

**Kurdistan Regional Government-Iraq
Ministry of Higher Education And
Scientific Research
University of Sulaimani
College of Education
Department of Physics**



The Nuclear Structure of Even – Even Zirconium-Isotopes by Using Interacting Boson Models (IBM-1 & IBM-2)

A Thesis

**Submitted to the Council of the College of Education/University of Sulaimani
in Partial Fulfillment of the Requirements for the Degree of Master of
Science in Physics
(Theoretical Physics)**

By

Berun Nasraddin Ghafoor

B.Sc. in physics (2012), University of Sulaimani

Supervised by

Assist. Prof. Dr. Saddon Taha Ahmad

Dr. Ari Karim Ahmed

December

2016

Sarmawarz

2716

Linguistic Evaluation Certificate

This is to certify that I, Arsto Nasir Ahmed, have proofread this thesis entitled **"The Nuclear Structure of Even-Even Zirconium- Isotopes by Using Interacting Boson Models (IBM-1 & IBM-2)"** conducted by Berun Nasraddin Ghafoor. After marking and correcting the mistakes, the thesis was handed again to the researcher to make the corrections in this last copy.



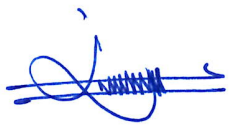
Proofreader: Arsto Nasir Ahmed

Date: 26/12/ 2016

Department of English, School of Languages, Faculty of Humanities,
University of Sulaimani.

Supervisor Certification

We certify that this thesis entitled "The Nuclear Structure of Even-Even Zirconium-Isotopes by Using Interacting Boson Models (IBM-1 & IBM-2)" accomplished by (Berun Nasralddin Ghafoor), was prepared under our supervisions in the College of Education at the University of Sulaimani, as partial fulfillment of the requirements for the degree of Master of Science in Physics

Signature: 
Name: **Dr. Saddon Taha Ahmad**
Title: **Assistant Professor**
Date: / / 2016

Signature: 
Name: **Dr. Ari Karim Ahmed**
Title: **Lecturer**
Date: / / 2016

In view of the available recommendation, I forward this thesis for debate by the examining committee.

Signature: 
Name: **Dr. Ari K. Ahmed**
Title: **Lecturer**
Date: / / 2016

Examining Committee Certification

We certify that we have read this thesis entitled " The Nuclear Structure of Even-Even Zirconium-Isotopes by Using Interacting Boson Models (IBM-1 & IBM-2)" prepared by (Berun Nasralddin Ghafoor), and as Examining Committee, examined the student in its content and in what is connected with it, and in our opinion it meets the basic requirements toward the degree of Master of Science in Physics.

Signature: 
Name: **Dr. Hiwa Y. Abdullah**
Title: **Assistant Professor**
Date: / / 2017
(Chairman)

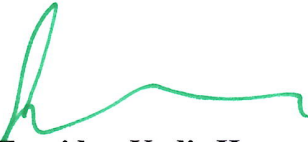
Signature: 
Name: **Dr. Jundi K. Yousif**
Title: **Assistant Professor**
Date: / / 2017
(Member)

Signature: 
Name: **Dr. Sarbast S. Ameen**
Title: **Lecturer**
Date: / / 2017
(Member)

Signature: 
Name: **Dr. Saddon T. Ahmad**
Title: **Assistant Professor**
Date: / / 2017
(Supervisor-Member)

Signature: 
Name: **Dr. Ari K. Ahmed**
Title: **Lecturer**
Date: **2/3** / 2017
(Supervisor-Member)

Approved by the Dean of the College of Education.

Signature: 
Name: **Dr. Faraidun Kadir Hamasalh**
Title: **Assistant Professor**
Date: **24** / / 2017

This thesis is dedicated to:

My lovely parents,

My sweet wife Tota,

My adorable sons Albert and Mali,

My dear brothers & sisters,

My entire sincere friends.

Berun

Acknowledgements

All praise is for my God compassionate and merciful almighty Allah, without the faith in the Almighty; I could not be able finish and succeed in my work.

I would like to thanks my supervisors, Dr. Saddon Taha Ahmad and Dr. Ari Karim Ahmed, for their continuous encouragements, invaluable supervisions, timely suggestions and inspiring guidance throughout the completion of this thesis. I would also like to acknowledge the financial support received through a studentship award by the College of Education for two years that enabled me to undertake this thesis.

I would like also to special thanks to head of Department of Physics of the College of Education, Dr. Ari Karim Ahmed, who always supported me and helped me during the M.Sc. Courses

It is my gratefulness to all my teachers in Sulaimani University who supported and guided me in completing this thesis. I would also like to thanks Dr. Jundi K. Yousif who helped me my thesis would be better.

Finally, special thanks to my dear family; Mother, father, wife, sisters, and brothers for their encouragement and support.

Berun

Abstract

The structure of the Zr-isotopes with proton number ($Z=40$), and with neutron's number $N=40,42,44,46,48,52, 54,56,58,60,62,64,66$, and 68 have been studied theoretically using the framework of the interacting boson models IBM-1 and IBM-2. The symmetry limits of the considered nuclei were studied using the energy of the second excited state relative to the first excited state. The considered nuclei were found to be transitional in the region $U(5) \rightarrow SU(3)$ and $O(6)$. The properties of the lowest mixed symmetry states such as the $1_M^+, 2_M^+$, and 3_M^+ states are calculated by IBM-2 model in the vibrational, rotational and gamma unstable ($SU(5)$, $SU(3)$, and $O(6)$) of Zr-isotopes and studied in detail. It was found that the mixed symmetry 1_M^+ and 3_M^+ levels are affected by the Majorana force parameters ξ_1 and ξ_3 respectively, while the parameter ξ_2 affects the energies of all levels which are considered to have mixed symmetry character, and it affects strongly the 2^+ states, as well as controlling the sharing between 2_M^+ state and its neighbors of 2^+ states. It is also found that the mixed symmetry character of 1_M^+ and 3_M^+ levels are confined to one level only in each isotope whereas the 2_M^+ state may share the mixed symmetry character with its neighboring levels.

In the framework of IBM-1 and IBM-2, the properties of energy level with positive parity of the ground, beta and gamma bands were studied. In general, the calculated low-lying positive parity energy spectra are better reproduced by the framework of IBM-2 than those of IBM-1 in most cases. This is due to the proton-neutron degree of freedom and the absence of these states in the IBM-1 model. The electromagnetic properties of E2 and M1 operators were investigated and the results were analyzed. The properties of E2 operator depend explicitly on the effective charges used in both IBM-1 and IBM-2. It is found that the different values of α_2 in the framework of IBM-1 for each Zr-isotopes also different values for both (e_π and e_ν) in the

framework of IBM-2 for each Zr-isotopes are used to generate the E2 properties such as B(E2) and Q(2⁺) throughout all considered Zr-isotopes. On the other hand the properties of the magnetic dipole operator have been studied only by the framework of IBM-2 because of the absence of the M1 transitions in the IBM-1. It is found that the M1 properties clearly depend on the g_π and g_ν in the framework of the IBM-2. Fixed values of ($g_\nu = -0.02\mu_N$) for all Zr-isotopes but changes the g_π for them were adopted in the calculations of IBM-2 to generate the M1 properties such as the B(M1), $\mu_{2_1^+}$ and $\delta(E2/M1)$ mixing ratios throughout these isotopes. It is found that the percentage of F-spin is to show the full symmetric and mixed symmetry of states. The small values of delta mixing ratios $\delta(E2/M1)$ was obtained with transition from mixed symmetry states to those of full symmetry.

Contents

Subject	Page
Abstract	I
List of figures	III
List of tables	VI
List of symbols	XII
Chapter One Introduction	1
1.1 Liquid drop model	1
1.2 The Fermi gas model	3
1.3 Shell model	4
1.4 Collective model	6
1.5 Interacting boson model (IBM)	9
1.6 Previous studies	15
1.7 Aims of the work	22
1.8 The outline of this thesis	22
Chapter Two The Interacting Boson Models (IBM)	23
2.1 IBM-1 Model	23
2.1.1 The Hamiltonian	24
2.1.2 Electromagnetic transition operator	28
2.1.3 Dynamical symmetries	31
2.1.3.1 Group Chain I: $U(5)$ symmetry	33
2.1.3.2 Group Chain II: $SU(3)$ symmetry	40
2.1.3.3 Group Chain III: $O(6)$ symmetry	45
2.2 Interacting Boson Model-2	54
2.2.1 IBM-2 Hamiltonian	55
2.2.2 Electromagnetic transition operator	57
2.2.3 Dynamical symmetry	59
2.2.3.1 Vibrational limit ($U_{\pi+\nu}(5)$): H^I Chain	61
2.2.3.2 Rotational limit ($SU_{\pi+\nu}(3)$): H^{II} Chain	64
2.2.3.3 γ -unstable limit ($O_{\pi+\nu}(6)$): H^{III} Chain	67
2.2.4 Mixed-symmetry	70
2.2.5 Delta mixing ratio	75
Chapter Three Computer programs for IBM-1 and IBM-2	76
3.1 IBM-1	76
3.2 IBM-2	79
Chapter Four Result and Discussion	86
4.1 Energy spectrum	87
4.1.1 ^{80}Zr -isotope	91
4.1.2 ^{82}Zr -isotope	92

Subject	Page
4.1.3 ^{84}Zr -isotope	93
4.1.4 ^{86}Zr -isotope	94
4.1.5 ^{88}Zr -isotope	95
4.1.6 ^{92}Zr -isotope	96
4.1.7 ^{94}Zr -isotope	97
4.1.8 ^{96}Zr -isotope	98
4.1.9 ^{98}Zr -isotope	99
4.1.10 ^{100}Zr -isotope	100
4.1.11 ^{102}Zr -isotope	101
4.1.12 ^{104}Zr -isotope	102
4.1.13 ^{106}Zr -isotope	103
4.1.14 ^{108}Zr -isotope	104
4.2 Mixed symmetry states	120
4.3 Electromagnetic properties	125
4.3.1 BE(2) transition properties	125
4.3.2 B (M1) transition properties	136
4.3.3 δ - mixing ratios	143
Chapter Five	159
Conclusions and future works	
5.1 Conclusions	159
5-2 Future works	160
References	161

List of Figures

Figure No.	Title	Page No.
(1-1)	Summary of liquid drop model treatment of the average binding energy.	3
(1-2)	Change the spherical shape of the nucleus to non-spherical due to a centrifugal pressure on the surface of the nucleus.	7
(1-3)	Nuclear deformation in the (β, γ) plane. The Lund conventions are used. The four cases ($\gamma = 120^\circ, 180^\circ, 240^\circ, 300^\circ$) correspond to the cases with $\gamma = 0^\circ$ and 60° but with different orientations of their axis. The area $0^\circ < \gamma < 60^\circ$ (in grey) is then sufficient to describe the nuclear deformation	9
(2-1)	low-lying levels of the U(5) symmetry of the IBM in the harmonic limit.	38
(2-2)	A typical spectrum with U(5) symmetry and N=6. in parentheses the quantum numbers (ν) and (n_d) appear	40
(2-3)	A typical spectrum with SU(3) symmetry and N=6. in parentheses the quantum numbers (λ) and (μ) appear	45
(2-4)	Low-lying levels of the O(6) limit, for N = 6	49
(2-5)	A typical spectrum with O(6) symmetry and N=6. in parentheses the quantum numbers (σ) and (ν_Δ) appear	50
(2-6)	Expectation values of \hat{n}_d in the yrast states for the three symmetries of the IBA N = 6	51
(2-7)	Casten triangle which shows the transitional regions between the three dynamical symmetries	53
(2-8)	A typical spectrum only the lowest states of the irrep [N] and [N-1] with $U_{\pi+\nu}(6) \supset U_{\pi+\nu}(5)$ symmetry in IBM-2, and $N_\pi = 2, N_\nu = 1$	64
(2-9)	A typical spectrum only the lowest states of the irrep [N] and [N-1] with $U_{\pi+\nu}(6) \supset SU_{\pi+\nu}(3)$ symmetry in IBM-2, and $N_\pi = 2, N_\nu = 1$	67
(2-10)	A typical spectrum only the lowest states of the irrep [N] and [N-1] with $U_{\pi+\nu}(6) \supset O_{\pi+\nu}(6)$ symmetry in IBM-2, and $N_\pi = 2, N_\nu = 1$	70
(2-11)	Geometric illustration of collective motion in symmetry and mixed-symmetry states in IBM-2	71
(2-12)	Illustration of states in a two boson $U_{\pi+\nu}(5)$ Hamiltonian using the IBM-2. F-spin is a good quantum number for this Hamiltonian, and the Majorana operator simply shifts the mixed-symmetry states up or down by the parameter λ	72
(3-1)	The structure of IBS1 code	78
(3-2)	structure of IBST program	79
(3-3)	structure of CFPGEN and NPCFPG programs	81
(3-4)	structure of RACFL and DDMEFL programs	82
(3-5)	structure of (NPBOSN) program	83
(3-6)	structure of NPBTRN program	84
(3-7)	Structure of Delta IBM2 program.	85

Figure No.	Title	Page No.
(4-1)	Variation of the energy ratios $\frac{E4_1^+}{E2_1^+}$ with neutron number in $^{80-108}\text{Zr}$ -isotops	88
(4-2)	a comparison between the experimental low -lying positive parity states in ^{80}Zr . With those obtained by IBM-1 and IBM-2 for the ground, gamma, and beta bands.	106
(4-3)	a comparison between the experimental low -lying positive parity states in ^{82}Zr with those obtained by IBM-1 and IBM-2 for the ground, gamma, and beta bands	106
(4-4)	a comparison between the experimental low -lying positive parity states in ^{84}Zr with those obtained by IBM-1 and IBM-2 for the ground, gamma, and beta bands.	107
(4-5)	a comparison between the experimental low -lying positive parity states in ^{86}Zr with those obtained by IBM-1 and IBM-2 for the ground, gamma, and beta bands.	107
(4-6)	a comparison between the experimental low -lying positive parity states in ^{88}Zr with those obtained by IBM-1 and IBM-2 for the ground, gamma, and beta bands	108
(4-7)	a comparison between the experimental low -lying positive parity states in ^{92}Zr with those obtained by IBM-1 and IBM-2 for the ground, gamma, and beta bands.	108
(4-8)	a comparison between the experimental low -lying positive parity states in ^{94}Zr with those obtained by IBM-1 and IBM-2 for the ground, gamma, and beta bands.	109
(4-9)	a comparison between the experimental low -lying positive parity states in ^{96}Zr with those obtained by IBM-1 and IBM-2 for the ground, gamma, and beta bands.	109
(4-10)	a comparison between the experimental low -lying positive parity states in ^{98}Zr with those obtained by IBM-1 and IBM-2 for the ground, gamma, and beta bands.	110
(4-11)	a comparison between the experimental low -lying positive parity states in ^{100}Zr with those obtained by IBM-1 and IBM-2 for the ground, gamma, and beta bands.	110
(4-12)	a comparison between the experimental low -lying positive parity states in ^{102}Zr with those obtained by IBM-1 and IBM-2 for the ground, gamma, and beta bands	111
(4-13)	a comparison between the experimental low -lying positive parity states in ^{104}Zr with those obtained by IBM-1 and IBM-2 for the ground, gamma, and beta bands	111
(4-14)	a comparison between the experimental low -lying positive parity states in ^{106}Zr with those obtained by IBM-1 and IBM-2 for the ground , gamma, and beta bands	112
(4-15)	a comparison between the experimental low -lying positive parity states in ^{108}Zr with those obtained by IBM-1 and IBM-2 for the ground, gamma, and beta bands	112

Figure No.	Title	Page No.
(4-16)	Experimental and calculated values of the energy ratios $\frac{E4_1^+}{E2_1^+}$ as a function of neutron number for $^{80-108}\text{Zr}$ isotopes.	113
(4-17)	Experimental and calculated values of the energy ratios $\frac{E2_2^+}{E2_1^+}$ as a function of neutron number for $^{80-108}\text{Zr}$ isotopes	114
(4-18)	Experimental and calculated values of the energy ratios $\frac{E6_1^+}{E2_1^+}$ as a function of neutron number for $^{80-108}\text{Zr}$ isotopes	114
(4-19)	A comparison between the calculated energy values of the IBM-1 and IBM-2 and those of experimental data in the $^{80-108}\text{Zr}$ -isotopes for the ground band of (a) 2_1^+ state (b) 4_1^+ state (c) 6_1^+ state.	116
(4-20)	A comparison between the calculated energy values of the IBM-1 and IBM-2 and those of experimental data in the $^{80-108}\text{Zr}$ -isotopes for the beta band of (a) 0_2^+ state (b) 2_2^+ state (c) 4_2^+ state	117
(4-21)	A comparison between the calculated energy values of the IBM-1 and IBM-2 and those of experimental data in the $^{80-108}\text{Zr}$ -isotopes for the gamma band of (a) 2_3^+ state (b) 3_1^+ state (c) 4_3^+ state (d) 5_1^+ .	119
(4-22)	Variation of the parameter ε_d with the neutron numbers in $^{80-108}\text{Zr}$ isotopes.	119
(4-23)	Variation of the parameter K with the neutron numbers in $^{80-108}\text{Zr}$ isotopes	120
(4-24)	(a)The change of the level energy in ^{104}Zr as a function of ξ_1 , (b)The change of the level energy in ^{108}Zr as a function of ξ_1 , (c) The change of the level energy in ^{102}Zr as a function of ξ_3 , and (d)The change of the level energy in ^{106}Zr as a function of ξ_3	124
(4-25)	(a) The change of the level energy in ^{102}Zr as a function of ξ_2 , (b) The change of the level energy in ^{108}Zr as a function of ξ_2 .	125
(4-26)	the $B(E2;2_1^+ \rightarrow 0_1^+)$ e^2b^2 transition for $^{80-106}\text{Zr}$ – isotopes as a function of neutron number.	134
(4-27)	the $B(E2;4_1^+ \rightarrow 2_1^+)$ e^2b^2 transition for $^{80-106}\text{Zr}$ – isotopes as a function of neutron number	134
(4-28)	the $B(E2;2_2^+ \rightarrow 2_1^+)$ e^2b^2 transition for $^{80-106}\text{Zr}$ – isotopes as a function of neutron number.	135
(4-29)	the ratios of $B(E2;4_1^+ \rightarrow 2_1^+) / B(E2;2_1^+ \rightarrow 0_1^+)$ for $^{80-106}\text{Zr}$ – isotopes as a function of neutron number	135
(4-30)	The multipole mixing ratio δ , of $2_i^+ \rightarrow 2_1^+$ transitions is plotted against ξ_2 for ^{106}Zr .	158

List of Tables

Table No.	Title	Page No.
(2-1)	Classification scheme for the group chain I	37
(2-2)	Classification scheme for the group chain II	43
(2-3)	Classification scheme for the group chain III	47
(2-4)	classification of the transitional region in the space of IBM	53
(2-5)	Partial classification scheme for <i>chain I</i>	63
(2-6)	Partial classification scheme for <i>chain II</i>	66
(2-7)	Partial classification scheme for <i>chain III</i>	69
(4-1)	The IBM-1 Hamiltonian parameters used for $^{80-108}\text{Zr}$ -isotopes	89
(4-2)	The IBM-2 Hamiltonian parameters used for $^{80-108}\text{Zr}$ - isotopes	91
(4-3)	the comparison between the calculated and the experimental energy levels values of (^{80}Zr)	92
(4-4)	the comparison between the calculated and the experimental energy levels values of (^{82}Zr)	93
(4-5)	the comparison between the calculated and the experimental energy levels values of (^{84}Zr)	94
(4-6)	the comparison between the calculated and the experimental energy levels values of (^{86}Zr)	95
(4-7)	the comparison between the calculated and the experimental energy levels values of (^{88}Zr)	96
(4-8)	the comparison between the calculated and the experimental energy levels values of (^{92}Zr)	97
(4-9)	the comparison between the calculated and the experimental energy levels values of (^{94}Zr)	98
(4-10)	the comparison between the calculated and the experimental energy levels values of (^{96}Zr)	99
(4-11)	the comparison between the calculated and the experimental energy levels values of (^{98}Zr)	100
(4-12)	the comparison between the calculated and the experimental energy levels values of (^{100}Zr)	101
(4-13)	the comparison between the calculated and the experimental energy levels values of (^{102}Zr)	102
(4-14)	the comparison between the calculated and the experimental energy levels values of (^{104}Zr)	103
(4-15)	the comparison between the calculated and the experimental energy levels values of (^{106}Zr)	104
(4-16)	the comparison between the calculated and the experimental energy levels values of (^{108}Zr)	105
(4-17)	the percentages of F-spin contribution in Zr-isotopes for states that have the mixed symmetry characters	121

Table No.	Title	Page No.
(4-18)	The experimental B (E2; $J_i \rightarrow J_f$) values , in the units (e^2b^2) ,and the quadruple moments ,in the unit of ($e.b$) ,for ^{80}Zr isotope are compared with those obtained by IBM-1 and IBM-2 results . the effective charges are taken as ($\alpha_2 = 0.17624 e.b$) in the IBM-1 and ($e_v = 0.175$, $e_\pi = 0.174$) $e.b$ in the IBM-2	127
(4-19)	The experimental B (E2; $J_i \rightarrow J_f$) values , in the units (e^2b^2) ,and the quadruple moments ,in the unit of ($e.b$) ,for ^{82}Zr isotope are compared with those obtained by IBM-1 and IBM-2 results . the effective charges are taken as ($\alpha_2 = 0.23794 e.b$) in the IBM-1 and ($e_v = 0.1833$, $e_\pi = 0.17$) $e.b$ in the IBM-2	127
(4-20)	The experimental B (E2; $J_i \rightarrow J_f$) values , in the units (e^2b^2) ,and the quadruple moments ,in the unit of ($e.b$) ,for ^{84}Zr isotope are compared with those obtained by IBM-1 and IBM-2 results . the effective charges are taken as ($\alpha_2 = 0.18127 e.b$) in the IBM-1 and ($e_v = 0.17$, $e_\pi = 0.156$) $e.b$ in the IBM-2	128
(4-21)	The experimental B (E2; $J_i \rightarrow J_f$) values , in the units (e^2b^2) ,and the quadruple moments ,in the unit of ($e.b$) ,for ^{86}Zr isotope are compared with those obtained by IBM-1 and IBM-2 results . the effective charges are taken as ($\alpha_2 = 0.139292 e.b$) in the IBM-1 and ($e_v = 0.1304$, $e_\pi = 0.11$) $e.b$ in the IBM-2	128
(4-22)	The experimental B (E2; $J_i \rightarrow J_f$) values , in the units (e^2b^2) ,and the quadruple moments ,in the unit of ($e.b$) ,for ^{88}Zr isotope are compared with those obtained by IBM-1 and IBM-2 results . the effective charges are taken as ($\alpha_2 = 0.13199 e.b$) in the IBM-1 and ($e_v = 0.04$, $e_\pi = 0.131$) $e.b$ in the IBM-2	129
(4-23)	The experimental B (E2; $J_i \rightarrow J_f$) values , in the units (e^2b^2) ,and the quadruple moments ,in the unit of ($e.b$) ,for ^{92}Zr isotope are compared with those obtained by IBM-1 and IBM-2 results . the effective charges are taken as ($\alpha_2 = 0.12943 e.b$) in the IBM-1 and ($e_v = 0.04$, $e_\pi = 0.125$) $e.b$ in the IBM-2	129
(4-24)	The experimental B (E2; $J_i \rightarrow J_f$) values , in the units (e^2b^2) ,and the quadruple moments ,in the unit of ($e.b$) ,for ^{94}Zr isotope are compared with those obtained by IBM-1 and IBM-2 results . the effective charges are taken as ($\alpha_2 = 0.10369 e.b$) in the IBM-1 and ($e_v = 0.044$, $e_\pi = 0.11$) $e.b$ in the IBM-2	130
(4-25)	The experimental B (E2; $J_i \rightarrow J_f$) values , in the units (e^2b^2) ,and the quadruple moments ,in the unit of ($e.b$) ,for ^{96}Zr isotope are compared with those obtained by IBM-1 and IBM-2 results . the effective charges are taken as ($\alpha_2 = 0.07 e.b$) in the IBM-1 and ($e_v = 0.0468$, $e_\pi = 0.09$) $e.b$ in the IBM-2	130
(4-26)	The experimental B (E2; $J_i \rightarrow J_f$) values , in the units (e^2b^2) ,and the quadruple moments ,in the unit of ($e.b$) ,for ^{98}Zr isotope are compared with those obtained by IBM-1 and IBM-2 results . the effective charges are taken as ($\alpha_2 = 0.15907 e.b$) in the IBM-1 and ($e_v = 0.0526$, $e_\pi = 0.16$) $e.b$ in the IBM-2	131

Table No.	Title	Page No.
(4-27)	The experimental $B (E2; J_i \rightarrow J_f)$ values , in the units $(e^2 b^2)$,and the quadruple moments ,in the unit of $(e.b)$,for ^{100}Zr isotope are compared with those obtained by IBM-1 and IBM-2 results . the effective charges are taken as $(\alpha_2 = 0.19766 e.b)$ in the IBM-1 and $(e_v = 0.2312, e_\pi = 0.19) e.b$ in the IBM-2	131
(4-28)	The experimental $B (E2; J_i \rightarrow J_f)$ values , in the units $(e^2 b^2)$,and the quadruple moments ,in the unit of $(e.b)$,for ^{102}Zr isotope are compared with those obtained by IBM-1 and IBM-2 results . the effective charges are taken as $(\alpha_2 = 0.17594 e.b)$ in the IBM-1 and $(e_v = 0.2387, e_\pi = 0.178) e.b$ in the IBM-2	132
(4-29)	The experimental $B (E2; J_i \rightarrow J_f)$ values , in the units $(e^2 b^2)$,and the quadruple moments ,in the unit of $(e.b)$,for ^{104}Zr isotope are compared with those obtained by IBM-1 and IBM-2 results . the effective charges are taken as $(\alpha_2 = 0.20041 e.b)$ in the IBM-1 and $(e_v = 0.26175, e_\pi = 0.21) e.b$ in the IBM-2	132
(4-30)	The experimental $B (E2; J_i \rightarrow J_f)$ values , in the units $(e^2 b^2)$,and the quadruple moments ,in the unit of $(e.b)$,for ^{106}Zr isotope are compared with those obtained by IBM-1 and IBM-2 results . the effective charges are taken as $(\alpha_2 = 0.17124 e.b)$ in the IBM-1 and $(e_v = 0.21, e_\pi = 0.1877) e.b$ in the IBM-2	133
(4-31)	The experimental $B (E2; J_i \rightarrow J_f)$ values , in the units $(e^2 b^2)$,and the quadruple moments ,in the unit of $(e.b)$,for ^{108}Zr isotope are compared with those obtained by IBM-1 and IBM-2 results . the effective charges are taken as $(\alpha_2 = 0.17124 e.b)$ in the IBM-1 and $(e_v = 0.21, e_\pi = 0.1877) e.b$ in the IBM-2	133
(4-32)	The $B(M1; J_i \rightarrow J_f)$ values , in the units of (μ_N^2) , and the magnetic dipole moments for the 2_1^+ states $(\mu_{2_1^+})$ in the unit of (μ_N) , for ^{80}Zr -isotopes obtained by IBM-2 results . The effective g- charges are taken as $g_v = -0.02$ and $g_\pi = 2.839$	136
(4-33)	The $B(M1; J_i \rightarrow J_f)$ values , in the units of (μ_N^2) , and the magnetic dipole moments for the 2_1^+ states $(\mu_{2_1^+})$ in the unit of (μ_N) , for ^{82}Zr -isotopes obtained by IBM-2 results . The effective g- charges are taken as $g_v = -0.02$ and $g_\pi = 2.839$	137
(4-34)	The $B(M1; J_i \rightarrow J_f)$ values , in the units of (μ_N^2) , and the magnetic dipole moments for the 2_1^+ states $(\mu_{2_1^+})$ in the unit of (μ_N) , for ^{84}Zr -isotopes obtained by IBM-2 results . The effective g- charges are taken as $g_v = -0.02$ and $g_\pi = 2.839$	137
(4-35)	The $B(M1; J_i \rightarrow J_f)$ values , in the units of (μ_N^2) , and the magnetic dipole moments for the 2_1^+ states $(\mu_{2_1^+})$ in the unit of (μ_N) , for ^{86}Zr -isotopes obtained by IBM-2 results . The effective g- charges are taken as $g_v = -0.02$ and $g_\pi = 2.995$	138

Table No.	Title	Page No.
(4-36)	The B(M1; $J_i \rightarrow J_f$) values , in the units of (μ_N^2), and the magnetic dipole moments for the 2_1^+ states ($\mu_{2_1^+}$) in the unit of (μ_N), for ^{88}Zr -isotopes obtained by IBM-2 results . The effective g- charges are taken as $g_v = -0.02$ and $g_\pi = 0.725$	138
(4-37)	The B(M1; $J_i \rightarrow J_f$) values , in the units of (μ_N^2), and the magnetic dipole moments for the 2_1^+ states ($\mu_{2_1^+}$) in the unit of (μ_N), for ^{92}Zr -isotopes obtained by IBM-2 results . The effective g- charges are taken as $g_v = -0.02$ and $g_\pi = 0.725$	139
(4-38)	The B(M1; $J_i \rightarrow J_f$) values , in the units of (μ_N^2), and the magnetic dipole moments for the 2_1^+ states ($\mu_{2_1^+}$) in the unit of (μ_N), for ^{94}Zr -isotopes obtained by IBM-2 results . The effective g- charges are taken as $g_v = -0.02$ and $g_\pi = 0.725$	139
(4-39)	The B(M1; $J_i \rightarrow J_f$) values , in the units of (μ_N^2), and the magnetic dipole moments for the 2_1^+ states ($\mu_{2_1^+}$) in the unit of (μ_N), for ^{96}Zr -isotopes obtained by IBM-2 results . The effective g- charges are taken as $g_v = -0.02$ and $g_\pi = 0.109$	140
(4-40)	The B(M1; $J_i \rightarrow J_f$) values , in the units of (μ_N^2), and the magnetic dipole moments for the 2_1^+ states ($\mu_{2_1^+}$) in the unit of (μ_N), for ^{98}Zr -isotopes obtained by IBM-2 results . The effective g- charges are taken as $g_v = -0.02$ and $g_\pi = 0.109$	140
(4-41)	The B(M1; $J_i \rightarrow J_f$) values , in the units of (μ_N^2), and the magnetic dipole moments for the 2_1^+ states ($\mu_{2_1^+}$) in the unit of (μ_N), for ^{100}Zr -isotopes obtained by IBM-2 results . The effective g- charges are taken as $g_v = -0.02$ and $g_\pi = 1.77$	141
(4-42)	The B(M1; $J_i \rightarrow J_f$) values , in the units of (μ_N^2), and the magnetic dipole moments for the 2_1^+ states ($\mu_{2_1^+}$) in the unit of (μ_N), for ^{102}Zr -isotopes obtained by IBM-2 results . The effective g- charges are taken as $g_v = -0.02$ and $g_\pi = 1.39$	141
(4-43)	The B(M1; $J_i \rightarrow J_f$) values , in the units of (μ_N^2), and the magnetic dipole moments for the 2_1^+ states ($\mu_{2_1^+}$) in the unit of (μ_N), for ^{104}Zr -isotopes obtained by IBM-2 results . The effective g- charges are taken as $g_v = -0.02$ and $g_\pi = 1.39$	142
(4-44)	The B(M1; $J_i \rightarrow J_f$) values , in the units of (μ_N^2), and the magnetic dipole moments for the 2_1^+ states ($\mu_{2_1^+}$) in the unit of (μ_N), for ^{106}Zr -isotopes obtained by IBM-2 results . The effective g- charges are taken as $g_v = -0.02$ and $g_\pi = 1.39$	142

Table No.	Title	Page No.
(4-45)	The $B(M1; J_i \rightarrow J_f)$ values, in the units of (μ_N^2) , and the magnetic dipole moments for the 2_1^+ states ($\mu_{2_1^+}$) in the unit of (μ_N) , for ^{108}Zr -isotopes obtained by IBM-2 results. The effective g- charges are taken as $g_v = -0.02$ and $g_\pi = 1.39$	143
(4-46)	The value of δ -mixing ratio obtained by IBM-2 for the ^{80}Zr isotope. The IBM-2 results are obtained using the parameters ($e_v = 0.175 eb$, $e_\pi = 0.174 eb$), $g_\pi = 2.839 \mu_N$ and $g_v = -0.02 \mu_N$	144
(4-47)	The value of δ -mixing ratio obtained by IBM-2 for the ^{82}Zr isotope. The IBM-2 results are obtained using the parameters ($e_v = 0.183 eb$, $e_\pi = 0.239 eb$), $g_\pi = 2.839 \mu_N$ and $g_v = -0.02 \mu_N$	145
(4-48)	The value of δ -mixing ratio obtained by IBM-2 for the ^{84}Zr isotope. The IBM-2 results are obtained using the parameters ($e_v = 0.17 eb$, $e_\pi = 0.156 eb$), $g_\pi = 2.839 \mu_N$ and $g_v = -0.02 \mu_N$	146
(4-49)	The value of δ -mixing ratio obtained by IBM-2 for the ^{86}Zr isotope. The IBM-2 results are obtained using the parameters ($e_v = 0.1304 eb$, $e_\pi = 0.11 eb$), $g_\pi = 2.995 \mu_N$ and $g_v = -0.02 \mu_N$	147
(4-50)	The value of δ -mixing ratio obtained by IBM-2 for the ^{88}Zr isotope. The IBM-2 results are obtained using the parameters ($e_v = 0.04 eb$, $e_\pi = 0.131 eb$), $g_\pi = 0.725 \mu_N$ and $g_v = -0.02 \mu_N$	148
(4-51)	The value of δ -mixing ratio obtained by IBM-2 for the ^{92}Zr isotope. The IBM-2 results are obtained using the parameters ($e_v = 0.04 eb$, $e_\pi = 0.125 eb$), $g_\pi = 0.725 \mu_N$ and $g_v = -0.02 \mu_N$	149
(4-52)	The value of δ -mixing ratio obtained by IBM-2 for the ^{94}Zr isotope. The IBM-2 results are obtained using the parameters ($e_v = 0.044 eb$, $e_\pi = 0.11 eb$), $g_\pi = 0.725 \mu_N$ and $g_v = -0.02 \mu_N$	150
(4-53)	The value of δ -mixing ratio obtained by IBM-2 for the ^{96}Zr isotope. The IBM-2 results are obtained using the parameters ($e_v = 0.0468 eb$, $e_\pi = 0.09 eb$), $g_\pi = 0.109 \mu_N$ and $g_v = -0.02 \mu_N$	151
(4-54)	The value of δ -mixing ratio obtained by IBM-2 for the ^{98}Zr isotope. The IBM-2 results are obtained using the parameters ($e_v = 0.0526 eb$, $e_\pi = 0.16 eb$), $g_\pi = 0.109 \mu_N$ and $g_v = -0.02 \mu_N$	152
(4-55)	The value of δ -mixing ratio obtained by IBM-2 for the ^{100}Zr isotope. The IBM-2 results are obtained using the parameters ($e_v = 0.2312 eb$, $e_\pi = 0.19 eb$), $g_\pi = 1.648 \mu_N$ and $g_v = -0.02 \mu_N$.	153
(4-56)	The value of δ -mixing ratio obtained by IBM-2 for the ^{102}Zr isotope. The IBM-2 results are obtained using the parameters ($e_v = 0.2387 eb$, $e_\pi = 0.178 eb$), $g_\pi = 1.39 \mu_N$ and $g_v = -0.02 \mu_N$.	154

Table No.	Title	Page No.
(4-57)	<p>The value of δ-mixing ratio obtained by IBM-2 for the ^{104}Zr isotope .The IBM-2 results are obtained using the parameters ($e_v=0.26175\text{ eb}$, $e_\pi=0.21\text{ eb}$), $g_\pi = 1.39\ \mu_N$ and $g_v = -0.02\ \mu_N$.</p>	155
(4-58)	<p>The value of δ-mixing ratio obtained by IBM-2 for the ^{106}Zr isotope .The IBM-2 results are obtained using the parameters ($e_v=0.21\text{ eb}$, $e_\pi=0.1877\text{ eb}$), $g_\pi = 1.39\ \mu_N$ and $g_v = -0.02\ \mu_N$.</p>	156
(4-59)	<p>The value of δ-mixing ratio obtained by IBM-2 for the ^{108}Zr isotope .The IBM-2 results are obtained using the parameters ($e_v=0.21\text{ eb}$, $e_\pi=0.1877\text{ eb}$), $g_\pi = 1.39\ \mu_N$ and $g_v = -0.02\ \mu_N$.</p>	157

List of Symbols

Symbol	Their meaning
IBM	Interacting boson model
N	Total numbers of boson
V	Boson-boson interaction potential
\hat{P}	Pairing operator
\hat{L}	Angular momentum operator
\hat{Q}	Quadrupole moments operator
\hat{T}_3	Octupole operator
\hat{T}_4	Hexadecupole operator
$\varepsilon_s, \varepsilon_d$	(s) and (d) single –boson energies
\hat{n}_d	Number of d-boson operator
$\hat{M}_{\pi\nu}$	Majorana interaction
\hat{T}^l	Transition operator
χ_π (χ_ν)	Proton (neutron) quadrupole deformation parameter
e_π (e_ν)	Proton (neutron) boson effective charge
g_π (g_ν)	Proton (neutron) bosons g-factor
N_π, N_ν	Proton , neutron – boson number
α_2	Boson effective charges
Ms	Mixed symmetry
M1	Magnetic dipole radiation
E2	Electric quadrupole radiation
Q(2_1^+)	Quadrupole moment of the first excited states 2_1^+
$\mu(2_1^+)$	Magnetic dipole moment of the first excited states 2_1^+
δ	Multipole mixing ratio
B(E2)	Electric quadrupole transition probabilities
B(E1)	Electric monopole transition probabilities
B(M1)	Magnetic dipole transition probabilities
γ	Gamma ray
L	Angular momentum
J_i	Initial spin
J_f	Final spin
π	Parity
W.u.	Weisskopf units
A	Mass number
i.e	That is
Eq.	Equation
et al	And other authors

Chapter One

Introduction

Chapter One

Introduction

The atomic nucleus is an incredibly complex system, where dozens and sometimes hundreds of particles interact in extremely complicated ways. That is a nucleus is quantum system of many nucleons interacting mainly by strong nuclear interaction. Each nucleon is made up of three quarks that interact via the strong force. The residual strong force is responsible for the short ranged attractive nuclear force that holds the nucleus together, and an additional Coulomb interaction between protons provides a repulsive force. Theory of atomic nuclei must describe the Structure of nucleus (distribution and properties of nuclear levels) and on the other hand Mechanism of nuclear reactions (dynamical properties of nuclei). It is clear that with such a complex system, a single model that describes all features of nuclei and includes all nuclear interactions will be impossible to implement. As such, identifying the underlying symmetries, the important degrees of freedom, and the most relevant interactions is extremely important for understanding the general behavior of the nucleus, here we can discuss briefly the nuclear models.

1.1 Nuclear models

1.1.1 Liquid drop model:

One of these models is liquid drop model that was the first model to describe nuclear properties. A detailed theory of the nuclear binding, based on highly sophisticated mathematical techniques and physical concepts, has been developed by Bruecknet and Co-Workers (1954-1961) [1]. A much cruder model exists in which the finer features in the nuclear force are ignored, but the strong inter-nucleon attraction is stressed [2]. This model is proposed in the

1935 by Bohr [3], and it provides a reasonable explanation for many nuclear phenomena such as, nuclear masses nuclear binding energy, nuclear fission, β -decay, radius, density, surface tension and the volume energy [4].

It assumes that the nucleus might be expected to behave very much like a droplet of some liquid in which the forces of attraction and repulsion between the particles in the liquid are balanced. The basis of this model is on the short range of the nuclear forces, together with the additivity of the volumes and binding energies [1,2,3,4]. The essential assumptions are:

- The nucleus like a droplet is incompressible matter so that $R \sim A^{1/3}$.
- The force between nucleons is considered to be spin independent as well as charge independent (the nuclear force is identical for every nucleon and in particular does not depend on whether it is a neutron or a proton).
- The nuclear forces have short-range character (saturation).

For most nuclei with $A > 20$ according to the liquid drop model, the binding energy is well reproduced by a semi-empirical mass formula. An excellent parameterization of the binding energies of nuclei in their ground state was proposed in 1935 by Bethe and Weizsäcker [5]. This formula relies on the liquid-drop analogy but also incorporates two quantum ingredients. One is an *asymmetry* energy which tends to favor equal numbers of protons and neutrons. The other is a *pairing* energy which favors configurations where two identical fermions are paired [4,5,6].

The mass formula of Bethe and Weizsäcker is

$$B(A,Z) = a_v A - a_s A^{2/3} - a_c [Z^2/A^{1/3}] - a_a [(N - Z)^2/A] + \delta(A) . \quad (1-1)$$

and a_v , a_s , a_c , a_a , δ are volume, surface, coulomb, asymmetry and pairing parameters term respectively [4,5].

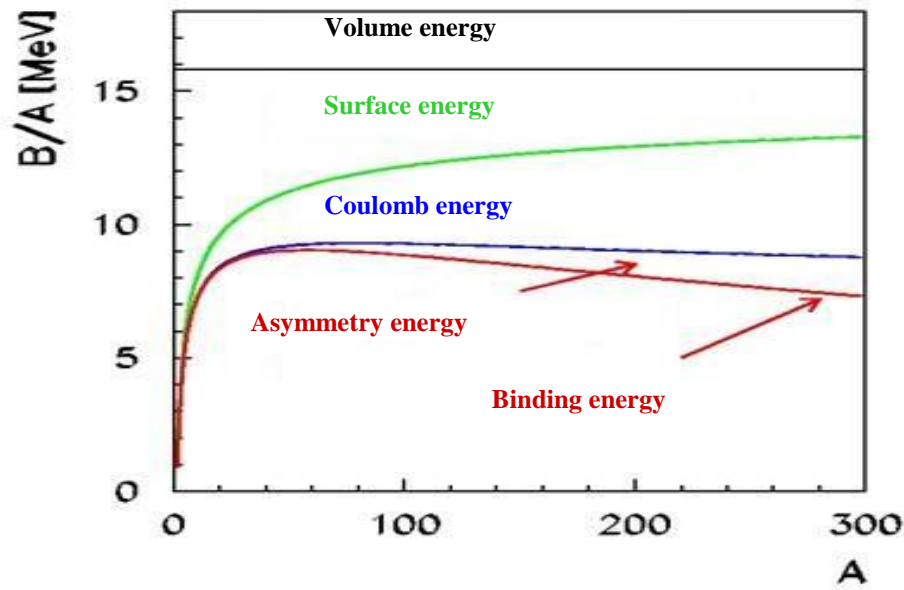


Fig. (1-1): summary of liquid drop model treatment of the average binding energy [5,6].

1.2 The Fermi gas model

In this model, nuclei are considered to be composed of two fermion gases, a neutron gas and a proton gas. The particles do not interact, but they are confined in a sphere which has the dimension of the nucleus. The Fermi model is based on the quantum statistics effects on the energy of confined fermions. The Fermi model provides a means to calculate the parameters term a_v , a_s and a_a in the Bethe–Weizsäcker formula, directly from the density ρ of the nuclear matter. According to this model, we can calculate the energy, momentum (called Fermi momentum) and wave number for the nucleus [5,6,7,8].

In a system of $A = Z + N$ nucleons, the densities of neutrons and protons are respectively $n_0(N/A)$ and $n_0(Z/A)$ where $n_0 \sim 0.15 \text{ fm}^{-3}$ is the nucleon density. The total kinetic energy is then [6]

$$E = E_Z + E_N = \frac{3}{5} \left[Z \frac{\hbar^2}{2m_p} \left(3\pi^2 \frac{Z n_0}{A} \right)^{2/3} + N \frac{\hbar^2}{2m_n} \left(3\pi^2 \frac{N n_0}{A} \right)^{2/3} \right] \quad (1-2)$$

1.3 Shell model

One important first step that was made by Jensen and Mayer was the development of the nuclear shell model [9]. In atomic systems, a central Coulomb potential is provided by the protons in the nucleus. Electrons are fermions, and as they are added to the system, they fill up electron orbits. With certain specific numbers of electrons, the orbits form closed shells that no longer interact as strongly with other atoms, or additional outer electrons. The nuclear system was found to behave in a similar way, but unlike the Coulomb central potential that exists in the atoms, the nuclear central potential is instead generated by the nucleons themselves. This assumption about the formation of shells in nuclei dramatically simplifies any attempts to model the structure of excited states in nuclei. The general energy spacing of possible proton and neutron orbits can be roughly predicted using a three-dimensional quantum Harmonic oscillator, an \hat{L}^2 interaction, and a spin-orbit coupling term. Constructing a basis out of the most likely configurations for the nucleons to occupy, and applying the relevant interactions, can in many cases reproduce the structure of the low-lying excited states of nuclei.

The main restriction with such a model is that even though the vastly complex system of the nucleus was dramatically simplified, it is still too complex to model nuclei with a large number of valence nucleons. The shell model is primarily applicable to nuclei that lie near closed shells, but as more valence nucleons are added to the system, an interesting type of behavior called collective motion arises.

The shell model that takes into account the behavior of individual nucleons and distribution of nucleons in the nuclear shells has been proposed to describe the stability of the magic numbers. In the nucleus, if the number of neutron (N) or the number of proton (Z) is equal to one of the following magic number (2, 8, 20, 28, 50, 82 and 126) or both are the magic numbers (called doubly magic) shell model can treat it. [10,11].

In the shell model, the nucleons in the nucleus form the shells (orbits) which are specified by their own potential and quantum numbers [12,13]. The nucleons are distributed due to the Pauli Exclusion Principle which requires that each nucleon has a unique set of quantum numbers to describe its motion in orbit [10]. The basic assumption of the shell model is that the effects of inter-nuclear interactions can be represented by single-particle potential [11,12]. Single particle model is a simple case of shell model, according to which the motion of an individual nucleon is particularly independent of that of any other nucleon, but the motion of any nucleon is governed by attractive average potential (self-consistent potential) that is formed as a result of interaction of the nucleon with other nucleons. This potential can be replaced as an approximation by a central potential that changes many body problem to one body problem [9,10].

For the harmonic oscillator potential, the stable nuclei are those which have closed proton and neutron shells, which represent the magic numbers 2, 8 and 20. To produce the other magic numbers (28, 50, 82 and 126) it must be used by another more realistic potential, harmonic oscillator with spin-orbit interaction. In 1949, M. G. Mayer and H. D. Jenson suggested that a spin-orbit potential [9,10,11,12,13] should be added to the centrally symmetric potential to generate the magic numbers (28, 50, 82, and 126). This term represents the interaction of spin of the nucleon (\vec{s}) and its orbital angular momenta (\vec{l}). The spin-orbit interaction, that is proportional to the quantity ($\vec{l} \cdot \vec{s}$), is strong comparing with the interaction between the nucleons themselves.

The shell model can predict the stability and abundance of the magic numbers, spin and parity of the ground states, magnetic dipole moment ($\vec{\mu}$), and Quadrupole moment. Even through the shell model is successful to predict these properties, it has some shortcomings to explain the following

- The large magnitude of the nuclear Quadrupole moments.
- The spin and parity for the ground state band of the nuclei $150 \leq A \leq 190$ and $A \geq 220$.
- The difference between experimental and theoretical magnetic dipole moments for some nuclei.
- The excited states of some even-even nuclei.

1.4 Collective model

This model is explaining the structure of nuclei with even numbers of protons and neutrons (known as *even-even* nuclei). Nuclei that have closed proton or neutron shells have a spherical shape. As valence nucleons are added to the system, the shape remains spherical but becomes softer, and vibrational structure is visible in the excited states of such nuclei. This softening of the spherical shape is the onset of collectivity, where collective motion refers to the valence nucleons moving together as a whole.

Excited states in nuclei decay to lower energy states via gamma-decay, where a gamma-ray of a particular multipolarity is emitted from the nucleus. The vibrational structure that appears at the onset of collectivity is a quadrupole oscillation around a spherical equilibrium shape, and the transitions that occur as a vibrational state decays to a more spherical state is typically an electric quadrupole (E2) transition. Strong transitions of this type are one of the signatures of collective behavior.

As even more valence nucleons are added to the system, a quadrupole deformed equilibrium shape becomes energetically favorable in nuclei. This deformed shape is associated with rotational structure in the excited states in such nuclei. The geometric nature of the transition from spherical to deformed makes using a geometric model a clear choice, and such a model was developed by Bohr and Mottelson [7],

In this model it is assumed that the outer most nucleons within the nucleus, exert a centrifugal pressure on the surface of the nucleus, as a result of it, the nucleus may be deformed into a permanent non spherical shape and hence, the surface may undergo oscillations due to the liquid drip model under the effect of exerted forces on the surface [14].

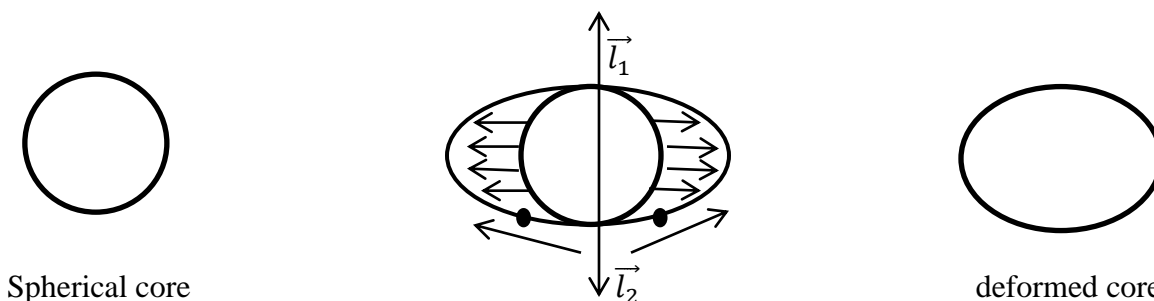


Fig.(1-2) : change the spherical shape of the nucleus to non-spherical due to a centrifugal pressure on the surface of the nucleus

As a result of the deformation, the surface of the nucleus may undergo oscillations and it rotates about an axis perpendicular to the symmetrical axis that causes to appear the excited states. The collective model generalizes the result of the shell model by considering the effect of a non-spherically symmetric potential, which leads to substantial deformations for heavy nuclei and consequently large value of electric quadrupole moments.

One of the most striking consequences of the collective model is the explanation of low – lying excited states of heavy nuclei. There are two major types of collective motion which are rotational motion that is a nucleus with a non-zero quadrupole moment that can have excited levels due to rotational perpendicular to the axis of symmetry, and the vibrational motion, in which there are modes of vibration in which the deformation of the nucleus due to the oscillation of electric quadrupole moment oscillates about its mean value. It could be that this mean value is very small, in which case the nucleus is oscillating between an oblate and a prolate spheroidal shape. It is also possible to have oscillations with different shapes, the small oscillations about the equilibrium shape perform simple harmonic motion [14, 15].

The shape of the nucleus can then be parametrized from a spherical shape corrected by the spherical harmonics $Y_{\lambda\mu}(\theta, \varphi)$

$$R(\theta, \varphi) = R_0 \left[1 + \sum_{\lambda=0}^{\infty} \sum_{\mu=-\lambda}^{\lambda} \alpha_{\lambda\mu} Y_{\lambda\mu}(\theta, \varphi) \right] \quad (1-3)$$

Where R_0 is the radius of a sphere of the same volume, $\alpha_{\lambda\mu}$ a variable to characterize the shape of the nucleus. The term $\lambda = 0$ describes volume variations, $\lambda = 1$ the translation of the system. The term with $\lambda = 2$ corresponds to quadrupole deformation and $\lambda = 3$ to octupole deformation. Using the transformation from the laboratory frame to the intrinsic frame, the five $\alpha_{\lambda=2,\mu}$ parameters are reduced to three real parameters $\alpha_{2,0}$, $\alpha_{2,2} = \alpha_{2,-2}$ and $\alpha_{2,1} = \alpha_{2,-1} = 0$. These variables can be parameterized as the following [14].

$$\alpha_{2,0} = \beta \cos \gamma \quad (1-4)$$

$$\alpha_{2,2} = \alpha_{2,-2} = \frac{1}{\sqrt{2}} \beta \sin \gamma \quad (1-5)$$

Where β represents the extent of the quadrupole deformation, γ gives the degree of axial asymmetry. Most nuclei are axially symmetric, or close to it, at least in their ground states. For an axially symmetric nucleus, the potential has a minimum at $\gamma = 0^\circ$. A common convention (Lund conventions) for the ranges of the β and γ variables is that $\beta > 0$, $\gamma = 0^\circ$ for an axially symmetric prolate nucleus and that $\beta > 0$, $\gamma = 60^\circ$ gives an axially symmetric oblate nucleus as it is shown in Fig.(1-3). Note that for $\beta < 0$, $\gamma = 0^\circ$, the nucleus is oblate [14,15]. If γ is not a multiple of 60° , one says that the nucleus is triaxial.

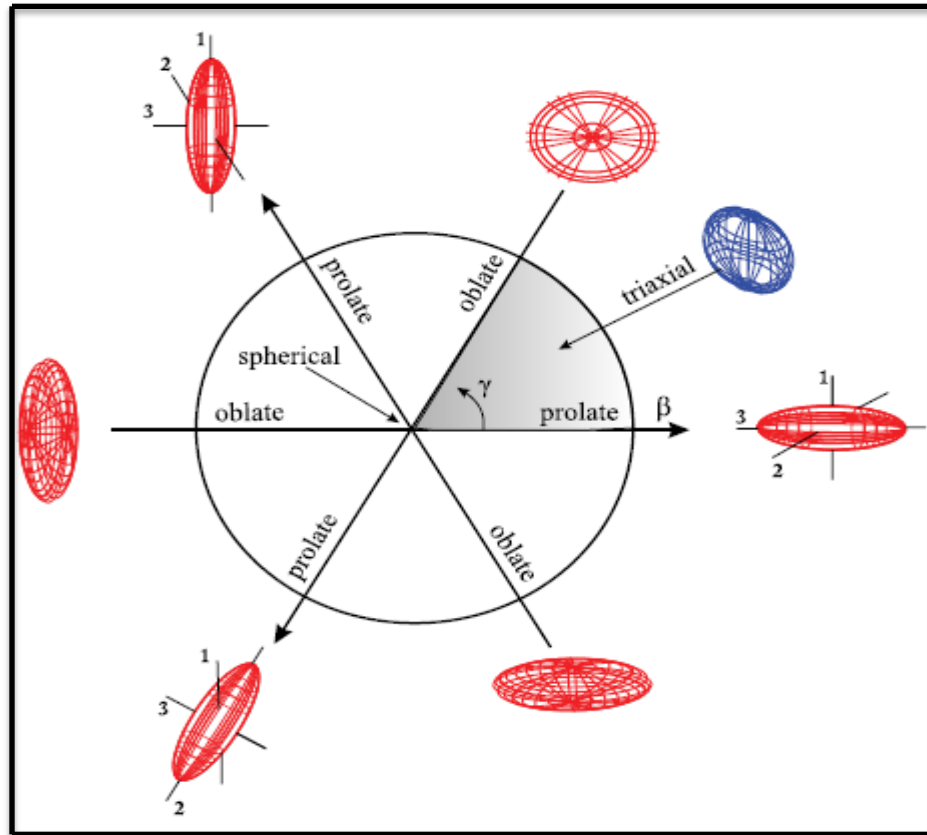


Fig. (1-3): Nuclear deformation in the (β, γ) plane. The Lund conventions are used. The four cases ($\gamma = 120^\circ, 180^\circ, 240^\circ, 300^\circ$) correspond to the cases with $\gamma = 0^\circ$ and 60° but with different orientations of their axis. The area $0^\circ < \gamma < 60^\circ$ (in grey) is then sufficient to describe the nuclear deformation

1.5 Interacting boson model (IBM)

The interacting boson model originated from early ideas of Feshbach and Iachello [15,16], who in 1969 described some properties of light nuclei in terms of interacting bosons, and from the work of Janssen, Jolos and Donau (1974) [16, 17], who in 1974 suggested a description of collective quadrupole states in nuclei in terms of a $SU(6)$ group. The latter description was subsequently cast into a different mathematical form by Arima and Iachello, 1975 [17, 18], with the introduction of an s-boson, which made the $SU(6)$, or rather $U(6)$, structure more apparent.

The success of this phenomenological approach to the structure of nuclei has led to major developments in the understanding of nuclear structure [15, 16, 17, 18].

The major new development was the realization that the bosons could be interpreted as nucleon pairs (Arima *et al.*, 1977) [18, 19, 20] in much the same way as Cooper pairs in the electron gas (Cooper, 1956). This provided a framework for a microscopic description of collective quadrupole states in nuclei and stimulated a large number of theoretical investigations. An immediate consequence of this interpretation was that, since one expected both neutron and proton pairs, one was led to consider a model with two types of bosons, proton bosons and neutron bosons. In order to make the distinction between proton and neutron bosons more apparent, the resulting model was called the interacting boson model-2, while the original version retained the name of interacting boson model-1 [20, 21, 22].

Subsequently, the model was further expanded by introducing explicitly unpaired fermions, thus allowing one to treat odd-even nuclei (Iachello and Scholten, 1979) [23]. Of this extension there exist now two versions, called the interacting boson-fermion model-1 and -2 [23,24]. In recent years, yet more extensions have been developed, including mixing of configurations, giant resonances, etc. As a result, there is hardly any aspect of nuclear structure that has not been touched by IBM [16, 17, 18, 19, 20, 21, 22].

The interacting boson model is an algebraic collective model that has a microscopic foundation in the shell model [16]. As mentioned above, one of the keys to understand nuclei is isolating the important interactions and degrees of freedom. The interacting boson model forgoes some of the single particle structure of the shell model, and focuses on the $L = 0$ and $L = 2$ couplings that play a dominant role in the low-lying states in even-even collective nuclei [17]. The symmetries in this model allow successful descriptions of vibrational, axially-symmetric deformed, and deformed gamma-soft collective structure.

When the proton-neutron degree of freedom is included in the interacting boson model, an additional class of states called mixed-symmetry states is allowed. When compared to their symmetric counterparts, these states have a negative phase factor between the proton and neutron boson components of the wave function. The experimental signatures for these mixed-symmetry states are strong M1 transitions to symmetric states [15].

The interacting boson model is a useful framework for the study of quantum phase transitions in nuclei. By using the method of coherent states, the algebraic structure of states in this model can be related to geometric variables β and γ [15]. With this formalism, an energy potential surface for the ground state can be found, which can help illustrate the transition from spherical to deformed between the symmetries. The behavior of the minima in energy potential surface shows that both first and second order phase transitions should occur in the model.

One of the most fundamental models in nuclear structure is the shell model, which was developed by Jensen and Mayer [11]. It is very useful for describing nuclei with a small number of valence nucleons, but as one moves away from closed shells, and collectivity takes hold, the model-space becomes much too large for calculations to be possible even on modern computers. At low energies in the shell model for even-even nuclei, pairs of identical valence nucleons occupy the same orbits, with the pairs coupling to $L = 0$ at the lowest energy and $L = 2$ at a higher energy. Many other configurations are possible, but at low energies, truncating the model space to include only those two-particle configurations that lead to an interesting model that has a much smaller model space, and wide applicability. This model is the interacting boson model (IBM) [25].

In the last decade the neutron-rich nuclei in the $40 \leq Z \leq 50$ region have attracted both theoretical and experimental attention. They were extensively studied via spontaneous or

induced fission reactions. Nuclei from this region of Segré chart exhibit vibrational, transitional, and rotational types of collectivity.

Such structures naturally appear in the framework of the interacting boson model (IBM) [26] which has been shown to be successful in the description of nuclear collective properties. The IBM in its first version, known as IBM-1, is based on the assumption that nuclear collectivity can be expressed in terms of s and d bosons [26, 27]. The model Hamiltonian is constructed from a set of 36 operators, bilinear in the boson creation and annihilation operators and generating the $U(6)$ Lie algebra. Dynamical symmetries occur if the Hamiltonian can be written as a combination of invariant (or Casimir) operators of specific subalgebras of $U(6)$ [26, 27] and three such cases occur, namely the spherical vibrational limit $U(5)$, the deformed limit $SU(3)$, and γ -soft limit $SO(6)$.

We begin from a strongly truncated model space, however, by keeping the pairing and quadrupole force components within the Interacting Boson Model (IBM) approximation [28]. This model approximates the interacting many-fermion problem using as the major degrees of freedom, N pairs of valence nucleons that are treated as bosons, carrying angular momentum either 0 (the s bosons) or 2 (the d bosons). This model is very appropriate in order to describe even-even medium-mass and heavy nuclei and transitional nuclei. Even here, treating proton and neutron bosons explicitly, one risks to be involved with too many model parameters. Therefore, in the present description of the Zr isotopes, we make use of an approach in which we restrict the use of identical bosons. This act of truncation naturally implies that one has to replace the Hamiltonian by an effective IBM Hamiltonian describing the interactions amongst these identical bosons [26, 27, 28].

The calculations are in the shell-model scheme and of the empirical structure of near closed-shell nuclei, in which 0^+ and 2^+ states lie considerably lower in energy than those of higher angular momentum. More specifically, this is characteristic feature of shell-model calculation of levels resulting from a short-range residual interaction in a two particle configuration of identical nucleons in the same orbit. Hence, it is reasonable to view the boson states as being constructed from the valence space only and to identify the bosons as correlated pairs of like nucleons. As such, the number $N = n_s + n_d$ is finite and conserved in a given nucleons and is simply given by half the total number of valence nucleons. In the original version of the model, the IBM-1, with which this review deals, no distinction is made between protons and neutrons. Moreover, the valence number counting is always done relative to the nearest closed shells. Calculate the number of difference between protons or neutrons relative to the nearest closed shell divided by two then adding both protons and neutrons bosons to give us the total number of bosons. For example, the nucleus $^{104}_{40}\text{Zr}_{64}$ has five valence proton bosons (relative to $Z=50$) and seven neutron bosons (relative to $N=50$), and so the boson number is $N = 5+7=12$, in this case protons are holes but neutrons are particles relative to the nearest close shell. And, in the $^{80}_{40}\text{Zr}_{40}$ has five valence protons and five neutrons (relative to $N=50$) and in this case both protons and neutrons are holes. Similarly, both $^{196}_{78}\text{Pt}_{118}$ and $^{128}_{54}\text{Xe}_{74}$ have $N = N_\pi + N_\nu = 2+4=6$ bosons and are taken to have the same basis states in the model, even though in one case both protons and neutrons are holes, while in the other the protons are particles and the neutrons holes. Nevertheless, despite this simplification, the key ingredient remains, namely, the explicit incorporation in the formalism of the finite number of valence nucleons available. This feature leads to many of the characteristic differences between the predictions of the IBA and earlier phenomenological models of collective nuclear structure, and also tends the former a

microscopic aspect, in that a substantial part of the predicted structural changes across a major shell arise automatically from the changes in boson number [15,16,17].

As a peculiarity of the IBM, there exist special cases in which certain linear combinations of matrix elements of this interaction potential vanish. In these cases, the energies of the nuclear states and the configurations can be expressed in a closed algebraic form. These special cases are named "dynamic symmetries". They correspond to the well-known "limits" allocated to the vibration, the rotation etcetera of the whole nucleus. However, most nuclei have to be calculated by diagonalising the Hamilton matrix as is usual in quantum mechanics.

The IBM is not only in connection with the shell model but also with the collective model of the atomic nucleus of Bohr and Mottelson [19, 20]. In this model the deformation of the nuclear surface is represented by five parameters from which a Hamiltonian of a five dimensional oscillator results. It contains fivefold generating and annihilating operators for oscillator quanta. The operators of these bosons correspond to the operators of the d-shell in the IBM.

However, the handling of the collective model is laborious. Moreover, the number of bosons is unlimited and is not a good quantum number in contrast to the situation in the IBM. The special cases mentioned above are reproduced by some versions of geometric models but they are not joined together continuously. In the IBM these relations exist. An additional relationship between both models consists in the fact that the form of the Hamilton operator (after suitable transformations) is similar to the one of the IBM. The total spin of a boson is identical with its angular momentum i.e. one does not attribute an intrinsic spin to the bosons. Since the angular momenta of the bosons are even ($l = 0, 2$) their parity is positive [21,22].

The application of the IBA to odd-mass nuclei, in which an odd nucleon is coupled to an IBA-1, description of the even-even core in the so-called interacting boson-fermion

approximation (IBFA) will also not be covered [23, 24]. And we can explain furthermore the interacting boson model in chapter two.

1.6 Previous studies

Zirconium with atomic number 40 and atomic weight 91.224(2)u has about thirty-three isotopes. Naturally occurring zirconium (Zr) is composed of four stable isotopes of which $^{90, 91, 92, 94}\text{Zr}$ and ^{96}Zr -isotope are nearly stable because they have a longer half-life than the age of the universe [29]. And ^{96}Zr is a primordial nuclide that decays via double beta decay with an observed half-life of 2.0×10^{19} years. It can also undergo single beta decay which is not yet observed, but the theoretically predicted value of $t_{1/2}$ is 2.4×10^{20} years [30]. The second most stable radioisotope is ^{93}Zr which has a half-life of 1.53 million years [29, 30]. Twenty-seven other radioisotopes have been observed. All have half-lives, less than a day except for ^{95}Zr (64.02 days), ^{88}Zr (63.4 days), and ^{89}Zr (78.41 hours). The primary decay mode is electron capture for isotopes lighter than ^{92}Zr , and the primary mode for heavier isotopes is beta decay [31].

Zirconium is the heaviest element that can be formed from symmetric fusion from either ^{45}Sc , or ^{46}Ca producing ^{90}Zr (after two beta-plus decays from ^{90}Mo) and ^{92}Zr respectively. All heavier elements are formed through asymmetric fusion or during the collapse of supernovae. As most of these are energy-absorbing processes, most nuclides of elements are heavier than it has been observed. The natural abundances of the Zirconium isotopes are ^{90}Zr (51.45%), ^{91}Zr (11.22%), ^{92}Zr (17.15%), ^{94}Zr (17.38%) and ^{96}Zr (2.80%) [30,31]. The nuclear structure of these isotopes have been the subject of several experiments and theoretical investigations such as:

- Studies of low-lying states in ^{94}Zr excited with the inelastic neutron scattering reaction [32]. In this study, the low-lying structure of $^{94}_{40}\text{Zr}$ has been studied with the $(n, n' \gamma)$

- reaction to identify symmetric and MS excitation in this nucleus. And used the γ -ray Spectroscopy, Doppler-shift Attenuation Method (DSAM), and Reduced Transition Probabilities.
- Zirconium isotopes are evidence for the heterogeneous distribution of s-process materials in the solar system [33]. In order to establish the occurrence and extent of such isotopic heterogeneities in Zr and to investigate the origin of widespread heterogeneities in our solar system, new high-precision Zr isotope data are reported for a range of primitive and differentiated meteorites. The majority of the carbonaceous chondrites (CV, CM, CO, CK) display variable $\epsilon^{96}\text{Zr}$ values (≤ 1.4) relative to the earth.
 - Discovery of Deformed Magic Number for Zirconium Isotopes (Deformed Magic Number Causes a Large Nuclear Deformation)[34], with some key points: Region of large deformation observed for neutron-rich zirconium (Zr) isotopes, degree of deformation of zirconium isotopes reaches the maximum when neutron number is 64 and equals the deformed magic number, and understanding changes in deformation may lead to understanding of the heavy element nucleosynthesis process in supernova explosions.
 - Hartree-Fock-Bogoliubov calculations in coordinate space using to study the properties of neutron-rich zirconium ($^{102,104}\text{Zr}$) [35]. In particular, they calculate two-neutron separation energies, Quadrupole moments, and rms-radii for proton and neutrons. And compare calculations with results from relativistic mean field theory and with available experimental data.
 - Microscopic study of nuclear structure for some Zr-isotopes using Skyrme-Hartree-Fock-Method [36]. By using the Skyrme parameterizations : SkM,S1,S3,SkM, and SkM .the charge, proton, neutron and mass densities together with their associated root mean

- square radii, neutron skin thickness, nuclear binding energies, and charge form factors have been calculated. Comparison between the theoretical and experimental results of charge form factors has likewise been performed.
- Shape co-existence and parity doublet in Zr isotopes [37]. They studied the ground and excited states properties for Zr isotopes starting from proton to neutron drip-lines using the relativistic and non-relativistic mean field formalisms with BCS and Bogoliubov pairing. The celebrity ML3 and SLy4 parameter sets are used in the calculations, and found spherical ground and low-lying large deformed excited states in most of the isotopes. Several couples of $\Omega^\pi = 1/2^\pm$ parity doublets configurations are found, while analyzing the single-particle energy levels of the large deformed configurations.
 - The role of the intrinsic E2 matrix element between the two 0^+ states in their configuration mixing in ^{100}Zr [38]. Shape coexistence in ^{100}Zr is a well-known phenomenon. And this study can describe the very important value of $B(E2)$ and lifetimes, with some work in the nuclear structure ^{100}Zr .
 - Neutron-rich Zr and Mo isotopes were populated as fission fragments produced by the $^{238}\text{U}(\alpha, f)$ fusion-fission reaction. Triaxiality and the aligned $h_{11/2}$ neutron orbitals in neutron-rich Zr isotopes [39]. The level schemes of these nuclei have been extended beyond the first band crossing region, which can be ascribed to the $h_{11/2}$ neutron pair alignment. The spin alignment and signature splitting for the $\nu h_{11/2}$ orbitals in term of triaxiality is addressed for calculations used the cranked shell model.
 - Proton-neutron structure of ^{92}Zr [40]. By using experimental data and shell model calculations show that both, single particle and collective degree of freedom are present in the low-lying levels of ^{92}Zr . The second excited quadrupole state shows the signatures of the one-phonon mixed-symmetric 2^+ state, whole calculations and data indicate an

almost pure neutron configuration for the 2_1^+ state, in contradiction with the F-spin symmetric limit and furthermore.

- Measurements of prompt γ rays in coincidence with isotopically-identified fission fragments, produced in collisions of ^{238}U on a ^9Be target, at energy around the coulomb barrier are reported. The structure evolution of the neutron-rich zirconium isotopes is discussed. With using the interacting boson model with a global parameterization that includes triaxiality. Towards the high spin-isospin frontier using isotopically-identified fission fragments [41].
- Using a schematic Interacting Boson Model (IBM) Hamiltonian to evaluate from spherical to deformed shapes along the chain of Zr isotopes from ^{96}Zr to ^{104}Zr , describing at the same time the excitation energies as well as the two-neutron separation energies. This is theoretical description of energy spectra and two-neutron separation energies for neutron-rich zirconium isotopes [42].
- Shape transition and collective dynamics in $^{94-100}\text{Zr}$ nuclei [43]. Quadrupole and octupole excitations in even $^{94-100}\text{Zr}$ nuclei are studied within the fully microscopic generator coordinate method using a basis generated by the self-consistent Hartree-Fock and GCM method.
- Interacting boson model-1 (IBM-1) used to calculations toward the neutron-rich nucleus ^{106}Zr [44], to study the energy levels and electric quardupole transition probabilities and compared with experimental information.
- Giant $M1$ states in Zr isotopes [45], by using the simple shell model. The newly observed $M1$ states in the (p,p') experiment on the Zr isotopes are considered the simple shell model. The calculation with a constant strength δ function interaction reproduces

- the excitation energies and the slight increase of the $M1$ strength at small momentum transfer with mass number.
- Microscopic study of oblate to prolate shape transition at higher spins in neutron-rich $^{100-104}\text{Zr}$ isotopes [46]. This study used the theoretical yrast spectra obtained in PSM framework compared with experimental data.
 - Anomaly in the nuclear charge radii of Zr isotopes [47], use the recent laser spectroscopic measurements, evaluate the nuclear root-mean-square charge radii on a chain of ^{90}Zr isotopes. A prominent kink is observed at Zr and a sharp change is noticed between ^{98}Zr and ^{100}Zr , in the neutron rich region.
 - Neutron separation energies of Zr isotopes [48], Q -value are reported for (d,t) reactions on all the stable isotopes of zirconium. Used the theoretical evaluation of Wapstra and Gova (WG) method and then compared to the experimental data.
 - Deformation parameters and nuclear radius of zirconium isotopes [49], using the deformed shell model. In this search he studied the most important deformation parameters (δ, β_2), intrinsic quadrupole moments (Q_0), root mean square of the nuclear radius and major with minor of ellipsoid axes (a,b) in addition to the difference between them.
 - Investigation of the neutron-rich zirconium (^{92}Zr , ^{94}Zr) [50], using interacting boson model. In this study calculated the low-lying levels structure and electric quadrupole transition by (IBM-1).and compared with experimental data.
 - A study of some nuclear properties of ^{102}Zr such as energy levels and $B(E2)$ transition [51], by using interacting boson model IBM-1 and IBM-2. Compared with experimental data.

- A study of some nuclear properties of ^{100}Zr such as energy levels and B(E2) transition [52], by using interacting boson model IBM-1 and IBM-2. Compared with experimental data.
- Gamow-Tellar strength distributions, β -decay half-lives, and β -delayed neutron emission are investigated in neutron-rich Zr isotopes with in a deformed quasiparticle random-phase approximation briefly β -decay properties [53]. Using self-consistent Skyrme Hartree-Fock mean field with correlations.
- Charge radii and structural evolution in Zr isotopes including both even-even and odd-A nuclei [54], is studied within self-consistent Skyrme Hartree-Fock-Bogoliubov (HFB).
- Study of spin rotation function for polarized proton incident on Zr isotopes [55]. In framework of first-order Brueckner theory employing Urbana V14, soft-core internucleon interaction along with relativistic mean field (RMF).
- Application of realistic effective interactions to the structure of the Zr isotopes [56]. The Zr isotopes undergo a clear and smooth shape transition with increasing neutron number. The isotopes which are displayed span from pure spherical nuclei that can be described in terms of simple shell-model configurations.
- Shell Model Calculations for Even Zirconium Isotopes [57], This contribution is a status report of the project aiming to describe the low-lying structure of the Zr isotopic chain by large scale shell model calculations.
- Lifetime measurements of the first 2^+ states in $^{104,106}\text{Zr}$ [58], Evolution of ground-state deformations. The first fast-timing measurements from nuclides produced via the in-flight fission mechanism are reported. The lifetimes of the first 2^+ states in $^{104,106}\text{Zr}$ nuclei have been measured via β -delayed γ -ray timing of stopped radioactive isotope beams

- Determination of the differences between the charge radii of zirconium [59], nuclei using laser-excited resonance fluorescence. The optical isotopic shifts of all the stable zirconium isotopes were determined for three atomic transitions of the $4d\ ^25s^2 \rightarrow 4d\ ^25s5p$ type by the method of laser-excited resonance fluorescence. The differences between the mean-square charge radii $\Delta\langle R^2 \rangle$ were determined for zirconium ions.
- A comparative study between semi-empirical oscillator strength parameterization and relativistic Hartree-Fock methods for computing the radiative parameters in Zr II spectrum [60].

1.7 Aims of the work

In the present work, the calculations have been performed for $^{80-108}\text{Zr}$ -isotopes (with $Z = 40$ and $40 \leq N \leq 68$) and to dedicate to study the following:

- Energy levels, nuclear shape and electromagnetic properties will be calculated.
- A detailed analysis of some spectroscopic observables, such as the ratio $R4/2$ of excitation energies of the first 2^+ and 4^+ levels or the amplitude of even-odd staggering in the γ band, The dynamical symmetries of even- even Zr- isotopes will be identified.
- The electric properties of the considered nuclei such as the E2 transition rates and the quadrupole moment of the first excited states 2_1^+ (i.e. $Q2_1^+$).
- The magnetic properties of the considered nuclei such as the M1 transition rates, mixing ratios and the magnetic dipole moments of the first excited states 2_1^+ (i.e. $\mu2_1^+$).

1.8 The outline

The outline of this thesis includes the following: the main characteristics of the theory of the interacting boson model of the IBM-1 and IBM-2 models, which are presented in chapter two. A brief description of the computer programs used in this work for the calculation of the energy and electromagnetic properties of IBM-1 and IBM-2 models is given in chapter three. The results and discussion of our theoretical calculation are presented in chapter four. The summary and the conclusions which are drawn by the present work and the suggested future works are presented in chapter five.

Chapter Two

The Interacting Boson Models (IBM)

Chapter Two

The Interacting Boson Models (IBM)

A nuclear model was proposed by Arima and Iachello, called Interacting Boson Model (IBM) to study the structure and properties of even– even nuclei and describing collective excitations in atomic nuclei. One of the advantages of the model is its use of the symmetries of the boson operators introduced in the model, which allows for analytic expressions of the states and expectation values for three different ideal limits of nuclei. In the IBM-1, the number of bosons is given by the number of pairs of protons and pairs of neutrons outside of closed shells. No distinction is made between proton type and neutron type bosons, but in IBM-2, distinction is made between proton type and neutron type bosons [16, 17, 18, 19].

2.1 IBM-1 Model

IBM-1 is (s-d) bosons system, which has six components that can be analogues to six-dimension space. In the view of group theory, this will lead to a description in terms of U(6). In the IBM-1, the nucleon or hole pairs must be the same type of nucleon. Meaning pairs consisting of a proton and neutron are not included. The IBM-1 is applicable only to even-even nuclei. The nuclear states are represented in the framework of second quantization. The boson creation operators are given by (s^\dagger) and (d^\dagger_μ) and the boson annihilation operators by (s) and (d_μ) where ($\mu = -2, -1, 0, 1, 2$) satisfy the following commutation relations [63].

$$[s, s] = [s^\dagger, s^\dagger] = 0 \quad (2-1)$$

$$[s, d_\mu] = [s^\dagger, d] = [s, d^\dagger] = [s^\dagger, d^\dagger] = 0 \quad (2-2)$$

$$[d_\mu, d_{\mu'}] = [d^\dagger_\mu, d^\dagger_{\mu'}] = 0 \quad (2-3)$$

$$[d_\mu, d_{\mu'}] = \delta_{\mu\mu'} \quad (2-4)$$

2.1.1 The Hamiltonian

The Hamiltonian, which connects the basis states, is written in the language of second quantization and, as such, can only involve combinations of the operators s , s^\dagger , d , d^\dagger . The specific combinations that appear are defined by the restriction limiting the complexity to a maximum of two-body interactions and by the need to conserve the total number of bosons. The former constraint implies that terms containing, for example, $d^\dagger d^\dagger$ or $s^\dagger s^\dagger$ are allowed, while combinations such as $d^\dagger d^\dagger d^\dagger$ are not. The latter demands that every creation operator be accompanied by an annihilation operator and vice versa. Such Hamiltonian operator (\hat{H}) contains one and two body operators

$$\hat{H} = \varepsilon_s s^\dagger \tilde{s} + \varepsilon_d \sum_m d^\dagger \tilde{d} + V \quad (2-5)$$

Where ε_s , ε_d are s and d single – boson energies, V is boson-boson interaction potential, s^\dagger (\tilde{s}) are creation and annihilation operators for the state (s), (s -boson), and d^\dagger (\tilde{d}) are creation and annihilation operators for the state(d), (d -boson). These rules result in the following form for the most general IBA-1 Hamiltonian [64, 65, 66, 67, 68].

$$\begin{aligned} \hat{H} = & E_0 + \varepsilon_s (s^\dagger \cdot \tilde{s}) + \varepsilon_d (d^\dagger \cdot \tilde{d}) + \sum_{L=0,2,4} \frac{1}{2} \sqrt{2L+1} C_L [[d^\dagger \otimes d^\dagger] \otimes [\tilde{d} \otimes \tilde{d}]^L]^0 \\ & + \tilde{V}_2 / \sqrt{2} [[d^\dagger \otimes d^\dagger]^2 \otimes [\tilde{d} \otimes \tilde{s}]^2 + [d^\dagger \otimes s^\dagger]^2 \otimes [d^\dagger \otimes \tilde{d}]^2]^0 \\ & + \tilde{V}_0 / 2 [[d^\dagger \otimes d^\dagger]^0 \otimes [\tilde{s} \otimes \tilde{s}]^0 + [s^\dagger \otimes s^\dagger]^0 \otimes [\tilde{d} \otimes \tilde{d}]^0]^0 \\ & + u_2 [[d^\dagger \otimes s^\dagger]^2 \otimes [\tilde{d} \otimes \tilde{s}]^2]^0 + u_0 / 2 [[s^\dagger \otimes s^\dagger]^0 \otimes [\tilde{s} \otimes \tilde{s}]^0]^0 \end{aligned} \quad (2-6)$$

where the coefficient in front of each term has been chosen according to the definitions of Arima and Iachello [17]. The operator \tilde{d} is defined by

$$\tilde{d}_m = (-1)^m d_{-m} \quad (2-7)$$

so that it maintains the character of a spherical tensor operator of rank two. This form of Hamiltonian is the most direct form which includes all allowed one-body and two-body interactions in the second quantization formalism. In this Hamiltonian E_0 is the core energy; ϵ_s and ϵ_d are the binding energies of the s and d boson (or we can say ϵ_s and ϵ_d are single boson energies for s-and d-boson respectively); the operators $(s^\dagger s)$ and $(d^\dagger \tilde{d})$ count the number of s and d bosons, respectively. Where n_s and n_d are number operators, the C_L , V_0 , V_2 , u_2 and u_0 are corresponding interaction parameters (The three constants C_0 , C_2 and C_4 specify the interaction between the d-bosons and similarly u_0 specifies the interaction strength among the s-bosons. The interaction of the s-bosons with the d-bosons is given by V_2 , V_0 and u_2). It is apparent that the full Hamiltonian of Eq. (2.6) involves two single-boson energies (multiplying the one body terms (ϵ_s, ϵ_d)), and seven boson-boson interaction strengths (multiplying the two-body terms $(C_0, C_2, C_4, V_0, V_2, u_2, u_0)$).

It can be shown that for the calculation of excitation energies only 6 of these 10 parameters are linearly independent. The effect of ϵ_s for example, can be absorbed into ϵ_d and E_0 by making use of the total boson number conservation, and the total number of boson is

$$\hat{N} = n_s + n_d \quad (2-8)$$

Also we can written as

$$\epsilon_s (s^\dagger s) + \epsilon_d (d^\dagger \tilde{d}) = \epsilon_s n_s + \epsilon_d n_d = \epsilon_s \hat{N} + (\epsilon_d - \epsilon_s) n_d = \epsilon_s \hat{N} + \epsilon_d n_d \quad (2-9)$$

Where $\epsilon_d - \epsilon_s$ is the difference in binding energy between the s-and the d-boson. Since $\epsilon_s \hat{N}$ is a constant for a given nucleus, its contribution can be absorbed in E_0 . Similarly the contribution of u_0 and u_2 can be absorbed in E_0 , ϵ_d and C_L using

$$\begin{aligned}
[(d^\dagger s^\dagger)^{(2)} (\tilde{d}s)^{(2)}]_0^{(0)} &= (s^\dagger s)_0^{(0)} (d^\dagger \tilde{d})_0^{(0)} = \frac{1}{\sqrt{5}}(\hat{N}n_d - n_d n_d) \\
&= \frac{1}{\sqrt{5}}\{ (\hat{N} - 1)n_d - \sum_{L=0,2,4} \sqrt{2L+1} [(d^\dagger d^\dagger)^L (\tilde{d}\tilde{d})^L]_0^{(0)} \} \quad (2-10)
\end{aligned}$$

, and

$$\begin{aligned}
[(s^\dagger s^\dagger)(s s)]_0^{(0)} &= n_s(n_s-1) = (\hat{N} - n_d - 1)(\hat{N} - n_d) \\
(\hat{N} - 1) \hat{N} - 2(\hat{N} - 1) n_d + \sum_{L=0,2,4} \sqrt{2L+1} [(d^\dagger d^\dagger)^L (\tilde{d}\tilde{d})^L]_0^{(0)} & \quad (2-11)
\end{aligned}$$

For a given nucleus E_0 is a constant affecting only the binding energy. The calculation of the matrix elements of this general Hamiltonian can be carried out in a straight forward way, using the coefficients of fractional parentage (cfp) [20]. From the above equations, N is a fixed for a given nucleus and only the excitation energy are considered, then only one of the one body terms and five of the two body terms are independent, and then the number is further reduced to six parameters. And we can express the number of s-boson and d-boson in terms of creation and annihilation operators,

The number of s-boson is

$$n_s = s^\dagger \tilde{s} \quad (2-12)$$

The number of d-boson is

$$n_d = d^\dagger \tilde{d} \quad (2-13)$$

the most commonly used form of the IBA Hamiltonian, and the one in which it is the easiest to understand the role of each term in determining the final structure of the nucleus under consideration, is the so-called multipole expansion. In this parametrization the various boson-boson interactions are grouped so that the Hamiltonian takes the form [15, 16, 17, 18, 19, 20].

$$\hat{H} = \varepsilon (n_d) + a_o (\hat{P} \cdot \hat{P}) + a_1 (\hat{L} \cdot \hat{L}) + a_2 (\hat{Q} \cdot \hat{Q}) + a_3 (\hat{T}_3 \cdot \hat{T}_3) + a_4 (\hat{T}_4 \cdot \hat{T}_4) \quad (2-14)$$

Where ε , a_0 , a_1 , a_2 , a_3 and a_4 are the model parameters, P , L , Q , T_3 and T_4 are the pairing, angular momentum, quadrupole, octupole and hexadecapole operators respectively. n_d is the d-boson number operator, and all operators in the Hamiltonian are the following [64,65,66,67,68]

Pairing operator is

$$\hat{P} = \frac{1}{2} [(\tilde{d} \cdot \tilde{d}) - (\tilde{s} \cdot \tilde{s})] = \frac{1}{2} (\tilde{d}^2 - \tilde{s}^2) \quad (2-15)$$

$$T_l = [d^\dagger \otimes \tilde{d}]^l \quad l=0,1,2,3,4,\dots \quad (2-16)$$

Angular momentum operator is

$$\hat{L} = \sqrt{10} [d^\dagger \otimes \tilde{d}]^1 = \sqrt{10} \hat{T}_1 \quad (2-17)$$

Quadrupole moment operator is

$$\begin{aligned} \hat{Q} &= [d^\dagger \otimes \tilde{s} + s^\dagger \otimes \tilde{d}]^2 - \frac{\sqrt{7}}{2} [d^\dagger \otimes \tilde{d}]^2 \\ &= [d^\dagger \otimes \tilde{s} + s^\dagger \otimes \tilde{d}]^2 - \frac{\sqrt{7}}{2} T_2 \end{aligned} \quad (2-18)$$

Octupole operator is

$$\hat{T}_3 = [d^\dagger \otimes \tilde{d}]^3 \quad (2-19)$$

Hexadecapole operator is

$$\hat{T}_4 = [d^\dagger \otimes \tilde{d}]^4 \quad (2-20)$$

Number of d-boson operator is

$$\hat{n}_d = \sqrt{5} \hat{T}_0 \quad (2-21)$$

In this form there appear terms that have, at least superficially, a more physical connotation, specifically an angular momentum operator, a quadrupole operator, octupole and hexadecapole terms, as well as the so-called pairing operator P . Note, however, that these are operators acting on boson states, not in the fermion space. It is in this form, therefore, that we shall usually

consider the application of the IBA-1 Hamiltonian to the set of basis states described earlier. We note that the definition of Q above uses a specific SU(3) choice of numerical coefficients.

The Hamiltonian also can be written in terms of Casimir operator [17].

$$\hat{H} = \varepsilon \hat{C}_{1U(5)} + \alpha \hat{C}_{2U(5)} + \beta \hat{C}_{2O(5)} + \gamma \hat{C}_{2O(3)} + \delta \hat{C}_{2SU(3)} + \eta \hat{C}_{O(6)} \quad (2-22)$$

Where ε , α , β , γ , δ , and η are parameters, $\hat{C}_{1U(5)}$ is linear Casimir operator and $\hat{C}_{2U(5)}$, $\hat{C}_{2O(5)}$, $\hat{C}_{2O(3)}$, $\hat{C}_{2SU(3)}$, and $\hat{C}_{O(6)}$ are quadratic Casimir operator.

As will become evident, an important concept is that of a *Casimir* operator of a group. This is an operator that commutes with *all* of the generators of the group. Such operators can be composed of linear or higher-order combinations of the generators and are appropriately called linear, quadratic, . . . , Casimir operators.

For example, in the case of O(3), the operator

$$J^2 = J_x^2 + J_y^2 + J_z^2 = J_+ J_- + J_z^2 \quad (2-23)$$

Commutates with J_z , J_+ , and J_- and is therefore the (quadratic) Casimir operator of O(3).

2.1.2 Electromagnetic transition operator

Many observable quantities can be calculated in the framework of IBM by evaluating the matrix elements of the appropriate operators. The construction of operators for the various nuclear structure observables of interest is again straightforward, given the fact that they must be built from the basic elements s , s^\dagger , \tilde{d} or d^\dagger . In the vast majority of applications to date, only the lowest-order contributions to these operators have been included [64, 65, 66, 67, 68]

The electric monopole transition operator is

$$T(E0) = \alpha \hat{n}_s + \frac{\beta}{\sqrt{5}} \hat{n}_d \quad (2-24)$$

The T(E0) operator can be rewritten as

$$T(E0) = \alpha(\hat{N} - \hat{n}_d) + \frac{\beta}{\sqrt{5}} \hat{n}_d = \alpha(\hat{N}) + \frac{\beta}{\sqrt{5}} \hat{n}_d \quad (2-25)$$

Where α and β are the coefficient of the various terms in the operator. The first term in $T(E0)$ vanishes, since N is conserved and therefore cannot induce transitions between the orthogonal basis states. Hence $E0$ transitions are simply proportional to the matrix elements of the d-boson number operator and thus rather directly sample the wave function structure, can be written as $T_0^{E0} = e_0 \hat{n}_d$.

The most important electromagnetic features are the E2 transitions. The B(E2) values were calculated by using the E2 operator. The E2 transition operator (electric quadrupole transition operator) must be a Hermitian tensor of rank two and therefore the number of bosons must be conserved. Since with these constraints the general E2 operator can be written as

$$T(E2) = e_B [(d^\dagger \tilde{s} + s^\dagger \tilde{d}) + \chi(d^\dagger \tilde{d})^{(2)}] = e_B Q \quad (2-26)$$

Where e_B plays the role of the effective boson charge. The parameter χ determines the relative importance of the two terms. The $E2$ operator, which is identical in form to the Q operator in the Hamiltonian, consists of one piece that changes n_d by unity and another that leaves n_d unchanged, the ratio of the two terms being given by the parameter χ .

Hexadecupole transition operator is a tensor of rank four (E4) and can be written as

$$T_m^{E4} = e_4 [d^\dagger \otimes \tilde{d}]_m^4 \quad (2-27)$$

the monopole operator $M^{(0)}$ can be constructed in a similar manner [19]

$$M^{(0)} = c + \alpha_0 (s^\dagger s)^{(0)} + \beta_0 (d^\dagger \tilde{d})^{(0)} \quad (2-28)$$

Where c is a constant, the monopole operator is used to calculate properties such as E0 transitions and mean square radii.

The magnetic dipole transition operator are [17,18,19]

$$T(M1) = g_B \hat{L} = g_B [d^\dagger \otimes \tilde{d}]_m^1 \quad (2-29)$$

In contrast, the $M1$ operator is proportional to the total angular momentum and therefore gives rise to no transitions. To investigate $M1$ transitions in the IBA-1 framework, it has therefore been necessary to introduce second-order terms [17] In this case, one has

$$T(M1) = (g_B + A \hat{N}) \hat{L} + B \hat{n}_d \hat{L} + C (Q\hat{L})^{(1)} \quad (2-30)$$

Then the magnetic octupole transition operator is a tensor to rank three

$$T_m^{M3} = e_3 [d^\dagger \otimes \tilde{d}]_m^3 \quad (2-31)$$

Electromagnetic transition rates can be calculated in the usual way. By taking the reduced matrix element of the corresponding transition operators between initial and final states as $\langle L_f || T^l || L_i \rangle$.

The relation could hold for electric and magnetic transition probability, $B(El)$ and $B(Ml)$ respectively as [17]

$$B(l; L_i \rightarrow L_f) = \frac{1}{2^{Li+1}} |\langle L_f || T^l || L_i \rangle|^2 \quad (2-32)$$

Where:

L_i : Angular momentum of the initial state.

L_f : Angular momentum of the final state.

T^l : Transition operator.

Turning now to other properties, the operator for the mean-square radius is, of course, closely related to that for the $E0$ transitions and is given by

$$r^2 = \langle r^2 \rangle_c + a \hat{n}_d + b \hat{N} \quad (2-33)$$

Where the first term represent the mean-square radius of the closed-shell core. a and b are constants.

2.1.3 Dynamical symmetries

As we have mentioned before, it is Hamiltonian exactly for certain sets of possible to solve the IBM parameters using group theoretical methods. In the following the relevant symmetries are discussed briefly. The $s(L=0)$ and $d(L=2)$ bosons of the IBM-1 have six components (substates) and therefore define a six-dimensional space. This leads to a description in terms of the unitary group in six dimensions, $U(6)$. The Hamiltonian (2-6) can be regarded as a general rotation in a six dimensional space. The six dimensions are formed by the s -boson and the five components of the d -boson, $d_2, d_1, d_0, d_{-1}, d_{-2}$. It is a unitary operator because the norm (i.e. the number of bosons) of the vectors is left invariant. This means that the general Hamiltonian can be discussed in terms of the group $U(6)$, of all unitary transformations in six dimensions.

As a consequence, many of the characteristic properties of the IBM can be derived by group-theoretical methods and expressed analytically. When we consider the different reductions of $U(6)$, three dynamical symmetries emerge [17,18,19] known as $U(5)$, $SU(3)$ and $O(6)$, which are related to the geometrical idea of the spherical vibrator, deformed rotor and symmetric (γ -soft) deformed, respectively [21]. According to the value of the (ϵ) and (V) in Eq.(2-5) that there are three limits in IBM-1: at the first limit $\epsilon \gg V$ this state named by vibration dynamical symmetry described by subgroup $U(5)$, at second limit when $V \gg \epsilon$ this state named by rotational dynamical symmetry described by subgroup $SU(3)$, and at third limit when $V \cong \epsilon$ then state named by γ -unstable symmetry described by subgroup $O(6)$ [17,18,19,20,21].

The number of generator in term of unitary group $U(n)$ [16] is

$$\text{Number of generator of } U(n) = n^2 \quad (2-34)$$

Thus we have 36 generators of the $U(6)$ group that can be written down explicitly [16]

$$G_{U(6)} = [s^\dagger \tilde{s}]_0^{(0)}, [d^\dagger \tilde{d}]_0^{(0)}, [d^\dagger \tilde{d}]_\mu^{(1)}, [d^\dagger \tilde{d}]_\mu^{(2)}, [d^\dagger \tilde{d}]_\mu^{(3)}, [d^\dagger \tilde{d}]_\mu^{(4)}, [d^\dagger \tilde{s}]_\mu^{(2)}, [s^\dagger \tilde{d}]_\mu^{(2)} \quad (2-35)$$

$$\begin{array}{cccccccc} \downarrow & \downarrow \\ 1 & 1 & 3 & 5 & 7 & 9 & 5 & 5 = 36 \end{array}$$

Since the generators are dependent on the angular momentum and the number of generator in term of angular momentum is $(2L+1)$. In special cases Hamiltonian can be expressed in terms of the generators of a subgroup of $U(6)$. The generators of a subgroup are a subset of these 36 $U(6)$, generators, that close under commutation. Under the restriction that each group contains the angular momentum group, $O(3)$, as a subgroup, three group chains can be assigned [16,17,18,19,20,21].

$$\begin{array}{l} \text{I. } U(6) \supset U(5) \supset O(5) \supset O(3) \\ \text{II. } U(6) \supset SU(3) \supset O(3) \\ \text{III. } U(6) \supset O(6) \supset O(5) \supset O(3) \end{array} \quad \left. \vphantom{\begin{array}{l} \text{I.} \\ \text{II.} \\ \text{III.} \end{array}} \right\} \quad (2-36)$$

These chains will be discussed more extensively in the following sections.

If the Hamiltonian can be written as the sum of the Casimir operators of one of the group chains (2-36) one says that it has a dynamical symmetry. Whenever a dynamical symmetry occurs the representations of a group are split in energy but not admixed with other representations. The eigenstates can then be classified according to the group reduction. In these cases there exists an analytic expression for the eigenvalues.

These analytic solutions arise only for certain values of the parameters in the Hamiltonian (2-6). We shall refer to them as limiting cases and label them by the first subgroup in the chain. The linear and quadratic Casimir operators of $U(6)$ and its various subgroups can be written in terms of the operators from Eq. (2.15) to(2-21) as

$$C_{1U(6)} = \hat{N} \quad (2-37)$$

$$C_{2U(6)} = \hat{N} (\hat{N} + 5) \quad (2-38)$$

$$C_{1U(5)} = \hat{n}_d \quad (2-39)$$

$$C_{2U(5)} = \hat{n}_d (\hat{n}_d + 4) \quad (2-40)$$

$$C_{2SU(3)} = \frac{4}{3} Q^2 + \frac{1}{2} \hat{L}^2 \quad (2-41)$$

$$C_{2O(6)} = 2 \hat{N} (\hat{N} + 4) - 8 P^\dagger P \quad (2-42)$$

$$C_{2O(5)} = \frac{2}{5} \hat{L}^2 + 4T_3^2 \quad (2-43)$$

$$C_{2O(3)} = 2 \hat{L}^2 \quad (2-44)$$

It should be commented that since these Casimir operators are defined by a set of vanishing commutators, any multiplicative form is also a generator. The definitions above are conventional and convenient ones. It now remains to identify the representation labels for each chain, and hence the quantum numbers of the basis states, as well as the physical structure for each limiting symmetry. In doing so, we shall from time to time make correspondences with various geometrical models.

2.1.3.1 Group chain I: U(5) symmetry

This symmetry group described the vibrational nuclei which have spherical shape, and it has 25 numbers of generator in term of unitary group with used the eq.(2-34). We can write it as [16]

$$G_{U(5)} = [d^\dagger \tilde{d}]_0^{(0)}, [d^\dagger \tilde{d}]_\mu^{(1)}, [d^\dagger \tilde{d}]_\mu^{(2)}, [d^\dagger \tilde{d}]_\mu^{(3)}, [d^\dagger \tilde{d}]_\mu^{(4)} \quad (2-45)$$

$$\begin{array}{ccccc} \downarrow & \downarrow & \downarrow & \downarrow & \downarrow \\ 1 & 3 & 5 & 7 & 9 = 25 \end{array}$$

These operators close under the algebra $U(5)$. The quantum number with which the representations of this group are labeled is n_d .

The set $G_{U(5)}$ contains a subset of 10 operators that close under commutation, the generators of the orthogonal algebra in five dimensions $O(5)$

$$\text{Number of generator } O(n) = \frac{1}{2}n(n-1) \quad (2-46)$$

and can be written as

$$G_{O(5)} = [\underset{\downarrow 3}{d^\dagger \tilde{d}}]_\mu^{(1)}, [\underset{\downarrow 7}{d^\dagger \tilde{d}}]_\mu^{(3)} = 10 \quad (2-47)$$

The representations of $O(5)$ are labeled by ν , the boson seniority, the eigenvalues of the quadratic Casimir operator of $O(5)$,

$$C_{O(5)} = \frac{1}{3} (d^\dagger \tilde{d})^{(1)} \cdot (d^\dagger \tilde{d})^{(1)} + \frac{1}{3} (d^\dagger \tilde{d})^{(3)} \cdot (d^\dagger \tilde{d})^{(3)} \quad (2-48)$$

Are given by $\frac{1}{6} \nu(\nu+3)$

The $O(5)$ group contains $O(3)$, the angular momentum, as subgroup or rotational algebra, it has three generators by using (2-46) as shown below

$$G_{O(3)} = [\underset{\downarrow 3}{d^\dagger \tilde{d}}]_\mu^{(1)} \quad (2-49)$$

The eigenvalues of the well-known Casimir operator of $O(3)$,

$$\hat{L}^2 = 10 (d^\dagger \tilde{d})^{(1)} \cdot (d^\dagger \tilde{d})^{(1)} \quad (2-50)$$

Are $L(L+1)$, where L , the angular momentum, labels the different $O(3)$ multiplets. In an $O(3)$ multiplet the levels are distinguished by M , the projection of L on the Z -axis.

Finally the single component generate of algebra $O(2)$ of rotation around z -axis its component of $O(3)$ by use eq.(2-46) is given by

$$G_{O(2)} = [d^\dagger \tilde{d}]_0^1 \quad (2-51)$$

$$\downarrow$$

$$1$$

This yields a possible chain of algebras [25,26,27,28]

$$U(6) \supset U(5) \supset O(5) \supset O(3) \supset O(2)$$

$$\downarrow \quad \downarrow \quad \downarrow \quad \downarrow \quad \downarrow$$

$$[N] \quad [n_d] \quad v, n_\Delta \quad L \quad M_L$$

This chain described by above six quantum numbers [16,17], and the eigenvectors can be labeled with the quantum numbers of the various groups, which can be written as

$$|\psi\rangle = |[N] [n_d] v, n_\Delta L M_L\rangle \quad (2-52)$$

Where [21]

$$n_d = 0, 1, \dots, N \quad (2-53)$$

N: is total number of bosons

v : is the d-boson seniority: represents the number of d-boson which are not coupled pairwise to angular momentum zero

L: angular momentum

M_L : component of angular momentum and

$$v = n_d, n_d - 2, \dots, 1 \text{ or } 0 ; n_d = \text{odd or even} \quad (2-54)$$

Another quantum number (n_β) which gives the number of d-boson pairs [17] which are coupled pairwise to angular momentum zero.

$$v = n_d - 2 n_\beta \rightarrow n_\beta = (n_d - v) / 2 \quad (2-55)$$

$$n_\beta = 0, 1, \dots, n_d/2 \text{ or } (n_d - 1) / 2 ; n_d = \text{even or odd} \quad (2-56)$$

The step from O(5) to O(3) is not fully decomposable then an extra quantum number required which is n_Δ as can be seen, an additional quantum number n_Δ has been introduced to describe the reduction from O(5) to O(3). This requirement indicates that within the basis states $|N n_d v\rangle$ which describe the representations of O(5) there can be more than one state with a particular value of L [21].

n_Δ : describes the number of d-boson triplets which are coupled to zero angular momentum.

Then (n_d) partition will be as

$$n_d = 2 n_\beta + 3 n_\Delta + \lambda \quad (2-57)$$

The value of (L) contained in each irrep n_d of U(5) are given by

$$L = \lambda, \lambda+1, \lambda+2, \dots, 2\lambda-2, 2\lambda \quad (2-58)$$

The value of M_L allowed for a given value of L is

$$-L \leq M_L \leq +L$$

We can classify scheme for the group chain I to show how it depended on the quantum numbers that are shown in table (2-1) [16].

Table (2-1) : Classification scheme for the group chain I

U(6)	U(5)	O(5)		O(3)
N	n_d	ν	n_Δ	L
0	0	0	0	0
1	0	0	0	0
	1	1	0	2
2	0	0	0	0
	1	1	0	2
	2	2	0	4,2
		0	0	0
3	0	0	0	0
	1	1	0	2
	2	2	0	4,2
		0	0	0
	3	3	0	6,4,3
			1	0
		1	0	2
4	0	0	0	0
	1	1	0	2
	2	2	0	4,2
		0	0	0
	3	3	0	6,4,3
			1	0
		1	0	2
	4	4	0	8,6,5,4
			1	2
		2	0	4,2
		0	0	0

The Hamiltonian for chain I can be written down in term of the Casimir operator as follows

$$\hat{H}_I = \alpha \hat{C}_{1U(5)} + \hat{C}_{2U(5)} + \gamma \hat{C}_{2O(5)} + \delta \hat{C}_{2O(3)} \quad (2-59)$$

Eigenvalues for this chain from the Hamiltonian in term of the Casimir operator eq.(2-59) is given by [17]

$$E = \alpha n_d + \beta n_d(n_d+4) + 2 \gamma \nu(\nu+3) + 2 \delta L(L+1) \quad (2-60)$$

Where each term in Eq. (2-60) is the eigenvalue of the corresponding Casimir operator of Eq.(2-59). While the Hamiltonian In terms of the operators of the multipole expansion, H_I reduces to [61,62,63].

$$\hat{H}_I = \varepsilon (n_d) + a_1(\hat{L} \cdot \hat{L}) + a_3(\hat{T}_3 \cdot \hat{T}_3) + a_4(\hat{T}_4 \cdot \hat{T}_4) \quad (2-61)$$

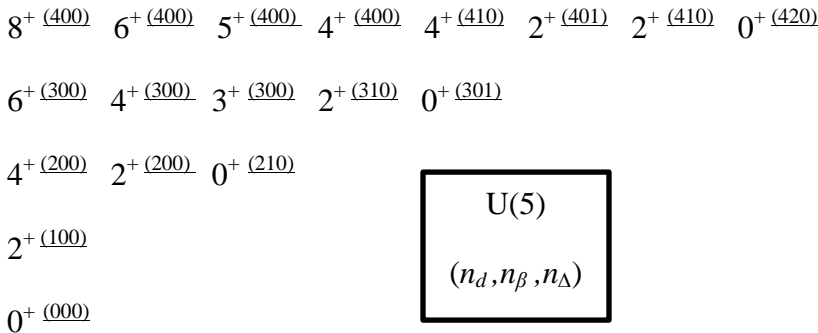


Figure (2-1): low-lying levels of the U(5) symmetry of the IBM in the harmonic limit.

The U(5) limit hasn't E0 transition since the E0 operator is proportional to \hat{n}_d

$$\langle i | TE0 | j \rangle \propto \hat{n}_{d_j} \langle i | j \rangle = 0 \quad (\text{if } i \neq j) \quad (2-62)$$

The general form for quadrupole electric transition operators for the U(5) chain T(E2) is given from equ.(2-26) has a term that changes n_d by ± 1 and a term with $\Delta n_d = 0$. Since the selection rule is

$$n_d = 0, \pm 1 \quad (2-63)$$

If the operator is chosen to be a generator of the U(5) symmetry, then only the latter term would be used. However, the predicted E2 matrix elements would then be 0 between states differing by 1 or more d bosons, while they would yield nonzero diagonal contributions (quadrupole moments). This situation is essentially the inverse of that expected and observed for vibrational nuclei, and hence it has been customary to use the first term of the EI operator in the U(5) limit, which produces results very similar to those of the geometric vibrational picture.

The general result B(E2) values [64]

$$\sum_{L'} B(E2; L_{n_d+1} \rightarrow L', n_d) = e_B^2 (n_d + 1) (N - n_d) \quad (2-64)$$

Where e_B is a boson effective charge. The sum on the left side of Eq. (2.64) accounts for the distribution of strength from a given initial state if the angular momentum selection rules allow decay to more than one level of the next lower multiplet. This sum contains more than one term only for decay of $n_d \geq 3$ states.

Equation (2.64) gives, for the transitions between the lowest levels,

$$B(E2; 2_1^+ \rightarrow 0_1^+) = e_B^2 N \quad (2-65)$$

$$B(E2; 4_1^+ \rightarrow 2_1^+) = 2 e_B^2 (N-1) \quad (2-66)$$

The ratio between these two transition probabilities:

$$R = \frac{B(E2; 4_1^+ \rightarrow 2_1^+)}{B(E2; 2_1^+ \rightarrow 0_1^+)} = 2 \frac{(N-1)}{N} < 2 \quad (2-67)$$

Since U(5) is usually relevant only near closed shells, where N is rather small, differences from the geometric model can thus be significant.

and for $N \rightarrow \infty$ then $R = 2$ [17]

The electric quadrupole moment for the ground state is given by [17]

$$Q_L = \beta_2 \sqrt{\frac{16\pi}{5}} \left(\frac{\sqrt{1}}{\sqrt{14}}\right) L \quad (2-68)$$

Where

$$\beta_2 = \frac{-0.7}{\sqrt{5}} \alpha_2, \text{ and it changes from } 0 \text{ to } \frac{-\sqrt{7}}{2} \text{ in this chain} \quad (2-69)$$

A typical spectrum obtained from this Hamiltonian is shown in figure (2-2)

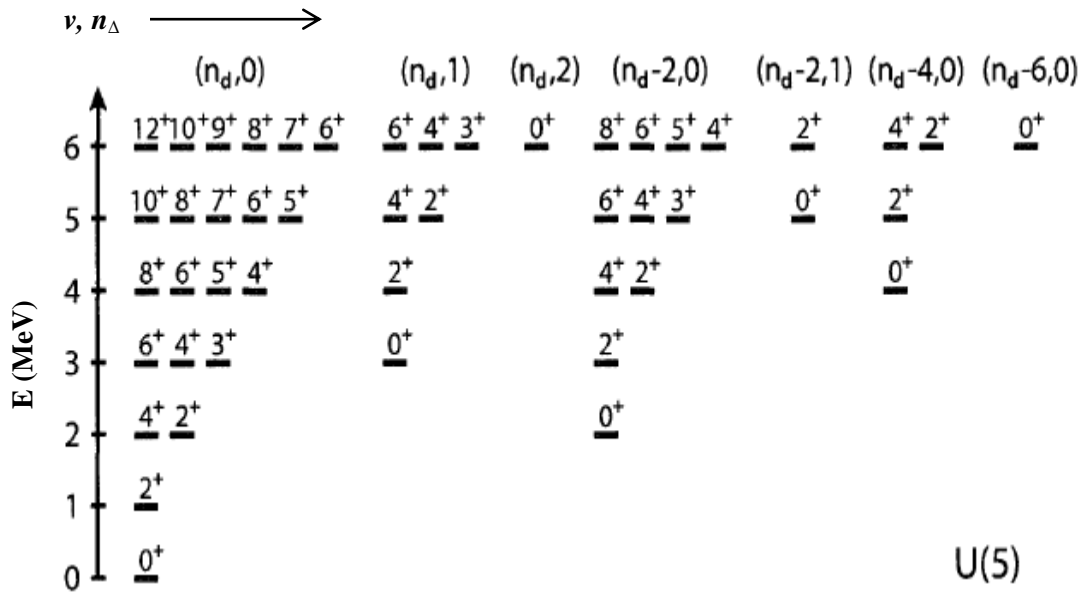


Figure (2-2): A typical spectrum with U(5) symmetry and N=6.in parentheses the quantum numbers (v) and (n_d) appear [17,18,19,20,21].

2.1.3.2 Group chain II: SU(3) symmetry

This symmetry group is used to describe the rotational spectra of nuclei, and it has 8 numbers of generator in term of special unitary group which used the following rule in the generator

$$\text{Number of generator of SU}(n) = n^2 - 1 \tag{2-70}$$

The generators are

$$G_{\text{SU}(3)} = \left[\begin{array}{c} d^\dagger \tilde{d} \Big|_{\mu}^{(1)} \\ \downarrow \\ 3 \end{array} \right], \left[\underbrace{\left[(d^\dagger \tilde{s} + s^\dagger \tilde{d}) \Big|_{\mu}^2 - \frac{1}{2} \sqrt{7} \left[d^\dagger \tilde{d} \Big|_{\mu}^{(2)} \right] \right]}_{\downarrow} \right] \tag{2-71}$$

5 = 8

These generators can be rewritten as

$$G_{\text{SU}(3)} = \{ L_m^{(1)}, Q_m^{(2)} \} \quad (2-72)$$

Where L and Q are angular momentum and quadrupole operators respectively from equ. (2-17) and equ.(2-18).

This group has again $O(3)$ as a subgroup and the generator is (2-49) with 3 number of generator and the itself component $O(2)$ from equ.(2-51) has only one number of generator. In the definition of the quadrupole operator in principle also $+\frac{1}{2}\sqrt{7}$ is allowed instead of $-\frac{1}{2}\sqrt{7}$. This sign change makes no difference in the calculation of excitation energies, it will only change the sign of the quadrupole moment

This yields a possible chain of algebras [17,18,19,20,21]

$$\begin{array}{cccc} U(6) \supset SU(3) \supset O(3) \supset O(2) \\ \downarrow \quad \downarrow \quad \downarrow \quad \downarrow \\ [N] \quad (\lambda, \mu) K \quad L \quad M_L \end{array}$$

The labels needed to classify the states in this chain are [16]. The $U(6)$ group is

$$U(6) = [N, 0, 0, 0, 0, 0] \equiv [N] \quad (2-73)$$

Because $U(6)$ known by the total number of boson (N).

In the $SU(3)$ scheme the states can be labeled as [10]

$$|\psi\rangle = |[N] (\lambda, \mu) K L M_L\rangle \quad (2-74)$$

The group of $SU(3)$ are characterized by two quantum numbers (λ, μ) the value of each (λ, μ) contained in each N are given by [16]

$$\begin{aligned}
[N] = (\lambda, \mu) = & (2N, 0) \oplus (2N-4, 2) \oplus (2N-8, 4) \oplus \dots \oplus \left\{ \begin{matrix} (0, N) \\ (2, N-1) \end{matrix} \right\} \left\{ \begin{matrix} N=even \\ N=odd \end{matrix} \right\} \\
& \oplus (2N-6, 0) \oplus (2N-10, 2) \oplus \dots \oplus \left\{ \begin{matrix} (0, N-3) \\ (2, N-4) \end{matrix} \right\} \left\{ \begin{matrix} N-3=even \\ N-3=odd \end{matrix} \right\} \\
& \oplus (2N-12, 0) \oplus (2N-16, 2) \oplus \dots \oplus \left\{ \begin{matrix} (0, N-6) \\ (2, N-7) \end{matrix} \right\} \left\{ \begin{matrix} N-6=even \\ N-6=odd \end{matrix} \right\} \\
& \oplus \dots
\end{aligned} \tag{2-75}$$

The step from SU(3) to O(3) is not fully decomposable, and then an extra quantum number is required which is denoted by (K). The corresponding number is called K. The values of L contained in each representation (λ, μ) are then given by the following algorithm [17]:

$$L = K, K+1, K+2, \dots, K + \max(\lambda, \mu) \tag{2-76}$$

Where

$$K = \text{integer} = \min(\lambda, \mu), \min(\lambda, \mu) - 2, \dots, 1 \text{ or } 0; \quad \{ \min(\lambda, \mu) = \text{odd or even} \} \tag{2-77}$$

With the expansion of $K = 0$ for which

$$L = \max(\lambda, \mu), \max(\lambda, \mu) - 2, \dots, 1 \text{ or } 0; \quad \{ \max(\lambda, \mu) = \text{odd or even} \} \tag{2-78}$$

and O(3), O(2) they are described by quantum number L and M_L respectively.

We can classify scheme for the group chain II to show how it depended on the quantum numbers shown in the table (2-2) [16].

Table (2-2): Classification scheme for the group chain II

U(6)	SU(3)		O(3)
N	(λ, μ)	$\tilde{\chi}$	L
0	(0,0)	0	0
1	(2,0)	0	2,0
2	(4,0)	0	4,2,0
	(0,2)	0	2,0
3	(6,0)	0	6,4,2,0
	(2,2)	0	4,2,0
		2	3,2
	(0,0)	0	0
4	(8,0)	0	8,6,4,2,0
	(4,2)	0	6,4,2,0
		2	5,4,3,2
	(0,4)	0	4,2,0
	(2,0)	0	2,0

The Hamiltonian is just a linear combination of the Casimir operators of SU(3) and O(3) and can be written [16,17,18,19,20,21,22]

$$\hat{H}_{II} = a_1 \hat{L}^2 + a_2 \hat{Q}^2 \tag{2-79}$$

Comparison with Eq. (2.42) and Eq.(2-45) shows that this form is equivalent to

$$\hat{H}_{II} = \frac{3}{4} a_2 C_{2SU(3)} + \left[\frac{1}{2} a_1 - \frac{3}{16} a_2 \right] C_{2O(3)} \tag{2-80}$$

The eigenvalue of the SU(3) Casimir operator as denned in Eq. (2.42) and Eq.(2-45) is given by

$$E_{C_{2su(3)}} = \frac{2}{3} (\lambda^2 + \mu^2 + \lambda\mu + 3\lambda + 3\mu) \tag{2-81}$$

And thus the resulting eigenvalue expression is [16]

$$E = \frac{a_2}{2} (\lambda^2 + \mu^2 + \lambda\mu + 3\lambda + 3\mu) + \left(a_1 - \frac{3a_2}{8} \right) L(L+1) \tag{2-82}$$

a_1 and a_2 can be calculated by [17]

$$a_1 = \frac{E_2^{\dagger}}{6} + \frac{3}{8} a_2 \tag{2-83}$$

$$a_2 = - \frac{[E_2^{\dagger} - E_2^{\ddagger}]}{3(2N-1)} \tag{2-84}$$

If the specific form of the quadrupole operator [16,17,18]

$$\hat{Q} = [d^\dagger \tilde{s} + s^\dagger \tilde{d}] - \frac{\sqrt{7}}{2} [d^\dagger \tilde{d}]^2$$

Then

$$T(E2) = \alpha_2 \hat{Q} \quad (2-85)$$

Where α_2 is the effective charge of E2 or before denoted by e_2 , $\beta = -\frac{\sqrt{7}}{2} \alpha_2$, and selection rules

for this symmetry are[16,17]

$$\left. \begin{array}{l} \Delta\lambda=0 \\ \Delta\mu=0 \end{array} \right\} \quad (2-86)$$

Since the operator (2-85) is a generator of the SU(3) group all quadrupole transitions between different multiplets are forbidden.

B(E2) is given by [69,70]

$$B(E2; (2N,0):L+2 \rightarrow L) = e_B^2 \frac{3}{4} \left[\frac{(L+2)(L+1)}{(2L+3)(2L+5)} \right] (2N-L)(2N+L+3) \quad (2-87)$$

Here the factor $(2N-L)(2N+L+3)$, which is not present in the equivalent expression for the rigid rotor, has its origin in the fact that the number of bosons (N) is conserved. This factor gives rise to the phenomenon that beyond a critical spin value the g.s. band B(E2) values actually decrease with increasing spin.

For L=0

$$B(E2; 2_1^+ \rightarrow 0_1^+) = \frac{e_B^2}{5} N(2N+3) \quad (2-88)$$

and for L=2

$$B(E2; 4_1^+ \rightarrow 2_1^+) = e_B^2 \frac{2}{7} (N-1)(2N+5) \quad (2-89)$$

The ratio between eq. (2-59) and (2-60) can be written as [62,63,64,65]

$$R = B(E2; 4_1^+ \rightarrow 2_1^+) / B(E2; 2_1^+ \rightarrow 0_1^+) = \frac{10}{7} \left[\frac{(N-1)(2N+5)}{N(2N+3)} \right] \quad (2-90)$$

If $N \rightarrow \infty$

$$R = \frac{10}{7} \tag{2-91}$$

The electric quadrupole moment for states is given by [61,62,63]

$$Q_L = -e_2 \sqrt{\frac{16\pi}{40}} \frac{L}{(2L+3)} (4N+3) \tag{2-92}$$

A typical spectrum obtained from this Hamiltonian is shown in figure (2-3)

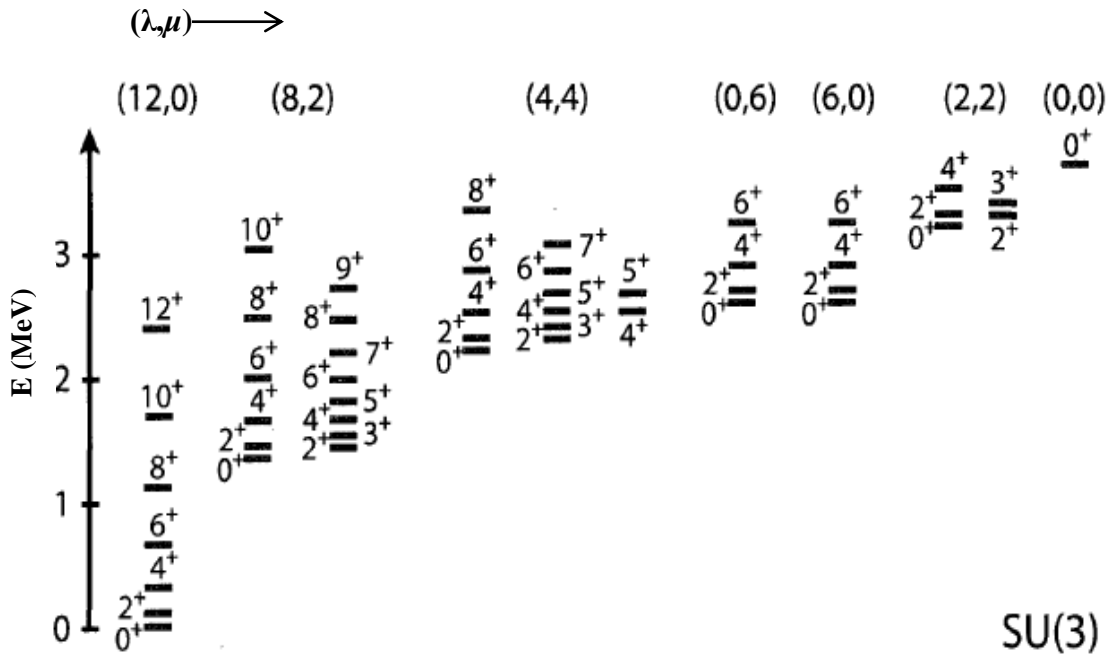


Figure (2-3): A typical spectrum with SU(3) symmetry and N=6. In parentheses the quantum numbers (λ) and (μ) appear [21].

2.1.3.3 Group Chain III: O(6) symmetry

The third symmetry in this model is known as (γ - unstable) symmetry, and it has 15 numbers of generator in term of orthogonal group which used this following rule

$$\text{Number of generator of } O(n) = \frac{1}{2}n(n-1) \tag{2-93}$$

The generators are

$$G_{O(6)} = [d^\dagger \tilde{d}]_\mu^{(1)}, [d^\dagger \tilde{d}]_\mu^{(3)}, [(d^\dagger \tilde{s} + s^\dagger \tilde{d})]_\mu^{(2)} \quad (2-94)$$

$$\begin{array}{ccc} \downarrow & \downarrow & \downarrow \\ 3 & 7 & 5 \end{array} = 15$$

We see immediately that also the generators of O(5), eq. (2.47) and those of O(3), eq. (2.49) are contained in this set, and its component O(2) from eq.(2-51) has only one number of generator.

This yields a possible chain of algebras [66,67,68,69,70,71,72,73,74,75]

$$U(6) \supset O(6) \supset O(5) \supset O(3) \supset O(2)$$

$$\begin{array}{ccccc} \downarrow & \downarrow & \downarrow & \downarrow & \downarrow \\ [N] & \sigma & (\tau, \nu_\Delta) & L & M_L \end{array}$$

Following the group reduction O(6) the states are labeled as [20]

$$|\psi\rangle = |[N] \sigma (\tau, \nu_\Delta) L M_L\rangle \quad (2-95)$$

O(6) in this chain described by σ which is a number of bosons which are not coupled to zero angular momentum, and take [16,17,18,19,20]

$$\sigma = N, N-2, \dots, 0 \text{ or } 1; \text{ for } N=\text{even or odd} \quad (2-96)$$

The selection rule for seniority is

$$0 \leq \nu \leq \sigma \quad (2-97)$$

Also O(5) defined by quantum number (τ)

$$\tau = \sigma, \sigma-1, \dots, 1, 0 \quad (2-98)$$

The step from O(5) to O(3) is not fully decomposable then a new quantum number found (ν_Δ), which described the number of triplet bosons which are coupled to zero angular momentum.

The partition of τ is

$$\tau = 3 \nu_{\Delta} + \lambda \quad (2-99)$$

Where

$$\nu_{\Delta} = 0, 1, 2, \dots \quad (2-100)$$

Then L takes

$$L = 2\lambda, 2\lambda-2, \dots, \lambda+1, \lambda, \dots \quad (2-101)$$

Or we can say

$$2\lambda \geq L \geq \lambda \quad (2-102)$$

We can classify scheme for the group chain III to show how it depended on the quantum numbers shown in the table (2-3) [16].

Table (2-3): Classification scheme for the group chain III

U(6)	O(6)	O(5)		O(3)
N	σ	τ	ν_{Δ}	L
0	0	0	0	0
1	1	1	0	2
		0	0	0
2	2	2	0	4,2
		1	0	2
		0	0	0
		0	0	0
3	3	3	0	6,4,3
			1	0
		2	0	4,2
		1	0	2
		0	0	0
		1	0	2
4	4	4	0	8,6,5,4
			1	2
		3	0	6,4,3
			1	0
		2	0	4,2
		1	0	2
		0	0	0
		2	0	4,2
		1	0	2
		0	0	0
	0	0	0	

The Hamiltonian in terms of the Casimir operator is given by [16,17,18,19,20,21]

$$\hat{H}_{III} = \beta \hat{C}_{O(5)} + \gamma \hat{C}_{2O(3)} + \xi \hat{C}_{2O(6)} \quad (2-103)$$

Where [21]

$$\hat{C}_{2O(6)} = 2N(N+4) - 2[(d^\dagger \cdot d^\dagger) - (s^\dagger \cdot s^\dagger)][(\tilde{d} \cdot \tilde{d}) - (\tilde{s} \cdot \tilde{s})] = 2N(N+4) - 8(\hat{P}^+ \cdot \hat{P}^-) \quad (2-104)$$

The eigenvalues are

$$E = 2 \xi \sigma (\sigma+4) + 2 \beta \tau (\tau+3) + 2 \gamma L (L+1) \quad (2-105)$$

Again, the various terms in the Casimir operators can be combined to write H_{III} in the convenient format of the multipole expansion [69,70,71]

$$\hat{H}_{III} = a_0 (P^+ P) + a_1 (\hat{L} \cdot \hat{L}) + a_3 (\hat{T}_3 \cdot \hat{T}_3) \quad (2-106)$$

Here the $P^+ P$ term stems from the C_{2O6} Casimir, that is, from the presence of the subgroup $O(6)$.

Due to the common use of the multipole Hamiltonian, the form of the (equivalent) eigenvalue expression that has most frequently appeared in the literature is [69,70,71,72,73,74,75]

$$E = \frac{a_0}{4} (N-\sigma)(N+\sigma+4) + \frac{a_3}{2} \tau(\tau+3) + (a_1 - \frac{a_3}{10}) L(L+1) \quad (2-107)$$

We can see that how change levels of energies with depended on their quantum number

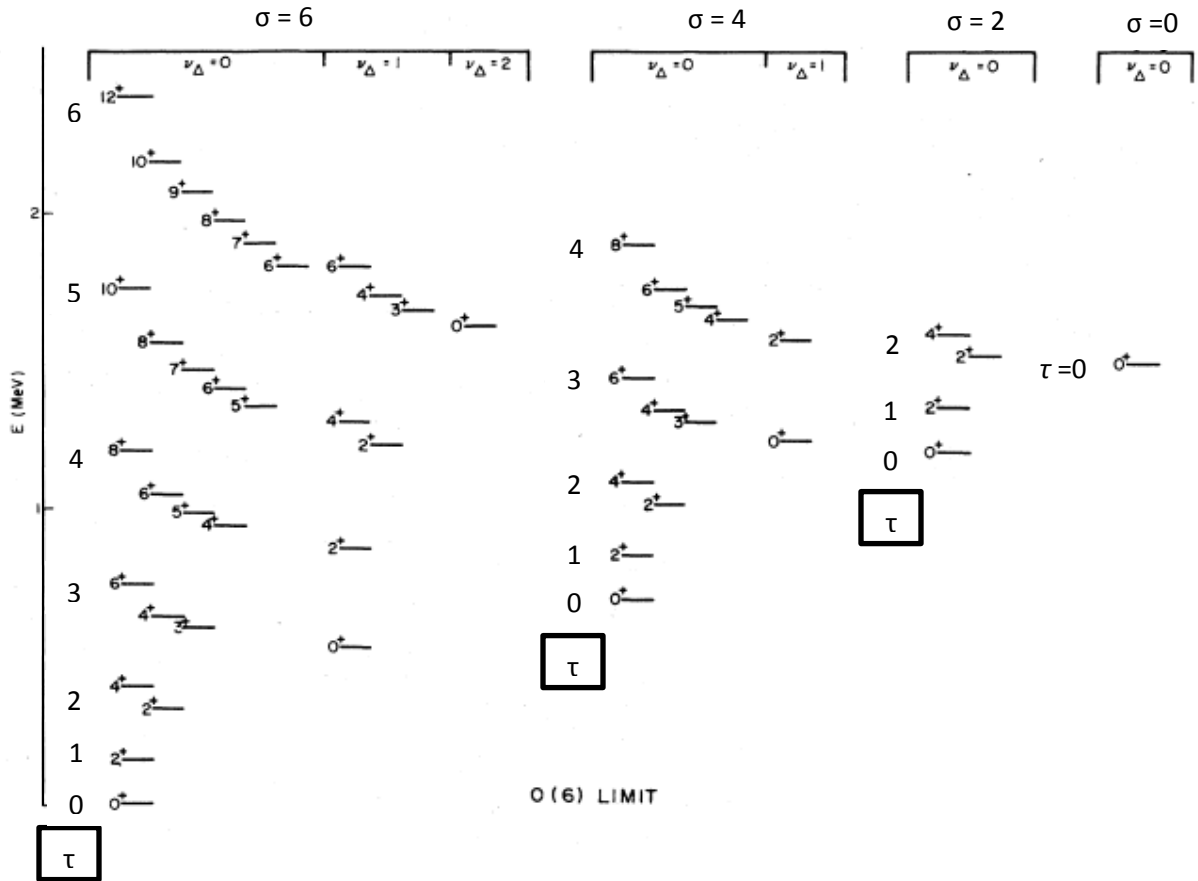


Figure (2-4): Low-lying levels of the O(6) limit, for N = 6 [16,17].

Since $T(E0)$ is diagonal in the U(5) basis states, it must require $\Delta\tau = 0$. Using Eq. (2-25), it is trivial to see that, in addition, $\Delta\sigma = \pm 2$ is necessary to avoid a cancellation in the contributing components. Thus the only predicted $E0$ strength to the ground state is from the $\sigma = N - 2, \tau = 0$ state, where the matrix elements take the form

$$\langle \sigma = N, \tau = 0, L = 0 | T(E0) | \sigma = N - 2, \tau = 0, L = 0 \rangle = e_0 \left[\frac{(N-1)(N+3)(2N+4)}{8(N+1)^2} \right]^{1/2} \quad (2-108)$$

Again electric quadrupole transition is given in Eq.(2-26) [17]

The B(E2) value for this symmetry connecting $\sigma = \sigma_{\max}$ and $L = 2 \tau$ is [16,17]

$$B(E2; \tau+1 \rightarrow \tau) = e_B^2 \frac{(\tau+1)}{2\tau+5} (N-\tau)(N+\tau+4) \quad (2-109)$$

For L=0 lower state Eq.(2-109) become

$$B(E2; 2_1^+ \rightarrow 0_1^+) = \frac{e_B^2}{5} N(N+4) \tag{2-110}$$

For L=2

$$B(E2; 4_1^+ \rightarrow 2_1^+) = e_B^2 \frac{2}{7} (N-1)(N+5) \tag{2-111}$$

The ratio between eq. (2-110) and (2-111) can be written as [16,17]

$$R = B(E2; 4_1^+ \rightarrow 2_1^+) / B(E2; 2_1^+ \rightarrow 0_1^+) = \frac{10}{7} \left[\frac{(N-1)(N+5)}{N(N+4)} \right] \tag{2-112}$$

If $N \rightarrow \infty$

$$R = \frac{10}{7} \tag{2-113}$$

Also from the second selection rule and from T^{E2} operator in the O(6), the electric quadrupole moment will be

$$Q_L = 0 \tag{2-114}$$

A typical spectrum generated by the Hamiltonian is shown in the figure (2-5)

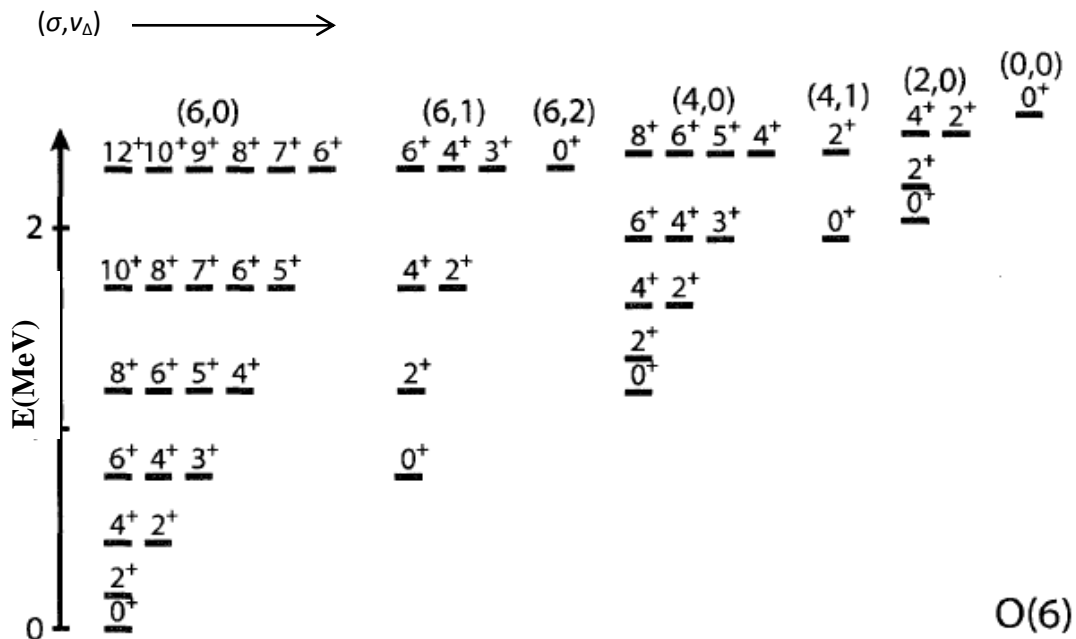


Figure (2-5): A typical spectrum with O(6) symmetry and N=6. In parentheses the quantum numbers (σ) and (ν_Δ) appear [17,18,19,20,21].

Since the SU(3) wave functions are complicated linear combinations of U(5) basis states with many n_d values, it is not surprising, first, that $\langle n_d \rangle_{g.s.}$ is larger than in either U(5) or O(6), or second that it changes little from state to state. Figure (2-6) illustrates this by showing the values of $\langle n_d \rangle$ for the yrast band calculated for all three limits by diagonalizing the appropriate Hamiltonian. In U(5), changes in the (single) n_d value characterizing each state are reflected directly in the state-dependent behavior of various observables. In contrast, in SU(3), the value of any matrix element normally results from subtle coherent effects, as befits a collective deformed intrinsic state.

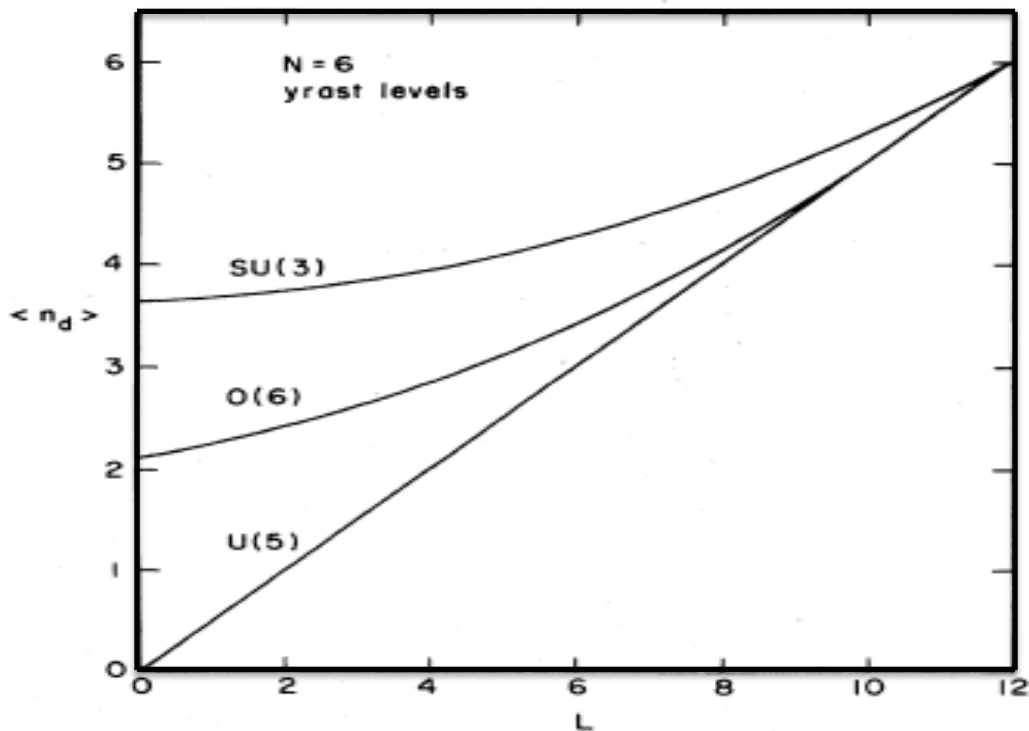


Figure (2-6): Expectation values of \hat{n}_d in the yrast states for the three symmetries of the IBA $N = 6$ [17].

Finally we can know Dynamical symmetry plays a major role in nuclear structure, they are best understood in terms of the interacting boson model. The IBM model predicts the existence of the dynamical symmetries which coincide with the geometrical shapes associated with the rotation of deformed, prolate nucleus, a spherical harmonic oscillator and an oblate deformed

rotor. Examples of all these cases have been found in nature. And each group described by self-quantum number and the ratio between energy levels in any nucleus in each group depended on that quantum number since like before discussion the ratio between energy levels are

$$E_2:E_4:E_6:E_8 = \begin{cases} E_{n_d=1}: E_{n_d=2}: E_{n_d=3}: E_{n_d=4} = 1:2:3:4 & \text{U(5)} \\ E_{\tau=1}: E_{\tau=2}: E_{\tau=3}: E_{\tau=4} = 1:2.5:4.5:7 & \text{O(6)} \\ E_{L=2}: E_{L=4}: E_{L=6}: E_{L=8} = 1:3.33:7:12 & \text{SU(3)} \end{cases} \quad (2-115)$$

The distinctive structures of the three dynamical symmetries in the IBA provide three clear-cut limits of the general Hamiltonian. Although evidence exists which suggests that some of the features of the pure symmetries are observed empirically in selected nuclei, in general, a realistic calculation will require a departure from the strict limits or indeed a transition between them. In this context the analytic limits emerging from the group theoretical treatment of the Hamiltonian can be viewed as "benchmarks" in constructing a more accurate description of the low-lying collective structure of a particular nucleus, or series of nuclei. This approach can be illustrated diagrammatically in the form of the symmetry triangle in the figure (2-7) [17].

The three apexes represent the limits of one of the exact symmetries, while the space enclosed by the three sides denotes the range of more general solutions that can be obtained numerically by diagonalizing the IBA-1 Hamiltonian of Eq. (2-14). A transition between two specific symmetries, without invoking any of the characteristics of the third, would correspond to a path along one of the three sides, but a more complex path between two limiting cases is clearly also possible [80,81]. For a transition along the sides, the structure at any point will be determined by the ratio of the two parameters [see Eq. (2-14)] that characterize the symmetries in question, and these are also indicated in the figure.

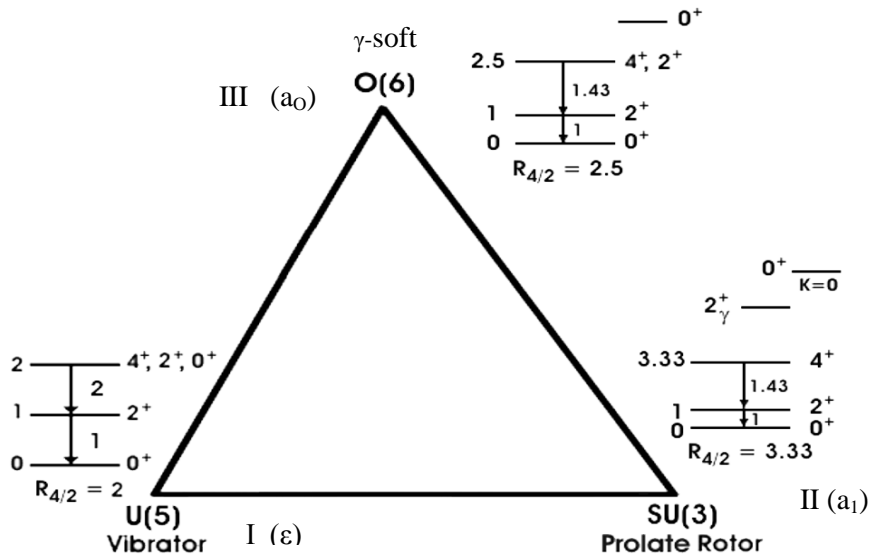


Figure (2-7): Casten triangle which shows the transitional regions between the three dynamical symmetries [17]

Three transitional regions can occur in the space of the IBM, as a result of perturbation of the two limits [70,71,72,73,74,75], can describe in the following table

Table (2-4): classification of the transitional region in the space of IBM

U(5)-SU(3)	SU(5) – O(6)	SU(3) – O(6)
It contains U(5) and SU(3) limits	its region contains both SU(5) and O(6) limits	this region contains both SU(3) and O(6) limits
$\hat{H}^{I+II} = \epsilon (n_d) + a_1(\hat{L} \cdot \hat{L}) + a_2(\hat{Q} \cdot \hat{Q})$ [2,3,65]	$\hat{H}^{I+III} = \epsilon (n_d) + a_o (\hat{P} \cdot \hat{P}) + a_1(\hat{L} \cdot \hat{L}) + a_3(\hat{T}_3 \cdot \hat{T}_3)$ [2,3,8]	$\hat{H}^{II+III} = a_o (\hat{P} \cdot \hat{P}) + a_1(\hat{L} \cdot \hat{L}) + a_2(\hat{Q} \cdot \hat{Q})$ [3]
The solution of Hamiltonian depended on the ratio (ϵ/a_2) , for large (ϵ/a_2) the spherical solution dominates or U(5). While for $(\epsilon/a_2) \rightarrow 0$ (small), the SU(3) will be dominates.	The nuclear structure depended on the ratio (ϵ/a_o) , for the large (ϵ/a_o) the U(5) will be dominates but for the small (ϵ/a_o) the O(6) will be dominates.	The solution of Hamiltonian depended on the ratio of (a_o/a_2) , for large (a_o/a_2) the O(6) limits dominates, while for $(a_o/a_2) \rightarrow 0$ (small) the SU(3) dominates.

2.2 Interacting Boson Model-2

Further developments were made to extend the space of IBM, in IBM-2 version, where distinction between neutron bosons and proton bosons was made. This assumption allows IBM to describe states interpreted as neutron-proton interaction. The microscopic picture of the IBM is very complicated. A commonly used microscopic picture is given in terms of collective pairs of nucleons. The s and d pairs of valence nucleons have angular momenta $J = 0$ and $J = 2$, respectively. These pairs correspond intuitively to the s and d bosons, respectively. The building blocks of the IBM-2 are the proton bosons s_π , d_π and the neutron bosons s_ν , d_ν . In the IBM-2 we tried to keep to a minimum number of free parameters in the Hamiltonian and we thus considered equal values for the neutron and proton d -boson excitation energy, in addition to the standard quadrupole interaction and Majorana term. We only considered the dipole neutron-proton boson interaction whose strength is characterized by a single parameter $M_{\pi\nu}$ [61,62,63,64,65,66]. One should expect, however, to obtain a more realistic description of nuclei by treating protons and neutrons as different particles, as they are. One introduces proton bosons s_p and d_p as well as neutron bosons s_n and d_n [16,17,18,19,20,21]. The total number of proton bosons introduced equals the number of valence proton pairs (particles or holes, whichever is minimum) in the nucleus under study. Similarly, the number of neutron bosons introduced equals the number of valence neutron pairs (particles or holes). Since in medium and heavy nuclei the valence protons and the valence neutrons occupy different major shells, no proton-neutron pairs can be treated as a mean field interaction between the proton bosons and the neutron bosons. The IBM-2 can be used to the description of the low-lying energy levels and the other spectroscopic properties of heavy nuclei such as quadrupole moment and M1 transition on proton-neutron degree of freedom and on the other hand can predict the mixed symmetry for the nuclei [69].

2.2.1 IBM-2 Hamiltonian

The IBM-2 has special practical significance because its parameters depend on a smoothed curve on π - and ν -boson numbers and it makes possible to calculate unknown nuclear spectra. The interest in the algebraic structure of the IBM-2 has even grown since states with special magnetic dipole properties are known which can be explained with group theoretical methods. The numbers of π -bosons N_π and ν -bosons N_ν are fixed equally. There is no boson composed of a proton and a neutron. There exist 12 creation operators for bosons

$$b_{\pi,jm}^\dagger = s_\pi^\dagger, d_{\pi,m}^\dagger \quad (m = -2, -1, \dots, 2) \quad (2-116)$$

, and

$$b_{\nu,jm}^\dagger = s_\nu^\dagger, d_{\nu,m}^\dagger \quad (m = -2, -1, \dots, 2) \quad (2-117)$$

And we have the same number of tensor operator for boson annihilation like this

$$\tilde{b}_{\pi,jm} = s_\pi, \tilde{d}_{\pi,m} \quad (m = -2, -1, \dots, 2) \quad (2-118)$$

, and

$$\tilde{b}_{\nu,jm} = s_\nu, \tilde{d}_{\nu,m} \quad (m = -2, -1, \dots, 2) \quad (2-119)$$

In analogy with commutation relation every d- or s-operator for protons commutes with every d- or s-operator for neutrons. We demand that both N_π and N_ν are good quantum numbers i.e. the Hamilton operator must meet the condition

$$[H, N_\pi] = [H, N_\nu] = 0 \quad (2-120)$$

The total number of the bosons (N), is equal to the total number of proton bosons (N_π) and neutron bosons (N_ν) [61] i.e.

$$N = N_\pi + N_\nu \quad (2-121)$$

With the operators

$$N_\pi = \sqrt{5} [d_\pi^\dagger \times \tilde{d}_\pi]^0 + s_\pi^\dagger s_\pi = \hat{n}_{s\pi} + \hat{n}_{d\pi} \quad (2-122)$$

The corresponding

$$N_v = \sqrt{5} [d_v^\dagger \times \tilde{d}_v]^0 + s_v^\dagger s_v = \hat{n}_{sv} + \hat{n}_{dv} \quad (2-123)$$

The IBM-2 Hamiltonian is modified with respect to the original IBM-1, therefore the vector space of the IBM-2 is then just product of all possible states $(s, d)^{N_v}$ with those of $(s, d)^{N_\pi}$, and where in each factor the set of states is the same as in IBM-1. [76,77,78,79]

$$\hat{H} = \hat{H}_\pi + \hat{H}_v + V_{\pi v} \quad (2-124)$$

Both \hat{H}_π and \hat{H}_v have the form of the IBM-1 Hamiltonian are for proton and neutron bosons respectively, but there is nothing than π - operator in \hat{H}_π and v -operator in \hat{H}_v , and the third part describes the interaction between them and can be written for proton and neutron both together as

$$\hat{V}_{\rho\rho} = \sum_{L=0,2,4} \frac{1}{2} \sqrt{2L+1} C_L^\rho \times [(d_\rho^\dagger \times d_\rho^\dagger)^L (\tilde{d} \times \tilde{d})^L]^{(0)} \quad (2-125)$$

Where

$$\rho = \pi \text{ or } v \quad (2-126)$$

The IBM-2 Hamiltonian which usually used in numerical calculation has form [76,77]

$$\hat{H} = \varepsilon_{d\pi} \hat{n}_{d\pi} + \varepsilon_{dv} \hat{n}_{dv} + \kappa \hat{Q}_\pi \cdot \hat{Q}_v + \omega_\pi \hat{L}_\pi \cdot \hat{L}_\pi + \omega_v \hat{L}_v \cdot \hat{L}_v + \hat{M}_{\pi v} \quad (2-127)$$

Where $\hat{n}_{d\pi}$ and \hat{n}_{dv} refer to the number of proton and neutron bosons and can take as

$$n_{d\rho} = (d_\rho^\dagger \otimes \tilde{d}_\rho) \quad (2-128)$$

Q and L in the equation(2-127) are quadrupole interactions and angular momentum respectively can be written as

$$\hat{Q}_\rho^x = [d_\rho^\dagger \times \tilde{s} + s_\rho^\dagger \times \tilde{d}_\rho]^2 + \chi_\rho [d_\rho^\dagger \otimes \tilde{d}_\rho]^2 \quad (2-129)$$

$$\hat{L}_\rho = \sqrt{10} [d_\rho^\dagger \otimes \tilde{d}_\rho]^{(1)} \quad (2-130)$$

the quadrupole operator in quadrupole-quadrupole interaction between proton and neutron, $\chi_\pi(\chi_\nu)$ represents the proton (neutron) quadrupole deformation parameter [77,78,79]. ω_ρ is the strength of the dipole among like nucleon interaction. And $\widehat{M}_{\pi\nu}$ is the Majorana interaction acts on the states, which are not fully symmetric under the interchange of the proton and neutron degrees of freedom. The (ξ_2) and (ξ_K) are the parameters of the strength of this interaction.

$$\widehat{M}_{\pi\nu} = \xi_2 [s_\nu^+ \times d_\pi^+ - s_\pi^+ \times d_\nu^+]^2 \cdot [\tilde{s}_\nu \times \tilde{d}_\pi - \tilde{s}_\pi \times \tilde{d}_\nu]^2 - 2 \sum_{K=1,3} \xi_K [d_\nu^+ \times d_\pi^+]^{(K)} \cdot [\tilde{d}_\nu \times \tilde{d}_\pi]^{(K)} \quad (2-131)$$

κ is the quadrupole-quadrupole interaction strength.

2.2.2 Electromagnetic transition operator

The IBM-2 can interest to calculate some other important observable quantities such as transition operator. For transition operators, it is convenient to introduce parameters with a direct physical meaning. These are called effective boson charges and moments, and in general the transition operator can be written as [61]

$$T^{(l)} = T_\pi^{(l)} + T_\nu^{(l)} \quad (2-132)$$

Where $T_\pi^{(l)}$ and $T_\nu^{(l)}$ are the already known IBM-1 operators with the proton or neutron label attached to them. Have the same as (2-24 to 2-31). They are defined in the following way. For E0 transitions we can written as [16]

$$T^{(E0)} = f_\pi n_{d_\pi} + f_\nu n_{d_\nu} \quad (2-133)$$

The most commonly used transition operator is quadrupole one (i.e. the E2 transition) which can be put in the form

$$T^{(E2)} = e_\pi \cdot \widehat{Q}_\pi + e_\nu \cdot \widehat{Q}_\nu \quad (2-134)$$

E4 transition is

$$T^{(E4)} = t_{\pi} \hat{V}_{\pi} + t_{\nu} \hat{V}_{\nu} \quad (2-135)$$

Where f_{ρ} (f_{π} , f_{ν}), e_{ρ} (e_{π} , e_{ν}) and t_{ρ} (t_{π} , t_{ν}) are the protons (neutrons) effective charges of the E0, E2 and E4 respectively. The protons (neutrons) boson effective charges are assumed to depend only on the number of protons (neutrons). In calculations they are usually kept constant. And can be calculated microscopically, and Q_{ρ} has in the Eq.(2-129) but \hat{V}_{ρ} can be written as

$$\hat{V}_{\rho} = [d_{\rho}^{\dagger} \otimes \tilde{d}_{\rho}]^{(4)} \quad (2-136)$$

For the magnetic transitions, one introduces boson effective g –factors. For M1 transitions (Magnetic dipole transitions) are also especially interesting, the relevant transition operator is

$$T^{(M1)} = \sqrt{\frac{3}{4\pi}} (g_{\nu} \hat{L}_{\nu} + g_{\pi} \hat{L}_{\pi}) \quad (2-137)$$

While for M3 transitions they are defined by

$$T^{(M3)} = \sqrt{\frac{7}{4\pi}} (m_{\nu} \hat{U}_{\nu} + m_{\pi} \hat{U}_{\pi}) \quad (2-138)$$

Where g_{ρ} (g_{π} , g_{ν}) and m_{ρ} (m_{π} , m_{ν}) are protons (neutrons) factors to the moments M1 and M3 respectively, and can be calculated microscopically. The g -factors are assumed to depend only on the number of protons (neutrons) boson number. Notice that while in IBM-1 all M1 transitions were forbidden if only lowest order terms were included in the transition operator, here this is no longer the case if $g_{\pi} \neq g_{\nu}$. Thus the need to include higher order terms in the M1 transition operator in IBM-1 in order to allow for M1 transitions to occur can be seen as a way to simulate the proton-neutron degree of freedom in the IBM-1 framework, and \hat{L}_{ρ} has in Eq.(2-130) but \hat{U}_{ν} can be written as

$$\hat{U}_{\nu} = [d_{\rho}^{\dagger} \otimes \tilde{d}_{\rho}]^{(3)} \quad (2-139)$$

We turn now to nuclear radii. Nuclear radii can be calculated in the interacting Boson model-2 from the expression [21]

$$\langle r_\pi^2 \rangle = \langle r_\pi^2 \rangle^{(c)} + A_\pi N_\pi + A_\nu N_\nu + \alpha_\pi \langle n_{d_\pi} \rangle \quad (2-140)$$

Here $\langle r_\pi^2 \rangle^{(c)}$ is the r.m.s. radius of the closed shell and $\langle n_{d_\pi} \rangle$ expectation value in the ground state of the nucleus with $N_\pi(N_\nu)$ is the proton (neutron) bosons and proton d-boson number operator n_{d_π} is $\hat{d}_\pi^\dagger \cdot \tilde{d}_\pi$. The two terms $A_\rho N_\rho$ ($\rho = \pi, \nu$) describe the overall increase in radius due to the increase in the number of particles, while the last term $\alpha_\pi \langle n_{d_\pi} \rangle$ describes the contribution to the radii due to the proton deformation. Nuclear radii are usually measured relative to the closed shell nuclei.

2.2.3 Dynamical symmetry

The algebraic structure of the interacting boson model-2 is at first sight a trivial extension of that of the interacting boson model-1. However, it turns out that if one wants to exploit the concept of dynamic symmetries introduced in IBM-1 dynamical symmetries, a much larger and richer variety occurs here. The proton bosons introduced span the dynamical group $U_\pi(6)$, while the neutron bosons span the dynamical group $U_\nu(6)$. Addition of the proton degrees of freedom to the neutron degree of freedom is achieved by taking the direct product of the two groups [69],

$$G_{[U_\rho(6)]} = U_\pi(6) \otimes U_\nu(6) \quad (2-141)$$

By using Eq.(2-34) the number of generator, this group has 72 generator, i.e. the 36 generators of $U_\pi(6)$ and the 36 generators of $U_\nu(6)$. Thus, We have 72 generators of the $U(6)$ group can be written down explicitly

$$G_{U_\rho(6)} = [s^\dagger \tilde{s}]_{0,\rho}^{(0)}, [d^\dagger \tilde{d}]_{0,\rho}^{(0)}, [d^\dagger \tilde{d}]_{\mu,\rho}^{(1)}, [d^\dagger \tilde{d}]_{\mu,\rho}^{(2)}, [d^\dagger \tilde{d}]_{\mu,\rho}^{(3)}, [d^\dagger \tilde{d}]_{\mu,\rho}^{(4)}, [d^\dagger \tilde{s}]_{\mu,\rho}^{(2)}, [s^\dagger \tilde{d}]_{\mu,\rho}^{(2)} \quad (2-142)$$

	↓	↓	↓	↓	↓	↓	↓	↓	
$\pi \rightarrow$	1	1	3	5	7	9	5	5	= 36
$\nu \rightarrow$	1	1	3	5	7	9	5	5	= 36

The main question then is how to reduce the algebra G to the rotation algebra [16], $O(3)$, which we want always as a subalgebra, since nuclear states are characterized by a good value of

the angular momentum. Since protons and neutrons are rotated simultaneously [69], the generators of O(3) are obtained by summing those of the two rotation algebras, $O_\pi(3)$ and $O_\nu(3)$

$$G_{O_\rho(3)} = [d^\dagger \tilde{d}]_{\pi,\mu}^{(1)} + [d^\dagger \tilde{d}]_{\nu,\mu}^{(1)} \quad (2-143)$$

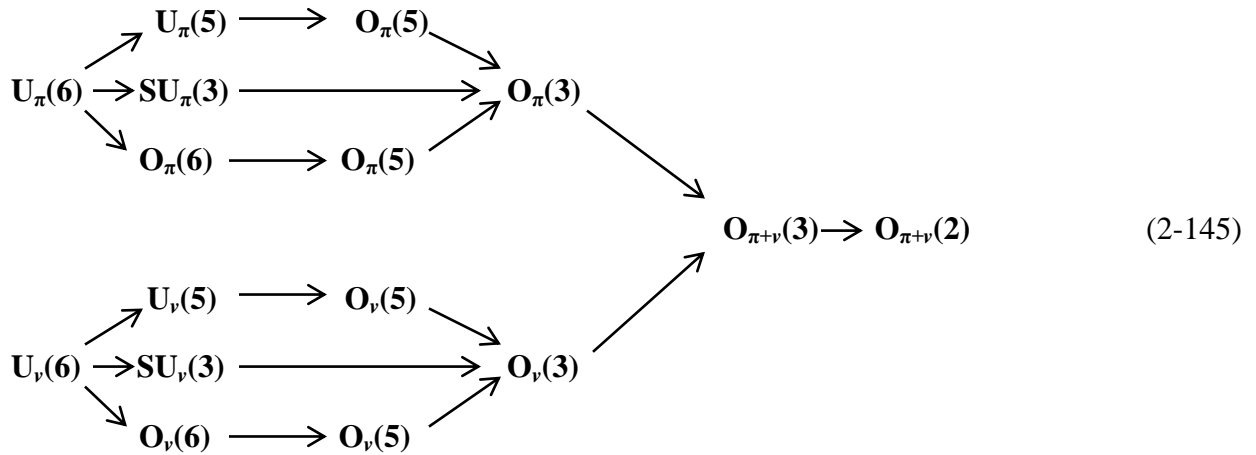
\downarrow
3

\downarrow
3

This corresponds to the familiar addition of angular momenta for protons and neutrons,

$$\hat{L} = \hat{L}_\pi + \hat{L}_\nu \quad (2-144)$$

Since each of the U(6) algebras has a rich subalgebra structure, there are a variety of ways in which the algebra $G_{[U_\rho(6)]} = U_\pi(6) \otimes U_\nu(6)$ can be reduced to O(3). These are called lattices of algebras and we shall discuss here some in detail. We begin by considering the trivial case in which the only common algebra is that of O(3). This can be schematically written as [15]



Where we have added a subscript $\pi + \nu$ to O(3) in order to indicate that it is obtained by summing the generators of $O_\pi(3)$ and $O_\nu(3)$. From the practical point of view, this case is not particularly interesting since it does not produce anything new, although in here yield the possible chains in the IBM-2 begging with $U_{\pi+\nu}(6)$ [15,16]

$$U_\pi(6) \otimes U_\nu(6) \supset U_{\pi+\nu}(6) \supset U_{\pi+\nu}(5) \supset O_{\pi+\nu}(5) \supset O_{\pi+\nu}(3) \supset O_{\pi+\nu}(2) \quad (H^I) \quad (2-146)$$

$$U_\pi(6) \otimes U_\nu(6) \supset U_{\pi+\nu}(6) \supset SU_{\pi+\nu}(3) \supset O_{\pi+\nu}(3) \supset O_{\pi+\nu}(2) \quad (H^{II}) \quad (2-147)$$

$$U_\pi(6) \otimes U_\nu(6) \supset U_{\pi+\nu}(6) \supset O_{\pi+\nu}(6) \supset O_{\pi+\nu}(5) \supset O_{\pi+\nu}(3) \supset O_{\pi+\nu}(2) \quad (H^{III}) \quad (2-148)$$

One thus recovers the symmetries contained in IBM-1. Clearly, these chains remain unchanged if the proton and neutron labels are interchanged. The states of the IBM-2 are characterized by two – row irreps $\{ N-f, f \}$ of $U_{\pi+\nu}(6)$ where N is the total number of bosons and

$$f = 0, 1 \dots \text{Min}(N_{\pi}, N_{\nu}) \quad (2-149)$$

2.2.3.1 Vibrational limit ($U_{\pi+\nu}(5)$) : (H^1) chain

In order to provide a complete classification scheme we now need to reduce representations of $U_{\pi+\nu}(6)$ to those of its subgroups. For totally-symmetric representations, which were the only ones occurring in the interacting boson model-1, the reduction was given in Sect. (2.2.3) here, however, we need the reduction also for mixed-symmetry states. The rules to obtain this reduction are much more complex. In general this chain describes the vibrational nucleus, it has 25 numbers of generator for proton bosons and 25 number of generator for neutron bosons in term of unitary group with used the eq.(2-34). We can write it [16]

$$G_{U_{\pi+\nu}(5)} = [d^+\tilde{d}]_{0,\rho}^{(0)}, [d^+\tilde{d}]_{\mu,\rho}^{(1)}, [d^+\tilde{d}]_{\mu,\rho}^{(2)}, [d^+\tilde{d}]_{\mu,\rho}^{(3)}, [d^+\tilde{d}]_{\mu,\rho}^{(4)} \quad (2-150)$$

	↓	↓	↓	↓	↓	
$\pi \longrightarrow$	1	3	5	7	9 = 25	
$\nu \longrightarrow$	1	3	5	7	9 = 25	

like IBM-1 in here $U(5)$ has subgroups $O(5)$ with contain $O(3)$ and component $O(2)$, but in here generated to protons and neutrons such as discusses in Eqs.(2-47 ,2-49 and 2-51) but in here separately for proton and neutron number [69]. Some quantum number is a good quantum number to characterized this chain, hence the quantum numbers needed to classify the states in this chain are [15, 16]

$$\begin{array}{ccccccc}
U_{\pi}(6) \otimes U_{\nu}(6) & \supset & U_{\pi+\nu}(6) & \supset & U_{\pi+\nu}(5) & \supset & O_{\pi+\nu}(5) \supset O_{\pi+\nu}(3) \supset O_{\pi+\nu}(2) \\
\downarrow & & \downarrow \\
[\widehat{N}_{\pi}][\widehat{N}_{\nu}] & & (N-f, f) & & (n_{d\pi}, n_{d\nu}) & & (v_{\pi}, v_{\nu})\alpha & & L & & M
\end{array}$$

The quantum number α is $[\tilde{n}_{\pi\Delta}, \tilde{n}_{\nu\Delta}]$ a quantum number required to completely specify the reduction $O(5) \supset O(3)$, that is $[\tilde{n}_{\pi\Delta}, \tilde{n}_{\nu\Delta}]$ represents missing labels. Because of the complex structure of the chain, we digress briefly here to discuss the question of how many labels are, in general, needed to classify uniquely basis states of a group generator.

For some special cases, the number of missing labels is reduced. For example, if the $O(5)$ representations are totally symmetric [16], the selection rule for seniority begin

$$v_{\pi} = \nu, v_{\nu} = 0 \quad (2-151-a)$$

As it is the case in the interacting boson model-1, only one missing label is needed,

$$\tilde{n}_{\pi\Delta} = \tilde{n}_{\Delta}, \tilde{n}_{\nu\Delta} = 0 \quad (2-151-b)$$

we note that the representations of $U_{\pi+\nu}(6)$, $U_{\pi+\nu}(5)$ and $O_{\pi+\nu}(5)$ are all two-rowed, i.e.

$$\left. \begin{array}{l}
[\widehat{N}_{\pi}, \widehat{N}_{\nu}] \equiv [\widehat{N}_{\pi}, \widehat{N}_{\nu}, 0, 0, 0, 0] \\
(n_{d\pi}, n_{d\nu}) \equiv (n_{d\pi}, n_{d\nu}, 0, 0, 0) \\
(v_{\pi}, v_{\nu}) \equiv (v_{\pi}, v_{\nu})
\end{array} \right\} \quad (2-152)$$

The values of $(n_{d\pi}, n_{d\nu})$ contained in the representation $[N, 0]$ of $U_{\pi+\nu}(6)$ are given by Eq.(2-53). For the representation $[N-1, 1]$ they are

$$\begin{aligned}
(n_{d\pi}, n_{d\nu}) &= (N-1, 0), (N-2, 0), \dots, (1, 0); \\
&(N-1, 1), (N-2, 1), \dots, (1, 1).
\end{aligned} \quad (2-153)$$

Similarly, the values of (v_{π}, v_{ν}) contained in the representation $(n, 0)$ of $U_{\pi+\nu}(6)$ are given by Eq. (2-54). For the representation $(n-1, 1)$ they are

$$\begin{aligned}
(v_{\pi}, v_{\nu}) &= (n-2, 0), (n-4, 0), \dots (2, 0) \text{ or } (1, 0); \quad (n = \text{odd or even}) \\
&(n-1, 1), (n-3, 1), \dots (2, 1) \text{ or } (1, 1); \quad (n = \text{odd or even}).
\end{aligned} \quad (2-154)$$

Finally, the values of L contained in a representation $(\nu, 0)$ are given by (2.58). Those contained in $(\nu - 1, 1)$ are

$$\begin{aligned}
 L = & 2\nu - 1, 2\nu - 2, \dots, 3; \\
 & \nu - 1, \nu - 2, \dots, 1, \quad (\nu \geq 2) \\
 & \nu + 1, \nu, \dots, 5, \quad (\nu \geq 4) \\
 & \nu + 2, \nu + 1, \dots, 7, \quad (\nu \geq 5) \\
 & \dots \dots \dots
 \end{aligned}
 \tag{2-155}$$

These rules give the results shown in Table (2-5)

Table (2-5): Partial classification scheme for chain I

$U_{\pi+\nu}(6)$	$U_{\pi+\nu}(5)$	$O_{\pi+\nu}(5)$	$O_{\pi+\nu}(3)$
$[N_\pi, N_\nu]$	$(n_{d\pi}, n_{d\nu})$	(ν_π, ν_ν)	L
[1,1]	(1,0)	(1,0)	2
	(1,1)	(1,1)	3,1
[2,1]	(2,0)	(2,0)	4,2
		(0,0)	0
	(1,0)	(1,0)	2
	(2,1)	(1,0)	2
		(2,1)	5,4,3,2,1
	(1,1)	(1,1)	3,1
[3,1]	(3,0)	(3,0)	6,4,3,0
		(1,0)	2
	(2,0)	(2,0)	4,2
		(0,0)	0
	(1,0)	(1,0)	2
	(3,1)	(2,0)	4,2
		(3,1)	7,6,5 ² ,4,3 ² ,2,1
		(1,1)	3,1
	(2,1)	(1,0)	2
		(2,1)	5,4,3,2,1
	(1,1)	(1,1)	3,1

The wave function which describes this chain is given as:[15,16,69]

$$|\psi\rangle = [[\widehat{N}_\pi][\widehat{N}_\nu] (N - f, f) (n_{d\pi}, n_{d\nu}) (\nu_\pi, \nu_\nu) \alpha. L M]
 \tag{2-156}$$

The Hamiltonian is given by

$$\widehat{H}^I = A_1 C_1 U_{\pi+\nu(5)} + A_2 C_2 U_{\pi+\nu(5)} + B C_2 O_{\pi+\nu(5)} + C (C_2 O_{\pi+\nu(3)}) + a M
 \tag{2-157}$$

The eigenvalue for this chain is given

$$\langle \hat{H}^I \rangle = A_1 (n_{d\pi} + C) + A_2 (n_{d\pi}(n_{d\pi} + 4) + n_{d\pi}(n_{d\pi} + 2)) + B (v_\pi (v_\pi + 3) + v_\nu (v_\nu + 1)) + CL(L+1) + a \left(\frac{N}{2} - F \right) \left(\frac{N}{2} + F + 1 \right) \quad (2-158)$$

$U_{\pi+\nu}(5)$ dynamical symmetry (vibrational nucleus) arises when $\chi_\rho = 0$ ($\rho = \pi, \nu$). The spectrum of states corresponding to energy level is shown in Fig. (2-8).

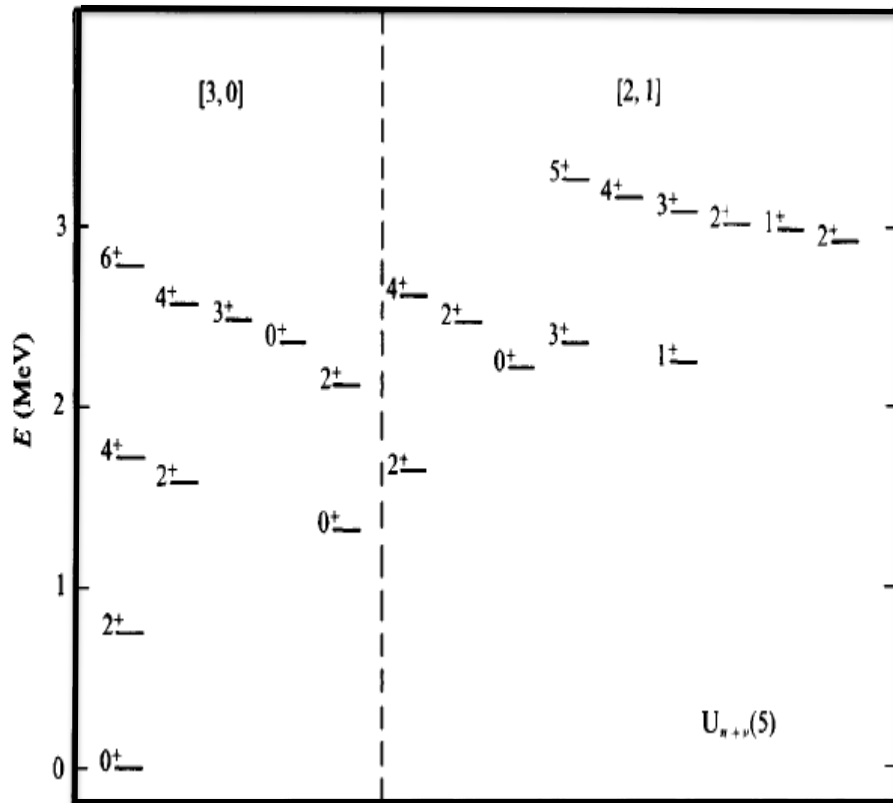


Fig. (2-8): A typical spectrum only the lowest states of the irrep $[N]$ and $[N-1]$ with $U_{\pi+\nu}(6) \supset U_{\pi+\nu}(5)$ symmetry in IBM-2, and $N_\pi = 2, N_\nu = 1$. [16].

2.2.3.2 Rotational limit ($SU_{\pi+\nu}(3)$) : (H^{II}) chain

In general this chain describes the rotational nucleus. It has 8 numbers of generator for proton bosons and 8 number of generator for neutron bosons in term of special unitary group with used the eq.(2-70). We can written as

$$G_{\text{SU}(3)_\rho} = [d^\dagger \tilde{d}]_{\mu,\rho}^{(1)}, [(d^\dagger \tilde{s} + s^\dagger \tilde{d})]_{\mu,\rho}^2 - \frac{1}{2}\sqrt{7} [d^\dagger \tilde{d}]_{\mu,\rho}^{(2)} \quad (2-159)$$

$$\begin{array}{ccc} \downarrow & \downarrow & \\ \pi \longrightarrow 3 & 5 & = 8 \\ \nu \longrightarrow 3 & 5 & = 8 \end{array}$$

These generators can be rewriting as

$$G_{\text{SU}(3)_\rho} = \{ L_{m,\rho}^{(1)}, Q_{m,\rho}^{(2)} \} \quad (2-160)$$

Where Q and L are angular momentum and quadrupole operators respectively from equ. (2-129) and equ.(2-130). This group has again $O(3)$ as a subgroup with 3 number of generator and its component $O(2)$ has only one number of generator but in here generated to protons and neutrons such as discusses in Eqs.(2-49 and 2-51) but in here done separately for proton and neutron number. In the definition of the quadrupole operator in principle also $+\frac{1}{2}\sqrt{7}$ is allowed instead of $-\frac{1}{2}\sqrt{7}$. This sign change makes no difference in the calculation of excitation energies, it will only change the sign of the quadrupole moment hence in the $\text{SU}_{\pi+\nu}(3)$ limit(rotational nucleus) arises when $\chi_\rho = \pm \frac{\sqrt{7}}{2} (\rho=\pi, \nu)$. Again some quantum number is a good quantum number to characterized this chain, hence the quantum numbers needed to classify the states in this chain are given by [15,16,69]

$$\begin{array}{cccccc} U_\pi(6) \otimes U_\nu(6) \supset U_{\pi+\nu}(6) \supset \text{SU}_{\pi+\nu}(3) \supset O_{\pi+\nu}(3) \supset O_{\pi+\nu}(2) \\ \downarrow \qquad \qquad \downarrow \qquad \qquad \downarrow \qquad \qquad \downarrow \qquad \qquad \downarrow \\ [\widehat{N}_\pi][\widehat{N}_\nu] \quad (N-f, f) \quad (\lambda, \mu) K \quad L \quad M \end{array}$$

In addition, a quantum number K is needed to fully specify the reduction from $\text{SU}(3)$ to $O(3)$. That K is missing labels. The representations (λ, μ) contained in a representation $[N,0]$ of $U(6)$ are given by (2.75). Those contained in a representation $[N-1,1]$ are

$$\begin{aligned}
 (\lambda, \mu) = & (\Gamma, 1), (\Gamma - 2, 2), (\Gamma - 3, 1), (\Gamma - 4, 3), (\Gamma - 4, 0), (\Gamma - 5, 2), \\
 & \Gamma \geq 1, \quad \Gamma \geq 4, \quad \Gamma \geq 5, \\
 & \dots \dots
 \end{aligned}
 \tag{2-161}$$

With Γ other quantum number is

$$\Gamma = 2N - 2, 2N - 8, 2N - 14, \dots \dots
 \tag{2-162}$$

Other selection rule and the reduction from SU(3) to O(3) is the same as in Eq.(2-76,2-77 and 2-78) are given in IBM-1 calculation. These rules give the results shown in table (2-6)

Table (2-6): Partial classification scheme for chain II

$U_{\pi+\nu}(6)$	$SU_{\pi+\nu}(3)$	$O_{\pi+\nu}(3)$
$[\widehat{N}_\pi, \widehat{N}_\nu]$	(λ, μ)	L
[1,1]	(2,1)	3,2, 1
[2,1]	(4,1)	5,4,3,2, 1
	(2,2)	4, 3,2 ² ,0
	(1,1)	2, 1
[3,1]	(6,1)	7,6, 5,4, 3,2, 1
	(4,2)	6, 5, 4 ² , 3, 2 ² , 0
	(3,1)	4,3,2, 1
	(2,3)	5, 4, 3 ² , 2, 1
	(2,0)	2,0
	(1,2)	3,2, 1

The wave function which describes the states of this chain are specified as

$$|\Psi\rangle = |[\widehat{N}_\pi][\widehat{N}_\nu] (N - f, f) (\lambda, \mu) K L M\rangle
 \tag{2-163}$$

Then the Hamiltonian in this chain is given by [15,16,21,69,75,76,77,78,79]

$$H^II = \alpha C_{2O(3)} + \beta C_{2SU(3)} + \gamma M
 \tag{2-164}$$

The eigenvalue is

$$\langle H^II \rangle = \alpha L(L+1) + \beta (\lambda^2 + \mu^2 + \lambda\mu + 3(\lambda + \mu)) + \gamma \left(\frac{N}{2} - F\right) \left(\frac{N}{2} + F + 1\right)
 \tag{2-165}$$

The Majorana term was written in terms of boson operator in Equ. (2-131) for $\xi_1 = \xi_2 = \xi_3$, the Majorana to the quadratic Casimir operator of $U_{\pi+\nu}(6)$ as

$$M = \frac{1}{2} [N(N+5) - C_{2U_{\pi+\nu}(6)}] \tag{2-166}$$

The spectrum of states corresponding to energy level is shown in Fig. (2-9).

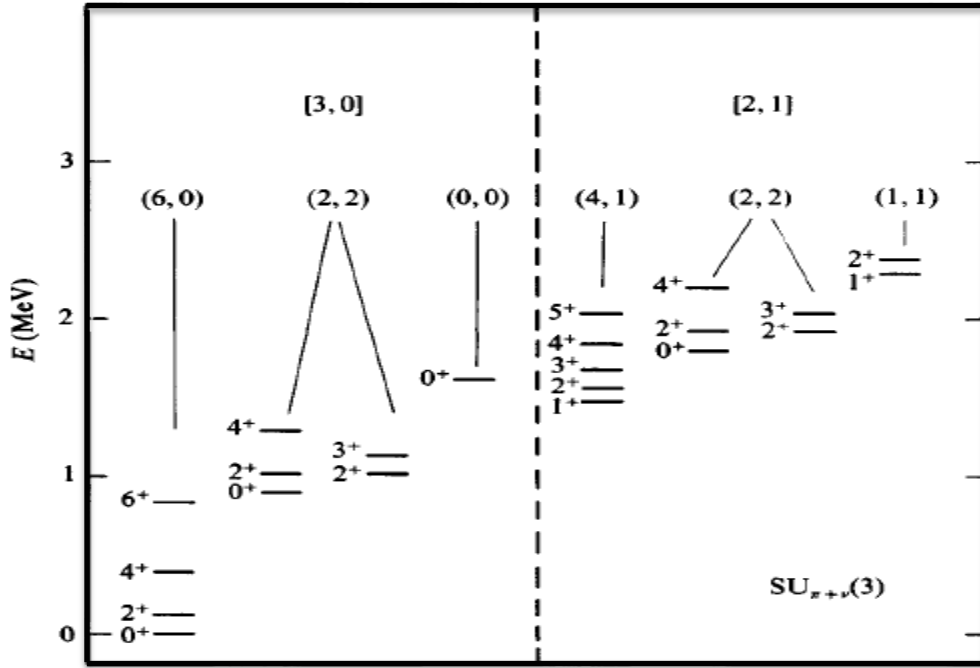


Fig. (2-9): A typical spectrum only the lowest states of the irrep [N] and [N-1] with $U_{\pi+\nu}(6) \supset SU_{\pi+\nu}(3)$ symmetry in IBM-2, and $N_{\pi} = 2, N_{\nu} = 1$. [16].

2.2.3.3 (γ - unstable) limit ($O_{\pi+\nu}(6)$) : (H^{III}) chain

In general this chain describes the (γ -unstable) nucleus, it has 15 numbers of generator for proton bosons and 15 number of generator for neutron bosons in term of orthogonal group with used the eq.(2-93). It can be written as [16]

$$G_{O(6)\rho} = [d^{\dagger} \tilde{d}]_{\mu,\rho}^{(1)}, [d^{\dagger} \tilde{d}]_{\mu,\rho}^{(3)}, [(d^{\dagger} \tilde{s} + s^{\dagger} \tilde{d})]_{\mu,\rho}^{(2)} \tag{2-167}$$

	↓	↓	↓	
π	3	7	5	= 15
ν	3	7	5	= 15

like IBM-1 in here $O(6)$ has subgroups $O(5)$ with contain $O(3)$ and component $O(2)$, but in here generated to protons and neutrons such as discussed in Eqs.(2-47 ,2-49 and 2-51) but in here

separately for proton and neutron number. And in the $O_{\pi+\nu}(6)$ dynamical (γ - unstable nucleus), the (χ_π) and (χ_ν) have opposite sign ($-\frac{\sqrt{7}}{2} < \chi_\pi < 0$ and $0 < \chi_\nu < +\frac{\sqrt{7}}{2}$). Again some quantum number is a good quantum number to characterize this chain, hence the quantum numbers needed to classify the states in this chain are [69]

$$\begin{array}{cccccc}
 U_\pi(6) \otimes U_\nu(6) \supset U_{\pi+\nu}(6) \supset O_{\pi+\nu}(6) \supset O_{\pi+\nu}(5) \supset O_{\pi+\nu}(3) \supset O_{\pi+\nu}(2) \\
 \downarrow \quad \quad \downarrow \\
 [\widehat{N}_\pi][\widehat{N}_\nu] \quad (N-f, f) \quad \langle \sigma_\pi, \sigma_\nu \rangle \quad (\tau_\pi, \tau_\nu) \gamma \quad L \quad M
 \end{array}$$

Where γ is $(\nu_{\pi\Delta}, \nu_{\nu\Delta})$ representing missing labels, it is necessary to completely specify the $O(5) \supset O(3)$ reduction. The representations of $O_{\pi+\nu}(6)$ and $O_{\pi+\nu}(5)$ are two-rowed

$$\begin{aligned}
 (\sigma_\pi, \sigma_\nu) &\equiv (\sigma_\pi, \sigma_\nu, 0) \\
 (\tau_\pi, \tau_\nu) &\equiv (\tau_\pi, \tau_\nu)
 \end{aligned} \tag{2-168}$$

The representations (σ_π, σ_ν) contained in a representation $[N, 0]$ of $U_{\pi+\nu}(6)$ are given in (2.96).

The representations (σ_π, σ_ν) contained in $[N-1, 1]$ are given by

$$\begin{aligned}
 (\sigma_\pi, \sigma_\nu) = &(N-2, 0), (N-4, 0) \dots, (2, 0) \text{ or } (1, 0) \quad (N = \text{even or odd}); \\
 &(N-1, 1), (N-3, 1), \dots, (2, 1) \text{ or } (1, 1); \quad (N = \text{odd or even})
 \end{aligned} \tag{2-169}$$

The representations (τ_π, τ_ν) contained in a representation of $(\sigma, 0)$ of $O_{\pi+\nu}(6)$ are given by

(2.98). Those contained in $(\sigma-1, 1)$ are given by [16]

$$\begin{aligned}
 (\tau_\pi, \tau_\nu) = &(\sigma-1, 0), (\sigma-2, 0), \dots, (1, 0); \\
 &(\sigma-1, 1), (\sigma-2, 1), \dots, (1, 1)
 \end{aligned} \tag{2-170}$$

The reduction from $O_{\pi+\nu}(5)$ to $O_{\pi+\nu}(3)$ is the same as in (2-158). These rules give the results shown in Table (2-7)

Table (2-7): Partial classification scheme for chain III

$U_{\pi+\nu}(6)$	$O_{\pi+\nu}(6)$	$O_{\pi+\nu}(5)$	$O_{\pi+\nu}(3)$
$[\widehat{N}_\pi, \widehat{N}_\nu]$	(σ_π, σ_ν)	(τ_π, τ_ν)	L
[1,1]	(1,1)	(1,0)	2
		(1,1)	3, 1
[2,1]	(1,0)	(1,0)	2
		(0,0)	0
	(2,1)	(2,0)	4,2
		(1,0)	2
		(2,1)	5,4,3,2,1
		(1,1)	3, 1
[3,1]	(2,0)	(2,0)	4,2
		(1,0)	2
		(0,0)	0
	(3,1)	(3,0)	6,4,3,0
		(2,0)	4,2
		(1,0)	2
		(3,1)	7,6,5 ² ,4,3 ² ,2,1
		(2,1)	5,4,3,2,1
		(1,1)	3, 1
	(1,1)	(1,0)	2
		(1,1)	3, 1

The wave function for the states are fully characterized as [69]

$$|\Psi\rangle = [[\widehat{N}_\pi][\widehat{N}_\nu] (N - f, f) \langle \sigma_\pi, \sigma_\nu \rangle (\tau_\pi, \tau_\nu) \gamma . L M \rangle \tag{2-171}$$

And the Hamiltonian will be as [67,69]

$$H^{III} = AC_{20\pi+\nu(6)} + BC_{20\pi+\nu(5)} + CC_{20\pi+\nu(3)} + aM \tag{2-172}$$

The eigenvalue is [75,76,77,78,79]

$$\begin{aligned} \langle H^{III} \rangle = & \mathbf{A} (\sigma_\pi(\sigma_\pi+4) + \sigma_\nu(\sigma_\nu+2)) + \mathbf{B} (\tau_\pi(\tau_\pi+3) + \tau_\nu(\tau_\nu+1)) \\ & + CL(L+1) + a \left(\frac{N}{2} - F \right) \left(\frac{N}{2} + F + 1 \right) \end{aligned} \tag{2-173}$$

The spectrum of states corresponding to energy level is shown in Fig. (2-10)

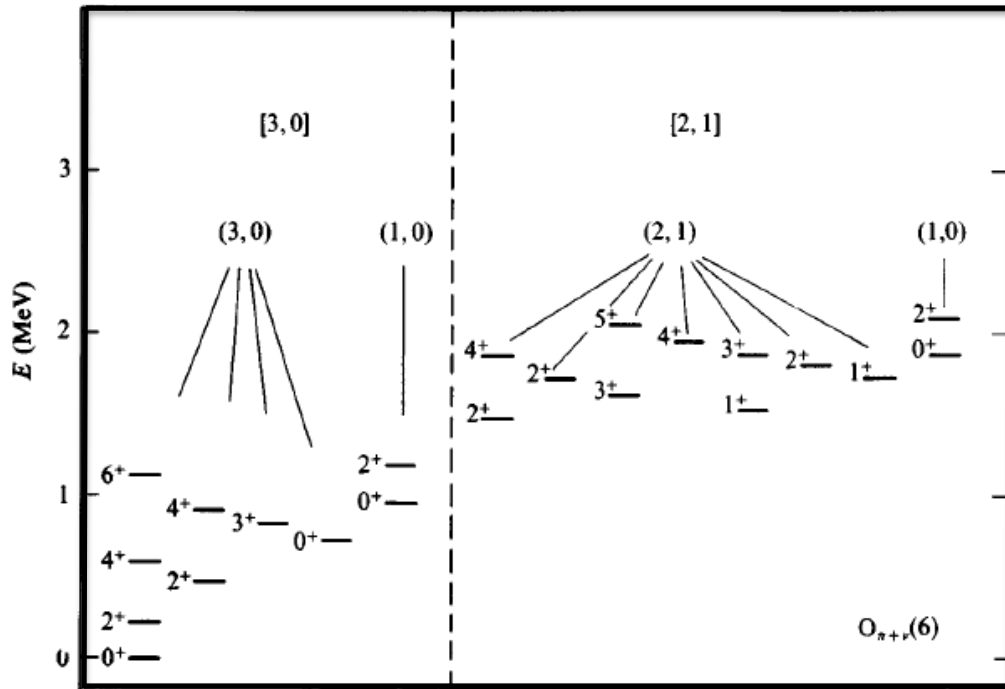


Fig. (2-10): A typical spectrum only the lowest states of the irrep $[N]$ and $[N-1]$ with $U_{\pi+\nu}(6) \supset O_{\pi+\nu}(6)$ symmetry in IBM-2, and $N_{\pi} = 2, N_{\nu} = 1$. [3].

2.2.4 Mixed-symmetry

When the proton-neutron degree of freedom is included in the interacting boson model, additional classes of states called mixed-symmetry states are allowed. When compared to their symmetric counterparts, these states have a negative phase factor between the proton and neutron boson components of the wave function. The experimental signatures for these mixed-symmetry states are strong M1 transitions to symmetric states. In the IBM-2, proton and neutron bosons are treated independently, and this results in an additional degree of freedom, which essentially can be thought of as a phase factor between proton and neutron components of the wave function. When all of the proton and neutron bosons in the system are in phase, the state is considered to be a symmetric state. These tend to appear at lower energies in the system and are

analogous to the states that are found in the sd-IBM-1. When some of the proton and neutron bosons in the system are out of phase, an additional class of states appears that are called mixed-symmetry states [15]. These states can be illustrated geometrically with some of the proton and neutron bosons oscillating or rotating out of phase, and an example of this can be seen in Fig.(2-11)

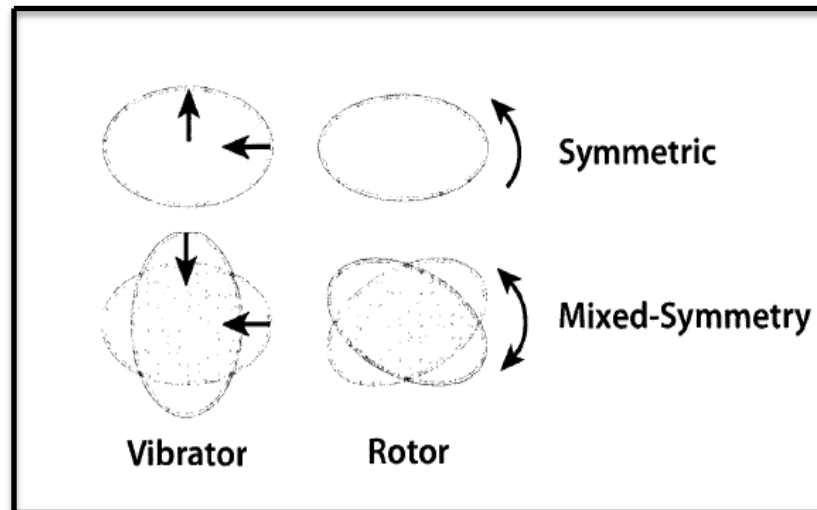


Fig.(2-11): Geometric illustration of collective motion in symmetry and mixed-symmetry states in IBM-2 [15].

As we have seen, the major difference between IBM-1 and IBM-2 is that the latter contains a whole class of states, the mixed symmetry states (MISS), which are completely missing from IBM-1. In the early days of the model the existence of MISS was a puzzle, since they were predicted to occur at rather low energies but no such state had been seen experimentally. It was then argued that “obviously” these states were lying very high in energy, and the coefficient of Majorana term in the Hamiltonian was made “big”, in order to push the MISS far up in the spectrum. Actually, this was the reason the Majorana term was introduced at all. In the IBM-2, matrix elements of the \hat{F}^2 operator can be directly calculated in order to evaluate the proton-neutron boson symmetry of each state. Experimentally, such matrix elements are not observable, so other signatures for mixed-symmetry states are important to identify. In the IBM-1, off-

diagonal MI transition matrix elements vanished, due to the L operator referring to total angular momentum, which is a good quantum number for each state. This means that \hat{L} only effects diagonal terms in the Hamiltonian [69]. The MI operator in the IBM-2 is constructed from a sum of \hat{L}_π and \hat{L}_ν , which can be seen in Eq. (2.137) To help illustrate how the MI operator behaves in the IBM-2, it can be rewritten in the following way:

$$\hat{T}(M1) = \sqrt{\frac{3}{16\pi}} ((g_\pi + g_\nu)(L_\pi + L_\nu) + (g_\pi - g_\nu)(L_\pi - L_\nu)) \quad (2-174)$$

The term with $(L_\pi + L_\nu)$ refers to the total angular momentum, which is a good quantum number for each state, and it therefore only affects diagonal terms of the Hamiltonian. That leaves the term with $(L_\pi - L_\nu)$ as the only part that contributes to MI transition matrix elements between states. The operators L_π and L_ν conserve the underlying U(5) quantum numbers, so the $(L_\pi - L_\nu)$ term effectively creates a phase difference between proton and neutron bosons, and can change the F-spin of a state [15]. The matrix elements of the MI transition operator can be large between states of different F-spin, and an example using the $U_{\pi+\nu}(5)$ Hamiltonian from Fig.(2-12) will help illustrate this.

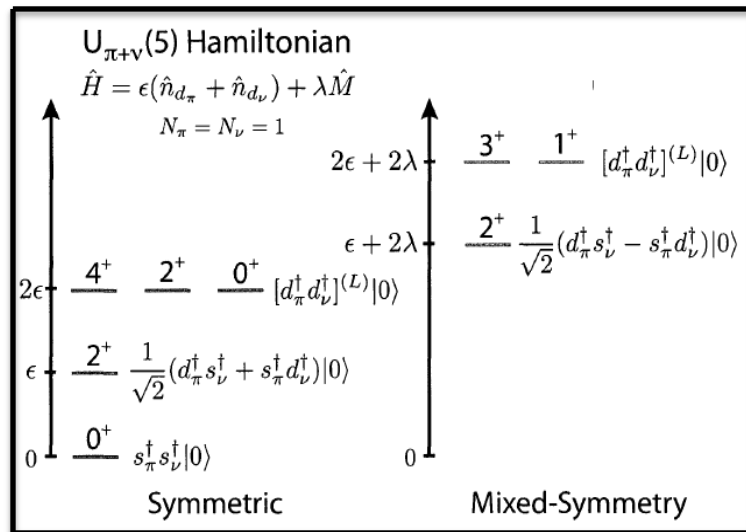


Figure (2-12): Illustration of states in a two boson $U_{\pi+\nu}(5)$ Hamiltonian using the IBM-2. F-spin is a good quantum number for this Hamiltonian, and the Majorana operator simply shifts the mixed-symmetry states up or down by the parameter λ [13].

The M1 transition matrix elements between states with $F = F_{max}$ vanish, because the phase difference created by the $(L_\pi - L_\nu)$ term of the operator causes the terms in the matrix element to completely cancel. That is, M1 transition can be used to identify the mixed symmetry of states.

Another interesting point is the Majorana terms ξ_i (with $i=1,2$ and 3) is to specify the mixed states from symmetric and controlling the energy of such states with cross pending to these in experimental data. This dependence of level energy on the Majorana term is a good indication that contains a mixed symmetry contributions. In the U(5) [15,69,75,80,81] limit the mixed-symmetry states can be interpreted as vibrations of the neutrons and the protons which are out of the phase, in contrast to the symmetric state, associated with a simultaneous vibration of the neutrons and the protons, in the SU(3) limit mixed-symmetry states formed if the deformation distributions of neutrons and protons do not coincide, however, that the shape of the distribution itself is the same for neutrons and protons (either prolate or oblate) in SU(3) which is the geometrical analogue of the conditions of F-spin symmetry in the algebraic model. Finally, for the O(6) limit the geometrical interpretation is similar to the SU(3), but in this case the shape of the neutron and protons distribution ranges continuous from prolate to oblate (γ -unstable) [75,80,81].

it is convenient at this point to introduce a quantum number called F-spin. A particularly important property of the IBM-2 is that each proton-neutron symmetry described of each state is specified in terms of a new quantum number called F-spin [15,16], The F-spin can be defined as

$$F = \frac{N}{2} - f \quad (2-175)$$

The zero- component is

$$\hat{F}_0 = \frac{1}{2} (\hat{N}_\pi - \hat{N}_\nu) \quad (2-176)$$

Then one can characterize the states by the quantum numbers N , F , and F_0 . Clearly the totally symmetric states span the one-row irrep of $U_{\pi+\nu}$ (6), $[N,0]$. Thus they are characterized by $f=0$, which implies that they possess the maximum possible value of the F-spin is

$$F_{\max} = \frac{1}{2}N = \frac{1}{2}[\widehat{N}_{\pi} + \widehat{N}_{\nu}] \quad (2-177)$$

It is clear that the states of maximum F-spin are in one to one correspondence with the states of IBM-1. States with F-spin less than the maximum value of $\frac{N}{2}$ have no counterparts in IBM-1. They have mixed proton-neutron symmetry character, thus they are called mixed symmetry states [75,76,77,78,79]. That is when $F = F_{\max}$, the IBM-2 states become fully symmetric and reduced to the state of the IBM-1, but if the $F < F_{\max}$, the states have no counterpart with IBM-1, they have mixed p-n symmetry and they are called mixed state symmetry (MS). The F-spin operator is constructed in the following way [15]

$$\widehat{F}^+ = s_{\pi}^+ \cdot \tilde{s}_{\nu} + d_{\pi}^+ \cdot \tilde{d}_{\nu} \quad (2-178)$$

$$\widehat{F}^- = s_{\nu}^+ \cdot \tilde{s}_{\pi} + d_{\nu}^+ \cdot \tilde{d}_{\pi} \quad (2-179)$$

$$\widehat{F}^0 = s_{\pi}^+ \cdot \tilde{s}_{\pi} - s_{\nu}^+ \cdot \tilde{s}_{\nu} + d_{\pi}^+ \tilde{d}_{\pi} - d_{\nu}^+ \tilde{d}_{\nu} \quad (2-180)$$

$$\widehat{F}^2 = \widehat{F}^+ \widehat{F}^- + \widehat{F}^0 \widehat{F}^0 - \widehat{F}^0 \quad (2-181)$$

The \widehat{F}^2 operator can be directly evaluated as a two-body matrix element of states from an IBM-2 calculation, which gives information about the proton-neutron boson symmetry of the state. When F-spin is a good quantum number for a Hamiltonian, the maximum value it can have is $F_{\max} = \frac{1}{2}[\widehat{N}_{\pi} + \widehat{N}_{\nu}]$ and this corresponds to a symmetric state. For a mixed-symmetry state with one proton boson and one neutron boson out of phase, $F = F_{\max} - 1$. The minimum value that F can have is $F_{\min} = \frac{1}{2}|\widehat{N}_{\pi} - \widehat{N}_{\nu}|$.

2.2.5 Delta mixing ratio

Delta mixing ratio can produce when the E2 and M1 transition between two states are allowed both together, and it is the reduced E2 and M1 matrix elements [15]

$$\Delta(E2/M1) = \frac{\langle J_f \| T(E2) \| J_i \rangle_{(eb)}}{\langle J_f \| T(M1) \| J_i \rangle_{(\mu_N)}} \quad (2-182)$$

And related to the conventional experimental mixing ratio δ (E2/M1) according to the ref.[80,81]

$$\delta (E2/M1) = 0.835 E_\gamma \times \Delta(E2/M1) \frac{(eb)}{(\mu_N)} \quad (2-183)$$

Where E_γ the transition energy in (Mev), whereas $\Delta(E2/M1)$ is essentially a geometrical factor depending on the angular momentum of the initial and final state. An interesting aspect of the IBM, from the point of view of the mixing ratio, is the treatment of the M1 operator [15]. In the IBM-1 the lowest M1 transition can be vanishing, since it is described as one body operator and characterized with $\beta_1 [d^+ \times \tilde{d}]_\mu^{(1)}$ since it is proportional with total angular momentum, but in higher-order term it cannot vanish. And in (IBM-2), the lowest-order M1 operator is no longer proportional to the total angular momentum operator and hence, in general, M1 transitions are allowed. In here the delta mixing ratio in IBM-2 is produced to reduce the matrix element between E2/M1.

Chapter Three

Computer programs for IBM-1 and IBM-2

Chapter Three

Computer programs for IBM-1 and IBM-2

In this chapter, we describe the computer program to calculate the nuclear properties for Zr-nuclei by using interacting boson model for both versions (one and two) [84,85]. We have already been installed on pc-computer and used the Fortran power station-90 software to help that purpose. We have two main versions for that program IBM-1 (called version one) and IBM-2 also (called version two).

3.1 IBM-1

By using this program, this version can calculate some properties of the nuclei theoretically as energies of states with possible angular momentum for states, the matrix elements for quadrupole moment and electromagnetic transition probabilities, and coefficients of the potential energy surface of the nucleus. In this version, we have a file called (IBS1.for), whose type is Fortran type and can be used to calculate the above properties when we can run from Fortran power station by connecting both (IBSL.for) and (Eigsad.for). This is schematically illustrated in figure (3-1). Both (IBSL.for) and (Eigsad.for) are two other main programs in this version, each of them which can be used for a special purpose. (IBSL.for) can be used to solve the Hamiltonian matrix elements of one and two body terms, because it contains a number of subroutines that work like sub-programs for a number of functions. On the other hand, (Eigsad) program can be used to calculate the binding energy and to produce the diagonalization of the Hamiltonian matrix elements, since this aim is useful to calculate the eigenvalues and eigenvectors for all levels with definite angular momentum of the state.

When we compile the (IBS1.for) in the Fortran power station to obtain the objective of that file at the same time, insert both (IBSL.for) and (Eigsad.for) program to that file and both together can be compiled in the Fortran, and we can produce a link between them to make an executable file or running file, called (IBS1.exe) whose type is (exe or application file). And, we can input data in here to found above properties of the nucleus. The input data that can be used for IBM-1 version are the total boson number of the nucleus, and the Hamiltonian parameters such as ϵ , \mathbf{a}_0 , \mathbf{a}_1 , \mathbf{a}_2 , \mathbf{a}_3 , \mathbf{a}_4 and χ . But to calculate the perfect energy levels here, we wanted the other main program called (CFP.for), must be compiled in the Fortran power station and linked to produce the executable (application) file since the output of this file (CFP.OUT) is used as an input parameter and can be calculates the one body coefficient of fractional parentage and the CFP.OUT file stored and then used to calculate the electromagnetic transitions between these levels. When we want to run the program (IBS1.EXE), the input file must have contained the information, data and parameter of Hamiltonian matrix. That file is the file.Dat type. We inputting the names of that file into IBS1.EXE and must be equal or less than 9 character because in the IBS1.FOR we mentioned that the input and output can take 9 characters or less than 9. Here, we can named the input files as ZrA.inp, where A is the total number of the nucleons (proton and neutron) of the nucleus. After running we can obtain the same file for output such as ZrA.out.

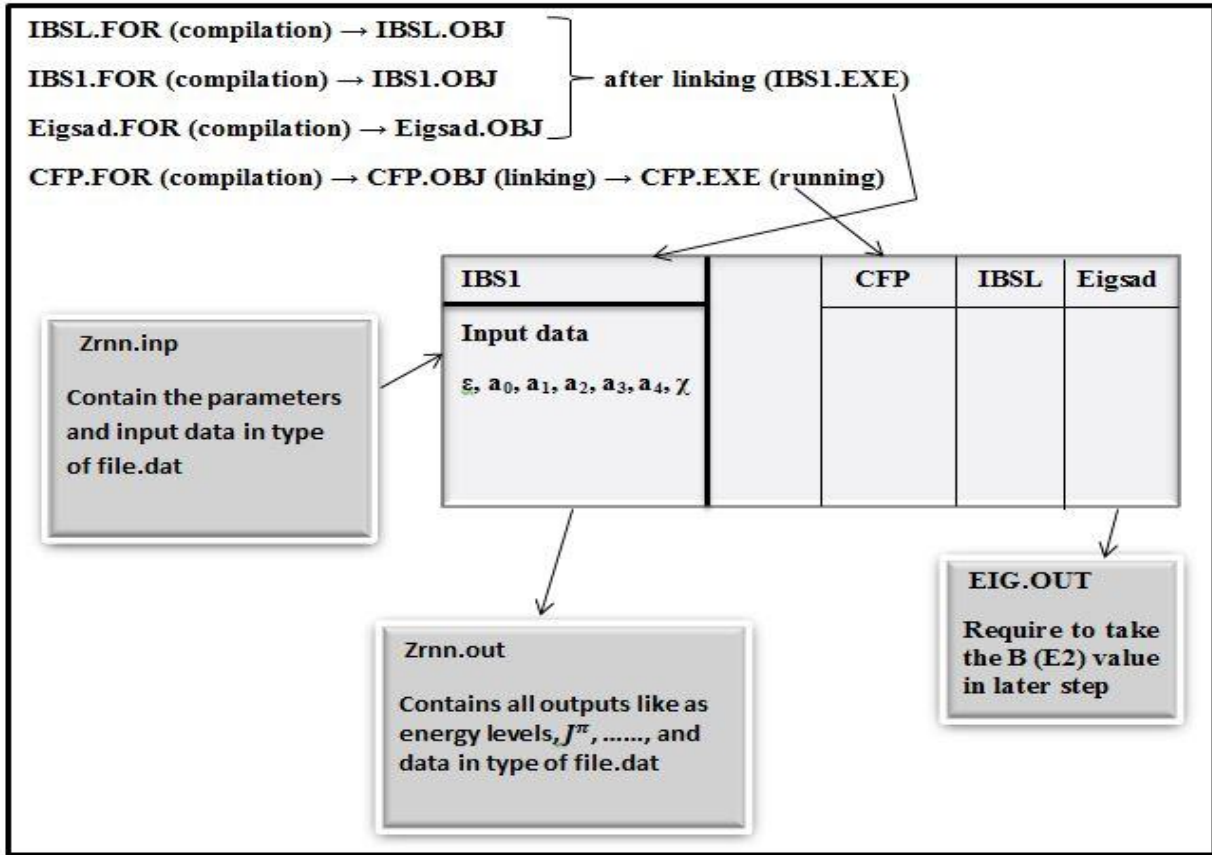


Figure (3-1): The structure of IBS1 code.

The above structure of IBS1 program cannot obtain the electric quadrupole moments (Q_2^+) and the electromagnetic transitions probabilities B(E2), so they must be found in another program in version one. That program is called (IBST.FOR) that contains the information about (Q_2^+ and B(E2)) and it's a main program of the version one to calculate the electric quadrupole moments and B(E2) values for the nucleus. The running of this program is similar to the IBS1 program, which we can compile in the Fortran power station connected with IBSL.FOR and EIGSAD.FOR together, and we make a link between them to produce the IBST.EXE file. As in IBS1 program, we need to compile and link the CFP.FOR file for this program. The IBST program should be executed directly after IBS1 program, because IBS1 program produces a file.dat from functional statement of the EIGSAD program called EIG.INP which contains data required in the calculations of B(E2). And, in the IBST program we need the input file.dat type

and named by BE2.INP, that contains the value of effective charge e_B^2 for protons and neutrons and in version one does not differentiate between the protons and neutrons. With χ , SO(6) parameter takes a constant value for all isotopes and the value of angular momentum(J), as well as an input parameter. This is required to find the electric quadrupole moments and initial and final states which are needed to find the B(E2) between them. And, the structure of the IBST is illustrated schematically in the figure (3-2).

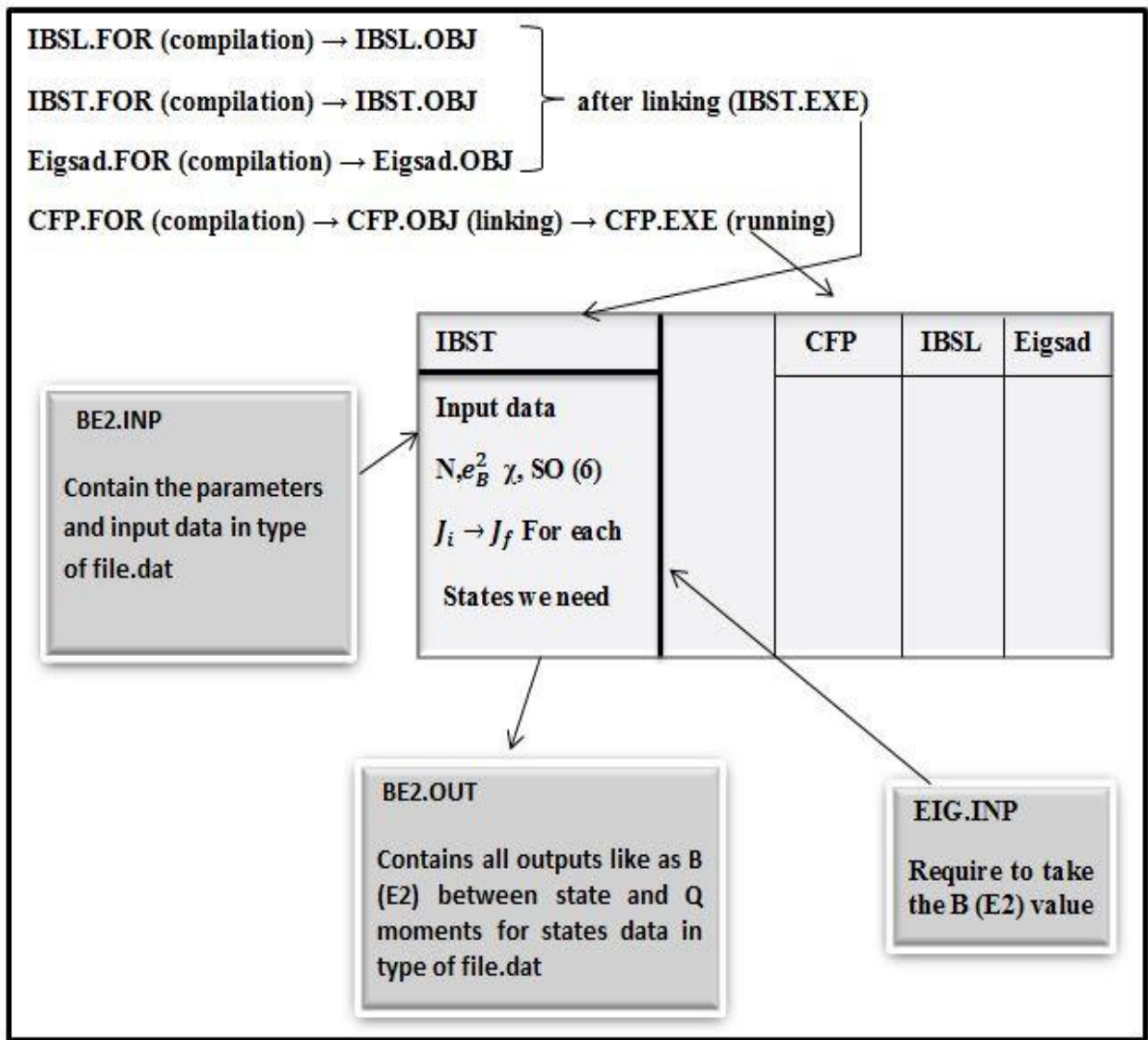


Figure (3-2): structure of IBST program

3.2 IBM-2

Here we can also calculate the properties of Zr- nuclei by using the interacting boson model-2, which is distinction between protons and neutrons. By using the Fortran power station, and in this version to calculate the eigenvalues and eigenvectors for all states with definite angular momentum itself, we can use the (NPBOSN) program, since in term of this program we can diagonalize the Hamiltonian matrix elements. And to calculate the electromagnetic transitions between states and moments of the nuclei, we can use another program called the (NPBTRN) program since in program has a useful function to calculate the electromagnetic matrix elements between eigenstates. For the first purpose to calculate eigenvalues and eigenvectors for all possible states, we need some coefficients and parameters to put into the (NPBOSN) program, such as coefficient of fractional parentage (c.f.p), Racah coefficient and d-boson number for one-body operator matrix element.

And, to create one body and two body c.f.p.'s for states we can use two other programs (CFPGEN) and (NPCFPG). By compiling and linking the (CFPGEN) program in the Fortran power station, the produced (CFPGE.EXE) file can create one body (c.f.p) for states and store in the file.dat called (cfp1). On the other hand, to produce the two-body (c.f.p) for states, we use the (NPCFPG) program in the Fortarn power station, when compiling and linking can obtain an output file.dat named by (cfp2). In the (CFPGEN) program, we need the total number of boson to input data and need the maximum number of d-boson to input data for (NPCFPG) program. (cfp1) and (cfp2) files are illustrated schematically in figure (3-3).

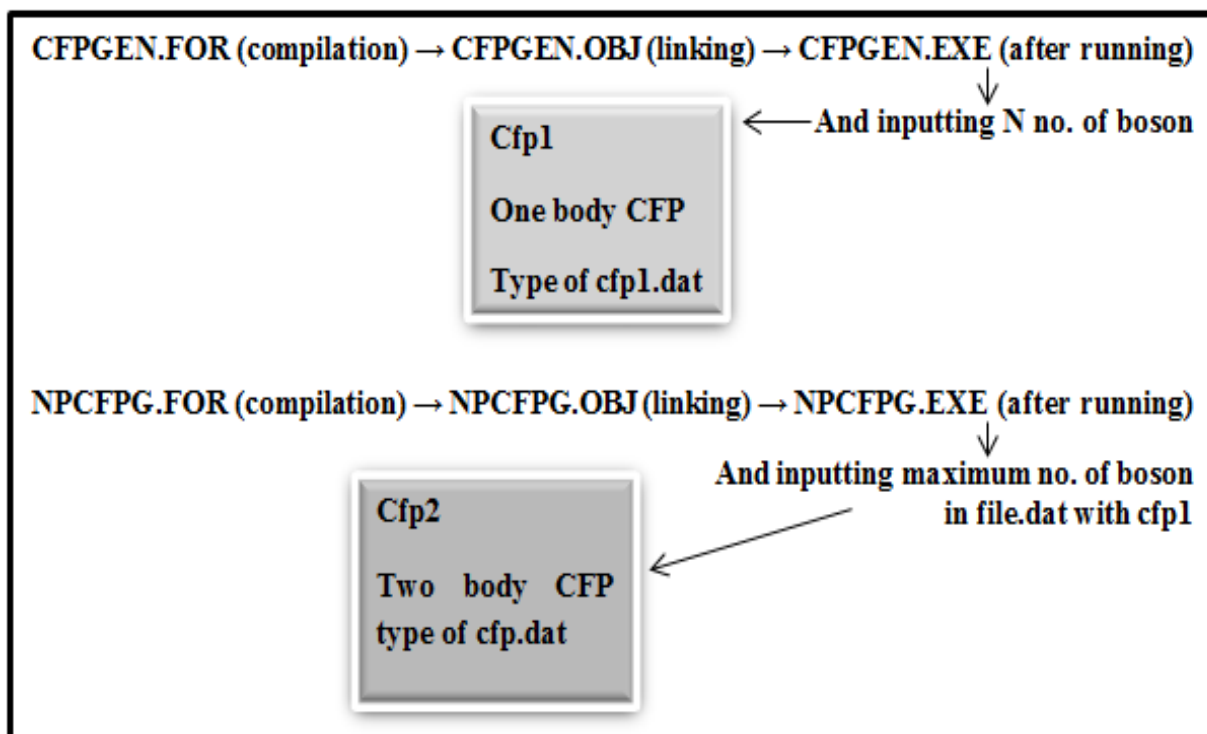


Figure (3-3): structure of CFPGEN and NPCFPG programs

And to calculate the Racah coefficient, (RACFL) program will be used. (RACFL) program can be compiled and linked to the Fortran power station, to produce the (RACFL.EXE) in which we put the input data and application file of this program then we run. The input file is called (Rac.dat) which contains the maximum number of d-boson (n_d) and maximum number of angular momentum with identifying name of output file. The output of Racah coefficient stored in the file.dat is called (Rac6). This is illustrated schematically in the figure (3-4). On the other hand, to calculate the d-boson of one-body operator matrix element, we use another program called (DDMEFL) program when compiled and linked. We can input in the executed file the maximum number of d-boson in the file with two-body CFP file (cfp2), and here we can take the one-body matrix elements in a file.dat called (ddmef) that are used in the (NPBOSN) program.

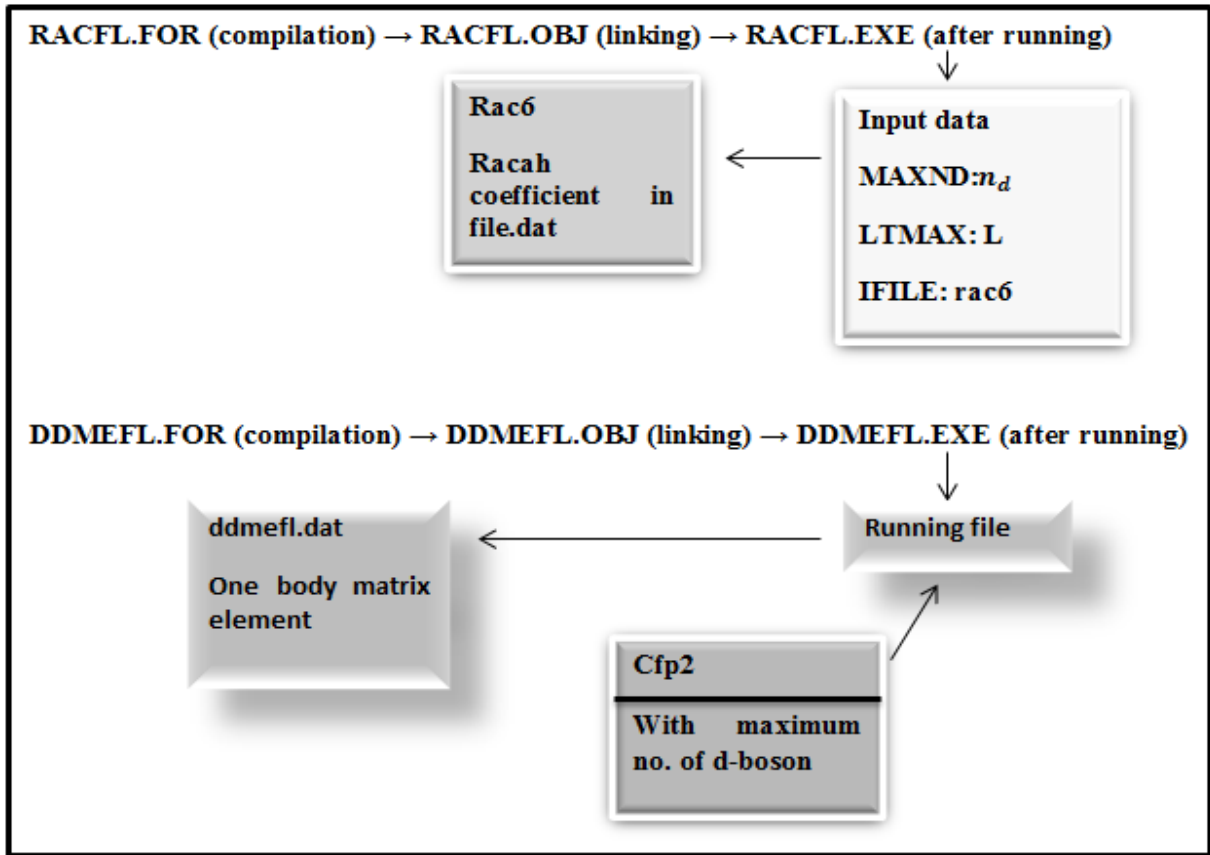


Figure (3-4): structure of RACFL and DDMEFL programs

With the above function, coefficients and parameters are taken by the programs can be used in the (NPBOSN) program to calculate the properties of Zr-nuclei as energy levels with its definite angular momentum. In the (NPBOSN) program, we have some input parameter for nuclei which needs to identify the properties of the nuclei. These input parameters reading from (NPBOSN) program are stored in the file.dat called (Zrnn.inp) where (nn) is the no. of atomic mass of Zr-nuclei. We can produce the structure of the (NPBSON) program schematically as illustrated in figure (3-5).

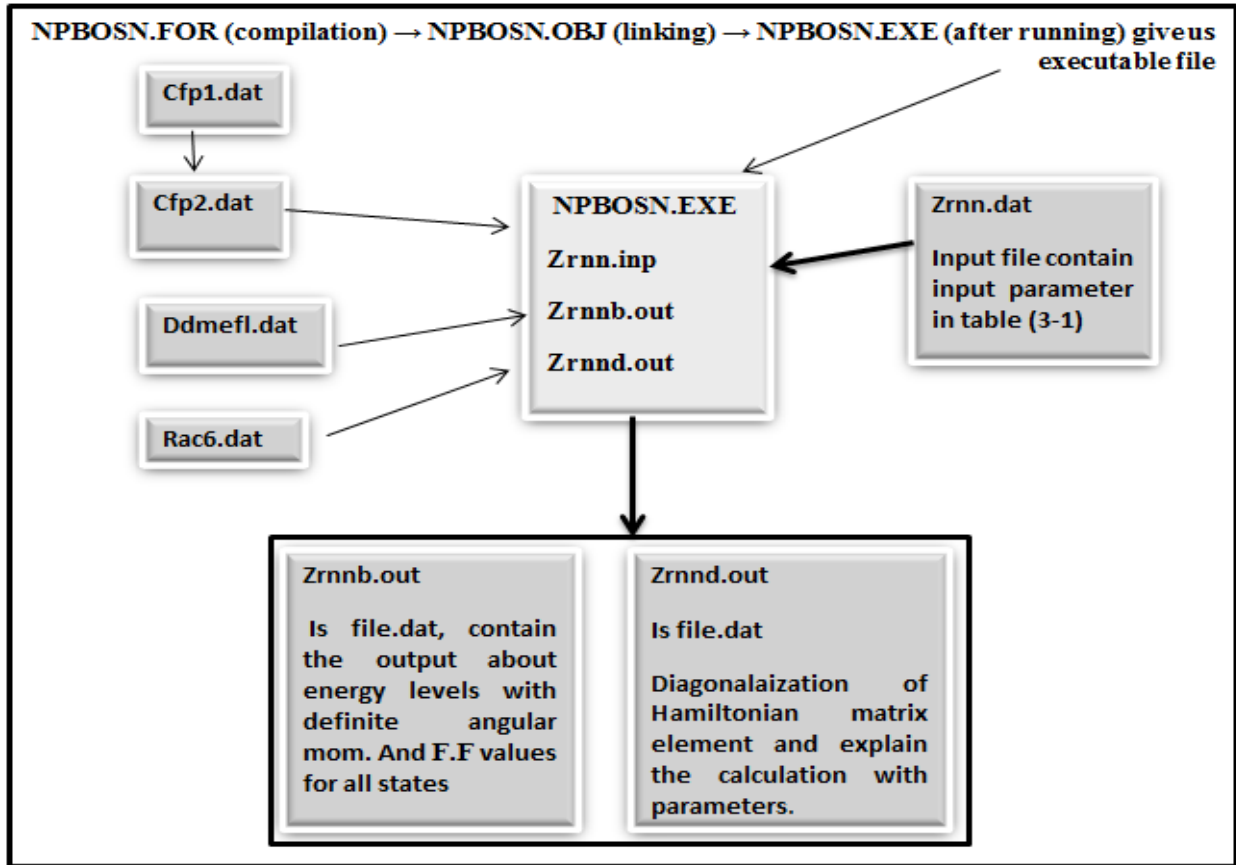


Figure (3-5): structure of (NPBOSN) program

On the other hand, in the IBM-2 version to calculate the electromagnetic matrix elements $B(E2)$, $B(M1)$, Q -moments and μ -moments we use the (NPBTRN) program running in the Fortran power station since information is stored in NPBTRN about these properties for Zr nuclei. Here, we need a file.dat named as Zr-nn, where nn is the no. of atomic mass of Zr-nucleus. It contains some input parameter to calculate the above properties of the Zr-nuclei. When we run the (NPBTRN) program, we can take the value of the $B(E2)$ and Q -moment with the value of $M1$ transition in the states in the same file.dat called Zr-nn.out. The NPBTRN can be illustrated schematically in figure (3-6).

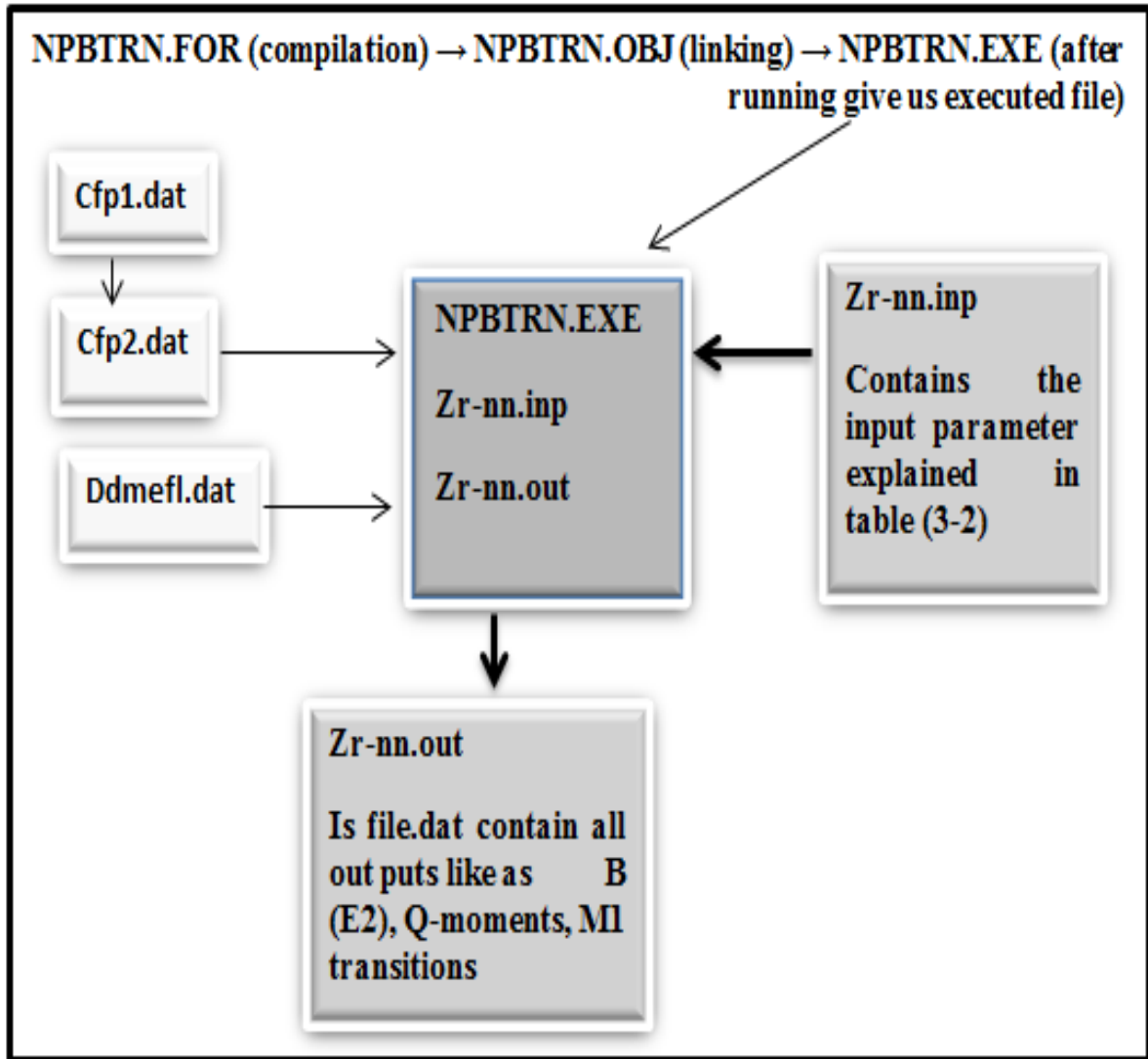


Figure (3-6): structure of NPBTRN program

The ratio between E2 transitions to M1 transitions are called delta mixing ratio that can be calculated from Delta_IBM2.for after running from the Fortran power station studio. Delta_IBM2.for contains all information about the delta mixing ratio as Hamiltonian parameters CHI (γ), effective charge boson and G-factor for both protons and neutrons. In this program, we must run the program for each isotopes and change the parameter since each parameter has selected parameters, and the input parameters in the input file are the electromagnetic

parameters from the output of B(E2) and B(M1) transitions called DS(N), DD(N), DS(P), and DD(P), with the gamma energy for each transition.

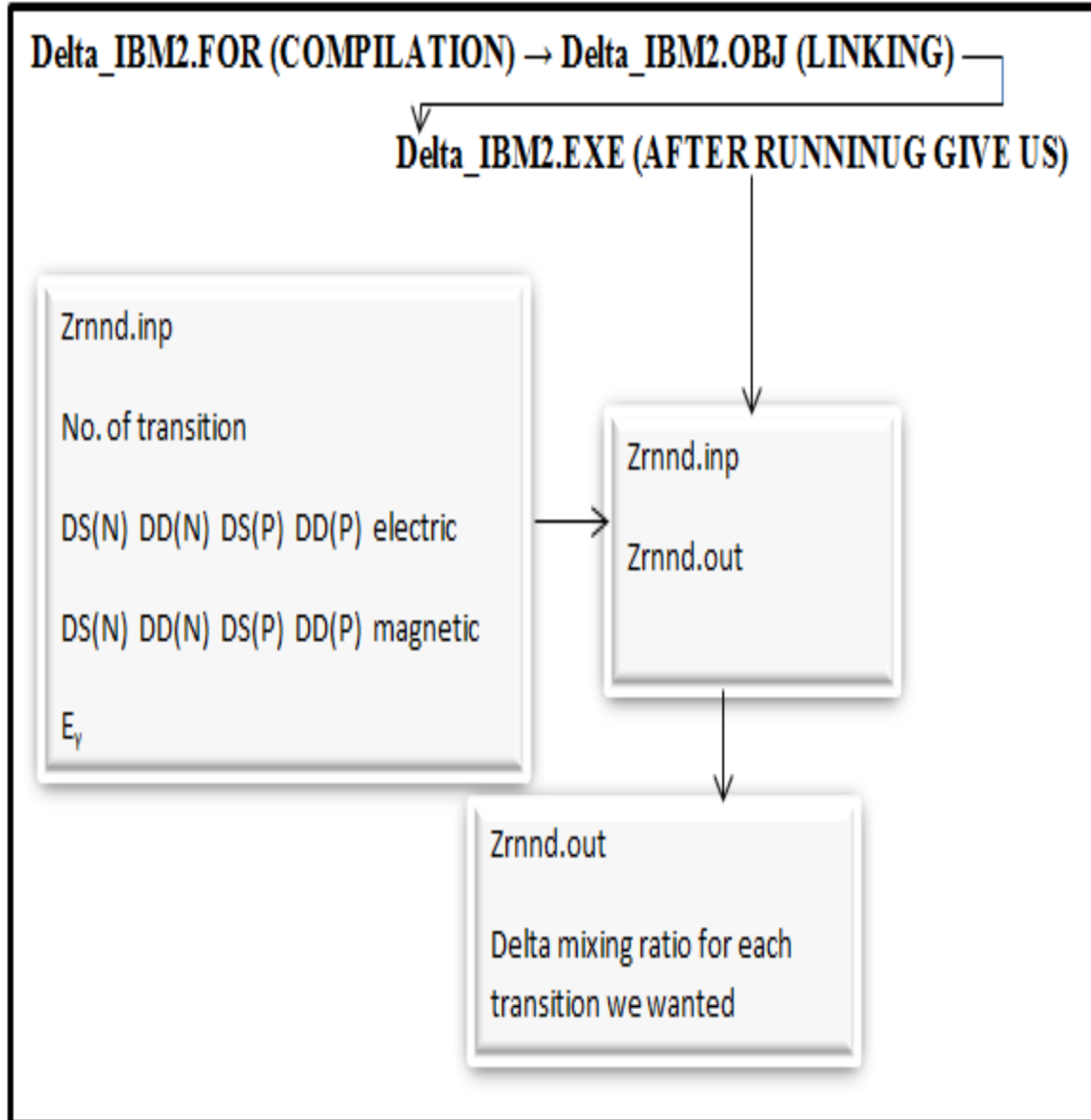


Figure (3-7): Structure of Delta_IBM2 program

Chapter Four

Result and Discussion

Chapter four

Results and Discussion

Introduction

In the framework of the Interacting Boson Models (IBM-1 and IBM-2), the nuclear structure of even-even Zr-isotopes are investigated. IBA-1 and IBA-2 Hamiltonian parameters are obtained as well as the extraction of the energy levels. Also, the electric quadrupole transition probabilities $B(E2:J_i \rightarrow J_f)$ of the Zr-isotopes were calculated. In calculations, the theoretical energy levels and the electric quadrupole transition probabilities have been obtained by using PHINT code. Good agreement was found from a comparison between the calculated energy levels and the electric quadrupole transition probabilities $B(E2)$ of the Zr-isotopes with the experimental data.

Calculations with IBM framework depend on the best fitting of Hamiltonian parameters to obtained the best result for the energy levels, $B(E2)$ values, etc.. For the best choosing of the parameters, we must depend on the experimental data. Important thing that we must know before all things is the shape of nuclei and to locate it in Casten triangle. To know the shape of the nuclei we used the energy value of experimental data for that purpose, where the ratio between the energy of $(\frac{E_{4^+}}{E_{2^+}})$ tell us what the shape of that nuclei is. From the Casten triangle of symmetry, three dynamical region produce SU(5),SU(3) and O(6), each of them is characterized by a specified parameter in Hamiltonian Eq.(2-14). For instance SU(5) controlling with (ϵ) , in SU(3) angular momentum and quadrupole moment interaction $(a_1L.L)$, and $(a_2Q.Q)$ are strong existence the rotational nuclei, and O(6) controlling with $(a_0P.P)$. SU(5) is the shape image of

vibrational nuclei, SU(3) is the shape image of rotational nuclei, and O(6) is of the γ -unstable nuclei.

Energy level calculations can be done by using the Hamiltonian Eq. (2-14), in the (IBM-1), and in (IBM-2) it can be done by using the Hamiltonian Eq. (2-127) in the Fortran power station program, such as IBM-1, each region of nuclei in IBM-2 specified by specific parameter in Eq. (2-127). For example the first term (ϵ_d) is dominated in vibrational like nuclei and second term (quadrupole-quadrupole interaction) is dominant in rotational nuclei with negative value of χ_π and χ_ν , and with condition $\chi_\pi = -\chi_\nu$ in second term may be obtained the γ -unstable nuclei.

This work contains the calculation of energy scheme of the bands (G-band, β -band, and γ -band), with the B(E2) and $Q(2_1^+)$ which can be reproduced in IBM by the inserting the effective charge (e_B^2) for IBM-1 and (e_π, e_ν) for IBM-2. The IBM-1 calculation cannot take us the B(M1) transition, while in IBM-2 can take the magnetic transition probability B(M1), and this is useful to find the delta mixing ratio since it can be calculated from matrix element of B(E2) and B(M1) transitions. The mixed symmetry is another property of IBM-2, and it's very sensitive to the Majorana terms in Hamiltonian of IBM-2. Where the state is fully symmetric the F-spin is maximum value, while the mixed symmetry state has F-spin with minimum value. If we have transition with strong B(M1), the transition occur from the mixed to full symmetric, and consequently δ -mixing ratio is small for gamma transitions.

4.1 Energy spectrum

The energy ratios between $E4_1^+$ to $E2_1^+$ energy levels tell us about the nucleus shape symmetry, it's necessary to produce the low-lying energy levels of a nucleus by IBM-1. SU(5) is vibrational nuclei with $R_{4/2}$ has a limit value of 2, 2.5 for γ -unstable nuclei O(6), and 3.33 for

rotational nuclei SU(3). The variation of the experimental $\frac{E_{4_1^+}}{E_{2_1^+}}$ value of Zr-nuclei with the neutron numbers is given in figure (4-1). It is clear that the $^{80-108}\text{Zr}$ -isotopes distributed between all limits, and we take the same result for those ratios in IBM-1 and IBM-2.

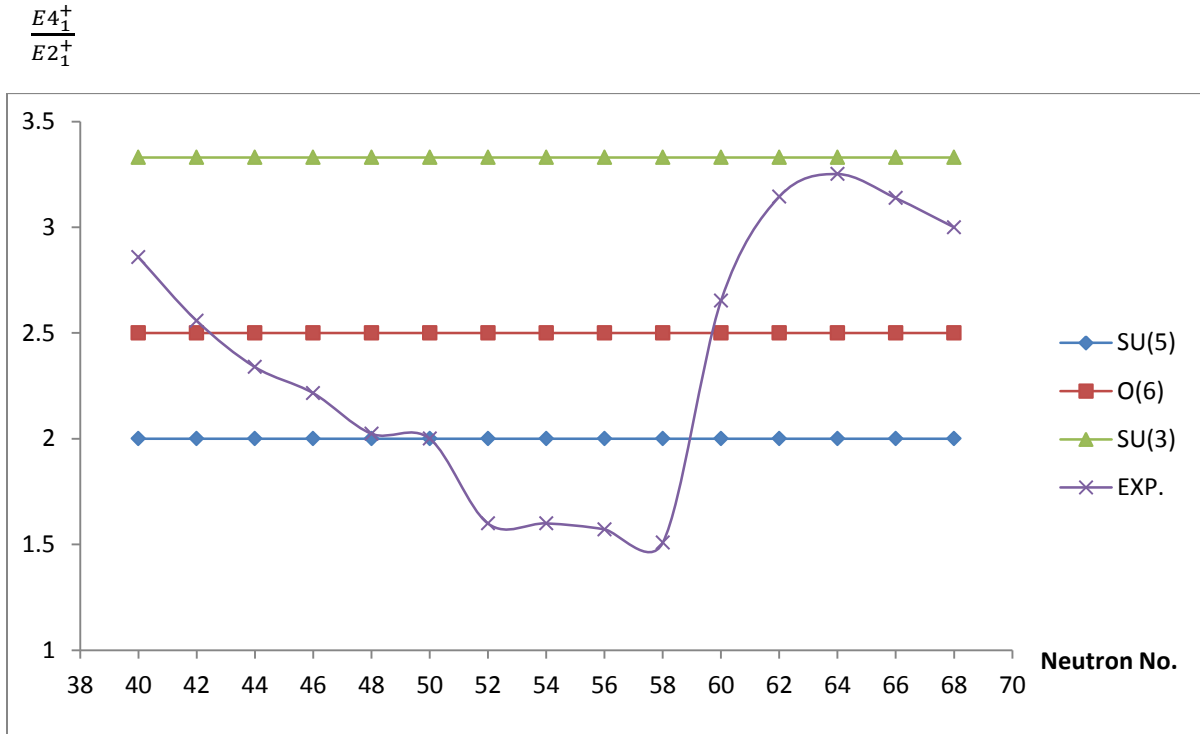


Fig. (4-1): Variation of the energy ratios $\frac{E_{4_1^+}}{E_{2_1^+}}$ with neutron number in $^{80-108}\text{Zr}$ -isotopes.

However, by using the parameters of Tables (4-1a, and b) and (4-2a, and b) in the Hamiltonian equations (2-14) and (2-127) of IBM-1 and IBM-2 respectively, the result for a low-lying positive parity energy spectra has been obtained for $^{80-108}_{40}\text{Zr}_N$ isotopes with neutron numbers $N= 40,42,44,46,48,52,54,56,58,60,62,64,66$, and 68. These low-lying energy spectra which obtained by IBM-1 and IBM-2 are within the SU(5), O(6), and SU(3) limits. We take the energy spectra for $^{80-108}\text{Zr}$ -isotopes from the program for three bands, ground band with angular momentum: $0_1^+, 2_1^+, 4_1^+, 6_1^+, 8_1^+$, beta band with angular momentum: $0_2^+, 2_2^+, 4_2^+, 6_2^+, 8_2^+$, and

gamma band with angular momentum: 2_3^+ , 3_1^+ , 4_3^+ , 5_1^+ , 6_3^+ , and can be compared with experimental data as shown in the tables (4-3)

Table (4-1a): The IBM-1 Hamiltonian parameters used for $^{80-88}\text{Zr}$ and $^{92-94}\text{Zr}$ isotopes

Parameters	Zr ⁸⁰	Zr ⁸²	Zr ⁸⁴	Zr ⁸⁶	Zr ⁸⁸	Zr ⁹²	Zr ⁹⁴
N	10	9	8	7	6	6	7
ϵ (Mev)	0.71	0.73	0.75	0.72	0.75	0.70	0.727
a_0 (Mev)	0.06	0.05	0.058	0.0	0.0	0.0	0.0
a_1 (Mev)	0.0105	0.0106	0.0108	0.011	0.0087	0.01	0.0115
a_2 (Mev)	-0.010	-0.008	-0.008	-0.008	0.016	0.02	0.012
a_3 (Mev)	0.0	0.0	0.0	0.0	0.0	0.0089	0.0
a_4 (Mev)	0.0	0.0	0.0	0.0	0.0	0.0098	0.0
CHI	-1.35	-1.35	-1.35	-1.35	-1.35	-1.35	-1.35
SO(6)	1.0	1.0	1.0	1.0	1.0	1.0	1.0

Table (4-1b): The IBM-1 Hamiltonian parameters used for $^{86-108}\text{Zr}$ isotopes

Parameters	Zr ⁹⁶	Zr ⁹⁸	Zr ¹⁰⁰	Zr ¹⁰²	Zr ¹⁰⁴	Zr ¹⁰⁶	Zr ¹⁰⁸
N	8	9	10	11	12	13	12
ϵ (Mev)	0.64	0.80	0.55	0.48	0.46	0.53	0.52
a_0 (Mev)	0.05	0.122	0.0	0.04	0.06	0.05	0.05
a_1 (Mev)	0.03	0.02	0.0087	0.0087	0.0105	0.0105	0.0105
a_2 (Mev)	0.08	0.04	-0.016	-0.013	-0.008	-0.008	-0.008
a_3 (Mev)	0.0	0.0	0.0	0.0	0.0	0.0	0.0
a_4 (Mev)	0.0	0.0	0.0	0.0	0.0	0.0	0.0
CHI	-1.35	-1.35	-1.35	-1.35	-1.35	-1.35	-1.35
SO(6)	1.0	1.0	1.0	1.0	1.0	1.0	1.0

Table (4-2a): The IBM-2 Hamiltonian parameters used for $^{80-88}\text{Zr}$ and $^{92-94}\text{Zr}$ isotopes

Parameters	Zr ⁸⁰	Zr ⁸²	Zr ⁸⁴	Zr ⁸⁶	Zr ⁸⁸	Zr ⁹²	Zr ⁹⁴
N_v	5	4	3	2	1	1	2
N_π	5	5	5	5	5	5	5
ε_d	0.51	0.645	0.20	0.575	0.93	0.90	0.91
k (RKAP)	-0.14	-0.24	-0.18	-0.15	-0.008	-0.008	-0.008
k_v (RKNN)	-0.05	-0.05	-0.05	-0.04	-0.001	-0.001	-0.001
k_π (RKPP)	-0.09	-0.19	-0.13	-0.11	-0.007	-0.007	-0.007
χ_v (CHN)	-0.22	-0.22	-0.22	-0.80	-1.7	-1.7	-1.7
χ_π (CHP)	0.0	0.0	0.0	0.0	-1.0	-1.0	-1.0
C_{L_v} (L=0)	0.0	0.0	-0.04	-0.001	0.0	0.0	0.0
C_{L_v} (L=2)	-0.1	-0.1	-0.04	-0.001	0.0	0.0	0.0
C_{L_v} (L=4)	-0.1	-0.1	0.275	0.3	0.0	0.0	0.1
C_{L_π} (L=0,2,4)	0,0,0	0,0,0	0,0,0	0,0,0	0,0,0	0,0,0	0,0,0
ξ_1	0.4	0.4	0.4	0.25	-0.1	-0.1	-0.1
ξ_2	-0.1	-0.25	-0.25	-0.6	0.285	0.285	0.385
ξ_3	0.4	0.4	0.4	0.25	-0.02	-0.02	-0.02

Where all parameter in unit (MeV) except CHN and CHP

Table (4-2b): The IBM-2 Hamiltonian parameters used for $^{96-108}\text{Zr}$ isotopes

Parameters	Zr ⁹⁶	Zr ⁹⁸	Zr ¹⁰⁰	Zr ¹⁰²	Zr ¹⁰⁴	Zr ¹⁰⁶	Zr ¹⁰⁸
N_v	3	4	5	6	7	8	7
N_π	5	5	5	5	5	5	5
ϵ_d	0.98	0.95	0.3	0.001	0.017	0.001	0.001
k (RKAP)	0.048	-0.03	-0.13	-0.15	-0.185	-0.180	-0.170
k_v (RKNN)	0.020	-0.01	-0.06	-0.07	-0.060	-0.055	-0.05
k_π (RKPP)	0.030	-0.02	-0.07	-0.08	-0.125	-0.125	-0.120
χ_v (CHN)	-2.40	-1.0	-0.24	-0.24	-0.20	-0.18	-0.18
χ_π (CHP)	-2.40	-1.0	-0.24	-0.24	0.0	0.0	0.0
C_{Lv} (L=0)	0.90	-1.0	-0.15	-0.10	-0.04	-0.04	-0.04
C_{Lv} (L=2)	0.90	0.05	-0.15	-0.10	-0.04	-0.04	-0.04
C_{Lv} (L=4)	0.90	-0.1	-0.04	-0.02	-0.02	0.05	0.09
$C_{L\pi}$ (L=0,2,4)	0,-0.598,0	-0.3,0.1,0.1	0,0,0	0,0,0	0,0,0	0,0,0	0,0,0
ξ_1	-0.15	-0.1	0.29	0.29	0.29	0.10	-0.10
ξ_2	0.40	0.1	-0.29	-0.29	-0.29	-0.29	-0.30
ξ_3	-0.15	-0.1	0.29	0.29	0.29	0.10	-0.10

Where all parameter in unit (MeV) except CHN and CHP

4.1.1 ^{80}Zr -isotope

The values of the low-lying positive parity states of ^{80}Zr -isotope calculated by IBM-1 and IBM-2 models have been compared with the experimental data [86] as shown in the table (4-3). It is clear from the table that the available data are limited to 2_1^+ , 4_1^+ , 6_1^+ , 8_1^+ , and 10_1^+ which are located at 0.289, 0.826, 1.605, 2.610, and 3.789 MeV respectively; are nicely reproduced by IBM-1 and IBM-2, but IBM-1 gives better fitting in comparison to IBM-2. The experimental

data for beta and gamma band for ^{80}Zr -isotope are not available and the IBM-2 energy value for these bands are pushed up and come higher than those of the IBM-1.

Table (4-3): the comparison between the calculated and the experimental energy levels values of (^{80}Zr)

J^+	Energy levels (Mev)			
	EXP.	Ref.[86]	IBM-1	IBM-2
0_1^+	0.0		0.0	0.0
2_1^+	0.289		0.328	0.386
4_1^+	0.826		0.845	0.886
6_1^+	1.605		1.537	1.529
8_1^+	2.610		2.390	2.294
10_1^+	3.789		3.397	3.201
2_2^+			0.940	0.985
3_1^+			1.452	1.586
4_2^+			1.576	1.619
5_1^+			2.176	2.341
6_2^+			2.347	2.364
7_1^+			3.047	3.233
0_2^+			0.947	1.218
2_3^+			1.658	1.934
4_3^+			2.170	2.146

4.1.2 ^{82}Zr -isotope

The values of the low-lying positive parity states of ^{80}Zr -isotope calculated by IBM-1 and IBM-2 models have been compared with the experimental data [87] as shown in the table (4-4). It is clear from the table that the available data are limited to 2_1^+ , 4_1^+ , 6_1^+ , 8_1^+ , and 10_1^+ which are located at 0.407, 1.041, 1.888, 2.909 and 4.036 MeV respectively; are nicely reproduced by IBM-1 and IBM-2, and in 12_1^+ , 14_1^+ with experimental data 5.213, 6.490 MeV respectively [87], the IBM-1 also produces best fitting, IBM-2 are pushing these states up. Again there are no

experimental data for beta and gamma band for ^{82}Zr -isotope are available. The predicted energy values for these bands by IBM-1 and IBM-2 takes from the program, but the IBM-2 pushed up the energy values of gamma and beta bands compared to the IBM-1, and the gamma band coming lower than the beta band.

Table (4-4): the comparison between the calculated and the experimental energy levels values of (^{82}Zr)

J^+	Energy levels (Mev)			
	EXP.	Ref.[87]	IBM-1	IBM-2
0_1^+	0.0		0.0	0.0
2_1^+	0.407		0.470	0.433
4_1^+	1.041		1.095	1.049
6_1^+	1.888		1.873	1.843
8_1^+	2.909		2.795	2.821
10_1^+	4.036		3.858	4.009
12_1^+	5.213		5.057	5.461
14_1^+	6.490		6.389	7.359
2_2^+			1.146	1.314
3_1^+			1.751	2.038
4_2^+			1.763	2.101
0_2^+			1.474	1.843
2_3^+			1.954	2.225

4.1.3 ^{84}Zr -isotope

The values of the low-lying positive parity states of ^{84}Zr -isotope calculated by IBM-1 and IBM-2 models have been compared with the experimental data [88] as shown in the table (4-5). It is clear from the table that the available data are limited to 2_1^+ , 4_1^+ , 6_1^+ , 8_1^+ , and 10_1^+ which are located at 0.540, 1.263, 2.136, 3.089 and 4.069 MeV respectively; are nicely reproduce by IBM-1 and IBM-2, and in 12_1^+ , 14_1^+ with experimental data 5.136, 6.303 MeV respectively [88], the

IBM-1 and IBM-2 are pushed up. The gamma band head comes lower than the beta band, with experimental data for 2_2^+ , 4_2^+ , 6_2^+ are 1.119, 1.888, and 2.740 MeV, are reproduced nicely energy value by both IBM-1 and IBM-2, but there are no experimental energy values available for beta band, and the values of energy for that band by IBM-1 and IBM-2 systematically are not bad.

Table (4-5): the comparison between the calculated and the experimental energy levels values of (^{84}Zr)

J^+	Energy levels (Mev)			
	EXP.	Ref.[88]	IBM-1	IBM-2
0_1^+	0.0		0.0	0.0
2_1^+	0.540		0.517	0.429
4_1^+	1.263		1.192	1.116
6_1^+	2.136		2.021	2.015
8_1^+	3.089		2.996	3.002
10_1^+	4.069		4.113	4.196
12_1^+	5.136		5.368	5.692
14_1^+	6.303		6.758	7.525
2_2^+	1.119		1.117	1.037
3_1^+			1.790	1.850
4_2^+	1.888		1.880	1.854
5_1^+			2.642	2.544
6_2^+	2.740		2.778	2.610
0_2^+			1.182	1.379
2_3^+			1.815	1.637
4_3^+			2.470	2.001

4.1.4 ^{86}Zr -isotope

The values of the low-lying positive parity states of ^{86}Zr -isotope calculated by IBM-1 and IBM-2 models have been compared with the experimental data [89] as shown in the table (4-6). It is clear from the table that the available data are limited to 2_1^+ , 4_1^+ which are located at 0.752, and 1.666 MeV respectively; are nicely reproduced by IBM-1, but IBM-2 are pulling down with

small amount compared by IBM-1. The 6_1^+ energy value with experimental [89] 2.669 MeV is well fitted with both IBM-1 and IBM-2. The 8_1^+ , and 10_1^+ energy values with experimental value 3.298 and 4.326 MeV are pushing up by both IBM-1 and IBM-2. The experimental data for 2_2^+ , 4_2^+ , 6_2^+ are 1.422, 2.343, and 3.254 MeV in beta band are reproduced nicely by IBM-1, and also best fitting by IBM-2 for 2_2^+ , and small pulling down for 4_2^+ and 6_2^+ by IBM-2. No experimental data are available for gamma band, and the systematic of IBM-1 and IBM-2 results are reasonable.

Table (4-6): the comparison between the calculated and the experimental energy levels values of (^{86}Zr)

J^+	Energy levels (Mev)			
	EXP.	Ref.[89]	IBM-1	IBM-2
0_1^+	0.0		0.0	0.0
2_1^+	0.752		0.698	0.513
4_1^+	1.666		1.507	1.394
6_1^+	2.669		2.431	2.401
8_1^+	3.298		3.473	3.544
10_1^+	4.326		4.634	4.976
0_2^+			1.259	1.420
2_2^+	1.422		1.393	1.428
4_2^+	2.343		2.244	2.008
6_2^+	3.254		3.209	3.053
2_3^+			2.020	1.814
3_1^+			2.168	2.272

4.1.5 ^{88}Zr -isotope

The values of the low-lying positive parity states of ^{88}Zr -isotope calculated by IBM-1 and IBM-2 models have been compared with the experimental data [90] as shown in the table (4-7). It is clear from the table that the available data are limited to 2_1^+ , 4_1^+ which are located at 1.057,

and 2.139 MeV respectively; are nearly best fitting reproduce by IBM-1 and IBM-2 but pulling down with small amount compared with experimental data. The 6_1^+ energy value with experimental 2.811 MeV is in good fit with both IBM-1 and IBM-2. The 8_1^+ energy values with experimental value 3.391 MeV is pushed up by both IBM-1 and IBM-2. The experimental data for beta band are reproduced nicely by both IBM-1 and IBM-2, but for 6_2^+ , 8_2^+ , and for gamma band the IBM-1 is better fitting than IBM-2.

Table (4-7): the comparison between the calculated and the experimental energy levels values of (^{88}Zr)

J^+	Energy levels (Mev)			
	EXP.	Ref.[90]	IBM-1	IBM-2
0_1^+	0.0		0.0	0.0
2_1^+	1.057		0.911	0.890
4_1^+	2.139		1.836	1.796
6_1^+	2.811		2.786	2.722
8_1^+	3.391		3.768	3.669
0_2^+	1.521		1.682	1.788
2_2^+	1.817		1.734	1.793
4_2^+	2.605		2.616	2.698
6_2^+	3.213		3.523	3.626
8_2^+	4.388		4.487	4.583
2_3^+	2.568		2.506	1.808
3_1^+			2.547	2.388
4_3^+	3.074		3.324	2.740
5_1^+	3.389		3.405	3.154
6_3^+			4.177	3.692
7_1^+	4.237		4.290	3.945

4.1.6 ^{92}Zr -isotope

The values of the low-lying positive parity states of ^{92}Zr -isotope calculated by IBM-1 and IBM-2 models have been compared with the experimental data [91] as shown in the table (4-8).

The available data are limited to 2_1^+ , 4_1^+ , 6_1^+ , and 8_1^+ ; both IBM-1 and IBM-2 almost fitting 2_1^+

and 6_1^+ nicely, but pushing up for 4_1^+ and 8_1^+ . In the beta band the experimental data for 0_2^+ , 2_2^+ , 4_2^+ , 6_2^+ are 1.383, 1.847, 2.398, and 3.304 MeV, both IBM-1 and IBM-2 pushed up the 0_2^+ , 4_2^+ , 6_2^+ states, while fitted nicely the 2_2^+ state. The experimental energy value for gamma band with 2_3^+ , 4_3^+ , and 5_1^+ states are 2.182, 2.864, and 3.675 MeV, the IBM-1 is better in fitting than IBM-2 for 2_3^+ and 5_1^+ states but for 4_3^+ state vice versa. Our results are better than those of ref [40, 50] in both IBM-1 and IBM-2.

Table (4-8): the comparison between the calculated and the experimental energy levels values of (^{92}Zr)

J^+	Energy levels (Mev)			
	EXP.	Ref.[91]	IBM-1	IBM-2
0_1^+	0.0		0.0	0.0
2_1^+	0.935		0.924	0.860
4_1^+	1.495		1.862	1.736
6_1^+	2.957		2.821	2.632
8_1^+	3.308		3.819	3.549
0_2^+	1.383		1.695	1.728
2_2^+	1.847		1.772	1.749
4_2^+	2.398		2.669	2.637
6_2^+	3.304		3.597	3.534
2_3^+	2.182		2.532	1.763
3_1^+			2.611	2.328
4_3^+	2.864		3.399	2.650
5_1^+	3.675		3.485	3.064
6_3^+			4.276	3.572
7_1^+			4.388	3.825

4.1.7 ^{94}Zr -isotope

The values of the low-lying positive parity states of ^{94}Zr -isotope calculated by IBM-1 and IBM-2 models have been compared with the experimental data [92] as shown in the table (4-9).

The available data are limited to 2_1^+ , 4_1^+ , 6_1^+ , and 8_1^+ ; both IBM-1 and IBM-2 achieved good

fitting for 2_1^+ and 8_1^+ , while both are slightly pushing up 4_1^+ and pulling down 6_1^+ . In the beta band experimental data for 0_2^+ , 2_2^+ , and 4_2^+ are 1.301, 1.672, and 2.330 MeV, both IBM-1 and IBM-2 pushed up 0_2^+ and 4_2^+ by small amount, but both fitted 2_2^+ nicely. The experimental energy value for gamma band for states 2_3^+ , 3_1^+ , and 4_3^+ are 2.152, 2.508, and 2.861 MeV, both IBM-1 and IBM-2 nearly best fit for 2_3^+ and 3_1^+ states, but both together are pushed up for 3_1^+ . Our result compared to the ref [42,43,50] is very good in both IBM-1 and IBM-2.

Table (4-9): the comparison between the calculated and the experimental energy levels values of (^{94}Zr)

J^+	Energy levels (Mev)			
	EXP.	Ref.[92]	IBM-1	IBM-2
0_1^+	0.0		0.0	0.0
2_1^+	0.919		0.901	0.863
4_1^+	1.470		1.853	1.746
6_1^+	3.143		2.860	2.849
8_1^+	3.632		3.928	3.576
0_2^+	1.301		1.638	1.733
2_2^+	1.672		1.703	1.753
4_2^+	2.330		2.621	2.660
6_2^+			3.596	3.589
2_3^+	2.152		2.473	2.268
3_1^+	2.508		2.530	2.662
4_3^+	2.861		3.340	3.170
5_1^+			3.451	3.442
6_3^+			4.273	4.080
7_1^+			4.428	4.167

4.1.8 ^{96}Zr -isotope

The results of ^{96}Zr -isotope calculated by IBM-1 and IBM-2 models have been compared with the experimental data [93] as shown in the table (4-10). The available data are limited to 2_1^+ , 4_1^+ , 6_1^+ , and 8_1^+ ; both IBM-1 and IBM-2 pulling down the 2_1^+ and 4_1^+ , and nearly producing

best fit for 6_1^+ and 8_1^+ . In the beta band both IBM-1 and IBM-2 pushing up 0_2^+ , but showing good fit for 2_2^+ , 4_2^+ , and 6_2^+ . The experimental energy value for gamma band for states 2_3^+ , 4_3^+ , 5_1^+ , 6_3^+ , and 7_1^+ are 2.668, 3.082, 3.309, 4.430, and 5.066 MeV, both IBM-1 and IBM-2 are fitting well the 2_3^+ state, but both pushed 4_3^+ and 5_1^+ states higher, while the 6_3^+ and 7_1^+ states are slightly pushed up by IBM-1, and slightly pulled down by IBM-2. Our result compared to the ref [42,43] are good fitted in both IBM-1 and IBM-2.

Table (4-10): the comparison between the calculated and the experimental energy levels values of (^{96}Zr)

J^+	Energy levels (Mev)			
	EXP.	Ref.[93]	IBM-1	IBM-2
0_1^+	0.0		0.0	0.0
2_1^+	1.750		1.284	1.277
4_1^+	2.750		2.322	2.407
6_1^+	3.483		3.374	3.443
8_1^+	4.390		4.622	4.475
0_2^+	1.581		1.828	1.998
2_2^+	2.226		2.179	2.349
4_2^+	2.857		3.091	2.881
6_2^+	3.772		4.052	3.578
2_3^+	2.668		2.464	2.609
3_1^+			3.235	3.043
4_3^+	3.082		3.590	3.378
5_1^+	3.309		3.892	3.501
6_3^+	4.430		4.594	3.858
7_1^+	5.066		5.269	4.262

4.1.9 ^{98}Zr -isotope

The values of the low-lying positive parity states of ^{98}Zr -isotope calculated by IBM-1 and IBM-2 models have been compared with the experimental data [94] as shown in the table (4-11). These available data are limited to 2_1^+ , 4_1^+ , 6_1^+ , and 8_1^+ . Both IBM-1 and IBM-2 nicely

fitted ground state band and the beta band states. The experimental energy values of gamma band for states 2_3^+ and 4_3^+ are 1.744, 3.271 MeV, both IBM-1 and IBM-2 fitted nicely the 2_3^+ state, but both are pulling down 4_3^+ state by small amount, schematically not bad result for other states. Our results in compare to the ref [42,43] are reasonable in both IBM-1 and IBM-2.

Table (4-11): the comparison between the calculated and the experimental energy levels values of (^{98}Zr)

J^+	Energy levels (Mev)			
	EXP.	Ref.[94]	IBM-1	IBM-2
0_1^+	0.0		0.0	0.0
2_1^+	1.222		0.814	0.943
4_1^+	1.843		1.580	1.539
6_1^+	2.491		2.363	2.384
8_1^+	3.217		3.260	3.280
0_2^+	0.854		1.195	1.136
2_2^+	1.590		1.595	1.596
4_2^+	2.277		2.315	2.461
6_2^+	3.117		3.222	3.359
2_3^+	1.744		1.964	1.771
3_1^+			2.502	2.346
4_3^+	3.271		2.814	2.534
5_1^+			3.235	3.065
6_3^+			3.617	3.366
7_1^+			3.997	3.828

4.1.10 ^{100}Zr -isotope

The values of the low-lying positive parity states of ^{100}Zr -isotope calculated by IBM-1 and IBM-2 models have been compared with the experimental data [95] as shown in the table (4-12). It is clear from the table that the available data are limited to 2_1^+ , 4_1^+ , 6_1^+ , and 8_1^+ which are located at 0.213, 0.565, 1.062, and 1.687 MeV respectively; both IBM-1 and IBM-2 are fitting well these states in G.S. band. In the beta band experimental data for 0_2^+ , 2_2^+ , 4_2^+ , and 6_2^+ are

0.829, 0.879, 1.294, and 1.856 MeV, both IBM-1 and IBM-2 reproduced acceptably good fit for 0_2^+ , 2_2^+ and 4_2^+ states, but the 6_2^+ is pushed up by IBM-1 and pulled down by IBM-2 by small amount. The experimental energy values for gamma band for states 2_3^+ , 3_1^+ and 7_1^+ are 1.196, 1.295, and 2.480 MeV, IBM-1 and IBM-2 predict best fit for these states. Our result compared to the ref [42,43,52] and look good in both IBM-1 and IBM-2.

Table (4-12): the comparison between the calculated and the experimental energy levels values of (^{100}Zr)

J^+	Energy levels (Mev)			
	EXP.	Ref.[95]	IBM-1	IBM-2
0_1^+	0.0		0.0	0.0
2_1^+	0.213		0.213	0.242
4_1^+	0.565		0.604	0.620
6_1^+	1.062		1.162	1.124
8_1^+	1.687		1.876	1.737
0_2^+	0.829		0.543	0.716
2_2^+	0.879		0.891	0.720
4_2^+	1.294		1.404	0.932
6_2^+	1.856		2.055	1.405
2_3^+	1.196		1.126	0.991
3_1^+	1.295		1.409	1.195
4_3^+			1.830	1.290
5_1^+			2.140	1.616
7_1^+	2.480		2.723	2.150

4.1.11 ^{102}Zr -isotope

The values of the low-lying positive parity states of ^{102}Zr -isotope calculated by IBM-1 and IBM-2 models have been compared with the experimental data [96] as shown in the table (4-13). The available data are limited to 2_1^+ , 4_1^+ , 6_1^+ , and 8_1^+ ; both IBM-1 and IBM-2 nearly produced best fit for these states in ground state band and in the beta band for 0_2^+ , 2_2^+ , 4_2^+ , and 6_2^+ states. The experimental energy value for gamma band for

states 2_3^+ , 3_1^+ , 4_3^+ , 6_3^+ and 7_1^+ are 1.211, 1.242, 1.538, 1.829 and 2.925 MeV, both IBM-1 and IBM-2 fitted 2_3^+ , 3_1^+ and 4_3^+ states nicely, but 6_3^+ in both IBM-1 and IBM-2 is pushed up by small amount, while both pulled down the 7_1^+ state. Our result in compare to the ref [42,51] is good in both IBM-1 and IBM-2.

Table (4-13): the comparison between the calculated and the experimental energy levels values of (^{102}Zr)

J^+	Energy levels (Mev)			
	EXP.	Ref.[96]	IBM-1	IBM-2
0_1^+	0.0		0.0	0.0
2_1^+	0.152		0.140	0.142
4_1^+	0.478		0.448	0.468
6_1^+	0.965		0.914	0.945
8_1^+	1.595		1.529	1.581
0_2^+	0.895		0.904	0.877
2_2^+	1.036		0.985	0.910
4_2^+	1.387		1.354	1.112
6_2^+	1.653		1.861	1.511
2_3^+	1.211		1.183	1.226
3_1^+	1.242		1.197	1.412
4_3^+	1.538		1.625	1.618
5_1^+			1.658	1.868
6_3^+	1.829		2.220	2.005
7_1^+	2.925		2.265	2.570

4.1.12 ^{104}Zr -isotope

The values of the low-lying positive parity states of ^{104}Zr -isotope calculated by IBM-1 and IBM-2 models have been compared with the experimental data [97] as shown in the table (4-14). It is clear from the table that the available data are limited to 2_1^+ , 4_1^+ , 6_1^+ , 8_1^+ , 10_1^+ , 12_1^+ , and 14_1^+ states are 0.139, 0.452, 0.926, 1.550, 2.315, 3.210, and

4.224 MeV, are well reproduced by both IBM-1 and IBM-2. The G-band, beta band and gamma band are well reproduced by both IBM-1 and IBM-2 in compare with ref [41], and best reproduce the G-band if compared to ref [42].

Table (4-14): the comparison between the calculated and the experimental energy levels values of (^{104}Zr)

J^+	Energy levels (Mev)			
	EXP.	Ref.[97]	IBM-1	IBM-2
0_1^+	0.0		0.0	0.0
2_1^+	0.139		0.141	0.140
4_1^+	0.452		0.450	0.471
6_1^+	0.926		0.913	0.950
8_1^+	1.550		1.522	1.563
10_1^+	2.315		2.271	2.316
12_1^+	3.210		3.155	3.231
14_1^+	4.224		4.171	4.346
2_2^+			0.745	0.955
3_1^+			0.949	1.246
4_2^+			1.113	1.370
5_1^+			1.400	1.785
6_2^+			1.613	1.886
7_1^+			1.995	2.295
0_2^+			0.848	1.094
2_3^+			1.133	1.389
4_3^+			1.517	1.769
6_3^+			2.093	2.222

4.1.13 ^{106}Zr -isotope

The values of the low-lying positive parity states of ^{106}Zr -isotope calculated by IBM-1 and IBM-2 models have been compared with the experimental data [98,99,100] as shown in the table (4-15). It is clear from the table that the available data are limited to 2_1^+ , 4_1^+ , 6_1^+ , and 8_1^+

states are 0.152, 0.477, 0.946, and 1.572 MeV, its best reproduced by both IBM-1 and IBM-2. The experimental data of 2_2^+ state is 0.607 MeV. The G-band, beta band and gamma band are well reproduced by both IBM-1 and IBM-2 if compared with ref [41], and best reproduce the G-band if compared to ref [44].

Table (4-15): the comparison between the calculated and the experimental energy levels values of (^{106}Zr)

J^+	Energy levels (Mev)			
	EXP.	Ref.[98,99,100]	IBM-1	IBM-2
0_1^+	0.0		0.0	0.0
2_1^+	0.152		0.154	0.114
4_1^+	0.477		0.483	0.455
6_1^+	0.946		0.971	0.950
8_1^+	1.572		1.609	1.612
10_1^+			2.390	2.433
12_1^+			3.308	3.431
14_1^+			4.360	4.621
2_2^+	0.607		0.794	0.888
3_1^+			1.028	1.160
4_2^+			1.192	1.284
5_1^+			1.511	1.669
6_2^+			1.724	1.880
7_1^+			2.139	2.347
0_2^+			0.827	1.001
2_3^+			1.145	1.294
4_3^+			1.592	1.682
6_3^+			2.204	2.141

4.1.14 ^{108}Zr -isotope

The values of the low-lying positive parity states of ^{108}Zr -isotope calculated by IBM-1 and IBM-2 models have been compared with the experimental data [98,99,101] as shown in the table (4-16). The available data are limited to 2_1^+ , 4_1^+ , 6_1^+ , and 8_1^+ states they have been nicely

reproduced by IBM-1 and IBM-2. The experimental data of 2_2^+ , 3_1^+ , 4_2^+ , and 6_2^+ states are 0.604, 0.947, 0.947, and 1.725 MeV, in gamma band are well reproduced in both IBM-1 and IBM-2. Also the experimental data of 2_3^+ in beta band with 0.948 MeV is good fitted by both IBM-1 and IBM-2. All bands are finely produced by both IBM-1 and IBM-2 in compare with ref [41].

Table (4-16): the comparison between the calculated and the experimental energy levels values of (^{108}Zr)

J^+	Energy levels (Mev)			
	EXP.	Ref.[98,99,101]	IBM-1	IBM-2
0_1^+		0.0	0.0	0.0
2_1^+		0.174	0.170	0.141
4_1^+		0.522	0.516	0.480
6_1^+		1.000	1.021	0.990
8_1^+		1.642	1.675	1.676
10_1^+			2.470	2.559
12_1^+			3.402	3.661
14_1^+			4.467	4.953
2_2^+	0.604		0.748	0.646
3_1^+	0.947		1.018	0.936
4_2^+	0.947		1.173	1.046
5_1^+			1.524	1.379
6_2^+	1.725		2.075	1.607
7_1^+			2.172	1.936
0_2^+			0.760	0.719
2_3^+	0.948		1.119	0.908
4_3^+			1.572	1.156
6_3^+			2.208	1.630

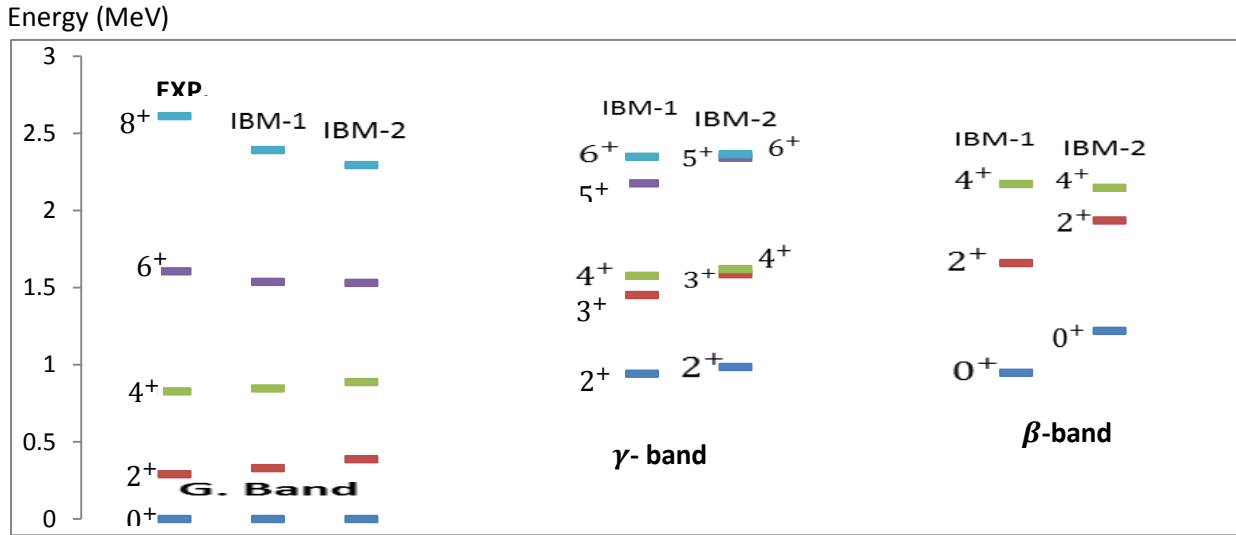


Figure (4-2): a comparison between the experimental low -lying positive parity states in ^{80}Zr [86]. With those obtained by IBM-1 and IBM-2 for ground, gamma, and beta bands.

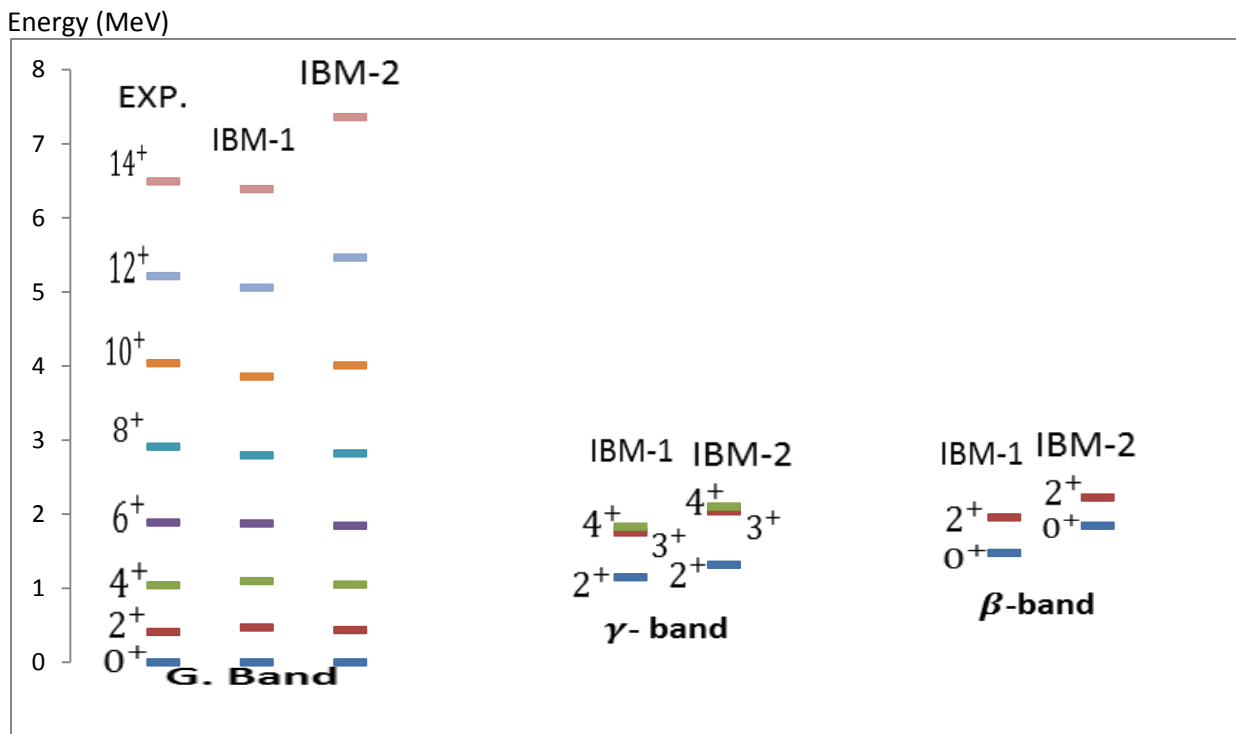


Figure (4-3): a comparison between the experimental low -lying positive parity states in ^{82}Zr [87] with those obtained by IBM-1 and IBM-2 for the ground, gamma, and beta bands.

Energy (MeV)

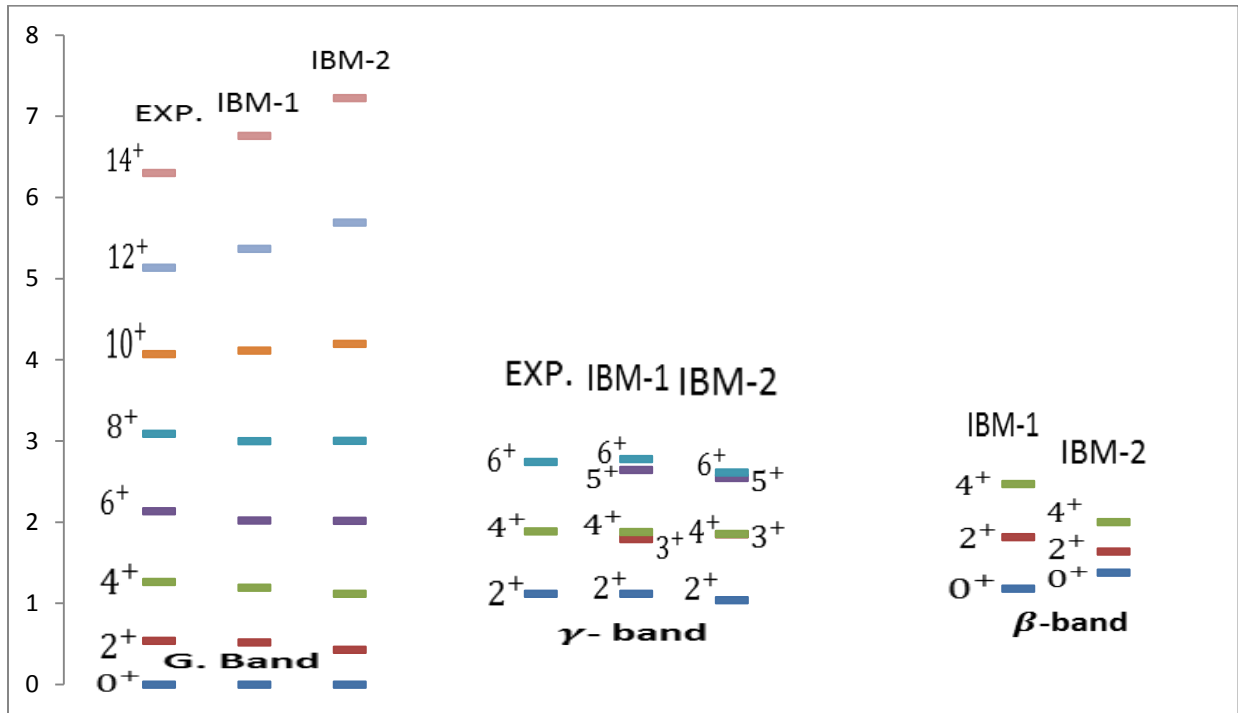


Figure (4-4): a comparison between the experimental low –lying positive parity states in ^{84}Zr [88] with those obtained by IBM-1 and IBM-2 for ground, gamma, and beta bands.

Energy (MeV)

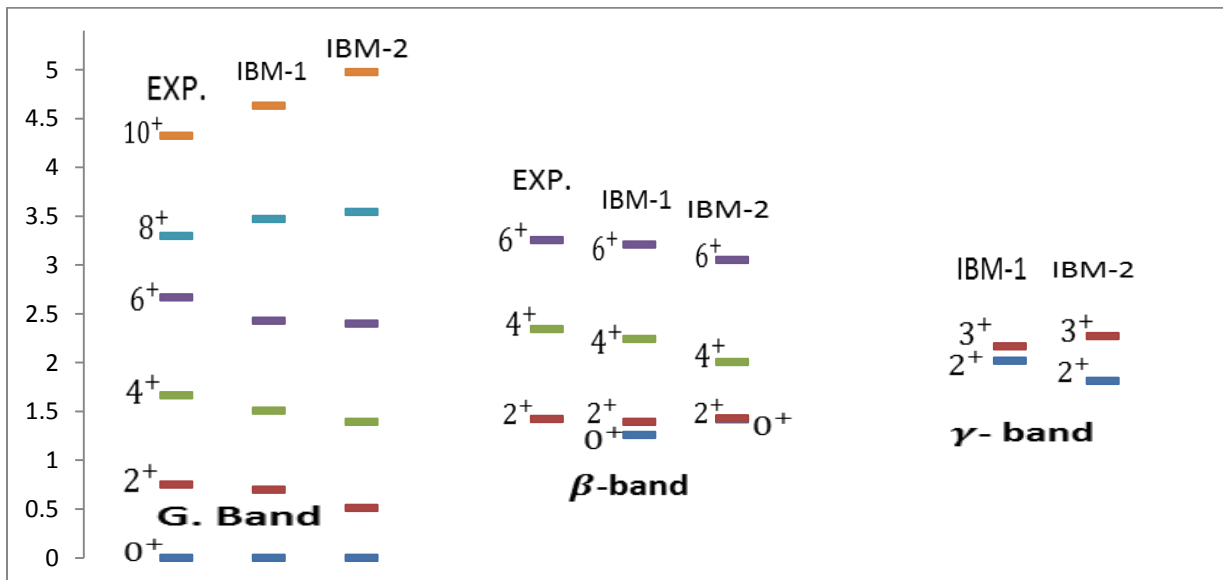


Figure (4-5): a comparison between the experimental low –lying positive parity states in ^{86}Zr [89] with those obtained by IBM-1 and IBM-2 for ground, gamma, and beta bands.

Energy (MeV)

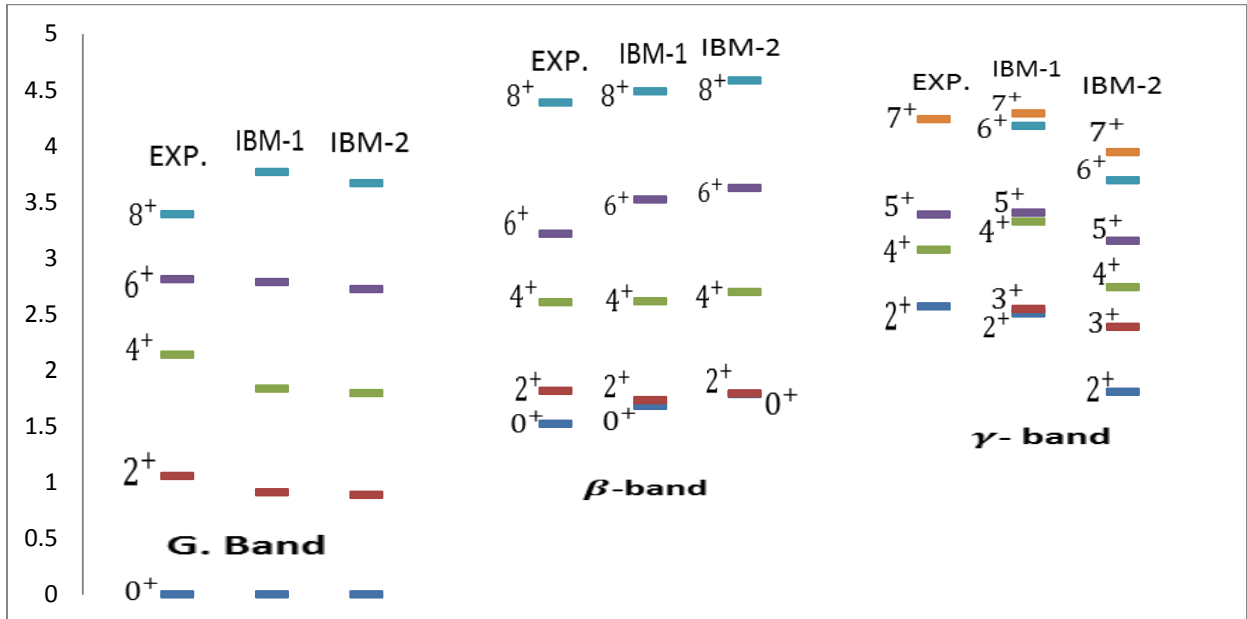


Figure (4-6): a comparison between the experimental low –lying positive parity states in ^{88}Zr [90] with those obtained by IBM-1 and IBM-2 for ground, gamma, and beta bands

Energy (MeV)

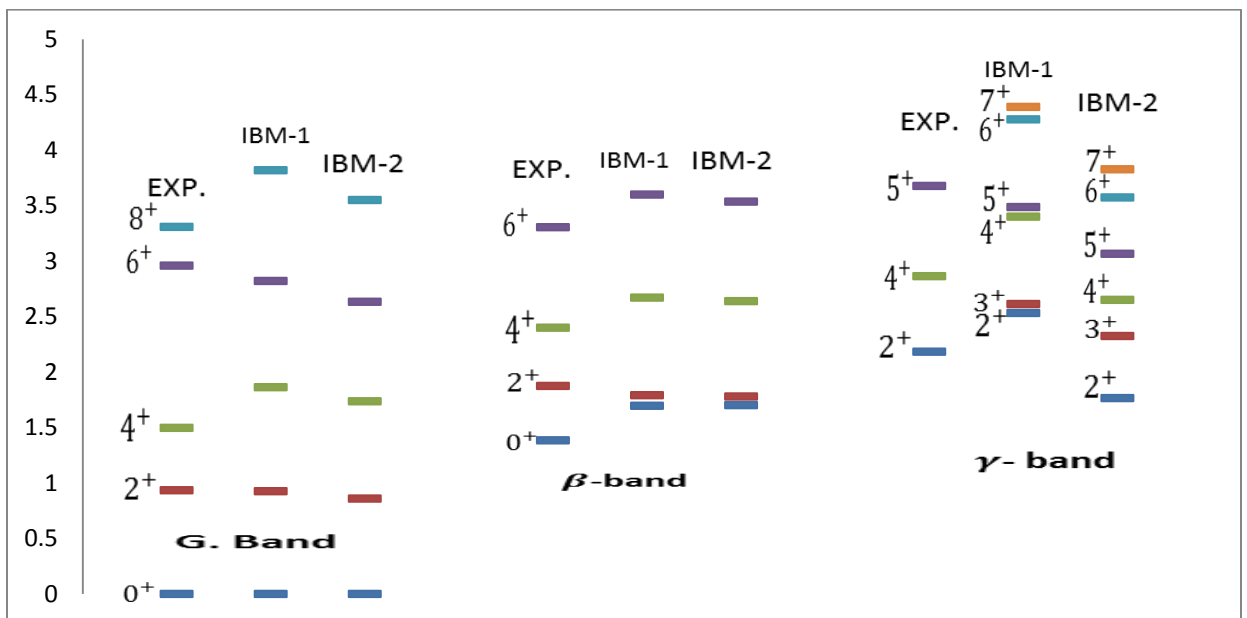


Figure (4-7): a comparison between the experimental low –lying positive parity states in ^{92}Zr [91] with those obtained by IBM-1 and IBM-2 for ground, gamma, and beta bands.

Energy (MeV)

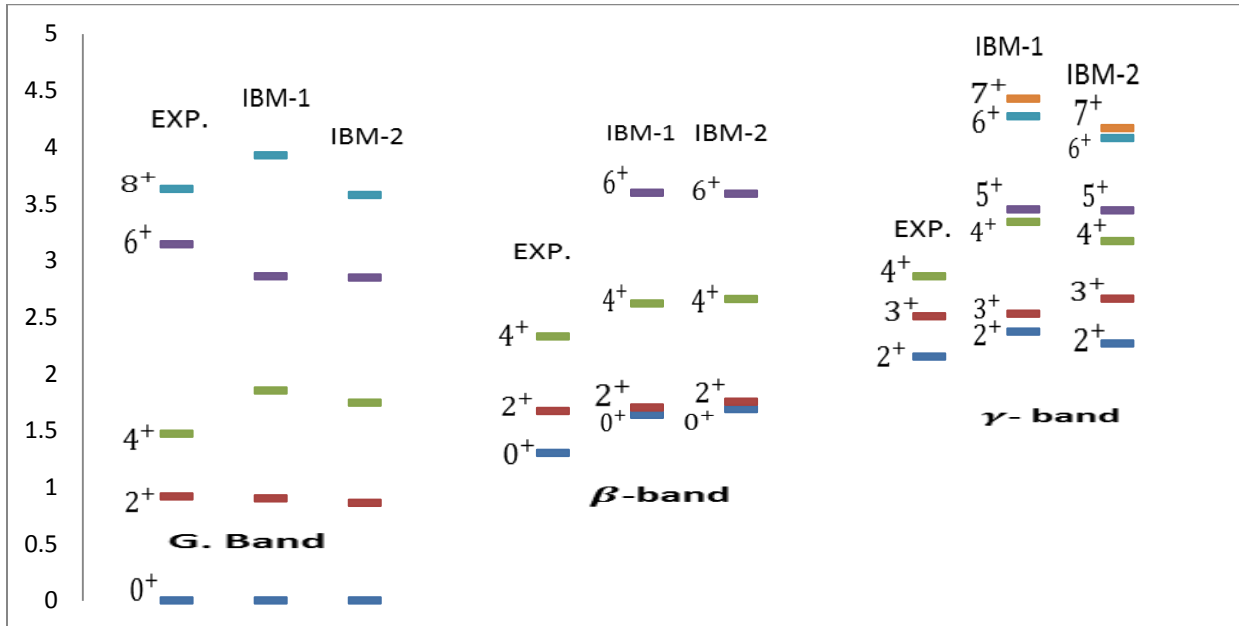


Figure (4-8): a comparison between the experimental low -lying positive parity states in ^{94}Zr [92] with those obtained by IBM-1 and IBM-2 for ground, gamma, and beta bands.

Energy (MeV)

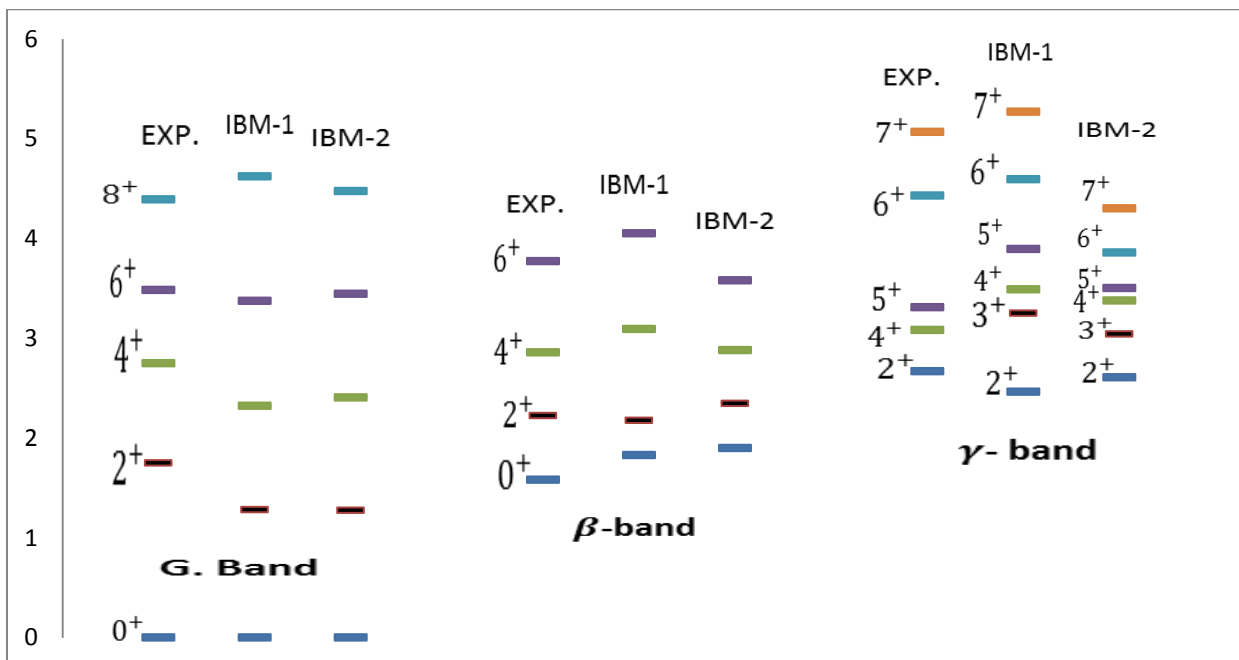


Figure (4-9): a comparison between the experimental low -lying positive parity states in ^{96}Zr [93] with those obtained by IBM-1 and IBM-2 for ground, gamma, and beta bands.

Energy (MeV)

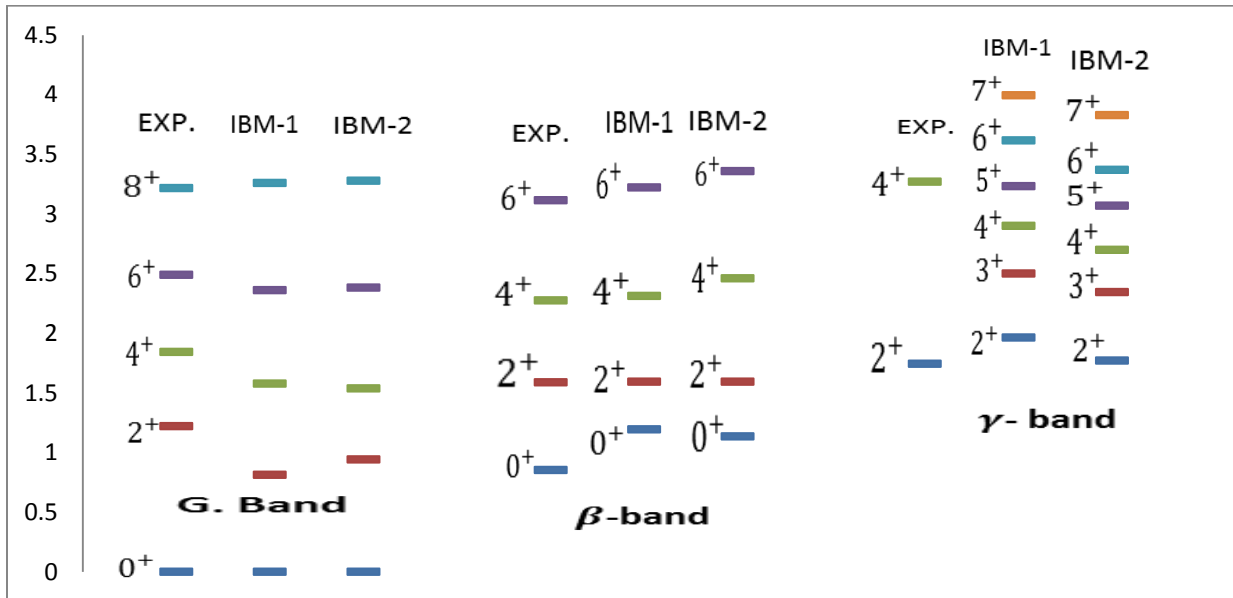


Figure (4-10): a comparison between the experimental low –lying positive parity states in ^{98}Zr [94] with those obtained by IBM-1 and IBM-2 for ground, gamma, and beta bands.

Energy (MeV)

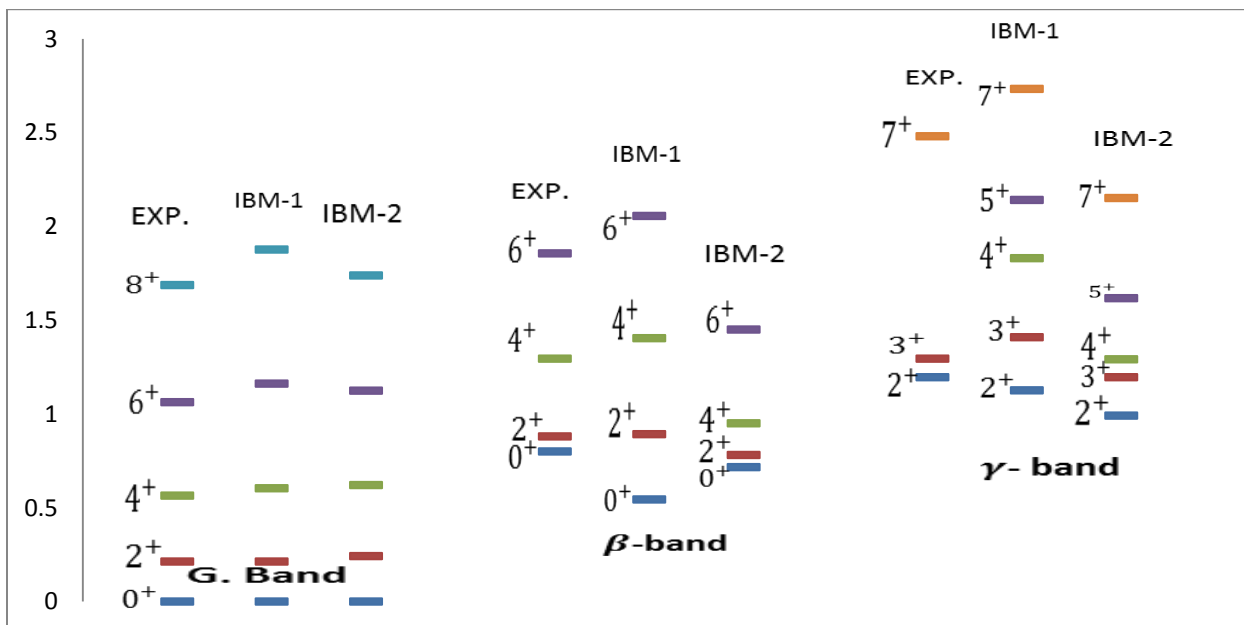


Figure (4-11): a comparison between the experimental low –lying positive parity states in ^{100}Zr [95] with those obtained by IBM-1 and IBM-2 for ground, gamma, and beta bands.

Energy (MeV)

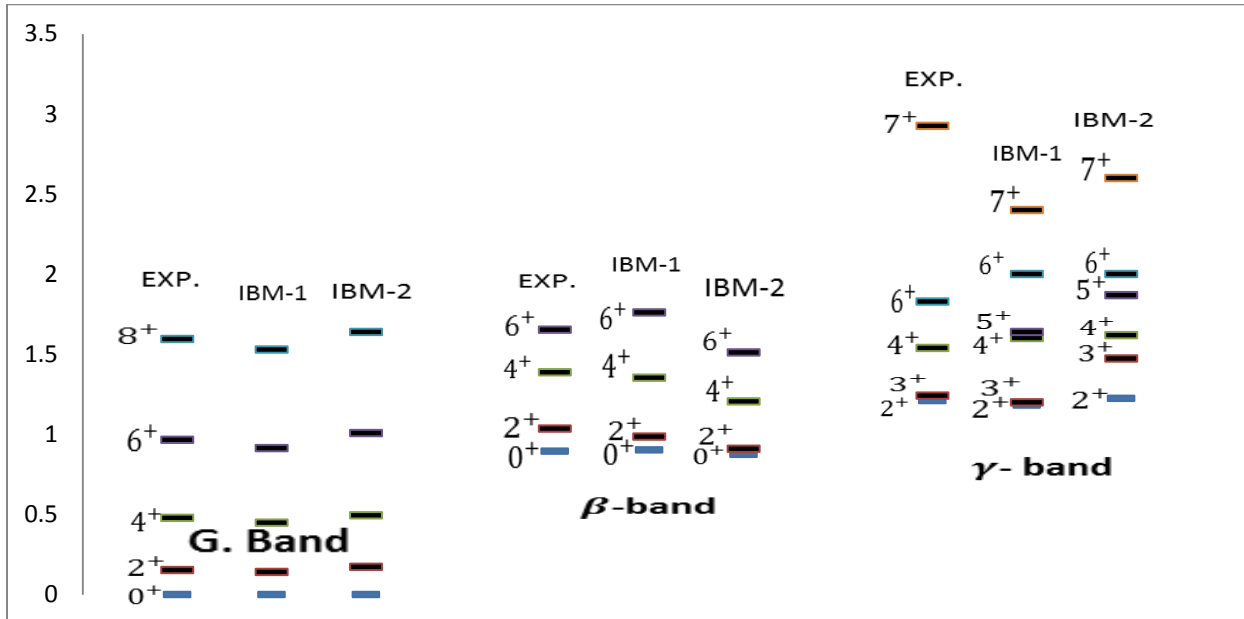


Figure (4-12): a comparison between the experimental low -lying positive parity states in ^{102}Zr [96] with those obtained by IBM-1 and IBM-2 for ground, gamma, and beta bands

Energy (MeV)

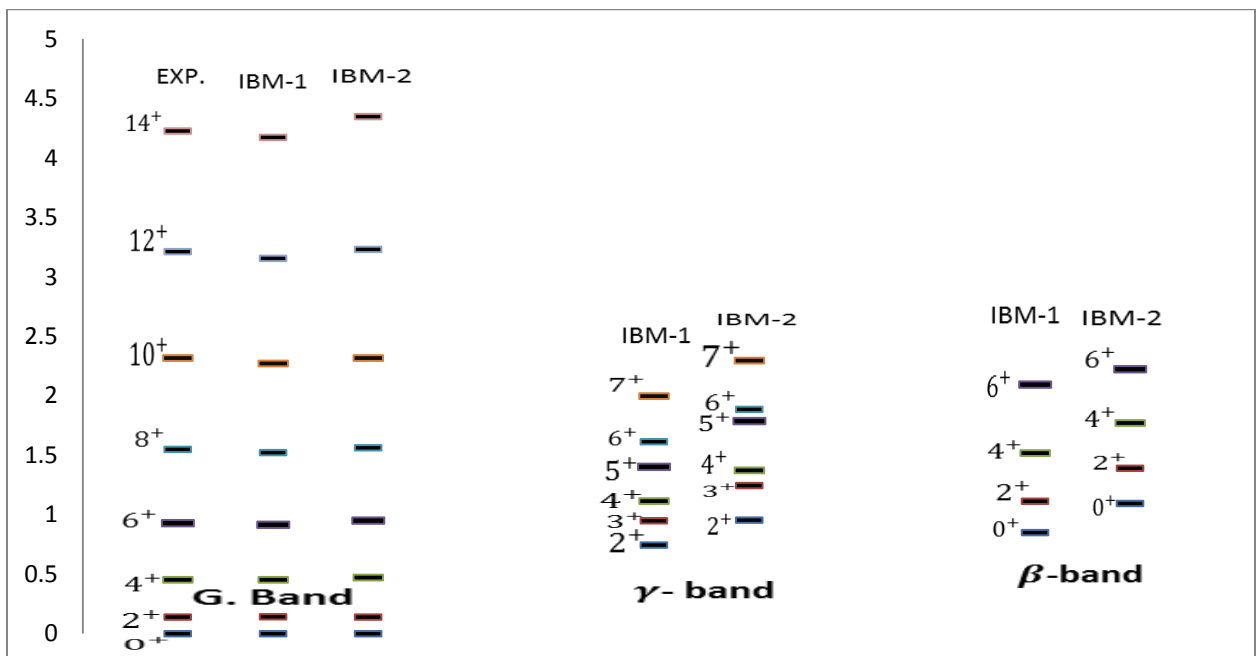


Figure (4-13): a comparison between the experimental low -lying positive parity states in ^{104}Zr [97] with those obtained by IBM-1 and IBM-2 for ground, gamma, and beta bands

Energy (MeV)

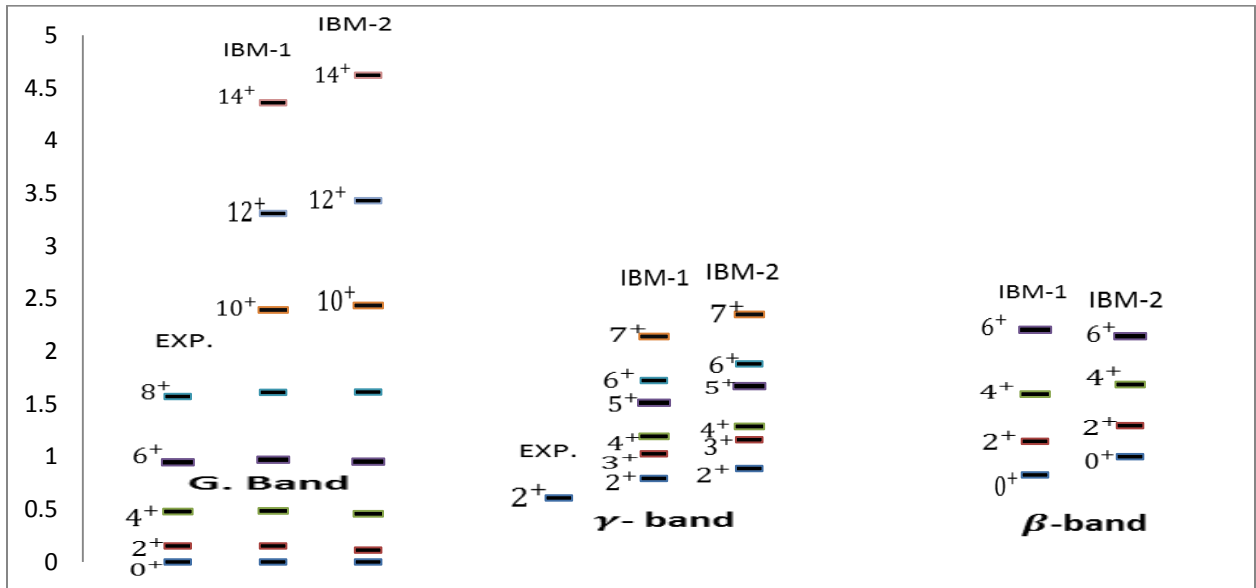


Figure (4-14): a comparison between the experimental low -lying positive parity states in ^{106}Zr [98,99,100] with those obtained by IBM-1 and IBM-2 for ground , gamma, and beta bands

Energy (MeV)

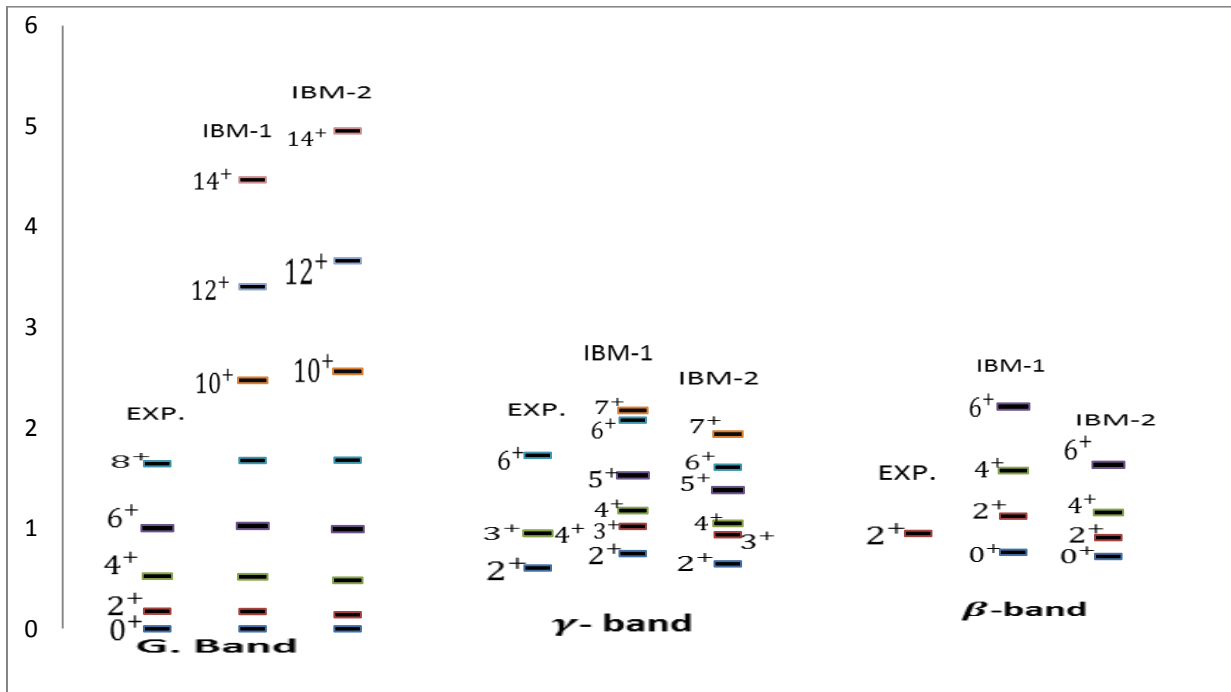


Figure (4-15): a comparison between the experimental low -lying positive parity states in ^{108}Zr [98, 99, 101] with those obtained by IBM-1 and IBM-2 for ground, gamma, and beta bands

The energy ratios $\left(\frac{E4_1^+}{E2_1^+}\right)$, $\left(\frac{E2_2^+}{E2_1^+}\right)$, and $\left(\frac{E6_1^+}{E2_1^+}\right)$ of the selected Zr-isotopes, has been calculated in the frame work of IBM-1, together with their corresponding experimental values are plotted respectively against the neutron numbers of Zr-isotopes and displayed in figures (4-16), (4-17), and (4-18). And the figures show that the Zr-isotopes evidence are considering as vibrational, rotational, and gamma soft symmetries. Generally the IBM-1 calculations of the values of above ratios are agree with the experimental energy ratios values.

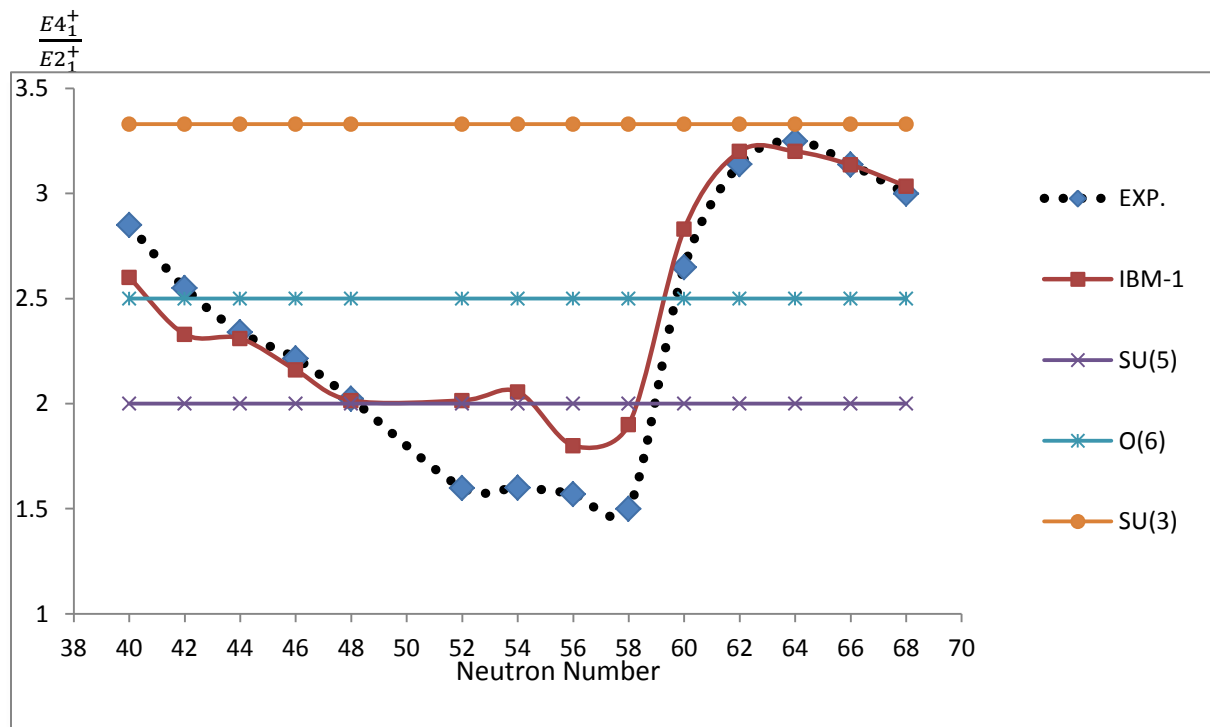


Figure (4-16): experimental and calculated values of the energy ratios $\frac{E4_1^+}{E2_1^+}$ as a function of neutron number for $^{80-108}\text{Zr}$ isotopes.

$$\frac{E2_2^+}{E2_1^+}$$

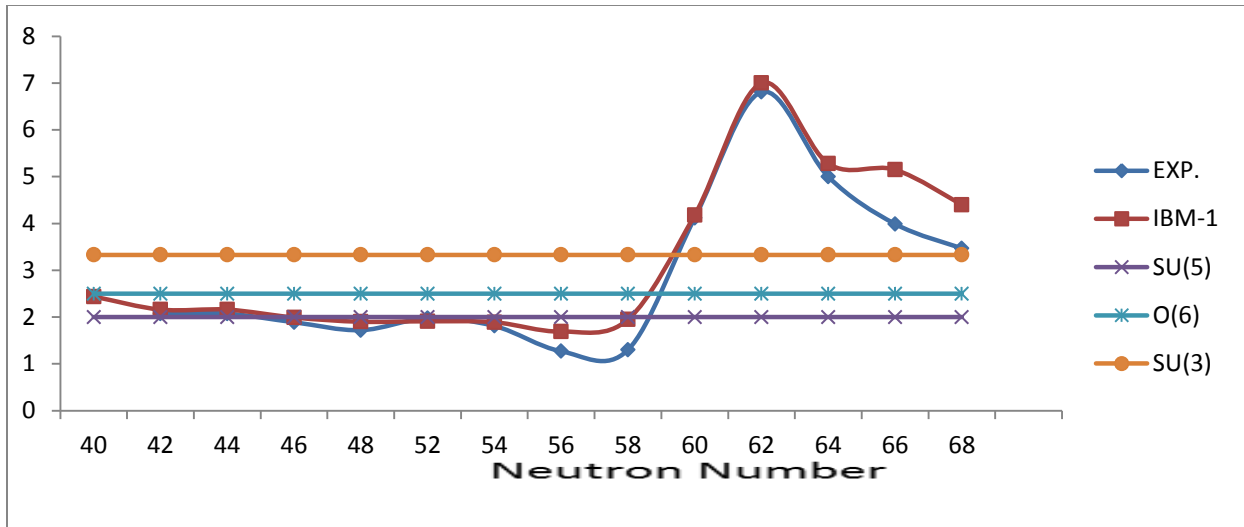


Figure (4-17): Experimental and calculated values of the energy ratios $\frac{E2_2^+}{E2_1^+}$ as a function of neutron number for $^{80-108}\text{Zr}$ isotopes.

$$\frac{E6_1^+}{E2_1^+}$$

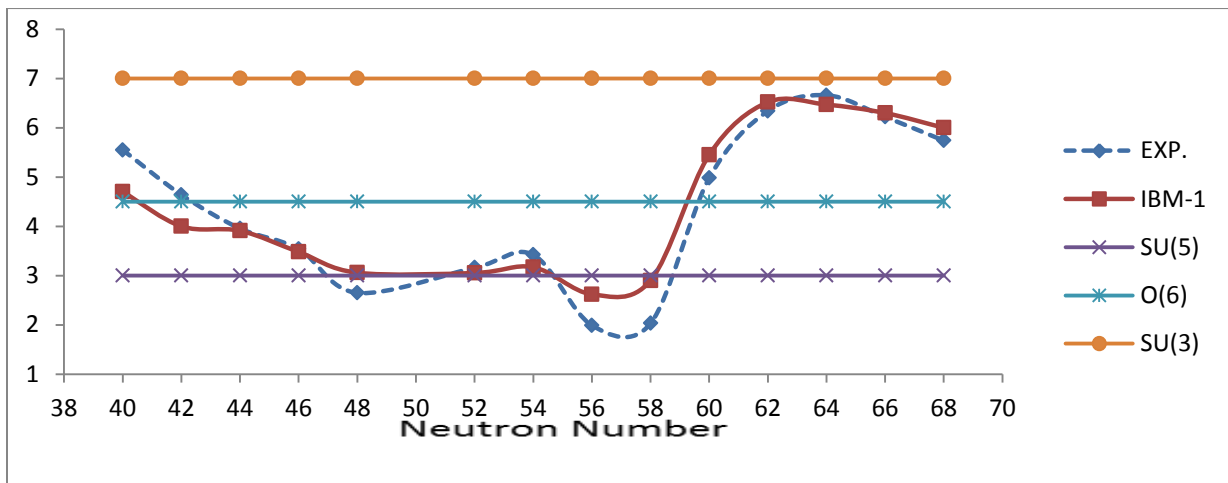
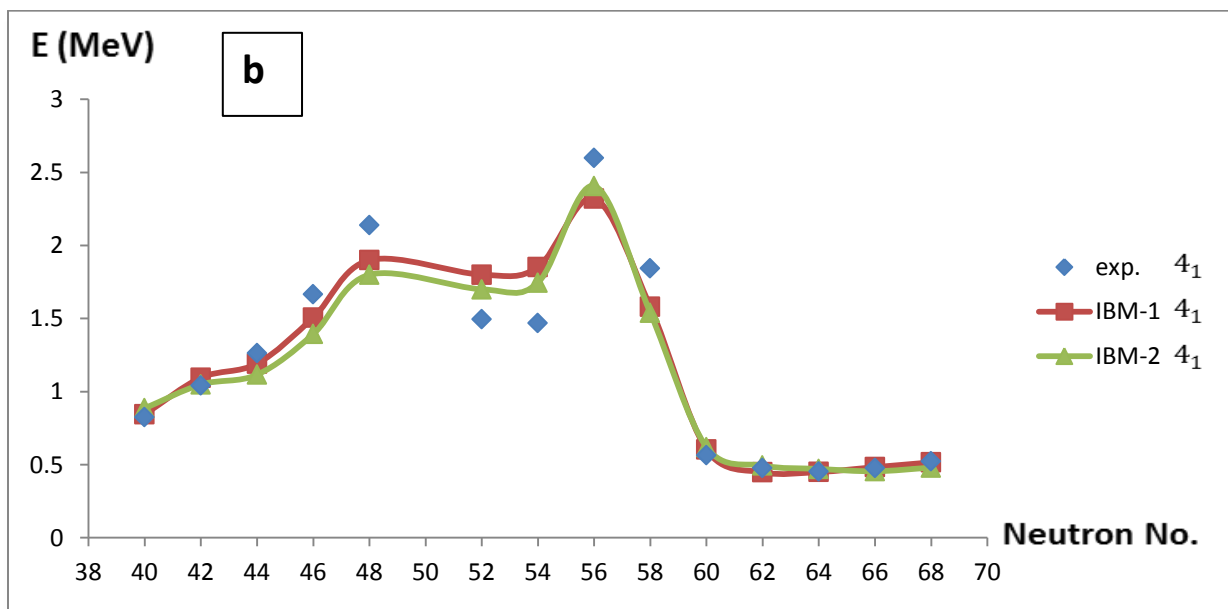
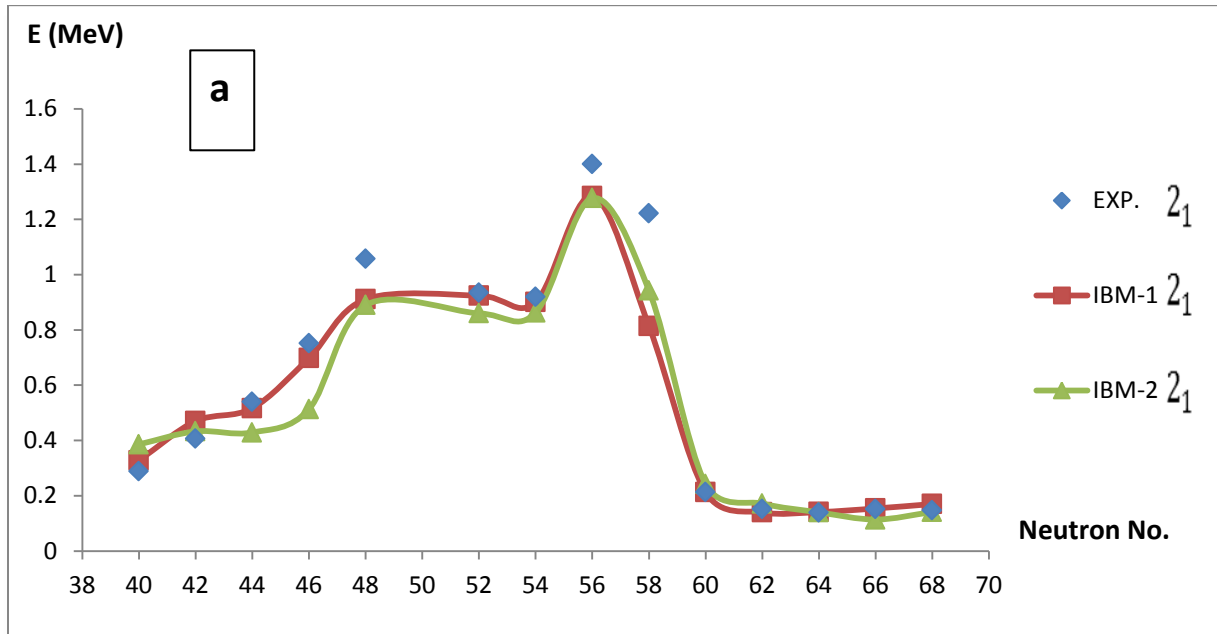


Figure (4-18): Experimental and calculated values of the energy ratios $\frac{E6_1^+}{E2_1^+}$ as a function of neutron number for $^{80-108}\text{Zr}$ isotopes.

In figure (4-19) the calculated IBM-1 and IBM-2 energy values of the ground band have been plotted as a function of the neutron numbers of $^{80-108}\text{Zr}$ -isotope. In figures (4-19a), (4-19b), and (4-19c) the energies for some selected states of the ground band, such as 2_1^+ , 4_1^+ , and 6_1^+ respectively are well fitted in both IBM-1 and IBM-2.



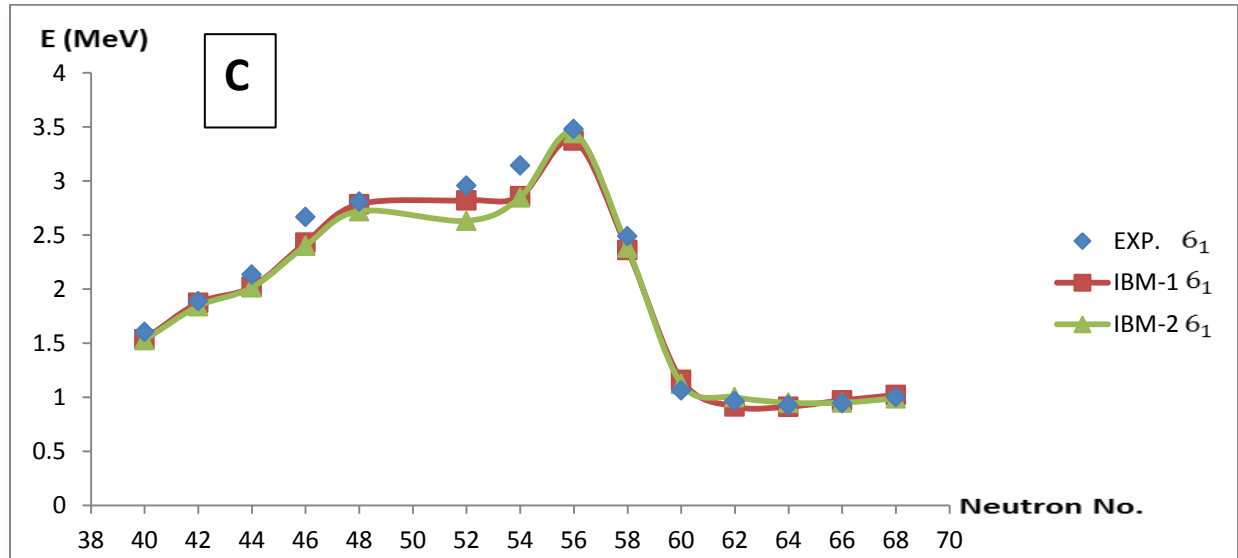
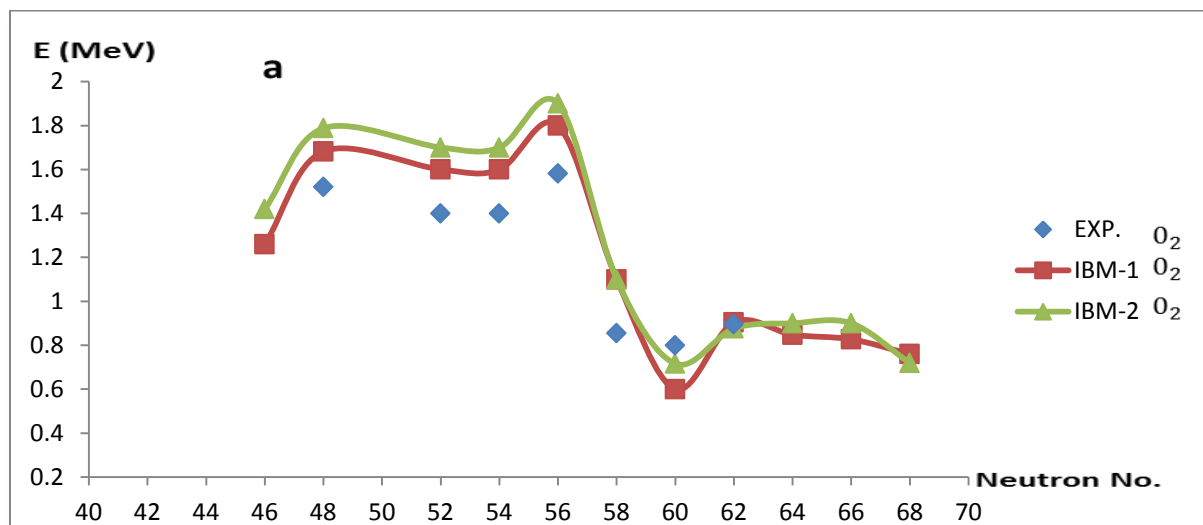


Figure (4-19): A comparison between the calculated energy values of the IBM-1 and IBM-2 and those of experimental data in the ⁸⁰⁻¹⁰⁸Zr-isotopes for the ground band of (a) 2₁⁺ state (b) 4₁⁺ state (c) 6₁⁺ state.

In figure (4-20) the calculated IBM-1 and IBM-2 energy values of the beta band have been plotted as a function of the neutron numbers of ⁸⁰⁻¹⁰⁸Zr-isotope. In figures (4-20a), (4-20b), and (4-20c) the energies for some selected states of beta band, such as 0₂⁺, 2₂⁺, and 4₂⁺ respectively are well fitted in both IBM-1 and IBM-2, and with increasing the neutron number both IBM-1 and IBM-2 are more acceptable result can be reproduced.



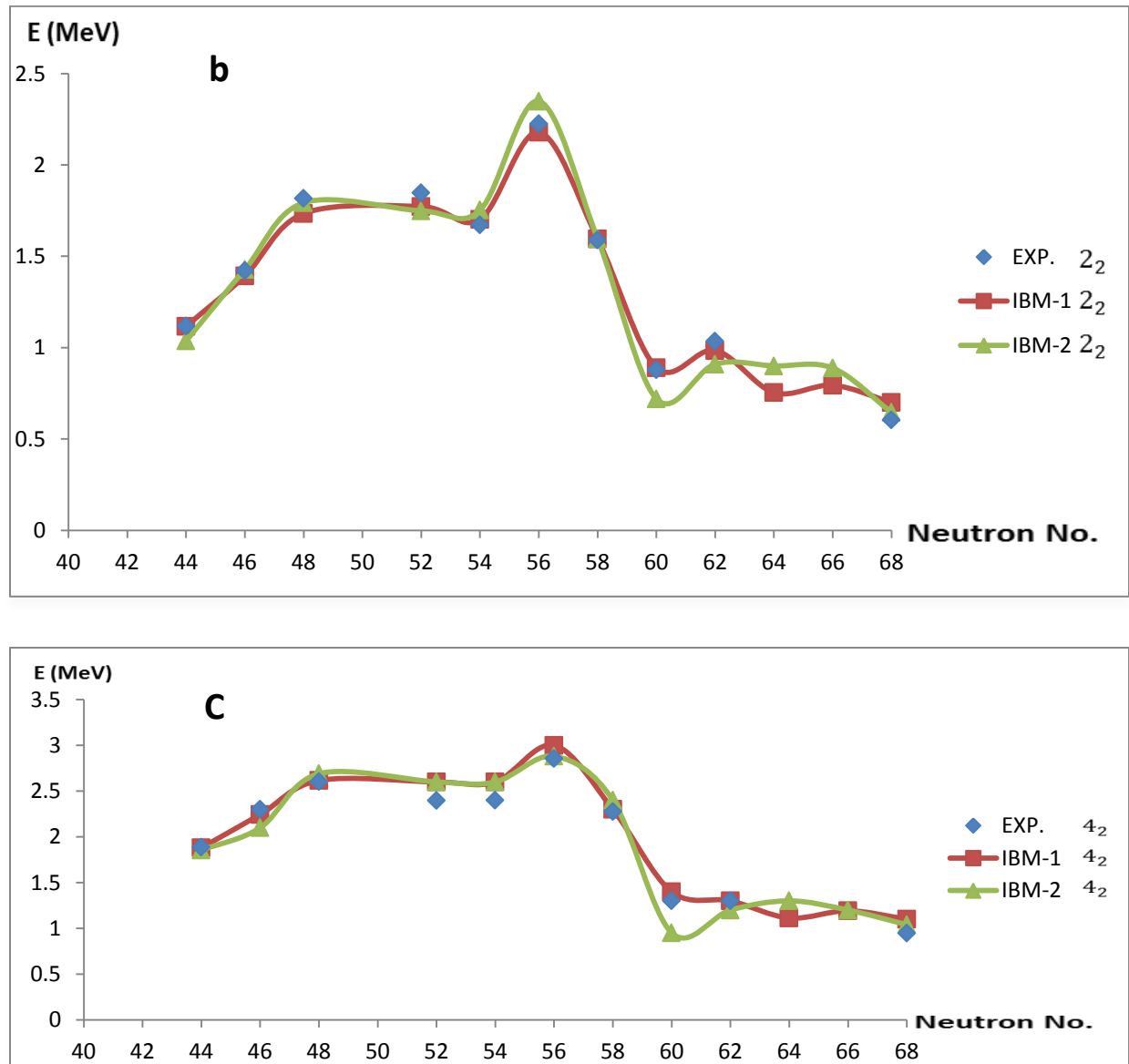
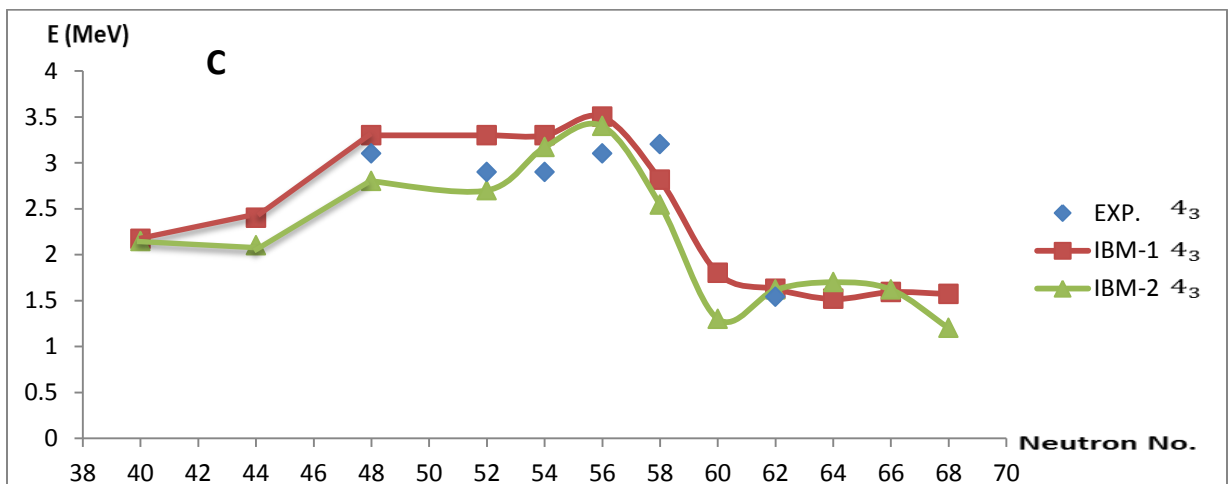
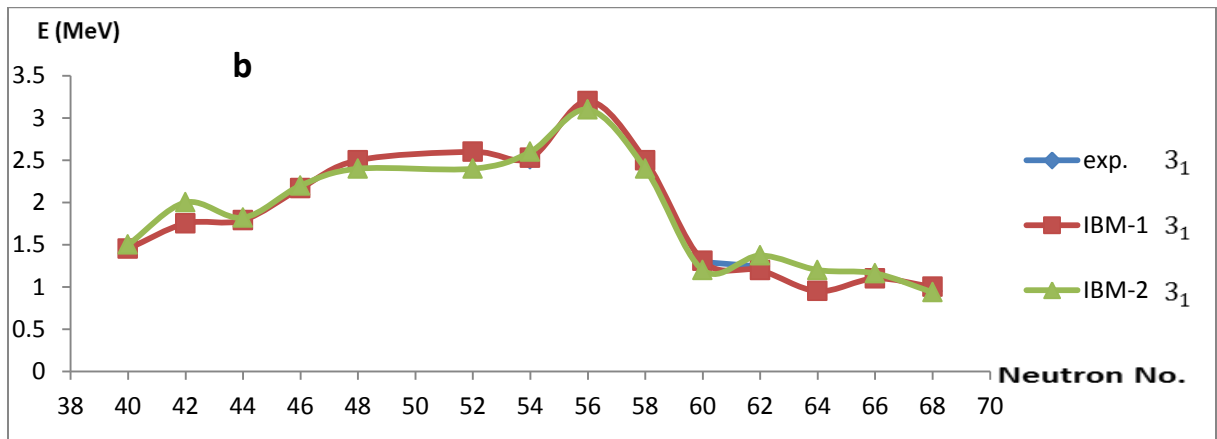
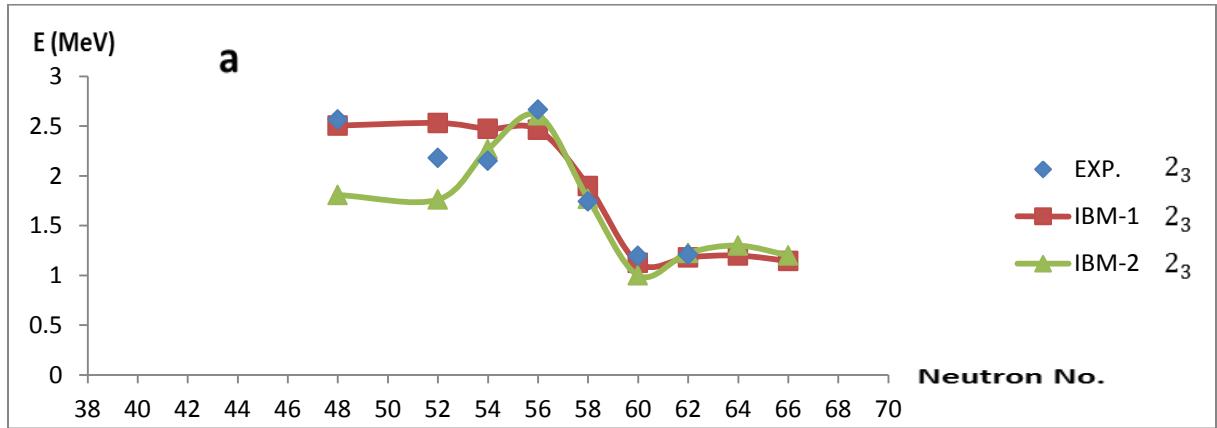


Figure (4-20): A comparison between the calculated energy values of the IBM-1 and IBM-2 and those of experimental data in the $^{80-108}\text{Zr}$ -isotopes for the beta band of (a) 0_2^+ state (b) 2_2^+ state (c) 4_2^+ state.

In the figure (4-21) the calculated IBM-1 and IBM-2 energy values of the gamma band have been plotted as a function of the neutron numbers of $^{80-108}\text{Zr}$ -isotope. In figures (4-21a), (4-21b), (4-21c), and (4-21d) the energies for some selected states of the gamma band, such as 2_3^+ , 3_1^+ , 4_3^+ , and 5_1^+ respectively are well best fitting in both IBM-1 and IBM-2, and with increasing the

neutron number both IBM-1 and IBM-2 are more acceptable result can be reproduced, in other hand we can say that the IBM-1 can reproduced the best result in some states and with increasing the neutron numbers compared to the IBM-2.



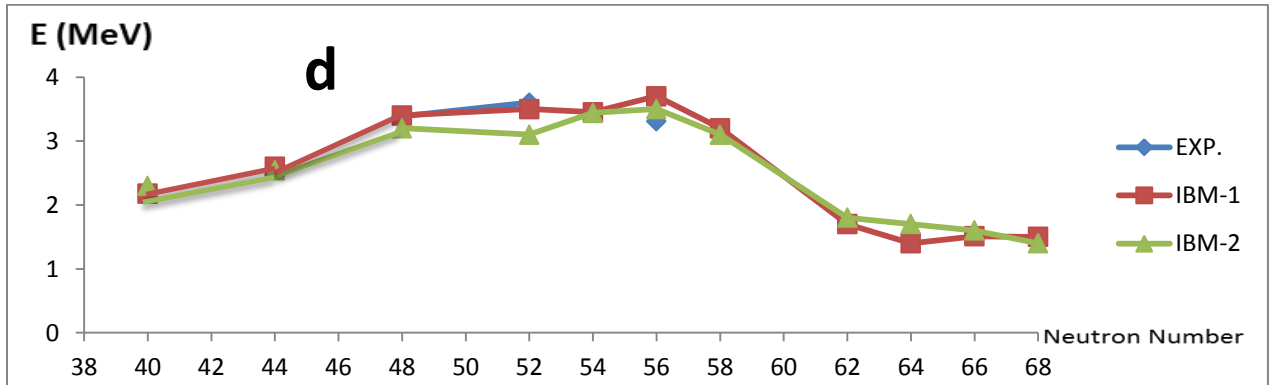


Figure (4-21): A comparison between the calculated energy values of the IBM-1 and IBM-2 and those of experimental data in the $^{80-108}\text{Zr}$ -isotopes for the gamma band of (a) 2_3^+ state (b) 3_1^+ state (c) 4_3^+ state (d) 5_1^+ .

From the resulting parameters that have been used in the calculation of IBM-2 which have been listed in table (4-2), one may conclude that the main features on nuclei are determined by the parameters (ε_d , K , χ_π , and χ_v). The parameters which have a great effect are plotted against the neutron numbers in $^{80-108}\text{Zr}$ -isotopes and presented in figures (4-22) and (4-23). Figure (4-22) shows (ε_d) as a function of the neutron numbers, and it is increasing and decreasing between ^{80}Zr and ^{86}Zr , and from ^{88}Zr starts to increasing and then nearly be constant until ^{98}Zr , then after increasing the neutron numbers from ^{100}Zr to ^{108}Zr the (ε_d) is decreasing and approaching zero. It is clear that K in the figure (4-23) has same behavior.

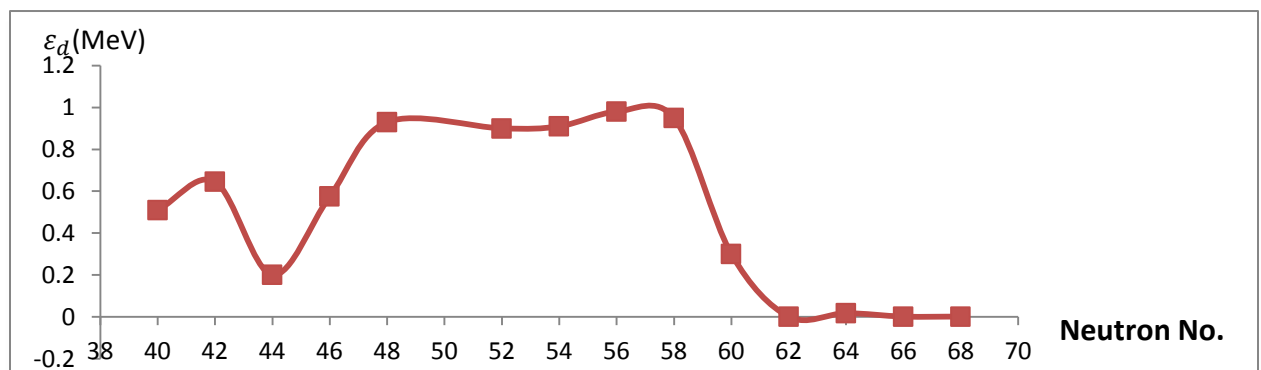


Figure (4-22): Variation of the parameter ε_d with the neutron numbers in $^{80-108}\text{Zr}$ isotopes for IBM-2.

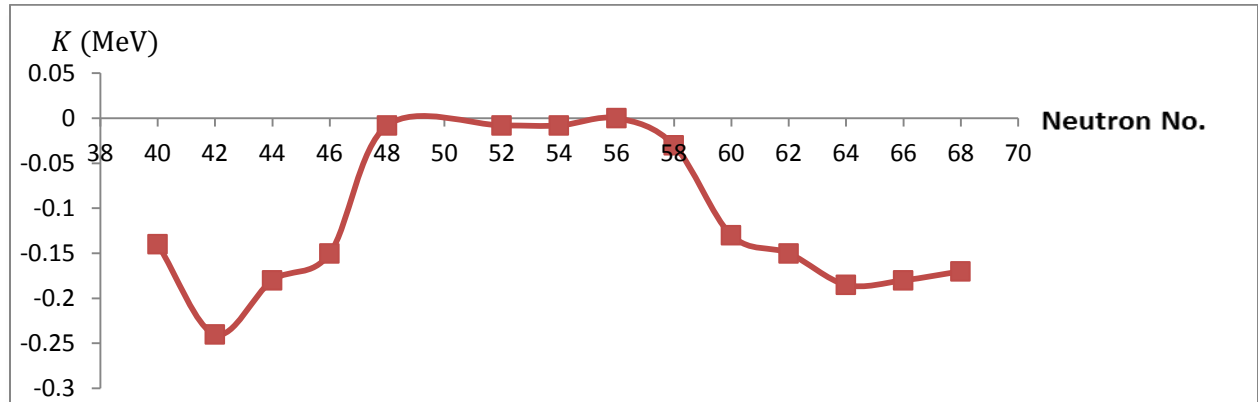


Figure (4-23): Variation of the parameter K with the neutron numbers in $^{80-108}\text{Zr}$ isotopes for IBM-2.

4.2 Mixed symmetry states

In the IBM-2 model, distinctions between neutron (ν) and proton (π) bosons are produced, and can reproduce all the results of IBM-1, but in addition contains extra states of what so called mixed symmetry states. These states are not totally symmetric in (sd) space and are allowed in IBM-2 because of the extra ($\nu \pi$) degree of freedom. A sensitive indication of mixed symmetry states description is due to the percentage of the F-spin contribution. Where $F = \frac{1}{2}$ for bosons with $F_{\max} = \frac{N_{\pi} + N_{\nu}}{2} = \frac{N}{2}$. Since states with maximum F-spin are symmetric. It should be remarked that states with $F_{\max} = \frac{N}{2}$ lie lowest in energy followed by $F = \frac{N}{2} - 1, \frac{N}{2} - 2, \dots$ etc., where the separation between states of mixed symmetry are determined by the Majorana terms. Table (4-17) shows the percentages of F-SPIN contribution in Zr- isotopes, some states in both three bands are fully symmetric for all Zr-isotopes such as 2_1^+ state, but in other hand 1_1^+ is a mixed symmetry state without e for all isotopes Zr^{96} , is not symmetric. The 2_2^+ state also is symmetric for all isotopes without ^{88}Zr , ^{100}Zr , and ^{102}Zr are mixed symmetry in 2_2^+ state. In the 2_3^+ state vice versa all isotopes are mixed symmetry without ^{88}Zr and ^{102}Zr are full symmetry, and ^{100}Zr also near mixed symmetry. In the 3_1^+ state ^{88}Zr , ^{92}Zr , ^{96}Zr , ^{100}Zr , and ^{108}Zr are mixed

symmetry, and ^{96}Zr is not symmetric, all other isotopes are full symmetric. In 0_3^+ state ^{94}Zr is full symmetric, ^{104}Zr and ^{106}Zr near symmetric, and ^{100}Zr is not symmetric, but all other isotopes are mixed symmetry.

Table (4-17): the percentages of F-spin contribution in Zr-isotopes for states that have the mixed symmetry characters.

isotopes	F-spin %100					
	2_1^+	2_2^+	2_3^+	1_1^+	3_1^+	0_3^+
Zr^{80}	%98.7	%97.7	%68.1	%64.7	%96	%79
Zr^{82}	%97.8	%95.6	%76.1	%60.7	%92.2	%73.4
Zr^{84}	%95.2	%88.5	%61.1	%57.9	%86.9	%70.7
Zr^{86}	%90.7	%82.6	%64.9	%54.9	%86.3	%55.1
Zr^{88}	%100	%50.9	%99.2	%50.0	%50	%50.2
Zr^{92}	%100	%99.1	%50.9	%50	%50	%50.7
Zr^{94}	%100	%100	%55.8	%55.6	%99.9	%100
Zr^{96}	%99.6	%84.5	%70.7	%28.2	%43.5	%70.6
Zr^{98}	%99.9	%99.5	%64.4	%63.5	%67.7	%63.9
Zr^{100}	%96.9	%64.6	%79	%61.6	%68.7	%43.7
Zr^{102}	%98	%68.5	%92.9	%66.1	%89.7	%52.2
Zr^{104}	%96.6	%95.6	%75.2	%68.4	%93.8	%85.1
Zr^{106}	%96.5	%94.1	%77.1	%70	%92.2	%81.3
Zr^{108}	%92.8	%80.1	%69.3	%64.2	%78.3	%63.4

Figures (4-24 and 4-25) are taken as an example to study the influence of the Majorana parameters ξ_1 , ξ_2 and ξ_3 on the mixed symmetry states or those contained mixed symmetry components, and some isotopes are taken for studying the affected the Majorana terms parameter. Figure (4-24a,b) shows that the $1_M^+ = 1_1^+$ in ^{104}Zr and ^{108}Zr levels is strongly affected by ξ_1 , show that 1_1^+ state is mixed symmetry for both isotopes, and figure(4-24c,d) shows that

3_M^+ ^{102}Zr and ^{106}Zr levels depends on the ξ_3 ,. The influence of ξ_2 parameter is shown in figure (4-25a,b), where it strongly effects the energies of all the levels considered to have a mixed symmetry components in ^{102}Zr and ^{108}Zr respectively and specially the 2^+ states. One of the important features is where two or more of states share the characters of mixed-symmetry, and that the case of 2_2^+ and 2_3^+ . With chosen values of ξ_2 , State 2_2^+ is effected by ξ_2 and carries totally or partially the properties of MS, and as the values of ξ_2 is increased such properties starts to be transferred to 2_3^+ . These characters in 2_2^+ states are less significant than that in 2_3^+ states, which can be seen in Figures (4-25a, and 4-25b) for the ^{102}Zr and ^{108}Zr respectively.

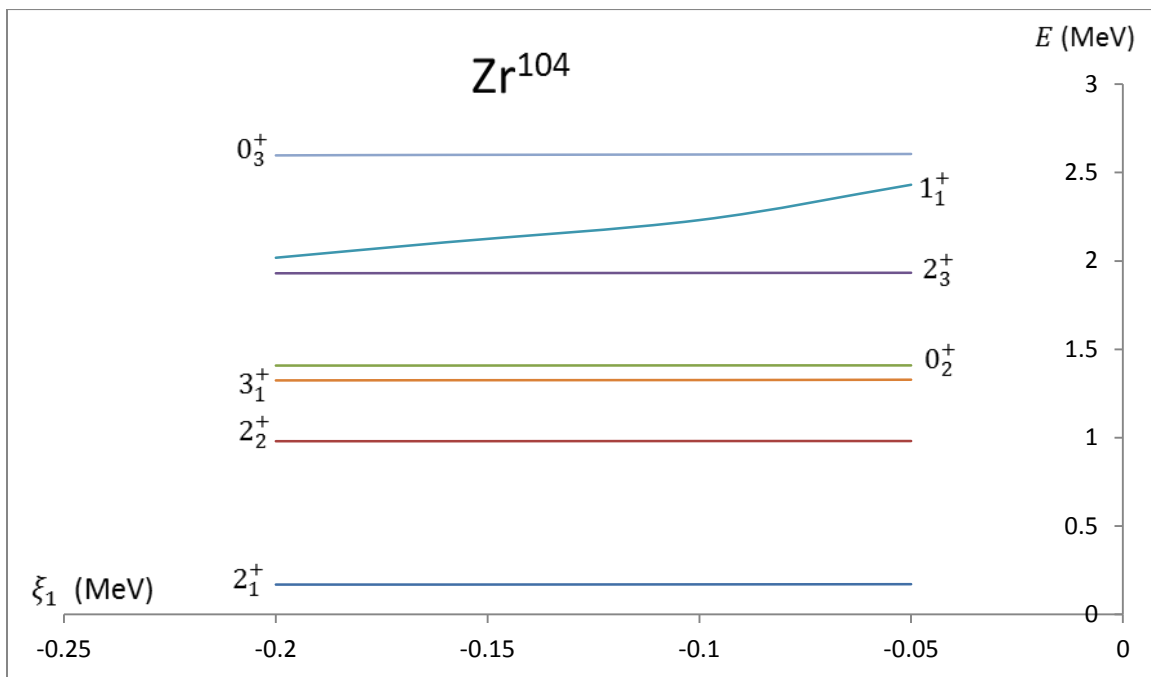


Figure (4-24 a): The change of the level energy in ^{104}Zr as a function of ξ_1 .

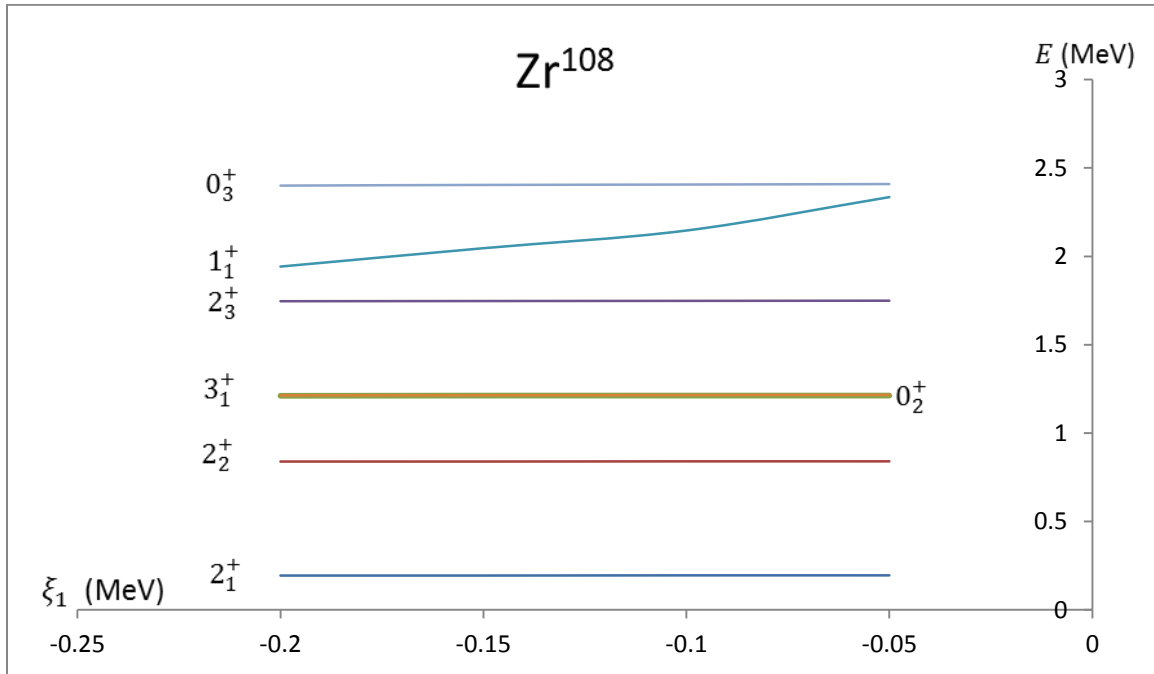


Figure (4-24 b): The change of the level energy in ^{108}Zr as a function of ξ_1 .

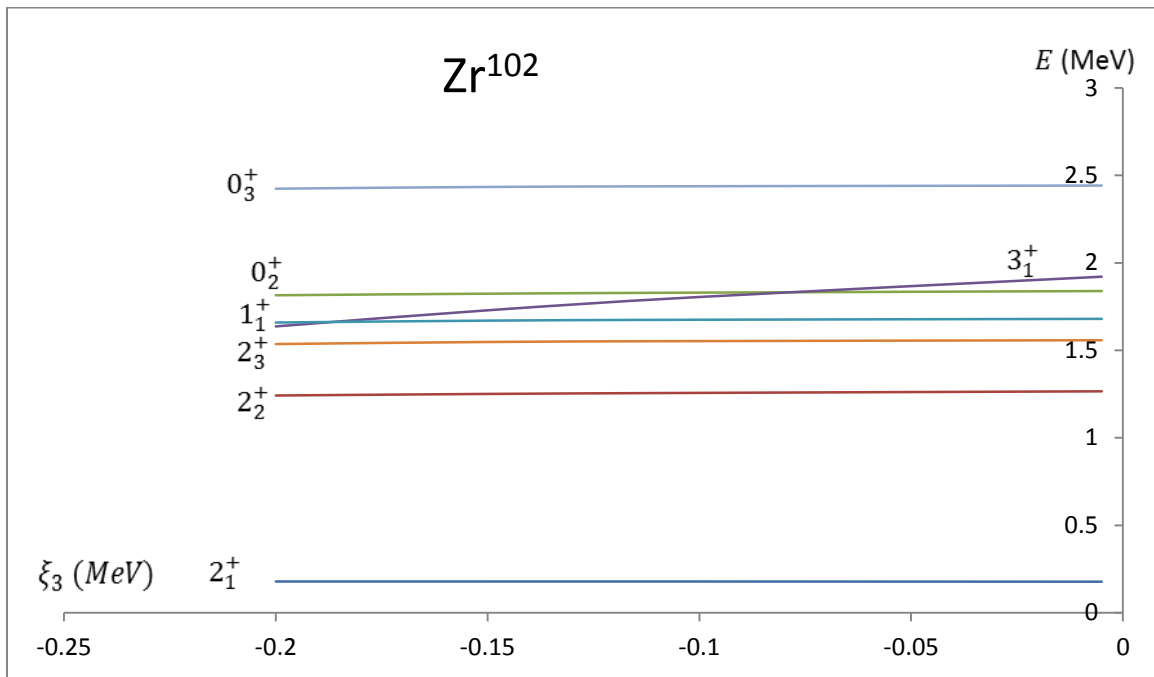


Figure (4-24 c): The change of the level energy in ^{102}Zr as a function of ξ_3 .

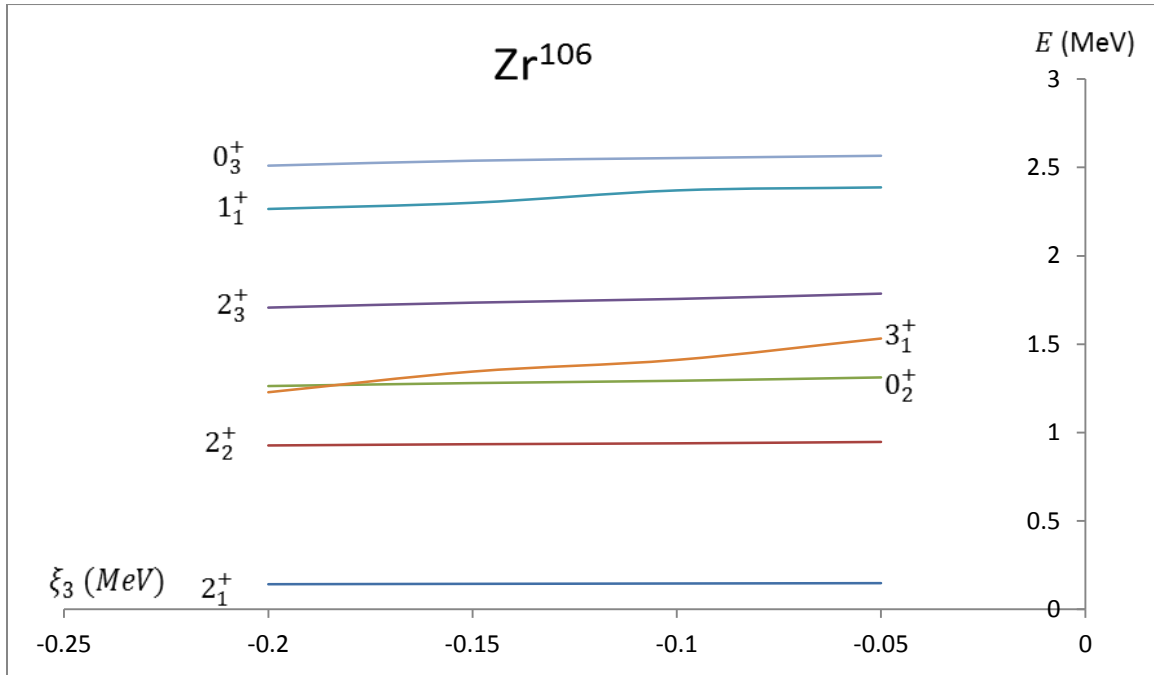


Figure (4-24 d): The change of the level energy in ^{106}Zr as a function of ξ_3 .

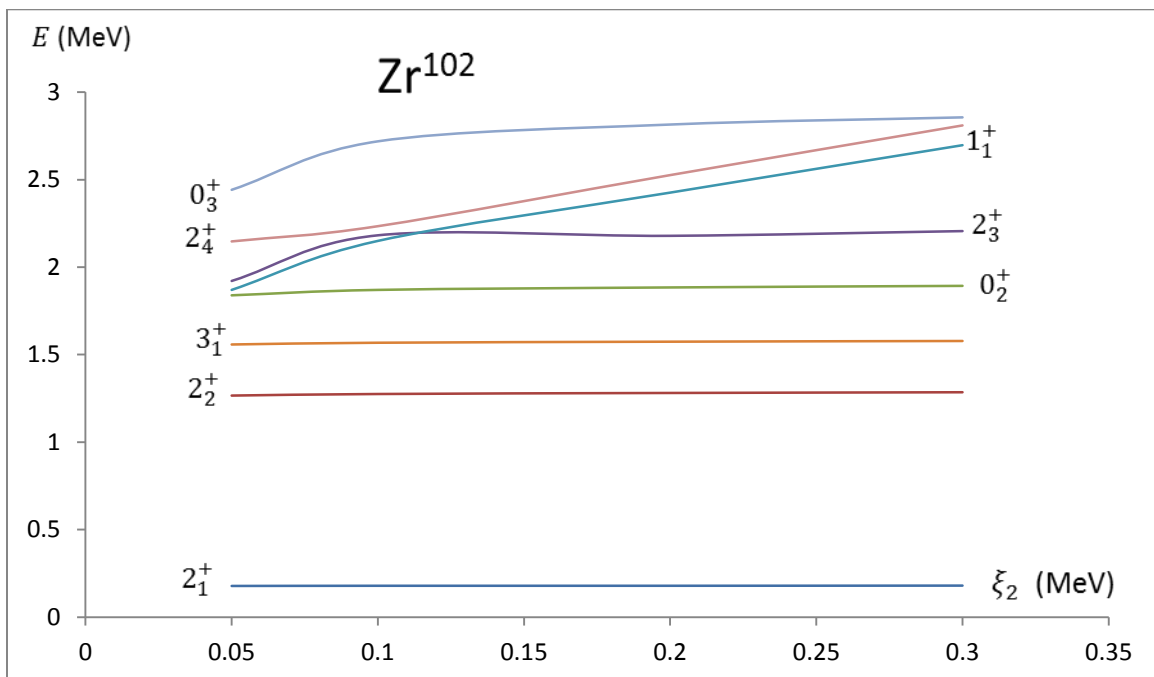


Figure (4-25 a): The change of the level energy in ^{102}Zr as a function of ξ_2 .

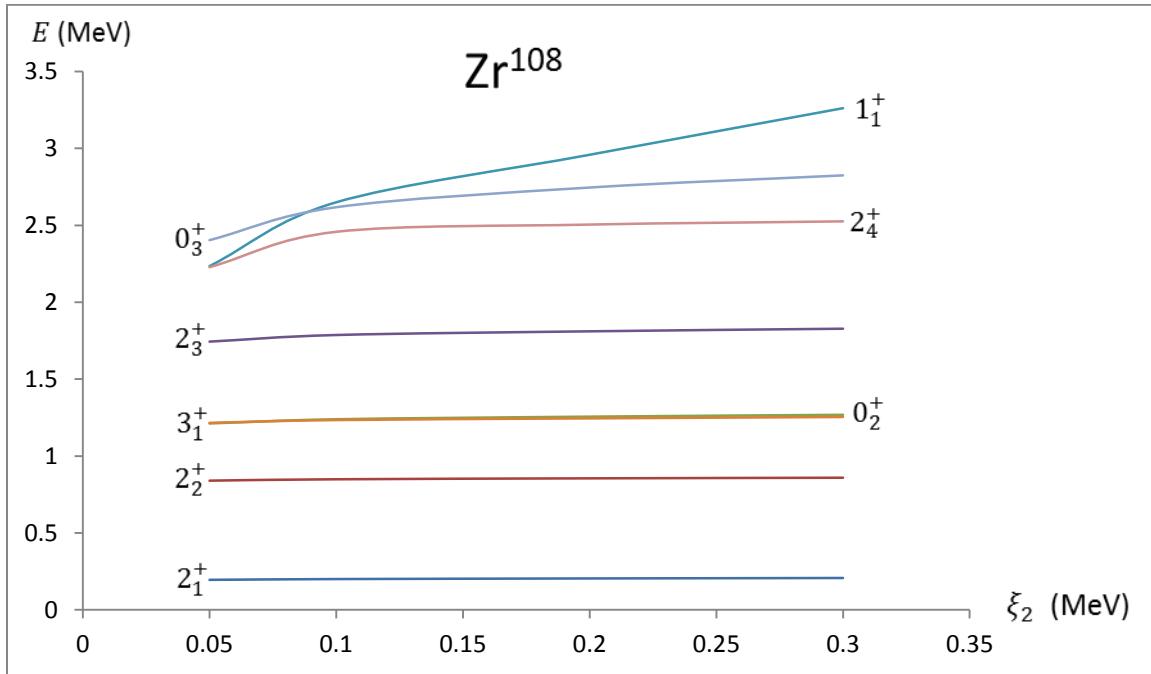


Figure (4-25 b): The change of the level energy in ^{108}Zr as a function of ξ_2 .

4.3 Electromagnetic properties:

4.3.1 BE(2) transition properties

The boson E2 operator in IBM-1, equation (2-26) and in IBM-2, equation (2-134), have been used for calculating the E2 transition rates and the quadrupole moments, for the low-lying excited states of the considered Zr-isotopes. In the principle that the value of the effective charge (α_2) of the IBM-1 was determined by normalizing to the experimental data $B(E2; 2_1^+ \rightarrow 0_1^+)$ of each isotopes (by using equation (2-65)). While in IBM-2 the values of e_ν and e_π in the present work are important and changed for each isotopes.

In Tables (4-18) to (4-31) the calculated results of the IBM-1 and IBM-2 and the experimental data for $B(E2; j_i \rightarrow j_f)$ transitions in units of (e^2b^2) are compared. The data of $B(E2; 2_1^+ \rightarrow 0_1^+)$, $B(E2; 4_1^+ \rightarrow 2_1^+)$ and $B(E2; 2_2^+ \rightarrow 2_1^+)$ transitions are plotted as a functions of neutron number of $^{80-106}\text{Zr}$ -isotopes in figures (4-26) to (4-29). As the neutron number is increasing the experimental $B(E2; 2_1^+ \rightarrow 0_1^+)$ changes increase and decrease, figure (4-26) which are in very good agreement with IBM-1 and IBM-2 for all isotopes, while in figure (4-27) sometime the IBM-2 results agree with experimental data for the transitions $B(E2; 4_1^+ \rightarrow 2_1^+)$ e^2b^2 for example when $N=44,52,60$ and sometime IBM-1 agrees with the experimental data for example when $N=46,52$, and some time both IBM-1 and IBM-2 are nearest fit like $N=92$, and in somewhere both together are far away from experimental data like $N=46,54$. Figure (4-27) shows that both IBM-1 and IBM-2 results are acceptable or expectant since don't have experimental data for these transitions. The other transitions haven't experimental data, except $N=52$ have the value of transition $B(E2; 6_1^+ \rightarrow 4_1^+)$, $B(E2; 2_1^+ \rightarrow 0_2^+)$ both IBM-1 and IBM-2 give us acceptable results, and $N=54$, have the value of transition $B(E2; 2_1^+ \rightarrow 0_2^+)$ also IBM-1 and IBM-2 give us the best nearest results.

The ratio of $\frac{B(E2; 4_1^+ \rightarrow 2_1^+)}{B(E2; 2_1^+ \rightarrow 0_1^+)}$ was calculated and compared with those of experimental data

and displayed. In the figure (4-28) show that $N=44$ IBM-2 nearest fit than IBM-1, but $N=46$ both IBM-1 and IBM-2 are far away, also $N=48,52$ both IBM-1 and IBM-2 are fitted, but when $N=60$ IBM-2 are the best fit than the IBM-2. The quadrupole moments of the first excited 2_1^+ states in $^{80-108}\text{Zr}$ -isotopes are also studied in this work and presented in Tables (4-18) to (4-31) have been calculated by using (IBM-1 and IBM-2) models.

Table (4-18): The experimental $B (E2; J_i \rightarrow J_f)$ values , in the units (e^2b^2) ,and the quadruple moments ,in the unit of $(e.b)$,for ^{80}Zr isotope are compared with those obtained by IBM-1 and IBM-2 results . the effective charges are taken as $(\alpha_2 = 0.17624 e.b)$ in the IBM-1 and $(e_\nu = 0.175 , e_\pi = 0.174) e.b$ in the IBM-2

$J_i \rightarrow J_f$	B (E2; $J_i \rightarrow J_f$) EXP. Ref.[102,103,104,105,106]	B (E2; $J_i \rightarrow J_f$) IBM-1	B (E2; $J_i \rightarrow J_f$) IBM-2
$2_1^+ \rightarrow 0_1^+$	0.760	0.760	0.761
$4_1^+ \rightarrow 2_1^+$		1.2303	1.073
$6_1^+ \rightarrow 4_1^+$		1.4465	1.174
$2_1^+ \rightarrow 0_2^+$		0.1298	0.3235
$2_2^+ \rightarrow 2_1^+$		0.3401	0.7345
$4_2^+ \rightarrow 2_1^+$		0.0002	0.0026
$4_2^+ \rightarrow 2_2^+$		0.5307	0.3455
$2_3^+ \rightarrow 2_2^+$		0.1519	0.0115
$Q 2_1^+$		- 2.1722	- 1.274

Table (4-19): The experimental $B (E2; J_i \rightarrow J_f)$ values , in the units (e^2b^2) ,and the quadruple moments ,in the unit of $(e.b)$,for ^{82}Zr isotope are compared with those obtained by IBM-1 and IBM-2 results . the effective charges are taken as $(\alpha_2 = 0.23794 e.b)$ in the IBM-1 and $(e_\nu = 0.1833 , e_\pi = 0.17) e.b$ in the IBM-2

$J_i \rightarrow J_f$	B (E2; $J_i \rightarrow J_f$) EXP. Ref.[102,103,104,105,106]	B (E2; $J_i \rightarrow J_f$) IBM-1	B (E2; $J_i \rightarrow J_f$) IBM-2
$2_1^+ \rightarrow 0_1^+$	0.910 \mp 0.13	0.910	0.911
$4_1^+ \rightarrow 2_1^+$		1.5469	1.2935
$6_1^+ \rightarrow 4_1^+$		1.9004	1.3970
$2_1^+ \rightarrow 0_2^+$		0.2286	0.1155
$2_2^+ \rightarrow 2_1^+$		0.8740	0.6370
$4_2^+ \rightarrow 2_1^+$		0.0001	0.0055
$4_2^+ \rightarrow 2_2^+$		0.7902	0.7551
$2_3^+ \rightarrow 2_2^+$		0.2576	0.0294
$Q 2_1^+$		- 1.9665	- 1.5

Table (4-20): The experimental $B (E2; J_i \rightarrow J_f)$ values , in the units (e^2b^2) ,and the quadruple moments ,in the unit of $(e.b)$,for ^{84}Zr isotope are compared with those obtained by IBM-1 and IBM-2 results . the effective charges are taken as $(\alpha_2 = 0.18127 e.b)$ in the IBM-1 and $(e_v = 0.17, e_\pi = 0.156) e.b$ in the IBM-2

$J_i \rightarrow J_f$	B (E2; $J_i \rightarrow J_f$) EXP. Ref.[88,102,103,104,105,106]	B (E2; $J_i \rightarrow J_f$) IBM-1	B (E2; $J_i \rightarrow J_f$) IBM-2
$2_1^+ \rightarrow 0_1^+$	0.437	0.437	0.437
$4_1^+ \rightarrow 2_1^+$	0.5157	0.7302	0.5989
$6_1^+ \rightarrow 4_1^+$		0.8845	0.6402
$2_1^+ \rightarrow 0_2^+$		0.1070	0.0230
$2_2^+ \rightarrow 2_1^+$		0.4613	0.4289
$4_2^+ \rightarrow 2_1^+$		0.0002	0.0042
$4_2^+ \rightarrow 2_2^+$		0.3767	0.2119
$2_3^+ \rightarrow 2_2^+$		0.1153	0.0039
$Q 2_1^+$		- 1.2791	- 0.6417

Table (4-21): The experimental $B (E2; J_i \rightarrow J_f)$ values , in the units (e^2b^2) ,and the quadruple moments ,in the unit of $(e.b)$,for ^{86}Zr isotope are compared with those obtained by IBM-1 and IBM-2 results . the effective charges are taken as $(\alpha_2 = 0.139292 e.b)$ in the IBM-1 and $(e_v = 0.1304, e_\pi = 0.11) e.b$ in the IBM-2

$J_i \rightarrow J_f$	B (E2; $J_i \rightarrow J_f$) EXP. Ref.[89,102,103,104,105,106]	B (E2; $J_i \rightarrow J_f$) IBM-1	B (E2; $J_i \rightarrow J_f$) IBM-2
$2_1^+ \rightarrow 0_1^+$	0.157	0.157	0.157
$4_1^+ \rightarrow 2_1^+$	0.082	0.2775	0.2306
$6_1^+ \rightarrow 4_1^+$		0.3523	0.2410
$2_1^+ \rightarrow 0_2^+$		0.0567	0.0425
$2_2^+ \rightarrow 2_1^+$		0.2177	0.0834
$4_2^+ \rightarrow 2_1^+$		0.0004	0.0015
$4_2^+ \rightarrow 2_2^+$		0.1670	0.1365
$2_3^+ \rightarrow 2_2^+$		0.0776	0.0179
$Q 2_1^+$		- 0.6921	- 0.6098

Table (4-22): The experimental $B (E2; J_i \rightarrow J_f)$ values , in the units (e^2b^2) ,and the quadruple moments ,in the unit of $(e.b)$,for ^{88}Zr isotope are compared with those obtained by IBM-1 and IBM-2 results . the effective charges are taken as $(\alpha_2 = 0.13199 e.b)$ in the IBM-1 and $(e_\nu = 0.04, e_\pi = 0.131) e.b$ in the IBM-2

$J_i \rightarrow J_f$	B (E2; $J_i \rightarrow J_f$) EXP. Ref.[90,102,103,104,105,106]	B (E2; $J_i \rightarrow J_f$) IBM-1	B (E2; $J_i \rightarrow J_f$) IBM-2
$2_1^+ \rightarrow 0_1^+$	0.086	0.086	0.086
$4_1^+ \rightarrow 2_1^+$	0.1256	0.1387	0.1405
$6_1^+ \rightarrow 4_1^+$		0.1580	0.1684
$2_1^+ \rightarrow 0_2^+$		0.0286	0.0258
$2_2^+ \rightarrow 2_1^+$		0.1666	0.0005
$4_2^+ \rightarrow 2_1^+$		0.0006	0.0025
$4_2^+ \rightarrow 2_2^+$		0.0945	0.0905
$2_3^+ \rightarrow 2_2^+$		0.0286	0.0001
$Q 2_1^+$	- 0.51	- 0.1494	- 0.2620

Table (4-23): The experimental $B (E2; J_i \rightarrow J_f)$ values , in the units (e^2b^2) ,and the quadruple moments ,in the unit of $(e.b)$,for ^{92}Zr isotope are compared with those obtained by IBM-1 and IBM-2 results . the effective charges are taken as $(\alpha_2 = 0.12943 e.b)$ in the IBM-1 and $(e_\nu = 0.04, e_\pi = 0.125) e.b$ in the IBM-2

$J_i \rightarrow J_f$	B (E2; $J_i \rightarrow J_f$) EXP. Ref.[42,50,102,103,104,105,106]	B (E2; $J_i \rightarrow J_f$) IBM-1	B (E2; $J_i \rightarrow J_f$) IBM-2
$2_1^+ \rightarrow 0_1^+$	0.0789	0.0789	0.0789
$4_1^+ \rightarrow 2_1^+$	0.1637	0.1271	0.1288
$6_1^+ \rightarrow 4_1^+$	0.3791	0.1440	0.1544
$2_1^+ \rightarrow 0_2^+$	0.0340	0.0270	0.0236
$2_2^+ \rightarrow 2_1^+$		0.1557	0.1158
$4_2^+ \rightarrow 2_1^+$		0.0007	0.0022
$4_2^+ \rightarrow 2_2^+$		0.0869	0.0855
$2_3^+ \rightarrow 2_2^+$		0.0265	0.0024
$Q 2_1^+$		- 0.1109	- 0.2529

Table (4-24): The experimental $B (E2; J_i \rightarrow J_f)$ values , in the units (e^2b^2) ,and the quadruple moments ,in the unit of ($e.b$) ,for ^{94}Zr isotope are compared with those obtained by IBM-1 and IBM-2 results . the effective charges are taken as ($a_2 = 0.10369 e.b$) in the IBM-1 and ($e_v = 0.044$, $e_\pi = 0.11$) $e.b$ in the IBM-2

$J_i \rightarrow J_f$	B (E2; $J_i \rightarrow J_f$) EXP. Ref.[42,50,102,103,104,105,106]	B (E2; $J_i \rightarrow J_f$) IBM-1	B (E2; $J_i \rightarrow J_f$) IBM-2
$2_1^+ \rightarrow 0_1^+$	0.0629	0.0629	0.0629
$4_1^+ \rightarrow 2_1^+$	0.0125	0.1052	0.1066
$6_1^+ \rightarrow 4_1^+$		0.1268	0.1330
$2_1^+ \rightarrow 0_2^+$	0.0235	0.0215	0.0199
$2_2^+ \rightarrow 2_1^+$		0.1216	0.0991
$4_2^+ \rightarrow 2_1^+$		0.0003	0.0002
$4_2^+ \rightarrow 2_2^+$		0.0734	0.0675
$2_3^+ \rightarrow 2_2^+$		0.0233	0.0010
$2_2^+ \rightarrow 0_1^+$	0.0050	0.0010	0.0010
$2_2^+ \rightarrow 0_2^+$	0.024	0.017	0.0211
Q 2_1^+		- 0.1318	- 0.2235

Table (4-25): The experimental $B (E2; J_i \rightarrow J_f)$ values , in the units (e^2b^2) ,and the quadruple moments ,in the unit of ($e.b$) ,for ^{96}Zr isotope are compared with those obtained by IBM-1 and IBM-2 results . the effective charges are taken as ($a_2 = 0.07 e.b$) in the IBM-1 and ($e_v = 0.0468$, $e_\pi = 0.09$) $e.b$ in the IBM-2

$J_i \rightarrow J_f$	B (E2; $J_i \rightarrow J_f$) EXP. Ref.[102,103,104,105,106]	B (E2; $J_i \rightarrow J_f$) IBM-1	B (E2; $J_i \rightarrow J_f$) IBM-2
$2_1^+ \rightarrow 0_1^+$	0.0314	0.0314	0.0314
$4_1^+ \rightarrow 2_1^+$		0.0436	0.0469
$6_1^+ \rightarrow 4_1^+$		0.0441	0.0415
$2_1^+ \rightarrow 0_2^+$		0.0107	0.0084
$2_2^+ \rightarrow 2_1^+$		0.0522	0.0471
$4_2^+ \rightarrow 2_1^+$		0.0017	0.0
$4_2^+ \rightarrow 2_2^+$		0.0274	0.0009
$2_3^+ \rightarrow 2_2^+$		0.0147	0.0
$2_2^+ \rightarrow 0_1^+$	>0.000157	0.00012	0.0001
$2_2^+ \rightarrow 0_2^+$	0.021195	0.0450	0.0380
Q 2_1^+		0.1108	0.0255

Table (4-26): The experimental $B (E2; J_i \rightarrow J_f)$ values , in the units (e^2b^2) ,and the quadruple moments ,in the unit of $(e.b)$,for ^{98}Zr isotope are compared with those obtained by IBM-1 and IBM-2 results . the effective charges are taken as $(\alpha_2 = 0.15907 e.b)$ in the IBM-1 and $(e_v = 0.0526, e_\pi = 0.16) e.b$ in the IBM-2

$J_i \rightarrow J_f$	B (E2; $J_i \rightarrow J_f$) EXP. Ref.[102,103,104,105,106]	B (E2; $J_i \rightarrow J_f$) IBM-1	B (E2; $J_i \rightarrow J_f$) IBM-2
$2_1^+ \rightarrow 0_1^+$	0.158 ∓ 0.11	0.158	0.158
$4_1^+ \rightarrow 2_1^+$		0.2674	0.2651
$6_1^+ \rightarrow 4_1^+$		0.3229	0.3325
$2_1^+ \rightarrow 0_2^+$	0.0264	0.0639	0.0470
$2_2^+ \rightarrow 2_1^+$		0.1674	0.2043
$4_2^+ \rightarrow 2_1^+$		0.0203	0.0002
$4_2^+ \rightarrow 2_2^+$		0.1900	0.2802
$2_3^+ \rightarrow 2_2^+$		0.1350	0.0014
$Q 2_1^+$		0.6623	-0.5145

Table (4-27): The experimental $B (E2; J_i \rightarrow J_f)$ values , in the units (e^2b^2) ,and the quadruple moments ,in the unit of $(e.b)$,for ^{100}Zr isotope are compared with those obtained by IBM-1 and IBM-2 results . the effective charges are taken as $(\alpha_2 = 0.19766 e.b)$ in the IBM-1 and $(e_v = 0.2312, e_\pi = 0.19) e.b$ in the IBM-2

$J_i \rightarrow J_f$	B (E2; $J_i \rightarrow J_f$) EXP. Ref.[95,102,103,104,105,106]	B (E2; $J_i \rightarrow J_f$) IBM-1	B (E2; $J_i \rightarrow J_f$) IBM-2
$2_1^+ \rightarrow 0_1^+$	1.110	1.110	1.111
$4_1^+ \rightarrow 2_1^+$	1.5307	1.7793	1.5372
$6_1^+ \rightarrow 4_1^+$	1.3593	2.0470	1.3990
$2_1^+ \rightarrow 0_2^+$		0.1707	0.2450
$2_2^+ \rightarrow 2_1^+$		0.1463	0.0040
$4_2^+ \rightarrow 2_1^+$		0.0001	0.0409
$4_2^+ \rightarrow 2_2^+$		1.1332	1.6644
$2_3^+ \rightarrow 2_2^+$		0.9956	0.0928
$Q 2_1^+$		-2.9137	-2.0106

Table (4-28): The experimental $B (E2; J_i \rightarrow J_f)$ values , in the units (e^2b^2) ,and the quadruple moments ,in the unit of $(e.b)$,for ^{102}Zr isotope are compared with those obtained by IBM-1 and IBM-2 results . the effective charges are taken as $(\alpha_2 = 0.17594 e.b)$ in the IBM-1 and $(e_v=0.2387, e_\pi=0.178) e.b$ in the IBM-2

$J_i \rightarrow J_f$	B (E2; $J_i \rightarrow J_f$) EXP. Ref.[102,103,104,105,106]	B (E2; $J_i \rightarrow J_f$) IBM-1	B (E2; $J_i \rightarrow J_f$) IBM-2
$2_1^+ \rightarrow 0_1^+$	1.350	1.350	1.350
$4_1^+ \rightarrow 2_1^+$		1.9429	1.9365
$6_1^+ \rightarrow 4_1^+$		2.1293	2.0490
$2_1^+ \rightarrow 0_2^+$		0.0419	0.0225
$2_2^+ \rightarrow 2_1^+$		0.0597	0.0006
$4_2^+ \rightarrow 2_1^+$		0.0001	0.0068
$4_2^+ \rightarrow 2_2^+$		0.6831	0.6919
$2_3^+ \rightarrow 2_2^+$		0.1773	0.1210
$Q 2_1^+$		-3.1162	-2.3521

Table (4-29): The experimental $B (E2; J_i \rightarrow J_f)$ values , in the units (e^2b^2) ,and the quadruple moments ,in the unit of $(e.b)$,for ^{104}Zr isotope are compared with those obtained by IBM-1 and IBM-2 results . the effective charges are taken as $(\alpha_2 = 0.20041 e.b)$ in the IBM-1 and $(e_v=0.26175, e_\pi=0.21) e.b$ in the IBM-2

$J_i \rightarrow J_f$	B (E2; $J_i \rightarrow J_f$) EXP. Ref.[102,103,104,105,106]	B (E2; $J_i \rightarrow J_f$) IBM-1	B (E2; $J_i \rightarrow J_f$) IBM-2
$2_1^+ \rightarrow 0_1^+$	1.958	1.958	1.958
$4_1^+ \rightarrow 2_1^+$		2.8382	2.8107
$6_1^+ \rightarrow 4_1^+$		3.1383	3.0428
$2_1^+ \rightarrow 0_2^+$		0.0625	0.0236
$2_2^+ \rightarrow 2_1^+$		0.1159	0.4481
$4_2^+ \rightarrow 2_1^+$		0.0000	0.0053
$4_2^+ \rightarrow 2_2^+$		0.9560	0.9113
$2_3^+ \rightarrow 2_2^+$		0.0339	0.1540
$Q 2_1^+$		-3.7313	-2.720

Table (4-30): The experimental $B (E2; J_i \rightarrow J_f)$ values , in the units (e^2b^2) ,and the quadruple moments ,in the unit of $(e.b)$,for ^{106}Zr isotope are compared with those obtained by IBM-1 and IBM-2 results . the effective charges are taken as $(\alpha_2 = 0.17124 e.b)$ in the IBM-1 and $(e_v=0.21, e_\pi=0.1877) e.b$ in the IBM-2

$J_i \rightarrow J_f$	B (E2; $J_i \rightarrow J_f$) EXP. Ref.[102,103,104,105,106]	B (E2; $J_i \rightarrow J_f$) IBM-1	B (E2; $J_i \rightarrow J_f$) IBM-2
$2_1^+ \rightarrow 0_1^+$	1.55	1.5501	1.551
$4_1^+ \rightarrow 2_1^+$		2.2771	2.2462
$6_1^+ \rightarrow 4_1^+$		2.5517	2.4612
$2_1^+ \rightarrow 0_2^+$		0.070	0.0788
$2_2^+ \rightarrow 2_1^+$		0.1229	0.2695
$4_2^+ \rightarrow 2_1^+$		0.0000	0.0043
$4_2^+ \rightarrow 2_2^+$		0.8023	0.7309
$2_3^+ \rightarrow 2_2^+$		0.0790	0.0778
Q 2_1^+		-3.3180	-2.4847

Table (4-31): The experimental $B (E2; J_i \rightarrow J_f)$ values , in the units (e^2b^2) ,and the quadruple moments ,in the unit of $(e.b)$,for ^{108}Zr isotope are compared with those obtained by IBM-1 and IBM-2 results . the effective charges are taken as $(\alpha_2 = 0.17124 e.b)$ in the IBM-1 and $(e_v=0.21, e_\pi=0.1877) e.b$ in the IBM-2

$J_i \rightarrow J_f$	B (E2; $J_i \rightarrow J_f$) EXP.	B (E2; $J_i \rightarrow J_f$) IBM-1	B (E2; $J_i \rightarrow J_f$) IBM-2
$2_1^+ \rightarrow 0_1^+$		1.2748	1.2394
$4_1^+ \rightarrow 2_1^+$		1.9016	1.7913
$6_1^+ \rightarrow 4_1^+$		2.1458	1.9403
$2_1^+ \rightarrow 0_2^+$		0.0818	0.1075
$2_2^+ \rightarrow 2_1^+$		0.1540	0.2134
$4_2^+ \rightarrow 2_1^+$		0.0000	0.0082
$4_2^+ \rightarrow 2_2^+$		0.6956	0.5961
$2_3^+ \rightarrow 2_2^+$		0.1055	0.0478
Q 2_1^+		-2.9963	-2.1959

$$B(E2; 2_1^+ \rightarrow 0_1^+) e^2 b^2$$

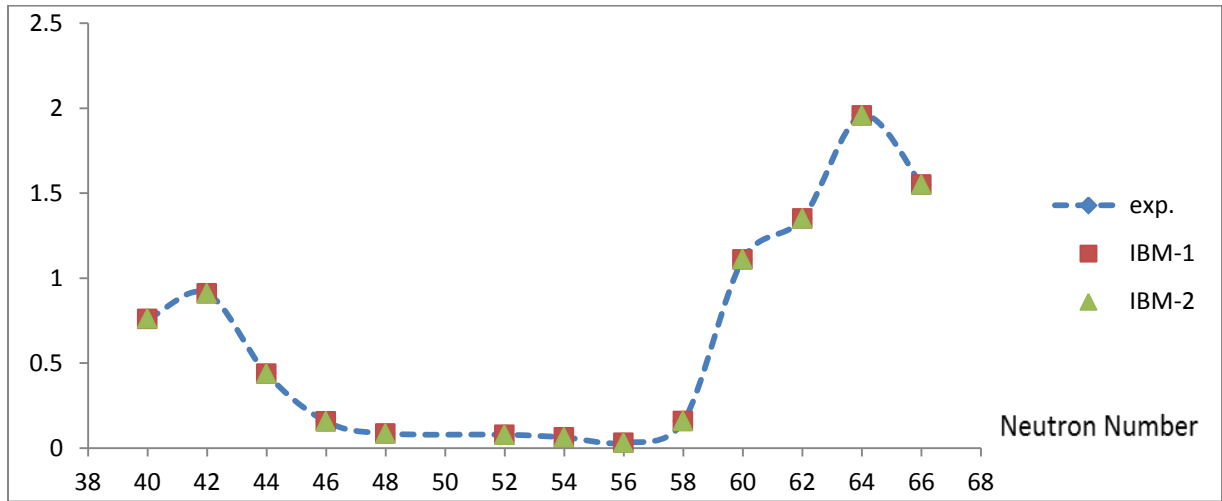


Figure (4-26): the $B(E2; 2_1^+ \rightarrow 0_1^+) e^2 b^2$ transition for $^{80-108}\text{Zr}$ – isotopes as a function of neutron number.

$$B(E2; 4_1^+ \rightarrow 2_1^+) e^2 b^2$$

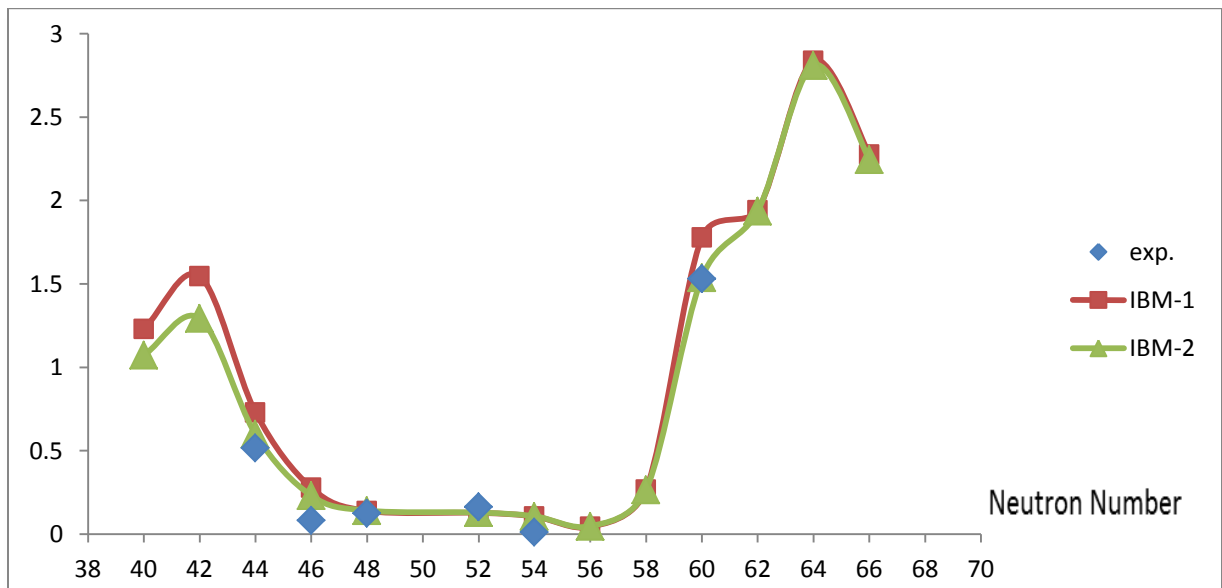


Figure (4-27): the $B(E2; 4_1^+ \rightarrow 2_1^+) e^2 b^2$ transition for $^{80-108}\text{Zr}$ – isotopes as a function of neutron number.

$$B(E2; 2_2^+ \rightarrow 2_1^+) e^2 b^2$$

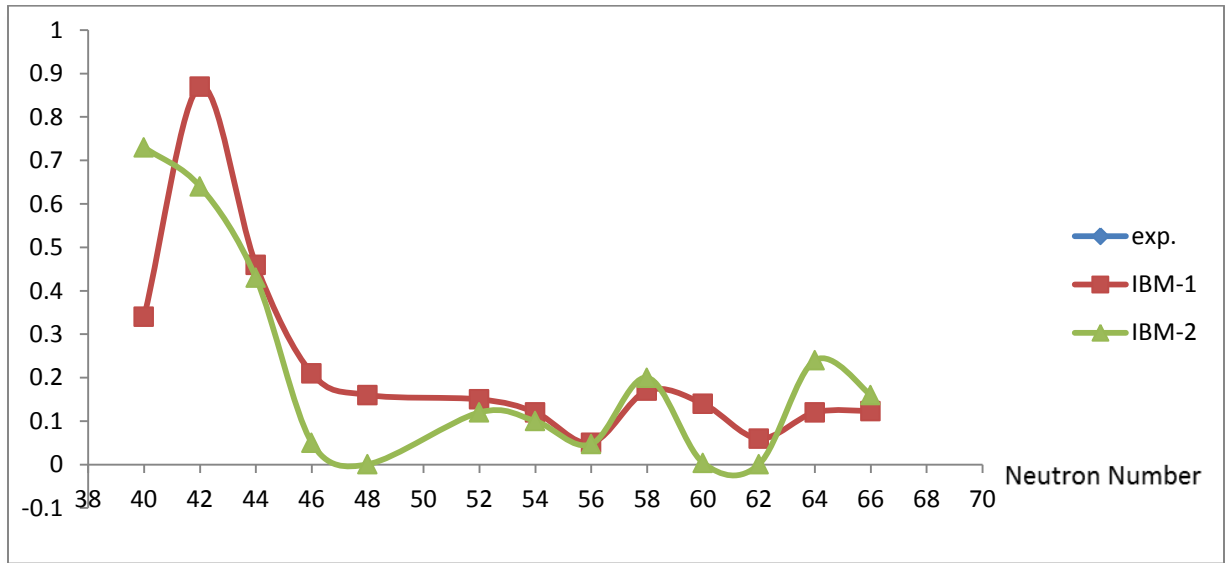


Figure (4-28): the $B(E2; 2_2^+ \rightarrow 2_1^+) e^2 b^2$ transition for $^{80-108}\text{Zr}$ – isotopes as a function of neutron number.

$$B(E2; 4_1^+ \rightarrow 2_1^+) / B(E2; 2_1^+ \rightarrow 0_1^+)$$

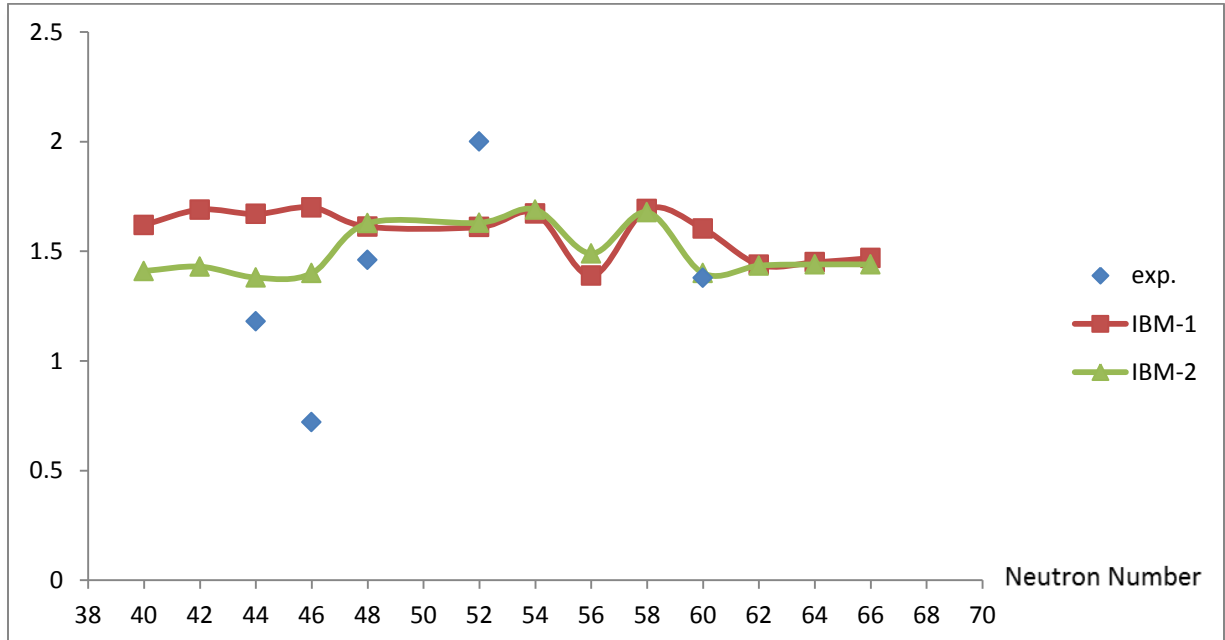


Figure (4-29): the ratios of $B(E2; 4_1^+ \rightarrow 2_1^+) / B(E2; 2_1^+ \rightarrow 0_1^+)$ for $^{80-108}\text{Zr}$ – isotopes as a function of neutron number.

4.3.2 B (M1) transition properties

The boson M1 operator of the IBM-2, have been used for calculating the M1 transitions rates and the magnetic dipole moments, for the first excited states 2_1^+ ($\mu_{2_1^+}$). However, these properties are influenced by the parameters of g_ν and g_π . A fixed values for $g_\nu = -0.02$, changed value for g_π shows above the tables, have been used to produce these properties throughout all $^{80-108}\text{Zr}$ -isotopes. The comparison between the calculated result for ($\mu_{2_1^+}$) moments of the IBM-2 model and those of experimental data are presented in Tables (4-32) to (4-45), and there are no experimental data available for B(M1) transitions.

Table (4-32): The B(M1; $J_i \rightarrow J_f$) values , in the units of (μ_N^2), and the magnetic dipole moments for the 2_1^+ states ($\mu_{2_1^+}$) in the unit of (μ_N), for ^{80}Zr -isotopes obtained by IBM-2 results . The effective g- charges are taken as $g_\nu = -0.02$ and $g_\pi = 2.839$

$J_i \rightarrow J_f$	B(M1; $J_i \rightarrow J_f$)	
	EXP.	IBM-2
$2_1^+ \rightarrow 1_1^+$		0.4072
$2_2^+ \rightarrow 1_1^+$		1.7556
$2_3^+ \rightarrow 1_1^+$		0.0575
$2_2^+ \rightarrow 2_1^+$		0.0301
$2_3^+ \rightarrow 2_1^+$		3.0222
$2_3^+ \rightarrow 2_2^+$		0.0194
$3_1^+ \rightarrow 2_1^+$		0.013
$3_1^+ \rightarrow 2_2^+$		0.0146
$3_1^+ \rightarrow 2_3^+$		0.0012
$3_1^+ \rightarrow 4_1^+$		0.008
$4_2^+ \rightarrow 4_1^+$		0.1509
$\mu_{2_1^+}$		1.0176

Table (4-33): The $B(M1; J_i \rightarrow J_f)$ values , in the units of (μ_N^2) , and the magnetic dipole moments for the 2_1^+ states ($\mu_{2_1^+}$) in the unit of (μ_N) , for ^{82}Zr -isotopes obtained by IBM-2 results . The effective g- charges are taken as $g_v = -0.02$ and $g_\pi = 2.839$

$J_i \rightarrow J_f$	$B(M1; J_i \rightarrow J_f)$	
	EXP.	IBM-2
$2_1^+ \rightarrow 1_1^+$		0.4570
$2_2^+ \rightarrow 1_1^+$		1.4665
$2_3^+ \rightarrow 1_1^+$		0.0832
$2_2^+ \rightarrow 2_1^+$		0.0123
$2_3^+ \rightarrow 2_1^+$		1.7126
$2_3^+ \rightarrow 2_2^+$		0.0573
$3_1^+ \rightarrow 2_1^+$		0.000
$3_1^+ \rightarrow 2_2^+$		0.0051
$3_1^+ \rightarrow 4_1^+$		0.0013
$\mu_{2_1^+}$		0.6889

Table (4-34): The $B(M1; J_i \rightarrow J_f)$ values , in the units of (μ_N^2) , and the magnetic dipole moments for the 2_1^+ states ($\mu_{2_1^+}$) in the unit of (μ_N) , for ^{84}Zr -isotopes obtained by IBM-2 results . The effective g- charges are taken as $g_v = -0.02$ and $g_\pi = 2.839$

$J_i \rightarrow J_f$	$B(M1; J_i \rightarrow J_f)$	
	EXP. [88]	IBM-2
$2_1^+ \rightarrow 1_1^+$		0.4072
$2_2^+ \rightarrow 1_1^+$		1.7556
$2_3^+ \rightarrow 1_1^+$		0.0575
$2_2^+ \rightarrow 2_1^+$		0.0301
$2_3^+ \rightarrow 2_1^+$		3.0222
$2_3^+ \rightarrow 2_2^+$		0.0194
$3_1^+ \rightarrow 2_1^+$		0.013
$3_1^+ \rightarrow 2_2^+$		0.0146
$3_1^+ \rightarrow 4_1^+$		0.008
$\mu_{2_1^+}$	0.96	0.96

Table (4-35): The $B(M1; J_i \rightarrow J_f)$ values , in the units of (μ_N^2) , and the magnetic dipole moments for the 2_1^+ states ($\mu_{2_1^+}$) in the unit of (μ_N) , for ^{86}Zr -isotopes obtained by IBM-2 results . The effective g- charges are taken as $g_v = -0.02$ and $g_\pi = 2.995$

$J_i \rightarrow J_f$	$B(M1; J_i \rightarrow J_f)$	
	EXP.[89]	IBM-2
$2_1^+ \rightarrow 1_1^+$		0.4339
$2_2^+ \rightarrow 1_1^+$		0.8849
$2_3^+ \rightarrow 1_1^+$		0.3050
$2_2^+ \rightarrow 2_1^+$		0.6839
$2_3^+ \rightarrow 2_1^+$		1.9012
$2_3^+ \rightarrow 2_2^+$		0.6210
$3_1^+ \rightarrow 2_1^+$		0.0956
$3_1^+ \rightarrow 2_2^+$		0.2582
$3_1^+ \rightarrow 4_1^+$		0.3217
$\mu_{2_1^+}$	1.0	0.9099

Table (4-36): The $B(M1; J_i \rightarrow J_f)$ values , in the units of (μ_N^2) , and the magnetic dipole moments for the 2_1^+ states ($\mu_{2_1^+}$) in the unit of (μ_N) , for ^{88}Zr -isotopes obtained by IBM-2 results . The effective g- charges are taken as $g_v = -0.02$ and $g_\pi = 0.725$

$J_i \rightarrow J_f$	$B(M1; J_i \rightarrow J_f)$	
	EXP.[90]	IBM-2
$2_1^+ \rightarrow 1_1^+$		0.0002
$2_2^+ \rightarrow 1_1^+$		0.0028
$2_3^+ \rightarrow 1_1^+$		0.0907
$2_2^+ \rightarrow 2_1^+$		0.1087
$2_3^+ \rightarrow 2_1^+$		0.0019
$2_3^+ \rightarrow 2_2^+$		0.0070
$3_1^+ \rightarrow 2_1^+$		0.0001
$3_1^+ \rightarrow 2_2^+$		0.0023
$3_1^+ \rightarrow 4_1^+$		0.0448
$\mu_{2_1^+}$	0.6	0.6006

Table (4-37): The $B(M1; J_i \rightarrow J_f)$ values , in the units of (μ_N^2) , and the magnetic dipole moments for the 2_1^+ states ($\mu_{2_1^+}$) in the unit of (μ_N) , for ^{92}Zr -isotopes obtained by IBM-2 results . The effective g- charges are taken as $g_v = -0.02$ and $g_\pi = 0.725$

$J_i \rightarrow J_f$	$B(M1; J_i \rightarrow J_f)$	
	EXP.	IBM-2
$2_1^+ \rightarrow 1_1^+$		0.0002
$2_2^+ \rightarrow 1_1^+$		0.0927
$2_3^+ \rightarrow 1_1^+$		0.0007
$2_2^+ \rightarrow 2_1^+$		0.0019
$2_3^+ \rightarrow 2_1^+$		0.1086
$2_3^+ \rightarrow 2_2^+$		0.0050
$3_1^+ \rightarrow 2_1^+$		0.0002
$3_1^+ \rightarrow 2_2^+$		0.0760
$3_1^+ \rightarrow 4_1^+$		0.0448
$\mu_{2_1^+}$		0.6005

Table (4-38): The $B(M1; J_i \rightarrow J_f)$ values , in the units of (μ_N^2) , and the magnetic dipole moments for the 2_1^+ states ($\mu_{2_1^+}$) in the unit of (μ_N) , for ^{94}Zr -isotopes obtained by IBM-2 results . The effective g- charges are taken as $g_v = -0.02$ and $g_\pi = 0.725$

$J_i \rightarrow J_f$	$B(M1; J_i \rightarrow J_f)$	
	EXP.	IBM-2
$2_1^+ \rightarrow 1_1^+$		0.0003
$2_2^+ \rightarrow 1_1^+$		0.1318
$2_3^+ \rightarrow 1_1^+$		0.0001
$2_2^+ \rightarrow 2_1^+$		0.0000
$2_3^+ \rightarrow 2_1^+$		0.1611
$2_3^+ \rightarrow 2_2^+$		0.0001
$3_1^+ \rightarrow 2_1^+$		0.0000
$3_1^+ \rightarrow 2_2^+$		0.0002
$3_1^+ \rightarrow 4_1^+$		0.0001
$\mu_{2_1^+}$		0.5131

Table (4-39): The $B(M1; J_i \rightarrow J_f)$ values , in the units of (μ_N^2) , and the magnetic dipole moments for the 2_1^+ states ($\mu_{2_1^+}$) in the unit of (μ_N) , for ^{96}Zr -isotopes obtained by IBM-2 results . The effective g- charges are taken as $g_v = -0.02$ and $g_\pi = 0.109$

$J_i \rightarrow J_f$	$B(M1; J_i \rightarrow J_f)$	
	EXP.[93]	IBM-2
$2_1^+ \rightarrow 1_1^+$		0.0000
$2_2^+ \rightarrow 1_1^+$		0.0000
$2_3^+ \rightarrow 1_1^+$		0.0001
$2_2^+ \rightarrow 2_1^+$		0.0021
$2_3^+ \rightarrow 2_1^+$		0.0031
$2_3^+ \rightarrow 2_2^+$		0.0008
$3_1^+ \rightarrow 2_1^+$		0.0000
$3_1^+ \rightarrow 2_2^+$		0.0001
$3_1^+ \rightarrow 4_1^+$		0.0001
$\mu_{2_1^+}$	0.0600	0.0605

Table (4-40): The $B(M1; J_i \rightarrow J_f)$ values , in the units of (μ_N^2) , and the magnetic dipole moments for the 2_1^+ states ($\mu_{2_1^+}$) in the unit of (μ_N) , for ^{98}Zr -isotopes obtained by IBM-2 results . The effective g- charges are taken as $g_v = -0.02$ and $g_\pi = 0.109$

$J_i \rightarrow J_f$	$B(M1; J_i \rightarrow J_f)$	
	EXP.	IBM-2
$2_1^+ \rightarrow 1_1^+$		0.0027
$2_2^+ \rightarrow 1_1^+$		0.0502
$2_3^+ \rightarrow 1_1^+$		0.0004
$2_2^+ \rightarrow 2_1^+$		0.0006
$2_3^+ \rightarrow 2_1^+$		0.0748
$2_3^+ \rightarrow 2_2^+$		0.0012
$3_1^+ \rightarrow 2_1^+$		0.0023
$3_1^+ \rightarrow 2_2^+$		0.0389
$3_1^+ \rightarrow 4_1^+$		0.0273
$\mu_{2_1^+}$		-0.0968

Table (4-41): The $B(M1; J_i \rightarrow J_f)$ values , in the units of (μ_N^2) , and the magnetic dipole moments for the 2_1^+ states ($\mu_{2_1^+}$) in the unit of (μ_N) , for ^{100}Zr -isotopes obtained by IBM-2 results . The effective g- charges are taken as $g_v = -0.02$ and $g_\pi = 1.77$

$J_i \rightarrow J_f$	$B(M1; J_i \rightarrow J_f)$	
	EXP. [95]	IBM-2
$2_1^+ \rightarrow 1_1^+$		0.3871
$2_2^+ \rightarrow 1_1^+$		0.0282
$2_3^+ \rightarrow 1_1^+$		0.0277
$2_2^+ \rightarrow 2_1^+$		0.5639
$2_3^+ \rightarrow 2_1^+$		0.0764
$2_3^+ \rightarrow 2_2^+$		0.1267
$3_1^+ \rightarrow 2_1^+$		0.0001
$3_1^+ \rightarrow 2_2^+$		0.0004
$\mu_{2_1^+}$	0.56	0.5602

Table (4-42): The $B(M1; J_i \rightarrow J_f)$ values , in the units of (μ_N^2) , and the magnetic dipole moments for the 2_1^+ states ($\mu_{2_1^+}$) in the unit of (μ_N) , for ^{102}Zr -isotopes obtained by IBM-2 results . The effective g- charges are taken as $g_v = -0.02$ and $g_\pi = 1.39$

$J_i \rightarrow J_f$	$B(M1; J_i \rightarrow J_f)$	
	EXP. [96]	IBM-2
$2_1^+ \rightarrow 1_1^+$		0.4264
$2_2^+ \rightarrow 1_1^+$		0.0290
$2_3^+ \rightarrow 1_1^+$		0.0461
$2_2^+ \rightarrow 2_1^+$		0.3557
$2_3^+ \rightarrow 2_1^+$		0.0067
$2_3^+ \rightarrow 2_2^+$		0.0106
$3_1^+ \rightarrow 2_1^+$		0.0011
$3_1^+ \rightarrow 2_2^+$		0.0000
$3_1^+ \rightarrow 2_3^+$		0.0051
$\mu_{2_1^+}$	0.44	0.4401

Table (4-43): The $B(M1; J_i \rightarrow J_f)$ values , in the units of (μ_N^2) , and the magnetic dipole moments for the 2_1^+ states ($\mu_{2_1^+}$) in the unit of (μ_N) , for ^{104}Zr -isotopes obtained by IBM-2 results . The effective g- charges are taken as $g_v = -0.02$ and $g_\pi = 1.39$

$J_i \rightarrow J_f$	$B(M1; J_i \rightarrow J_f)$	
	EXP.	IBM-2
$2_1^+ \rightarrow 1_1^+$		0.3528
$2_2^+ \rightarrow 1_1^+$		0.0971
$2_3^+ \rightarrow 1_1^+$		0.1102
$2_2^+ \rightarrow 2_1^+$		0.0115
$2_3^+ \rightarrow 2_1^+$		0.1082
$2_3^+ \rightarrow 2_2^+$		0.0081
$3_1^+ \rightarrow 2_1^+$		0.0030
$3_1^+ \rightarrow 2_2^+$		0.0017
$3_1^+ \rightarrow 2_3^+$		0.0016
$\mu_{2_1^+}$		0.2065

Table (4-44): The $B(M1; J_i \rightarrow J_f)$ values , in the units of (μ_N^2) , and the magnetic dipole moments for the 2_1^+ states ($\mu_{2_1^+}$) in the unit of (μ_N) , for ^{106}Zr -isotopes obtained by IBM-2 results . The effective g- charges are taken as $g_v = -0.02$ and $g_\pi = 1.39$

$J_i \rightarrow J_f$	$B(M1; J_i \rightarrow J_f)$	
	EXP.	IBM-2
$2_1^+ \rightarrow 1_1^+$		0.4028
$2_2^+ \rightarrow 1_1^+$		0.0246
$2_3^+ \rightarrow 1_1^+$		0.0873
$2_2^+ \rightarrow 2_1^+$		0.0150
$2_3^+ \rightarrow 2_1^+$		0.0741
$2_3^+ \rightarrow 2_2^+$		0.0138
$3_1^+ \rightarrow 2_1^+$		0.0112
$3_1^+ \rightarrow 2_2^+$		0.0000
$3_1^+ \rightarrow 2_3^+$		0.0024
$\mu_{2_1^+}$		0.1332

Table (4-45): The $B(M1; J_i \rightarrow J_f)$ values , in the units of (μ_N^2) , and the magnetic dipole moments for the 2_1^+ states ($\mu_{2_1^+}$) in the unit of (μ_N) , for ^{108}Zr -isotopes obtained by IBM-2 results . The effective g- charges are taken as $g_v = -0.02$ and $g_\pi = 1.39$

$J_i \rightarrow J_f$	$B(M1; J_i \rightarrow J_f)$	
	EXP.	IBM-2
$2_1^+ \rightarrow 1_1^+$		0.3727
$2_2^+ \rightarrow 1_1^+$		0.0141
$2_3^+ \rightarrow 1_1^+$		0.0202
$2_2^+ \rightarrow 2_1^+$		0.0146
$2_3^+ \rightarrow 2_1^+$		0.6103
$2_3^+ \rightarrow 2_2^+$		0.0695
$3_1^+ \rightarrow 2_1^+$		0.0284
$3_1^+ \rightarrow 2_2^+$		0.0061
$3_1^+ \rightarrow 2_3^+$		0.0106
$\mu_{2_1^+}$		0.0179

4.3.3 δ - mixing ratios

The δ -mixing ratios of the γ -transitions from the excited states in $^{80-108}\text{Zr}$ -isotopes is also calculated in the present work using the following relationship

$$\delta(E2/M1) = 0.835 E_\gamma \times \Delta(E2/M1) (e.b/\mu_N)$$

Where E_γ is the transition energy in (MeV) and $\Delta(E2/M1)$ is in units of $(\frac{e.b}{\mu_N})$ and defined as the ratio of the reduced E2 matrix element to the M1 matrix elements.

The δ -mixing ratios calculated in the present work which are results of IBM-2 have been shown in the Table (4-46) to (4-59), these results were obtained by using same boson effective charges e_π , e_v for E2 and g_π , g_v factors for M1 strengths. Figure (4-30) shows the variation of δ for the group of $2_i^+ \rightarrow 2_1^+$ ($i = 2, 3, 4$ and 5) transitions and can be seen that both the magnitude and sign of δ obtained with chosen value of Majorana term $\xi_2 = -0.29$ which is the value obtained from the energy fit for ^{106}Zr .

Table (4-46): The value of δ -mixing ratio obtained by IBM-2 for the ^{80}Zr isotope .The IBM-2 results are obtained using the parameters ($e_\nu=0.175\text{ eb}$, $e_\pi=0.174\text{ eb}$), $g_\pi=2.839\mu_N$ and $g_\nu=-0.02\mu_N$.

E_i (MeV)	Transition $J_i \rightarrow J_f$	E_γ (MeV)	δ -mixing ratios (eb/ μ_N)
			IBM-2
0.985	$2_2^+ \rightarrow 2_1^+$	0.599	2.46551
1.934	$2_3^+ \rightarrow 2_1^+$	1.557	-0.04417
2.119	$2_4^+ \rightarrow 2_1^+$	1.733	0.27901
2.252	$2_5^+ \rightarrow 2_1^+$	1.866	-0.091357
1.934	$2_3^+ \rightarrow 2_2^+$	0.949	-0.60543
1.586	$3_1^+ \rightarrow 2_1^+$	1.200	5.84383
1.586	$3_1^+ \rightarrow 2_2^+$	0.601	3.7561
1.586	$3_1^+ \rightarrow 2_3^+$	0.348	0.8727777
1.586	$3_1^+ \rightarrow 2_4^+$	0.533	0.2502842
1.586	$3_1^+ \rightarrow 2_5^+$	0.666	16.34244
2.628	$1_1^+ \rightarrow 2_1^+$	2.242	-0.1953517
2.628	$1_1^+ \rightarrow 2_2^+$	1.643	-0.0287342
2.628	$1_1^+ \rightarrow 2_3^+$	0.694	1.343335
2.628	$1_1^+ \rightarrow 2_4^+$	0.509	-0.156789
2.628	$1_1^+ \rightarrow 2_5^+$	0.376	0.481479

Table (4-47): The value of δ -mixing ratio obtained by IBM-2 for the ^{82}Zr isotope .The IBM-2 results are obtained using the parameters ($e_\nu=0.183\text{ eb}$, $e_\pi=0.239\text{ eb}$), $g_\pi = 2.839\mu_N$ and $g_\nu = -0.02\mu_N$.

E_i (MeV)	Transition $J_i \rightarrow J_f$	E_γ (MeV)	δ -mixing ratios(eb/ μ_N)
			IBM-2
1.232	$2_2^+ \rightarrow 2_1^+$	0.799	5.3219
2.225	$2_3^+ \rightarrow 2_1^+$	1.792	-0.104313
2.627	$2_4^+ \rightarrow 2_1^+$	2.194	0.520509
2.781	$2_5^+ \rightarrow 2_1^+$	2.348	-0.308158
2.225	$2_3^+ \rightarrow 2_2^+$	0.993	-0.429784
1.965	$3_1^+ \rightarrow 2_1^+$	1.532	-1821.5030
1.965	$3_1^+ \rightarrow 2_2^+$	0.733	7.891340
1.965	$3_1^+ \rightarrow 2_3^+$	0.260	1.224160
1.965	$3_1^+ \rightarrow 2_4^+$	0.662	0.4902483
1.965	$3_1^+ \rightarrow 2_5^+$	0.816	-2.373418
3.192	$1_1^+ \rightarrow 2_1^+$	2.759	-0.7736616
3.192	$1_1^+ \rightarrow 2_2^+$	1.960	-0.01503187
3.192	$1_1^+ \rightarrow 2_3^+$	0.967	1.305612
3.192	$1_1^+ \rightarrow 2_4^+$	0.565	-0.2280955
3.192	$1_1^+ \rightarrow 2_5^+$	0.411	0.2969277

Table (4-48): The value of δ -mixing ratio obtained by IBM-2 for the ^{84}Zr isotope .The IBM-2 results are obtained using the parameters ($e_\nu=0.17\text{ eb}$, $e_\pi=0.156\text{ eb}$), $g_\pi=2.839\mu_N$ and $g_\nu=-0.02\mu_N$.

E_i (MeV)	Transition $J_i \rightarrow J_f$	E_γ (MeV)	δ -mixing ratios(eb/ μ_N)
			IBM-2
1.037	$2_2^+ \rightarrow 2_1^+$	0.608	1.829340
1.637	$2_3^+ \rightarrow 2_1^+$	1.208	-0.02552702
1.743	$2_4^+ \rightarrow 2_1^+$	1.314	-1.324562
2.206	$2_5^+ \rightarrow 2_1^+$	1.777	-0.01460117
1.637	$2_3^+ \rightarrow 2_2^+$	0.600	-0.06959940
1.850	$3_1^+ \rightarrow 2_1^+$	1.421	1.350493
1.850	$3_1^+ \rightarrow 2_2^+$	0.813	2.622810
1.850	$3_1^+ \rightarrow 2_3^+$	0.213	0.08233342
1.850	$3_1^+ \rightarrow 2_4^+$	0.107	0.07387262
1.850	$3_1^+ \rightarrow 2_5^+$	0.356	29.243050
2.420	$1_1^+ \rightarrow 2_1^+$	1.991	-0.3482842
2.420	$1_1^+ \rightarrow 2_2^+$	1.383	-0.02812837
2.420	$1_1^+ \rightarrow 2_3^+$	0.783	2.146860
2.420	$1_1^+ \rightarrow 2_4^+$	0.677	0.05121828
2.420	$1_1^+ \rightarrow 2_5^+$	0.214	-0.4272834

Table (4-49): The value of δ -mixing ratio obtained by IBM-2 for the ^{86}Zr isotope .The IBM-2 results are obtained using the parameters ($e_\nu=0.1304\text{ eb}$, $e_\pi=0.11\text{ eb}$), $g_\pi = 2.995\mu_N$ and $g_\nu = -0.02\mu_N$.

E_i (MeV)	Transition $J_i \rightarrow J_f$	E_γ (MeV)	δ -mixing ratios(eb/ μ_N)
			IBM-2
1.428	$2_2^+ \rightarrow 2_1^+$	0.915	0.2667982
1.714	$2_3^+ \rightarrow 2_1^+$	1.201	-0.1110435
1.914	$2_4^+ \rightarrow 2_1^+$	1.401	-0.4773804
2.549	$2_5^+ \rightarrow 2_1^+$	2.036	-0.4375679
1.714	$2_3^+ \rightarrow 2_2^+$	0.286	-0.04053773
2.272	$3_1^+ \rightarrow 2_1^+$	1.759	0.7120001
2.272	$3_1^+ \rightarrow 2_2^+$	0.844	0.5286462
2.272	$3_1^+ \rightarrow 2_3^+$	0.558	-0.005777884
2.272	$3_1^+ \rightarrow 2_4^+$	0.358	0.2049621
2.272	$3_1^+ \rightarrow 2_5^+$	0.277	0.02532076
2.753	$1_1^+ \rightarrow 2_1^+$	2.240	-0.2399552
2.753	$1_1^+ \rightarrow 2_2^+$	1.325	-0.1402560
2.753	$1_1^+ \rightarrow 2_3^+$	1.039	0.4003437
2.753	$1_1^+ \rightarrow 2_4^+$	0.839	0.08978785
2.753	$1_1^+ \rightarrow 2_5^+$	0.204	0.008834369

Table (4-50): The value of δ -mixing ratio obtained by IBM-2 for the ^{88}Zr isotope .The IBM-2 results are obtained using the parameters ($e_\nu=0.04\text{ eb}$, $e_\pi=0.131\text{ eb}$), $g_\pi = 0.725\mu_N$ and $g_\nu = -0.02\mu_N$.

E_i (MeV)	Transition $J_i \rightarrow J_f$	E_γ (MeV)	δ -mixing ratios(eb/ μ_N)
			IBM-2
1.793	$2_2^+ \rightarrow 2_1^+$	0.903	0.04952659
1.808	$2_3^+ \rightarrow 2_1^+$	0.918	-6.426427
2.707	$2_4^+ \rightarrow 2_1^+$	1.817	64.261670
2.713	$2_5^+ \rightarrow 2_1^+$	1.823	-0.2337036
1.808	$2_3^+ \rightarrow 2_2^+$	0.015	-0.001094273
2.388	$3_1^+ \rightarrow 2_1^+$	1.498	8.566548
2.388	$3_1^+ \rightarrow 2_2^+$	0.595	3.025233
2.388	$3_1^+ \rightarrow 2_3^+$	0.580	-0.1105472
2.388	$3_1^+ \rightarrow 2_4^+$	0.319	-0.03135578
2.388	$3_1^+ \rightarrow 2_5^+$	0.325	0.04473265
2.291	$1_1^+ \rightarrow 2_1^+$	1.401	-5.773053
2.291	$1_1^+ \rightarrow 2_2^+$	0.498	-1.829359
2.291	$1_1^+ \rightarrow 2_3^+$	0.483	0.01897847
2.291	$1_1^+ \rightarrow 2_4^+$	0.416	-0.02519172
2.291	$1_1^+ \rightarrow 2_5^+$	0.422	-0.1079777

Table (4-51): The value of δ -mixing ratio obtained by IBM-2 for the ^{92}Zr isotope .The IBM-2 results are obtained using the parameters ($e_\nu=0.04\text{eb}$, $e_\pi=0.125\text{eb}$), $g_\pi=0.725\mu_N$ and $g_\nu=-0.02\mu_N$.

E_i (MeV)	Transition $J_i \rightarrow J_f$	E_γ (MeV)	δ -mixing ratios(eb/ μ_N)
			IBM-2
1.748	$2_2^+ \rightarrow 2_1^+$	0.888	5.699437
1.763	$2_3^+ \rightarrow 2_1^+$	0.903	-0.1585751
2.623	$2_4^+ \rightarrow 2_1^+$	1.763	1.408785
2.647	$2_5^+ \rightarrow 2_1^+$	1.787	88.099220
1.763	$2_3^+ \rightarrow 2_2^+$	0.012	0.006987436
2.328	$3_1^+ \rightarrow 2_1^+$	1.468	7.574205
2.328	$3_1^+ \rightarrow 2_2^+$	0.580	0.02739461
2.328	$3_1^+ \rightarrow 2_3^+$	0.565	-5.376200
2.328	$3_1^+ \rightarrow 2_4^+$	0.295	-0.2776594
2.328	$3_1^+ \rightarrow 2_5^+$	0.319	-0.02881465
2.231	$1_1^+ \rightarrow 2_1^+$	1.371	-5.088652
2.231	$1_1^+ \rightarrow 2_2^+$	0.483	-0.05810928
2.231	$1_1^+ \rightarrow 2_3^+$	0.468	3.115738
2.231	$1_1^+ \rightarrow 2_4^+$	0.392	0.5311691
2.231	$1_1^+ \rightarrow 2_5^+$	0.416	-0.02497165

Table (4-52): The value of δ -mixing ratio obtained by IBM-2 for the ^{94}Zr isotope .The IBM-2 results are obtained using the parameters ($e_v=0.044\text{ eb}$, $e_\pi=0.11\text{ eb}$), $g_\pi = 0.725\mu_N$ and $g_v = -0.02\mu_N$.

E_i (MeV)	Transition $J_i \rightarrow J_f$	E_γ (MeV)	δ -mixing ratios(eb/ μ_N)
			IBM-2
1.753	$2_2^+ \rightarrow 2_1^+$	0.890	-1.689853E+08
2.268	$2_3^+ \rightarrow 2_1^+$	1.405	-0.05394498
2.634	$2_4^+ \rightarrow 2_1^+$	1.771	0.1807715
3.151	$2_5^+ \rightarrow 2_1^+$	2.288	-79.538620
2.268	$2_3^+ \rightarrow 2_2^+$	0.515	-1.352146
2.662	$3_1^+ \rightarrow 2_1^+$	1.799	-22.313180
2.662	$3_1^+ \rightarrow 2_2^+$	0.909	-16.742700
2.662	$3_1^+ \rightarrow 2_3^+$	0.394	3.655371
2.662	$3_1^+ \rightarrow 2_4^+$	0.028	-0.3643988
2.662	$3_1^+ \rightarrow 2_5^+$	0.489	-0.2542454
2.640	$1_1^+ \rightarrow 2_1^+$	1.777	-5.280875
2.640	$1_1^+ \rightarrow 2_2^+$	0.887	-0.02394567
2.640	$1_1^+ \rightarrow 2_3^+$	0.372	-7.450555
2.640	$1_1^+ \rightarrow 2_4^+$	0.006	-0.06170274
2.640	$1_1^+ \rightarrow 2_5^+$	0.511	-0.04909090

Table (4-53): The value of δ -mixing ratio obtained by IBM-2 for the ^{96}Zr isotope .The IBM-2 results are obtained using the parameters ($e_\nu=0.0468\text{ eb}$, $e_\pi=0.09\text{ eb}$), $g_\pi = 0.109\mu_N$ and $g_\nu = -0.02\mu_N$.

E_i (MeV)	Transition $J_i \rightarrow J_f$	E_γ (MeV)	δ -mixing ratios(eb/ μ_N)
			IBM-2
2.349	$2_2^+ \rightarrow 2_1^+$	1.072	4.255815
2.609	$2_3^+ \rightarrow 2_1^+$	1.332	-3.195287
2.705	$2_4^+ \rightarrow 2_1^+$	1.428	-13.034730
3.900	$2_5^+ \rightarrow 2_1^+$	1.623	5.812901
2.609	$2_3^+ \rightarrow 2_2^+$	0.260	-0.02330888
3.043	$3_1^+ \rightarrow 2_1^+$	1.766	3.761372
3.043	$3_1^+ \rightarrow 2_2^+$	0.694	3.954921
3.043	$3_1^+ \rightarrow 2_3^+$	0.434	-0.1015568
3.043	$3_1^+ \rightarrow 2_4^+$	0.338	-0.6457117
3.043	$3_1^+ \rightarrow 2_5^+$	0.143	0.1516502
2.830	$1_1^+ \rightarrow 2_1^+$	1.553	2.870311
2.830	$1_1^+ \rightarrow 2_2^+$	0.481	-0.08794313
2.830	$1_1^+ \rightarrow 2_3^+$	0.221	0.3822096
2.830	$1_1^+ \rightarrow 2_4^+$	0.125	0.1998432
2.830	$1_1^+ \rightarrow 2_5^+$	0.070	0.04755854

Table (4-54): The value of δ -mixing ratio obtained by IBM-2 for the ^{98}Zr isotope .The IBM-2 results are obtained using the parameters ($e_\nu=0.0526\text{ eb}$, $e_\pi=0.16\text{ eb}$), $g_\pi = 0.109\mu_N$ and $g_\nu = -0.02\mu_N$.

E_i (MeV)	Transition $J_i \rightarrow J_f$	E_γ (MeV)	δ -mixing ratios(eb/ μ_N)
			IBM-2
1.596	$2_2^+ \rightarrow 2_1^+$	0.653	-35.914020
1.771	$2_3^+ \rightarrow 2_1^+$	0.828	-0.2862242
2.253	$2_4^+ \rightarrow 2_1^+$	1.310	3.862088
2.540	$2_5^+ \rightarrow 2_1^+$	1.597	-34.147740
1.771	$2_3^+ \rightarrow 2_2^+$	0.175	-0.5657341
2.346	$3_1^+ \rightarrow 2_1^+$	1.403	11.337900
2.346	$3_1^+ \rightarrow 2_2^+$	0.750	-2.643913
2.346	$3_1^+ \rightarrow 2_3^+$	0.575	29.769620
2.346	$3_1^+ \rightarrow 2_4^+$	0.093	-2.680118
2.346	$3_1^+ \rightarrow 2_5^+$	0.194	-0.8363773
2.292	$1_1^+ \rightarrow 2_1^+$	1.349	-10.706490
2.292	$1_1^+ \rightarrow 2_2^+$	0.696	-0.1230151
2.292	$1_1^+ \rightarrow 2_3^+$	0.521	-24.225770
2.292	$1_1^+ \rightarrow 2_4^+$	0.034	-0.05422030
2.292	$1_1^+ \rightarrow 2_5^+$	0.248	-0.7176009

Table (4-55): The value of δ -mixing ratio obtained by IBM-2 for the ^{100}Zr isotope .The IBM-2 results are obtained using the parameters ($e_\nu=0.2312\text{ eb}$, $e_\pi=0.19\text{ eb}$), $g_\pi = 1.648\mu_N$ and $g_\nu = -0.02\mu_N$.

E_i (MeV)	Transition $J_i \rightarrow J_f$	E_γ (MeV)	δ -mixing ratios(eb/ μ_N)
			IBM-2
0.720	$2_2^+ \rightarrow 2_1^+$	0.484	0.03353068
0.992	$2_3^+ \rightarrow 2_1^+$	0.756	-0.9954945
1.149	$2_4^+ \rightarrow 2_1^+$	0.913	0.2352935
1.246	$2_5^+ \rightarrow 2_1^+$	1.010	1.711900
0.992	$2_3^+ \rightarrow 2_2^+$	0.272	-0.1865394
1.192	$3_1^+ \rightarrow 2_1^+$	0.956	25.080570
1.192	$3_1^+ \rightarrow 2_2^+$	0.472	4.986140
1.192	$3_1^+ \rightarrow 2_3^+$	0.200	-1.905698
1.192	$3_1^+ \rightarrow 2_4^+$	0.043	-0.6732090
1.192	$3_1^+ \rightarrow 2_5^+$	0.054	5.349079
1.539	$1_1^+ \rightarrow 2_1^+$	1.303	-0.09050661
1.539	$1_1^+ \rightarrow 2_2^+$	0.819	1.929985
1.539	$1_1^+ \rightarrow 2_3^+$	0.547	0.6091802
1.539	$1_1^+ \rightarrow 2_4^+$	0.390	-0.3323646
1.539	$1_1^+ \rightarrow 2_5^+$	0.293	-0.06083475

Table (4-56): The value of δ -mixing ratio obtained by IBM-2 for the ^{102}Zr isotope .The IBM-2 results are obtained using the parameters ($e_\nu=0.2387\text{ eb}$, $e_\pi=0.178\text{ eb}$), $g_\pi = 1.39\mu_N$ and $g_\nu = -0.02\mu_N$.

E_i (MeV)	Transition $J_i \rightarrow J_f$	E_γ (MeV)	δ -mixing ratios(eb/ μ_N)
			IBM-2
0.908	$2_2^+ \rightarrow 2_1^+$	0.766	0.02224118
1.243	$2_3^+ \rightarrow 2_1^+$	1.101	-4.881112
1.577	$2_4^+ \rightarrow 2_1^+$	1.435	0.05617370
1.658	$2_5^+ \rightarrow 2_1^+$	1.516	1.445071
1.243	$2_3^+ \rightarrow 2_2^+$	0.335	-0.7882174
1.412	$3_1^+ \rightarrow 2_1^+$	1.270	12.417440
1.412	$3_1^+ \rightarrow 2_2^+$	0.504	14.256380
1.412	$3_1^+ \rightarrow 2_3^+$	0.169	-2.546024
1.412	$3_1^+ \rightarrow 2_4^+$	0.165	-2.519345
1.412	$3_1^+ \rightarrow 2_5^+$	0.246	-0.4391804
1.752	$1_1^+ \rightarrow 2_1^+$	1.610	-0.05685129
1.752	$1_1^+ \rightarrow 2_2^+$	0.844	1.998139
1.752	$1_1^+ \rightarrow 2_3^+$	0.509	0.1459061
1.752	$1_1^+ \rightarrow 2_4^+$	0.175	-0.2716937
1.752	$1_1^+ \rightarrow 2_5^+$	0.094	-0.01538062

Table (4-57): The value of δ -mixing ratio obtained by IBM-2 for the ^{104}Zr isotope .The IBM-2 results are obtained using the parameters ($e_\nu=0.26175\text{ eb}$, $e_\pi=0.21\text{ eb}$), $g_\pi = 1.39\mu_N$ and $g_\nu = -0.02\mu_N$.

E_i (MeV)	Transition $J_i \rightarrow J_f$	E_γ (MeV)	δ -mixing ratios(eb/ μ_N)
			IBM-2
0.955	$2_2^+ \rightarrow 2_1^+$	0.815	4.250752
1.389	$2_3^+ \rightarrow 2_1^+$	1.249	-0.5118751
1.852	$2_4^+ \rightarrow 2_1^+$	1.712	-0.1669035
1.907	$2_5^+ \rightarrow 2_1^+$	1.767	0.3689441
1.389	$2_3^+ \rightarrow 2_2^+$	0.434	-1.569667
1.264	$3_1^+ \rightarrow 2_1^+$	1.124	9.923706
1.264	$3_1^+ \rightarrow 2_2^+$	0.309	8.871681
1.264	$3_1^+ \rightarrow 2_3^+$	0.125	1.694591
1.264	$3_1^+ \rightarrow 2_4^+$	0.588	76.942990
1.264	$3_1^+ \rightarrow 2_5^+$	0.643	0.2765769
2.309	$1_1^+ \rightarrow 2_1^+$	2.169	-0.4581255
2.309	$1_1^+ \rightarrow 2_2^+$	1.354	-0.3243822
2.309	$1_1^+ \rightarrow 2_3^+$	0.920	0.7976437
2.309	$1_1^+ \rightarrow 2_4^+$	0.457	0.8771442
2.309	$1_1^+ \rightarrow 2_5^+$	0.402	-0.2950890

Table (4-58): The value of δ -mixing ratio obtained by IBM-2 for the ^{106}Zr isotope .The IBM-2 results are obtained using the parameters ($e_\nu=0.21\text{ eb}$, $e_\pi=0.1877\text{ eb}$), $g_\pi = 1.39\mu_N$ and $g_\nu = -0.02\mu_N$.

E_i (MeV)	Transition $J_i \rightarrow J_f$	E_γ (MeV)	δ -mixing ratios(eb/ μ_N)
			IBM-2
0.888	$2_2^+ \rightarrow 2_1^+$	0.774	2.733126
1.294	$2_3^+ \rightarrow 2_1^+$	1.180	-0.4048875
1.601	$2_4^+ \rightarrow 2_1^+$	1.487	0.7446577
1.709	$2_5^+ \rightarrow 2_1^+$	1.595	31.067320
1.294	$2_3^+ \rightarrow 2_2^+$	0.376	-0.7490517
1.160	$3_1^+ \rightarrow 2_1^+$	1.046	4.471070
1.160	$3_1^+ \rightarrow 2_2^+$	0.272	115.413300
1.160	$3_1^+ \rightarrow 2_3^+$	0.089	1.002137
1.160	$3_1^+ \rightarrow 2_4^+$	0.441	1.568506
1.160	$3_1^+ \rightarrow 2_5^+$	0.549	-0.8948597
1.819	$1_1^+ \rightarrow 2_1^+$	1.705	-0.3919338
1.819	$1_1^+ \rightarrow 2_2^+$	0.931	-0.4949175
1.819	$1_1^+ \rightarrow 2_3^+$	0.570	0.4231160
1.819	$1_1^+ \rightarrow 2_4^+$	0.218	-0.9410841
1.819	$1_1^+ \rightarrow 2_5^+$	0.110	0.001133918

Table (4-59): The value of δ -mixing ratio obtained by IBM-2 for the ^{108}Zr isotope .The IBM-2 results are obtained using the parameters ($e_\nu=0.21\text{ eb}$, $e_\pi=0.1877\text{ eb}$), $g_\pi = 1.39\mu_N$ and $g_\nu = -0.02\mu_N$.

E_i (MeV)	Transition $J_i \rightarrow J_f$	E_γ (MeV)	δ -mixing ratios(eb/ μ_N)
			IBM-2
0.646	$2_2^+ \rightarrow 2_1^+$	0.505	1.612056
0.908	$2_3^+ \rightarrow 2_1^+$	0.767	0.06726045
1.023	$2_4^+ \rightarrow 2_1^+$	0.891	1.228737
1.189	$2_5^+ \rightarrow 2_1^+$	1.048	-0.3634193
0.908	$2_3^+ \rightarrow 2_2^+$	0.262	-0.1810648
0.936	$3_1^+ \rightarrow 2_1^+$	0.795	1.830920
0.936	$3_1^+ \rightarrow 2_2^+$	0.290	-3.190639
0.936	$3_1^+ \rightarrow 2_3^+$	0.028	0.1271712
0.936	$3_1^+ \rightarrow 2_4^+$	0.096	0.4352536
0.936	$3_1^+ \rightarrow 2_5^+$	0.253	-0.09108128
1.039	$1_1^+ \rightarrow 2_1^+$	0.898	-0.2917548
1.039	$1_1^+ \rightarrow 2_2^+$	0.393	0.2580431
1.039	$1_1^+ \rightarrow 2_3^+$	0.131	-0.5663972
1.039	$1_1^+ \rightarrow 2_4^+$	0.016	-0.001844530
1.039	$1_1^+ \rightarrow 2_5^+$	0.150	0.1302961

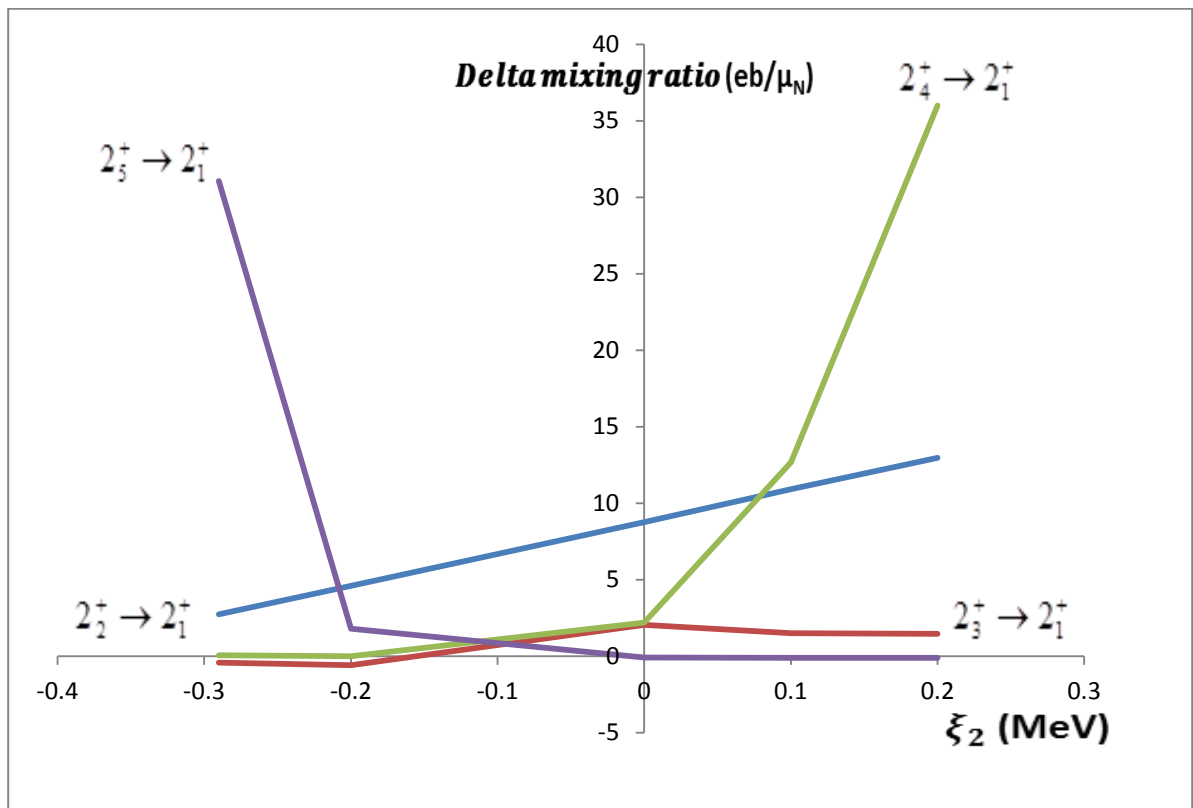


Figure (4-30): The multipole mixing ratio δ , of $2_i^+ \rightarrow 2_1^+$ transitions is plotted against ξ_2 for ^{106}Zr .

Chapter five

Conclusions and future works

Chapter five

Conclusions and future works

5-1 Conclusions

- It is concluded that the mixed symmetry 1_M^+ and 3_M^+ levels are affected by the Majorana force parameters ξ_1 and ξ_3 respectively, while the parameter ξ_2 affects the energies of all levels which are considered to have mixed symmetry character, and it affects strongly the 2^+ states.
- The mixed symmetry character of 1_M^+ and 3_M^+ levels are confined to one level only whereas the 2_M^+ state may share the mixed symmetry character with its neighboring levels and this leads to some difficulties in identifying these states since the sharing weakens the mixed symmetry character over a number of 2_M^+ levels.
- In general, the calculated result of IBM-1 and IBM-2 for B(E2) transitions in all considered Zr-isotopes nearly best fit, and show an increase in their values for N= 40 and 42, then decreasing with the increase in the neutron number until N=58, again the values is increasing with increase in the neutron number for most transitions. On other hand the calculated values of B(E2) transition are decreasing with the increase in the neutron number and approaching the experimental values, like as B(E2; $2_2^+ \rightarrow 2_1^+$). The experimental B(E2) values were not always in good agreement throughout all considered Zr - isotopes. The calculated electric quadrupole moments for the first excited states $Q(2_1^+)$ in Zr – isotopes are in reasonable agreement between IBM-1 and IBM-2 results and agree with the available experimental data.
- The properties of the magnetic dipole operator have been studied only by the framework of IBM-2 because of the absence of the M1 transitions in the IBM-1. It is concluded that

the properties of M1 operator are exclusively determined by the parameters of g_π and g_ν factors, the magnetic dipole moments $\mu_{2_1^\dagger}$ and there was agreement between the calculated and experimental data.

- The calculated delta mixing ratios using IBM-2 model are reflecting the characteristic of initial state as symmetry or mixed symmetry state. It is concluded that the delta mixing ratios are very sensitive to the Majorana terms.

5-2 Future Works

1- It is interesting to study the odd- even nuclei (isotopes) by using the interacting boson - fermions model (IBFM) to examine the behaviors of the IBM parameters through the isotopes.

2- Comparison study of Zr isotopes with Ru, Mo and Pb groups of isotopes may be beneficial to overcome the lack of experimental data and extrapolate or interpolate the descriptions of these nuclei.

References

References

- [1]. Walter E. Meyerhof “**Elements of nuclear physics**” published by HcGraw-Hill, Inc. library of Congress, USA, 67- 15247, (1976).
- [2]. J. L. Basdevant J. Rich, and M. Spiro “**Fundamentals In Nuclear Physics**”, published by Springer Science and Business Media, Inc., 233, NY 10013, USA (2005).
- [3]. F. F. Mende “**Liquid-Drop Model of Electron and Atom**”, published by *AASCIT Journal of Physics*. Vol. 1, No. 2, pp. 107-110, (2015)
- [4]. Nader Ghahramany, Shirvan Gharaati, and Mohammad Ghanaatian “**New approach to nuclear binding energy in integrated nuclear model**”, published by Springer, ResearchGate, *Journal of Theoretical and Applied Physics* 6, 3, (2012)
- [5]. A. Das and T. Ferbel “**INTRODUCTION TO NUCLEAR AND PARTICLE PHYSICS (2nd Edition)**”, published by World Scientific Publishing Co. Pte. Ltd., USA. (2003).
- [6]. W. N. Cottingham and D. A. Greenwood “**An introduction to nuclear physics**”, published by Cambridge University Press, CB2 2RU,UK, USA, (2004).
- [7]. K. S. Krane “**Introductory Nuclear Physics**”, published by Congress Library, 87-10623, 537-7, (1988) .
- [8]. H. Hassanabadi · A. Armat and L. Naderi “**Relativistic Fermi-Gas Model for Nucleus**”, published by Springer Science and Business Media, ResearchGate, NY, (2014).
- [9]. A. F. Lisetskiy, N. Pietralla, C. Fransen, R. V. Jolos, and P. von Brentano “**Shell model description of “mixed-symmetry” states in ⁹⁴Mo**”, published by *nucl-th*, Vol. 1, 7035, (2000).
- [10]. Norman D. Cook “**Models of the Atomic Nucleus**”, published by Springer Science, Library of Congress, CN.2010936431, (2010).
- [11]. Mirzaei Vahid, Askari Mohammad Bagher and Mirhabibi Mohsen. “**Study of Nuclear Shell Model**”, published by *Open Science Journal of Modern Physics*. Vol. 2, No. 3, pp. 19-22, (2015).

References

- [12]. Charles W. Lucas, Jr. Eric C. Baxter, Edward A. Boudreaux, and Roger A. Rydin “**A classical electro-dynamic theory of the nucleus**”, published by PHYSICS ESSAYS Journal, Vol. 26, No. 3, (2013).
- [13]. A Gargano, L Coraggio, A Covello and N Itaco “**Realistic shell-model calculations and exotic nuclei**”, Published by IOP, Journal of Physics, 527, 012004, (2014).
- [14]. P.O. Hess, M. Seiwert, J. Maruhn and W. Greiner “**General Collective Model and its Application to $^{238}_{92}\text{U}$** ”, published by Journal of Atoms and Nuclei, Vol. 296, pp. 147-163, (1980).
- [15]. Robert James Casperson “**Experimental and Numerical Analysis of Mixed-Symmetry States and Large Boson Systems**”, Published by UMI 3415010-2010 and by ProQuest LLC, ProQuest LLC 789, 17, United States Code. (2010).
- [16]. F. Iachello, and A. Arima, “**The Interacting Boson Model**”, published in the USA by Cambridge University Press, NY, (1987).
- [17]. R. F. Casten, and D. D. Warner “**The Interacting Boson Approximation**”, published by Reviews of Modern Physics, The American Physical Society Vol. 60, No. 2, April (1988).
- [18]. J. Engel, and F. Iachello, “**Interacting Boson Model of Collective Octupole States (I). The Rotational limit**”, published by Nuclear Physics, A-472, 61-84, (1987)
- [19]. R.F. Cassten “**Nuclear Structure from a Simple Perspective**”, published by Oxford University Press, P.314 (1990).
- [20]. Olaf Scholten, “**The interacting boson approximation model and applications**”, published in Geboren Te Madium INDONESIA (1980).
- [21]. A. Frank, J. Jolie and P. Van Isacker “**Symmetries in Atomic Nuclei**”, published by Springer Science, modern physics, LLC (2009).

References

- [22]. Enrique López-Moren and Octavio Castanos “**Shapes and stability within the interacting boson model: Effective Hamiltonians**”, published by ResearchGate, *Rev. Mex. Fiz.* 44S2, pp. 48-54, (1998).
- [23]. F. Iachello and P. Van Isacker, “**The Interacting Boson-Fermion Model**”, published by Cambridge University Press, Cambridge (1991).
- [24]. N. Yoshida, and F. Iachello “**Two-neutrino double β -decay in the interacting boson-fermion model**”, published by Prog. Theor. Exp. Phys. (PTEP), Vol. 43, No. 1, 1-25, (2013).
- [25]. K. Zajac and S. Szpikowski “**The new diagonalization procedure in the interacting boson model and its application**”, published by Acta Physica Polonica, Vol. B17 No. 12 (1986).
- [26]. Muhsen Cadem Motleb and Heiyam Najy Hady Dam “**Investigation of nuclear energy levels in ^{90}Sr nucleus**”, published by Journal of Babylon university, pure and applied Sciences, No. 2, Vol. 19. (2011).
- [27]. Imam Hossain, Hewa Y. Abdullah, Imad M. Ahmed, and Mohammad A Saeed, “**Ground-state energy band of even $^{104-122}\text{Cd}$ isotopes under the framework of interacting boson model-1**”, published by Springer science, Journal of Theoretical and Applied Physics, (2013).
- [28]. Vidya Devi, “**structure and odd-even staggering of Mo, RU and Pd even-even nuclei in the framework of IBM-1**”, published by Turkish Journal of Physics, Turk J phys TUBTAK, 37, 330-347. (2013).
- [29]. K. J. R. Rosman and P. D. P. Taylor “**Table of Isotopic Masses and Natural Abundances**”, published by Pure Appl. Chem., 71, 1593-1607, (1999).

References

- [30]. P. D. Desai, H. M. James, and C. Y. Ho “**Electrical Resistivity of Vanadium and Zirconium**”, published by J. Phys. Chem. Ref. Data, Vol. 13, No. 4, (1984).
- [31]. J. E. Sansonetti and W. C. Martin “**Handbook of Basic Atomic Spectroscopic Data**,” published by J. Phys. Chem. Ref. Data, Vol. 34, No. 4, (2005).
- [32]. Elhami, Esmat, “**Studied of low-lying states in ^{94}Zr excited with the inelastic neutron scattering reaction**”, published by University of Kentucky Doctoral Dissertations, paper 624 (2008).
- [33]. W. Akram, M. Schönabächler, S. Bisterzo and R. Gallino, “**Zirconium isotope evidence for the heterogeneous distribution of s-process materials in solar system**”, Published by Elsevier Ltd. Vol. 165, p. 484-500. (2015).
- [34]. Toshiyuki Sumikama, “**Discovery deformed Magic Number for Zirconium Isotopes**”, published in *Physical Review Letters*. (2011).
- [35]. V. E. Oberacker, A. S. Umar, E. Teran and A. Blazkiewicz, “**Hartree-Fock-Bogoliubov calculations in coordinate space: neutron-rich Sulfur, Zirconium, Cerium and Samarium Isotopes**”, published by Nuclear theo. Ltd. (2003).
- [36]. Ali A. Alzubadi, Z. A. Dakhil and Sheimaa T. Aluboodi, “**Microscopic study of nuclear structure for some Zr-isotopes using Skyrme-Hartree-Fock Method**”, published by Journal of Nuclear and Particle Physics 4(6): 155-163. (2014).
- [37]. Baharat Kumar, S. K. Singh, and S. K. Patra, “**Shape co-existence and parity doublet in Zr isotopes**”, published by International Journal of Modern Physics E. (2014).
- [38]. C. Y. Wu, H. Hua and D. Cline, “**The role of the intrinsic E2 matrix element between the first two 0^+ states in their configuration mixing in ^{100}Zr** ”, published by Elsevier, ScienceDirect, Physics letters B, 541, 59-63. (2002).

References

- [39]. H. Hua, C. Y. Wu, A. B. Hayes, and R. Teng with R. M. Clark, P. Fallon, A. Goergen, A. O. Macchiavelli, and K. Vetter, “**Triaxiality and the aligned $h_{11/2}$ neutron orbital in neutron-rich Zr and Mo isotopes**”, published by American Physical Society, PHYSICAL REVIEW C 69, 014317, (2004).
- [40]. V. Werner, D. Belic, P. von Brentano, C. Fransen, A. Gade, H. von Garrel, J. Jolei, U. Kneissl, C. Kohstall, A. Linnemann, A. F. Lisetskiy, N. Pietralla, H. H. Pitz, M. Scheck, K. –H. Speidel, F. Stedile, and S. W. Yates. “**Proton-neutron structure of the N=52 nucleus ^{92}Zr** ” published by ScienceDirect, ELSEVIER, Physics Letters B, 550, 140-146, (2002).
- [41]. A. Navin, M. Rejmund, C. Schmitt, S. Bhattacharyya, G. Lhersonneau, P. Van Isacker, M. Caamaño, E. Clément, O. Delaune, F. Farget, and G. de France. “**Towards the high spin-isospin frontier using isotopically-identified fission fragments**” published by, ELSEVEIR, Physics Letters B, 728, 136-140, (2014).
- [42]. J. E. Garcia-Ramos, K. Heyde, R. Fossion, V. Hellemans, and S. De Baerdemacher “**A theoretical description of energy spectra and two-neutron separation energies for neutron-rich zirconium isotopes**”, published by Nuclear Th. physics, (2005).
- [43]. J. Skalski, P. –H. Heenen, P. Bonche, and H. Flocard, “**Shape transition and collective dynamics in even $^{94-100}\text{Zr}$ nuclei**”, published by Zakopane School of Physics, ZAKOPANE, Poland ,Vol. 24, pp. 413-416, (1992).
- [44]. S. Lalkovski, and P. Van Isacker, “**IBM-1 calculations towards the neutron-rich nucleus ^{106}Zr** ”, published by American Physical Society, Physical Review C, Vol. 79, No. 1, (2009).
- [45]. H. Toki, D. Cha, and G. Bertsch, “**Giant M1 states in Zr isotopes within the simple shell model**”, published by Physical Review C, Vol. 24, No. 3, (1981).

References

- [46]. Ritu Chaudhary, Rani Devi, and S. K. Khosa, **“Microscopic study of oblate to prolate shape transition at higher spins in neutron-rich $^{100-104}\text{Zr}$ isotopes”**, Published by Nuclear Physics, Vol. 60, pp. 88-89, (2015).
- [47]. Hemalatha M., Bhagwat A., Shrivastava A., Kailas S., and Gambhir Y. K., **“Anomaly in the nuclear charge radii of Zr isotopes”**, published by Physical Review C, vol. 70, Issue 4, id. 044320. (2004).
- [48]. L. C. Gomes, and O. Dietzsch, **“Neutron separation energies of Zr isotopes”**, published in Sao Paulo, Brazil, Z. Naturforsch. 31a, 393-394. (1976).
- [49]. Ali Abdulwahab Ridha, **“Deformation parameters and nuclear radius of Zirconium (Zr) isotopes using the deformed shell model”**, published by Wasit Journal for science & Medicine, 2(1), 115-125, (2009).
- [50]. Shetha Farhan AboAlhose, **“Investigation of the neutron-rich zirconium ($A=92,94$) nuclei with the interacting boson model”**, published by Journal of Kerbala University, Vol. 10 No. 1, Scientific, (2012).
- [51]. A. R. H Subber, Mohammed A. Al Sharefi, and Ahmed M. Shuaib, **“A study of some nuclear properties of a nuclei with mass numbers ($A=100,102$) using interacting boson model”**, published by Journal of Kerbala University, Vol. 10, No. 1 Scientific, (2012).
- [52]. A. R. H Subber, Mohammed A. Al Sharefi, and Ahmed M. Shuaib, **“Investigation of some even-even nuclei with mass numbers ($A= 98,100$) by interacting boson model”**, published by Journal of Kerbala University, Vol. 10, No. 1, Scientific, (2012).
- [53]. P. Sarriguren and J. Pereira, **“ β -decay properties of Zr and Mo neutron-rich isotopes”**, published by National Superconducting Cyclotron Laboratory Journal (NSCL) PHY- 01-10253, (2010).

References

- [54]. R. Rodriguez-Guzman, P. Sarriguren, L. M. Robledo and S. Perez-Martin, **“Charge radii and structural evolution in Sr, Zr and Mo isotopes”**, published by Physical Letters B, Vol. 691, pp. 202-207, (2010).
- [55]. M. Hemalatha, S. Kailas, W. Haider, and Y. K. Gambhir, **“Study of spin rotation function for polarized proton incident on Zr and Sn isotopes”**, published by International Symposium on Nuclear Physics, (2009).
- [56]. A. Holt, T. Engeland, M. Hjorth-Jensen and E. Osnes, **“Application of realistic effective interactions to the structure of the Zr isotopes”** published by Nucl-th, Vol.1, N-0316, (2000).
- [57]. S.S. Dimitrova¹, D. Bianco, N. Lo Iudice, F. Andreozzi, and A. Porrino, **“Shell Model Calculations for Even Zirconium Isotopes”**, published by Heron Press, NUCLEAR THEORY, Vol. 32, (2013).
- [58]. F. Browne, A. M. Bruce, T. Sumikama, I. Nishizuka, S. Nishimura, P. Doornenbal, G. Lorusso, P.-A. Söderström, H. Watanabe, R. Daido, Z. Patelf, S. Ricef, L. Sinclairg, J. Wuh, Z. Y. Xu, A. Yagi, H. Baba, N. Chigac, R. Carroll, F. Didierjean, Y. Fang, N. Fukuda, G. Geyl, E. Ideguchi, N. Inabe, T. Isobe, D. Kameda, I. Kojouharov, N. Kurz, T.Kubo, S. Lalkovski, Z. Li, R. Lozeva, H. Nishibata, A. Odahara, Zs. Podolyák, P. H. Regan, O. J. Roberts, H. Sakurai, H. Schaffner, G. S. Simpson, H. Suzuki, H. Takeda, M. Tanaka, J. Taprogge, V. Werner, and O. Wieland, **“ Lifetime measurements of the first 2^+ states in $^{104,106}\text{Zr}$: Evolution of ground-state deformations”**, published by ScienceDirect, ELSEIVER, Physics Letters B, Vol.750, P. 448–452 (2015).
- [59]. Yu. P. Gangrskii, S. G. Zemlyanoi, B. K. Kul'dzhanov, K. P. Marinova, B. N. Markov, Hoang Thi Kim Hue, and Chan Kong Tam, **“Determination of the differences between the charge radii of zirconium nuclei using laser-excited resonance fluorescence”**, published by American Institute of Physics. Sov. Physics, JETP, 67(6), 0038-5646, (1988) .

References

- [60]. P. Quinet, S. Bouazza, and P. Palmeri, “**A comparative study between semi-empirical oscillator strength parametrization and relativistic Hartree-Fock methods for computing the radiative parameters in Zr II spectrum**”, published at Research Director, Scientific Research F.R.S.-FNRS, (2015).
- [61]. Saad N. Abood and Laith A. Najim, “**Interacting Boson Model (IBM-2) calculations of selected even-even Te nuclei**”, published by Pelagia Research Library, Adv. Appl. Sci. Res. 4(1), 444-451, (2013).
- [62]. Vidya Devi, “**The study of transition probabilities in low-lying levels of light Mg-Zr nuclei**”, published by Nucl. Phys. Vol. 60, pp. 186-187, (2015).
- [63]. Sundus Yaseen Hasan, Heiyam Najy Hady, “**The Interacting Boson model-1 Applied to the even-even $^{106-116}\text{Pd}$ Isotopes**”, published by Journal of Kuka-Physics, Vol. 2 no.1 (2010).
- [64]. K. A. Al-Maqtary, “**IBM-1 Calculations of Energy Levels and Electric Transition Probabilities B(E2) in $^{158-160}\text{Gd}$ Isotopes**”, published by Jordan Journal of Physics, Volume 6, Number 2, pp. 95-102, (2013).
- [65]. Mohammed Abdul Ameer, Mushtaq A. H. Al-Shimmary, “**IBM-1 INVESTIGATION FOR THE EVEN-EVEN $^{180-190}\text{W}$ ISOTOPES**”, published by Armenian Journal of Physics, vol. 4, issue 3, pp. 146-153. (2011).
- [66]. Muhsen Cadem motelb, “**Investigation of the low laying energy levels structure of the rich neutron isotopes $^{78-88}\text{Kr}$** ”, published by Journal of Babylon University, Pure and Applied Sciences, No.(3), Vol.(19), (2011).
- [67]. Atalay Küçük bursa and Kaan Manisa, “**IBM-1 CALCULATIONS ON THE EVEN-EVEN $^{122-128}\text{Te}$ ISOTOPES**”, published by Mathematical and Computational Applications, Vol. 10, No. 1, pp. 9-17, (2005).

References

- [68]. D. Bucurescu, G. Cata, D. Cutoiu, G. Constantinescu, M. Ivascu, and N. V. Zamfir, **“Description of the neutron deficient Sr and Zr isotopes in the interacting boson model”**, published by Nuclear Physics A, Vol. 401, PP. 22- 40, (1983).
- [69]. D. Bonatsos, **“Interacting boson models of nuclear structure”**, published by oxford university press, Clarendon press oxford. (1988).
- [70]. Ahmad K. Mheemeed, **“Calculation of Energy Levels and The Reduced Transitions Probability for Even-Even Number of Isotones (N=90)”**, published by J. Edu. & Sci., Vol. (21), No. (4), (2008).
- [71]. Fouad A. MAJEED and Kalid S. JASSIM ,**“Study of Phase Transitions and Critical Points in the Rare-Earth Region in the Framework of the Interacting Boson Model (IBM-1)”**, published by Babylon University, P.O.Box 4, Hilla-Babel, Iraq. (2003).
- [72]. Nurettin Turkan, Davut Olgun, and Yhsan Uluer, **“IBM-2 calculations of some even-even selenium nuclei”**, published by Central European Journal of Physics, Research article CEJP 4(1), pp. 124–154, (2006).
- [73]. Feng Pan, J. P. Draayer, **“New algebraic solutions for $SO(6) \leftrightarrow U(5)$ transitional nuclei in the interacting boson model”**, published by Elsevier, Nuclear Physics A, Vol. 636, pp. 156-168, (1998).
- [74]. H. M. Mittal and Vidya Devi, **“EVIDENCE FOR POSSIBLE $O(6)$ SYMMETRY IN $A=120-200$ MASS REGION”**, Armenian Journal of Physics, vol. 2, issue 3, pp. 146-156, (2009).
- [75]. Harun Resit Yazar and Ihsan Uluer, **“A CORRESPONDENCE BETWEEN IBA-I AND IBA-II MODEL AND ELECTROMAGNETIC TRANSITIONS OF SOME ERBIUM ISOTOPES”**, published by Mathematical and Computational Applications, Vol. 12, No. 2, pp. 69-76, (2007).

References

- [76]. Jundi Khalat Yousif, “**Nuclear structure of even-even $^{104-110}\text{Mo}$ isotopes**”, published by International Journal Scientific & Engineering Research Vol. 3, Issue 12, (2012).
- [77]. Zhang Dali and Ding BingGang, “**Description of the properties of the low-lying energy states in ^{100}Mo with IBM2**”, published by Science China, Physics, Mechanics & Astronomy, Vol. 57, No. 3, pp. 447- 452, (2014).
- [78]. M. A. Al-Shareefi and A. A. O. Musa, “**IBM-2 Calculation of the energy levels of $^{90-94}\text{Sr}$ and $^{156-160}\text{Yb}$** ”, published by Journal of Babylon University, Pure and Applied Science, No. 1, Vol. 22, 480-485, (2012).
- [79]. Saad Naji Abood, Abdul Kader Saad, Abdul Kader and Laith Ahmed Najim, “**IBM-2 Calculations for even-even Xe Isotopes**”, published by Pure and Applied Science, Vol. 1, Issue 1, Page 28-43, (2013).
- [80]. Rana Oday Al-Habib, “**Potential Energy Surfaces for Heavy Nuclei $^{228}_{88}\text{Ra}$, $^{230}_{90}\text{Th}$, and $^{232}_{92}\text{U}$** ”, published by Al- Mustansiriyah J. Sci. Vol. 23, No 7, (2012).
- [81]. Ali Abid Abojasseem, Ibtisam J. A. Fatlawi, Faeq A . AL-Tememe, and Suha H.Kadhem, “**Calculation of the Energy levels, the Square of rotational energy and The moment of inertia of $^{170-176}\text{Yb}$ Isotopes by the Interacting Boson Model-1**”, published by JOURNAL OF KUFA- PHYSICS, VOL.4, NO.1, (2012).
- [82]. Saddon Taha Ahmad and Diary Omar Kakil, “**The Prediction of the Electromagnetic Properties and the $\delta(E2/M1)$ of $^{110-116}\text{Cd}$ -Isotopes in IBM Model**”, published by Baghdad Science Journal Vol. 8, No. 3, (2011).
- [83]. F. I. Sharrad, H. Y. Abdullah, N. Al-Dahan, A. A. Okhunov, and H. A. Kassim, “**A CORRESPONDENCE BETWEEN IBA-1 AND IBA-2 MODELS OF EVEN ISOTOPES OF Sm**”, published by Armenian Journal of Physics, vol. 5, issue 3, pp. 111-121, (2012).

References

- [84]. Olaf Scholten, “**THE PROGRAM-PACKAGE PHINT**”, Kernfysisch Versneller Instituut, Zernikelaan 25, 9747 AA, Groningen, (1982).
- [85]. T. Otsuka and N. Yoshida, “**User’s Manual of the program NPBOS**”, published by Theoretical Division, Los Alamos National Laboratory, Los Alamos, New Mexico, 87545, U.S.A, (1985).
- [86]. BALRAJ SINGH, “**Live Chart of Nuclides - Levels for ^{80}Zr** ”, published by Nuclear Data Sheets 105, 223, (2005).
- [87]. J. K. Tuli, “**Live Chart of Nuclides - Levels for ^{82}Zr** ”, published by Nuclear Data Sheets 98, 209, (2003).
- [88]. T. Kibedi and J. Timar, “**Live Chart of Nuclides - Levels for ^{84}Zr** ”, published by Nuclear Data Sheets 110, 2815, (2009).
- [89]. ALEXANDRU NEGRET, and BALRAJ SINGH, “**Live Chart of Nuclides - Levels for ^{86}Zr** ”, published by Nuclear Data Sheets 124, 1, (2015).
- [90]. E.A. McCutchan and A.A. Sonzogni, “**Live Chart of Nuclides - Levels for ^{88}Zr** ”, published by Nuclear Data Sheets 115, 135, (2014).
- [91]. CORAL M. BAGLIN, “**Live Chart of Nuclides - Levels for ^{92}Zr** ”, published by Nuclear Data Sheets 113, 2187, (2012).
- [92]. D. Abriola, A.A. Sonzogni, “**Live Chart of Nuclides - Levels for ^{94}Zr** ”, published by Nuclear Data Sheets 107, 2423, (2006).
- [93]. D. Abriola, A.A. Sonzogni “**Live Chart of Nuclides - Levels for ^{96}Zr** ” published by Nuclear Data Sheets 109, 2501, (2008).
- [94]. BALRAJ SINGH, ZHIQIANG HU “**Live Chart of Nuclides - Levels for ^{98}Zr** ” published by Nuclear Data Sheets 98, 335, (2003).

References

- [95]. BALRAJ SINGH “**Live Chart of Nuclides - Levels for ^{100}Zr** ” published by Nuclear Data Sheets 109, 297, (2008).
- [96]. D. DE FRENNE “**Live Chart of Nuclides - Levels for ^{102}Zr** ” published by Nuclear Data Sheets 110, 1745, (2009).
- [97]. JEAN BLACHOT “**Live Chart of Nuclides - Levels for ^{104}Zr** ” published by Nuclear Data Sheets 108, 2035, (2007)
- [98]. BALRAJ SINGH AND MICHAEL BIRCH, “**Live Chart of Nuclides - Levels for $^{106-108}\text{Zr}$** ”, published by Nuclear Data Sheets, ENSDF program, (2011).
- [99]. BALRAJ SINGH, “**Live Chart of Nuclides - Levels for $^{106-108}\text{Zr}$** ”, published by Nuclear Data Sheets, ENSDF program, (2011).
- [100]. D. DE FRENNE AND A. NEGRET, “**Live Chart of Nuclides - Levels for ^{106}Zr** ”, published by Nuclear Data Sheets 109, 943, (2008).
- [101]. Jean Blachot, “**Live Chart of Nuclides - Levels for ^{108}Zr** ”, published by Nuclear Data Sheets 91, 135, (2000) .
- [102]. B. Pritychenko, M. Birch, B. Singh, and M. Horoi, “**Tables of E2 transition probabilities from the first 2^+ states in even–even nuclei**”, published by Elsevier, SciencDirect, Atomic Data and Nuclear Data Tables, 107, 1–139, (2016).
- [103]. B. Pritychenko, M. Birch, B. Singh, and M. Horoi, “**Tables of E2 transition probabilities from the first 2^+ states in even–even nuclei**”, published by Nucl-th, at arXiv:1312.5975v6 [nucl-th] 2 Oct 2015, (2015).
- [104]. R. C. Nayak, and S. Pattnaik, “**B(E2) \uparrow PREDICTIONS FOR EVEN-EVEN NUCLEI IN THE DIFFERENTIAL EQUATION MODEL**”, published by Nucl-th, at arXiv:1405.3191v1 [nucl-th] 13 May 2014, (2014).

References

- [105]. S. Raman, C. W. Nestor, JR., and P. Tikkanen, **“Transition probability from the ground state to the first –excited 2^+ state of even-even nuclides”**, published by Atomic Data and Nuclear Data Tables, Vol. 78, No.1, 1-128, (2001).
- [106]. S. Raman, C. W. Nestor, JR., S. KAHANE, and K. H. BHATT, **“PREDICITONS OF $B(E2;0_1^+ \rightarrow 2_1^+)$ VALUES FOR EVEN-EVEN NUCLEI”**, published by ATOMIC DATA AND NUCLEAR DATA TABLES, Vol. 42, No. 1, 1-54, (1989).
- [107]. P. Raghavan, **“Table of Isotopes”**, published by and Atomic Data and Nuclear Data Tables, Vol. 42, 189, (1989).

الخلاصة

لقد تم دراسة التركيب النووي لنظائر الزركونيوم التي عددها النيوتروني ($N = 40, 42, 44, 46, 48, 52, 54, 56, 58$) نظريا ضمن اطار عمل نموذج البوزونات المتفاعلة (IBM-1, BM-2). تم دراسة حدود التماثل تعتبر نواة استخدام الطاقة في الثانية متحمس الدولة بالنسبة إلى الحالة المثارة الأولى. تم العثور على اعتبار نوى أن تكون انتقالية في المنطقة $SU(5)$ الى $SU(3)$, و $O(6)$. ان صفات المستويات الأوطأ ذات التناظر المختلط مثل 1^+ , 2^+ , 3^+ التي استخرجت بواسطة نموذج (IBM-2) لنظائر الزركونيوم ذات التناظرات ($SU(5)$, $SU(3)$, و $O(6)$) الاهتزازية, الدورانية و جاما الغير مستقرة على التوالي قد درست بالتفصيل. لقد وجد بأن مستويات التناظر المختلط 1_M^+ , 3_M^+ تتأثر بمعاملتي قوة ماجورانا ξ_1 و ξ_3 على التوالي, بينما يؤثر المعامل ξ_2 على كل المستويات التي تحمل خاصية التناظر المختلط, حيث أنه يؤثر بقوة على مستويات 2^+ , كما أنه يتحكم في الشراكة بين المستوي 2_M^+ وجيرانه من مستويات 2^+ . كما وجد بأنه خاصية التناظر المختلط 1_M^+ , 3_M^+ تعود الى مستوي واحد فقط في كل نظير بينما المستوي 2_M^+ يمكن أن يشترك بخاصية التناظر المختلط مع جيرانه من المستويات.

في إطار IBM-1 و IBM-2، وتمت دراسة خصائص مستوى الطاقة مع تماثل إيجابي من الأرض وبيتا وجاما العصابات. بشكل عام، وأفضل مستنسخة أطيف الطاقة تعادل إيجابي المنخفض الكذب وتحسب على أساس إطار IBM-2 من تلك التي IBM-1 في معظم الحالات. ويرجع ذلك إلى درجة البروتون نيوترون الحرية وغياب هذه الدول في نموذج IBM-1. ان الصفات الكهرومغناطيسية ضمن اطار عمل IBM-2, IBM-1 قد درست وحللت نتائجها. ان صفات المؤثر $E2$ تعتمد صراحة على الشحنات المؤثرة المستخدمة في كل من IBM-2, IBM-1. لقد وجد أن لقيم مختلفة من α_2 في إطار IBM-1 وكذلك قيم مختلفة لكل من e_π و e_ν في إطار IBM-2 لكل نظير من نظائر Zr قد استخدمت لتوليد صفات $E2$ مثل ($E2$) و $Q(2^+)$ لجميع نظائر Zr المعنية. من ناحية أخرى فإن صفات M1 قد درست فقط في إطار IBM-2 بسبب غياب انتقالات M1 في IBM-1, كما وجد أن صفات M1 تعتمد بوضوح على g_π و g_ν في إطار IBM-2. أعطيت قيم ثابتة ل ($g_\nu = -0.02\mu_N$) لجميع نظائر Zr ولكن قيم مختلفة ل g_π في تلك الحسابات ل IBM-2 لتوليد صفات M1 مثل μ_{21}^+ , $B(M1)$ و نسب المزج $\delta(E2/M1)$ في هذه النظائر. لقد وجدنا النسبة المئوية ل برم F والتي من خلالها بيننا التناظر التام والمخلط للحالات. ان القيم الصغيرة لنسب المزج $\delta(E2/M1)$ التي لوحظت بالنسبة للانتقالات من الحالات ذات التناظر المختلط الى الحالات ذات التناظر التام.

**التركيب النووي لنظائر الزركونيوم الزوجية - الزوجية باستخدام أنموذج
البوزونات المتفاعلة (IBM-1 و IBM-2)**

رسالة

مقدمة الى مجلس كلية التربية في جامعة السليمانية
كجزء من متطلبات نيل درجة ماجستير في علوم الفيزياء
(الفيزياء نظرية)

من قبل

بيرون نصرالدين غفور

بكالوريوس فيزياء (2012)، جامعة السليمانية

باشراف

أ.م.د.سعدون طه أحمد

د.نارى كريم أحمد

كانون الاول

2016

سه رماوهرز

2716

بارگه کارتیکه ره به کارهینراوه کان له م دوو مۆدیله دا، بینرا که له بنچینهی کاری مۆدیلی IBM-1 دا به های α_2 به گۆراو دانرا بۆ ههر هاوتایهك , ههروهها به های گۆراو دانرا بۆ ههر یه که له $(e_\nu$ و e_π) له بنچینهی کاری IBM-2 دا بۆ ههر یه که له هاوتاکانی زرکونیوم , بۆ دست کهوتنی به های $B(E2)$ وه $Q(2^+)$ بو هه موو هاوتا ناماژه پیکراوهکانی زرکونیوم . له لایهکی تره وه لیکۆئینه وه کرا له سه ر تاییه تمه ندیهکانی موکنا تییسی جوت جه سه ریی کارتیکه ر ته نها به بنچینهی کاری IBM-2 له بهر نه وهی تاییه ت مه ندی M1 له IBM-1 توانای هاتنی نیه , وه بینرا که تاییه تمه ندی سیفه تی M1 به روونی به ند ده بییت له سه ر هاوکۆکه ی g_π و g_ν که به های نه گۆر دانرا بۆ ($g_\nu = -0.02$) بۆ هه موو هاوتاکانی زرکونیوم به لام به های گۆراو دانرا بۆ g_π بۆ هه رییه که له هاوتاکانی زرکونیوم , بۆ به دست هیئانی $B(M1)$ وه μ_1^+ وه ریژه ی تیکه ل $\delta(E2/M1)$ له م هاوتایانه دا . وه ریژه ی سه دی خولانه وهی (F-SPIN) F دۆزرایه وه و له ریگه یه وه هاوجییوونی ته واوه تی و هاوجییوونی تیکه ل پیشاندرایا بۆ ناسته کان به های بچوکی ریژه ی هاوجییوونی تیکه ل که ده ستخراوه ده توانییت گواسته نه وه بکات له ناستهکانی هاوجییوونی تیکه ل بۆ ناستهکانی هاوجییوونی ته واو .

پوختە

نەم توپۆئىنە ۋە يەدا دەست كرا بە ئىكۆئىنە ۋە يىكەتە ئاۋوكى بۇ ھاۋتاكانى ئاۋوكى زىكۆئىنەم كە ژمارەى پىرۆتۆنەكەى (40) ۋ ژمارەى نىوترونەكانى (N=40,42,44,46,48,52,54,56,58,60,62,64,66,68) بە شىۋەى تىۋرى بە بەكارهينانى چوارچىۋەى كارى مۆدلىكەكانى بۆزۋنى كارلىكراۋ (IBM-1, IBM-2). ئىكۆئىنە ۋە كرا ئە سەر سنورەكانى ھاۋجىبۋونى ھاۋتاكانى زىكۆئىنەم بە بەكارهينانى ئاستە ۋوزى ۋوزوئاۋى دوۋم بۇ ئاستە ۋزى ۋوزوئاۋى يەكەم. بىنرا كە ھاۋتا بە كارهينراۋەكان گۋاستنە ۋە ئە نىۋانپان رۋودەدات ئە ناۋچەى SU(5) بۇ SU(3), O(6). تايىبە تەندى سىفەتى ئاستە نزمەكانى ھاۋجىبۋونى تىكەلى ۋەك 1^+ , 2^+ , 3^+ كە دەرھىنراۋە ئە بۇشايى (IBM-2) بۇ ھاۋتاكانى زىكۆئىنەم كە دەكەۋىتە ناۋچەكانى (SU(5), SU(3), O(6)) ئەم ئىكۆئىنە ۋەدا بە ۋوردى باسى ئىۋەكرا. بىنرا كە ئاستەكانى ھاۋجىبۋونى تىكەلاۋەى 1^+ ۋ 3^+ كارى تىدەكرىت بە ھەردوۋ ھاۋكۆلكەى ھىزى (Majorana) ξ_1 ۋ ξ_3 يەك ئەدۋاى يەك, ئە كاتىكدا ھاۋكۆلكەى ξ_2 بە شىۋەىيەكى بەھىزكاردەكاتە سەر ھەموۋ ئەۋ ئاستانەى كە ھەنگرى تايىبە تەندى ھاۋجىبۋونى تىكەن بە تايىبەتى ئاستى 2^+ ھەر ۋەك چۆن كۆنترۆلى ھاۋبەشى دەكات ئە نىۋان ئاستى ھاۋتابۋونى تىكەلى 2_M^+ ۋە ھاۋسىكانى ئەۋ ئاستانەى كە ھەمان گۆشەى تەۋژمىيان ھەيە. ۋە ھەرۋەھا تىبىنى ئەۋە كرا كەۋا سىفەتى ھاۋجىبۋونى تىكەن بۇ ئاستەكانى 1_M^+ , 3_M^+ دەگەرپتەۋە بۇ يەك ئاست بۇ ھەرپەكىكىيان ئە ھەموۋ ھاۋتاكان. ئەكاتىكدا سىفەتى ئاستى 2_M^+ دابەش دەبىت بۇ زىاتر ئە ئاستىكدا ئە كۆمەلى 2^+ ئەگەن ئاستەكانى ھاۋسىيى.

ئەسەر بىنچىنەى كارى بوزۋنى كارلىكراۋ IBM-1 ۋ IBM-2 ئىكۆئىنە ۋە كرا ئە ئاستەكانى ۋوزە بۇ پارىتتە مۇجەبەكان ئە ھەرىپەكە ئە باندى بىنچىنەى ۋىباندى بىتتا ۋىباندى گاما. بە گشتى، نرخی ھەژماركراۋى ئاستە نزمەكانى شەبەنگى ۋوزەى پارىتتە مۇجەبەكان باشتەر دروستدەبىت بە بىنچىنەى كارى IBM-2 ئە چاۋ IBM-1 دا بۇ زۆرىنەى كەيسەكان. ئەمە دەگەرپتەۋە بۇ پەلى ئازادى پىرۆتۆن- نىوترونەكان ئە IBM-2 ۋ ئەھاتنى ئەۋ ئاستانە ئە IBM-1. تايىبە تەندى كارۋمۇگناتىسى ھەردوۋ كارتىكەرى E2 ۋە M1 ئىكۆئىنە ۋە بۇكرا ۋ ئە نجامەكانىشى شىكرانەۋە. شىكرانەۋەى ئە نجامەكان دەرىدەخات كە تايىبە تەندى E2 بە ئاشكرا بەندە ئەسەر

**پېكها تهى ناووكى هاوتاكانى جوت-جوت زرگونىوم به به كارهيئانى مؤديله كانى بوزونى
كارنيكراو (IBM-1 و IBM-2)**

نامه يه كه

**پيشكەش كراوه به نه نجومه نى كولپيژى په روه رده له زانكوى سليمانى
وهك به شيك له پيداويستيه كانى پلهى زانستى ماسته ر له زانستى فيزيا
(فيزياى تيورى)**

له لايه ن

بيرون نصرالدين غفور

به كالوريوس له فيزيا (2012)، زانكوى سليمانى

به سه رپه رشتى

پ.ى.د. سه عدون ته ها نه حمه د

د. نارى كريم نه حمه د